

City of San Diego La Jolla Area of Special Biological Significance Site Specific Dilution and Dispersion Model

June 2013

City of San Diego



Prepared by:
 AMEC Environment and Infrastructure, Inc.
 Project No. 5025121039



**LA JOLLA AREA OF SPECIAL BIOLOGICAL SIGNIFICANCE
SITE SPECIFIC DILUTION AND DISPERSION MODEL**

**Prepared for:
City of San Diego
Transportation and Storm Water Department
9370 Chesapeake Drive, Suite 100
San Diego, California 92123**

**Submitted by:
AMEC Environment & Infrastructure, Inc.
9210 Sky Park Court, Suite 200
San Diego, California 92123**

May 2013

AMEC Project No. 5025121039

This special study report is prepared for the City of San Diego, Transportation and Storm Water Department (City of San Diego) to complement multiple, ongoing storm water monitoring programs within the La Jolla Area of Special Biological Significance, No 29, located in La Jolla, California. In particular, this study is designed to provide a quantitative, site specific dilution and dispersion model to aid in determination of appropriate dilution factors per guidance provided in the California Ocean Plan (2009).

1.0 REGULATORY BACKGROUND

On October 18, 2004, the State Water Resources Control Board (State Water Board) notified the City of San Diego, as a responsible party, to cease storm water and non point source waste discharges into Areas of Biological Significance (ASBS) or to request an exception from the California Ocean Plan waste discharge prohibition. On December 15, 2004, the City of San Diego requested an exception for ASBS No. 29. On March 20, 2012, the State Water Board adopted Resolution No 2012-0012, approving an exception to the California Ocean Plan, *General Exception to the California Ocean Plan for Areas of Special Biological Significance Waste Discharge Prohibition for Storm Water and Nonpoint Source Discharges, with Special Protections* (herein referred General Protections). These general protections are in accordance with the Porter-Cologne Water Quality Control Act, California Water Code §13000 et seq., and implementing regulations, including the current Ocean Plan (2009).

Under the California Ocean Plan (2009), Section III, C.4.a, Effluent limitations for water quality objectives listed in Table B shall be determined through the use of the following equation:

$$C_e = C_o + D_m (C_o - C_s)$$

where (in ug/l):

- C_e = the effluent concentration limit,
- C_o = the concentration (water quality objective) to be met at the completion of initial dilution,
- C_s = background seawater concentration (references in Table C of Ocean Plan)
- D_m = minimum probable initial dilution expressed as parts seawater per part wastewater.

Furthermore, the Ocean Plan provides guidance for the identification of dilution models for use in determining the initial dilution, D_m. Specifically, per Section III, C.4.a;

The Executive Director of the SWRCB shall identify standard dilution models for use in determining D_m, and shall assist the Regional Board in evaluating D_m for specific waste discharges. Dischargers may propose alternative methods of calculating D_m, and the Regional Board may accept such methods upon verification of its accuracy and applicability.

2.0 HYDRODYNAMIC MODELING DESIGN

This study is designed to provide site specific dilution and dispersion model results for ASBS No. 29 to the San Diego Regional Water Quality Control Board (SDRWQCB). The effluents from three permitted outfalls within the La Jolla ASBS were studied using the SEDXPORT hydrodynamic modeling system. The model is designed to numerically simulate dry weather and wet weather case scenarios. The dilution study incorporated historical site specific outfall data on water mass boundary properties (bathymetry, salinity, temperature, ocean level/tides) and forcing functions (waves, currents and winds).

The SEDXPORT modeling system was developed at Scripps Institution of Oceanography (SIO) for the US Navy's *Coastal Water Clarity System* and *Littoral Remote Sensing Simulator*. The model has been reviewed and vetted by multiple regulatory agencies and has been calibrated for six previous water quality projects in the Southern California Bight. Due to the large number of oceanographic measurements that have been made in ASBS No 29 and the adjacent ASBS No 31, the model for this site is considered particularly robust. These include long term water quality, wind, wave, water height, tidal and temperature measures at the SIO pier as well as multiple special studies of currents and storm water inputs into La Jolla Bay and environs.

This model was selected as the most relevant model available for the following reasons;

- 1) The State Water Board required SIO to perform a similar study to determine the initial dilution and dispersion of the discharge during storm and non-storm periods at the adjacent ASBS No. 31 (San Diego-Scripps) as a requirement of SIO's NPDES Permit Exception, Order No. R9-2005-0008. SIO used the SEDXPORT modeling system to fulfill this requirement and the study was provided on February 9 2007 to the San Diego Regional Board and the California SWRCB for approval.
- 2) The model design and results of the SIO study were evaluated by the Natural Water Quality Committee (NWQC), and deemed appropriate (Summation of Findings, Natural Water Quality Committee, 2006-2009, SCCWRP Technical Report 625, September 2010). The NWQC was a scientific oversight committee established as a requirement of the SIO permit to evaluate monitoring results and special studies. With technical review and input from the NWQC, the SDRWQCB revised the initial 2:1 dilution factor in the initial waste discharge requirements (WDR) to a 7:1 dilution factor (representative of the minimum dilution ratio) and this 7:1 dilution factor was incorporated into the November 2008 revision of SIO's permit.
- 3) This study utilizes the same modeling program (SEDXPORT) and modeling assumptions and integrating the most recent long term historical trend data. In addition, the model calibration and outputs were generated by the same SIO scientists (Scott Jenkins, Ph.D. and Joseph Wasyl) that published the SDRWQCB approved 2007 SIO study.

- 4) The mass flow model inputs are based on actual discharge data (flow and mass) measured from permitted outfalls; SDL-157, SDL-062 and SDL-186. To model the beach discharges, flow and chemistry results collected in November 2011 provided data representative of the worse case proxy scenario. These data were merged with the long term probability assessment in order to bracket possible dilution outcomes. The study provide the same data endpoints (dilution ranges of the outer far field [$>-10\text{m}$] of ASBS No. 29 and the near field [$<-10\text{m}$] surf zone dilution ranges) for wet weather discharges under various ocean mixing conditions as used in the aforementioned SIO study. In addition, the extreme worse case probabilities (high storm water flow/low surf and currents) at the zone of initial dilution (ZID) were evaluated to determine minimum dilution factors.

3.0 HYDRODYNAMIC MODELING RESULTS

On behalf of the City of San Diego, AMEC Earth and Infrastructure, Inc. contracted with Dr. Scott A Jenkins Consulting to provide hydrodynamic modeling of storm drain discharges in the vicinity of ASBS No.29. The complete hydrodynamic modeling report is provided as Attachment A.

In order to model possible dilution scenarios, long term trends for boundary and force function data (i.e., 32 year record from 1980-2012) provides a representative basis for the model to incorporate the Pacific Decadal Oscillation (aka alternating periods of strong and weak El Niño). Site specific storm water flow and mass data (three events spanning from November 2011 to March 2012) were obtained from three monitored outfalls within ASBS No 29; SDL-157, SDL-062 and SDL-186.

These data sets (parameters for long term functions and outfall flux/hydrographs) are coupled and the model produces the dilution and dispersion outcomes (aka ranges of dilution factors) by analyzing the possible daily outcomes (maximum and minimum) of the input variables over 32 years (a total of 11,688 distinct combinations). This analysis was performed for each of the outfalls.

These probabilities can be plotted as a density functions and the dilution factors presented relative to the likelihood of occurrence. The resultant density plots span from the highest modeled dilution factor (low flow/high energy ocean conditions) to the lowest “worst case” dilution (high storm water flow/calm ocean conditions). The likelihood of occurrence corresponding to these conditions decreases for both the best and worst case scenarios as the model search criteria plots the possible combinations. See Attachment A, Table 3 for search criteria.

These wet weather worse case scenarios for the dilution and mass are plotted as dilution contour maps, by merging the results for both the offshore and surfzone bathymetry regions. See Attachment A, Figures 30-36. In general, dilutions for storm water range between a minimum of 10^2 to 10^4 in the nearshore and dilution magnitude of 10^4 to 10^7 characterize the outer half offshore of ASBS No. 29.

In the immediate zone of initial dilution, where there is irreversible turbulent mixing, the dilution factor for 90% of the potential outcomes produced a minimum dilution of 20 to 1 for the 48-inch Outfall SDL-157, and 15 to 1 for the 72-inch SDL-062 outfall using the worse case November 2011 storm event. Of the three flow monitored outfalls, the 36-inch SDL-186 (the Devil's slide) has significantly lower storm water discharges, and therefore correspondingly higher near shore dilution factors. Dilution factors for the SDL-186 near shore area were in the range of 10^3 .

The largest and single contributing dilution footprint was found at SDL-062, the discharge at the end of Avenita de la Playa Street. This is the largest outfall within ASBS No. 29 and drains the largest fraction of the La Jolla Shores watershed. Therefore, this outfall generates the lowest modeled dilution factors. The median outcome minimum surfzone dilution for SDL-062 is 22 to 1. The minimum worst case value for SDL062, with a probability of occurrence of 0.13%, is 13 to 1 (12.6:1 calculated value) in a peak storm water flow and low energy ocean mixing condition.

4.0 STUDY CONCLUSIONS

Using the SEDXPORT hydrodynamic model, the storm water discharges from monitored outfalls into the La Jolla ASBS No 29 generated dilution factors ranging from 10^2 in the near shore, to 10^7 in the seaward boundary during wet weather. Further resolution of the model at the zone of initial dilution (ZID) produced a worse case dilution factor of 15 to 1 for 90% of the possible outcomes for the largest discharge outfall, SDL-062. The extreme worst case (0.13% probability in conditions of high discharge, calm sea state) generated a 13:1 dilution factor for this outfall.

It was this extreme worse case dilution value that was approved by the SDRWQCB as described in hydrodynamic modeling section, item 2 above.

In addition, it is fortuitous that the lowest flow outfall, SDL-186 at the Devils Slide, has the most high value, hard bottom marine habitat and that dilution outcomes are greater than 3 orders of magnitude in the nearshore area. There is a hard bottom tidal flat in the immediate vicinity of the Devils Slide intertidal zone that is exposed at low tide, that may be subject to acute fresh water exposure during storm events. Conversely, the higher flow SDL-062 discharges across the southern border of La Jolla Shores beach and discharges into the surf zone onto sandy soft bottom marine habitat.

The high dilution factors expected in the vicinity of the Devils Slide area of ASBS No.29 is consistent with other localized water quality measurements during storm water discharge from Outfall SDL-186. These include the La Jolla Shores ASBS Protection Implementation Program administered under Prop 84 funding (Grant agreement No 10-413-550, La Jolla Shores Watershed Management Group [LJSWGM], 2008) and, ASBS No. 29 compliance monitoring under the General Protections, and a corresponding bioaccumulation study (AMEC, 2013).

City of San Diego
La Jolla Area of Special Biological Significance
Draft Dilution and Dispersion Model
AMEC Project No. 5025121039
June 2013



APPENDIX A

HYDRODYNAMIC MODELING OF STORM DRAIN DISCHARGES IN THE NEIGHBORHOOD OF ASBS 29 IN LA JOLLA, CALIFORNIA

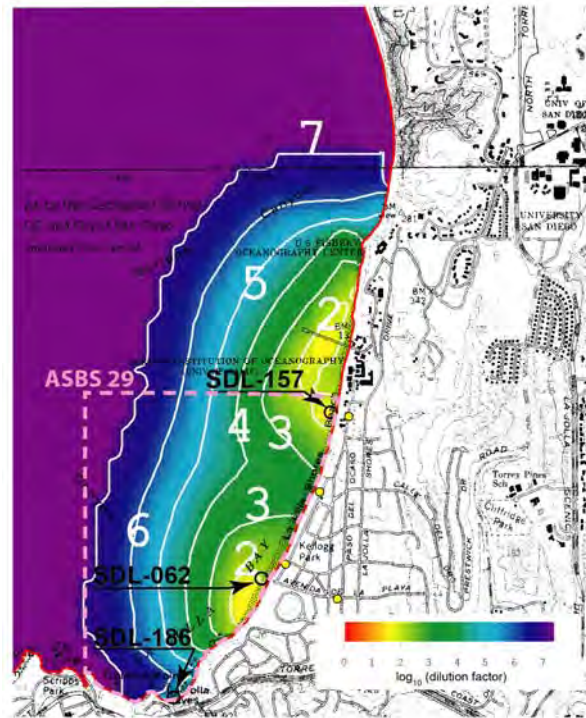
City of San Diego
La Jolla Area of Special Biological Significance
Draft Dilution and Dispersion Model
AMEC Project No. 5025121039
June 2013



This page intentionally left blank

HYDRODYNAMIC MODELING OF STORM DRAIN DISCHARGES IN THE NEIGHBORHOOD OF ASBS 29 IN LA JOLLA, CALIFORNIA

by: Scott A. Jenkins, Ph. D. and Joseph Wasyl



Submitted by:

Dr. Scott A. Jenkins Consulting
14765 Kalapana Street
Poway, CA 92064

Submitted to:
City of San Diego
Transportation and Storm Water Department
9370 Chesapeake Dr., Suite 100
San Diego, CA 92123, USA

Final: 12 May 2013

TABLE OF CONTENTS

	Page
EXECUTIVE SUMMARY	1
1.0 INTRODUCTION	1-1
2.0 MODEL DESCRIPTION AND CAPABILITIES	2-1
3.0 MODEL INITIALIZATION	3-1
3.1 Boundary Conditions	3-4
3.2 Forcing Functions	3-21
3.3 Model Scenarios.....	3-37
3.4 Calibration.....	3-39
4.0 RESULTS	4-1
4.1 Wet Weather Worst Case Dilution Results.....	4-1
4.2 Long Term Minimum Dilution in the Surf Zone and Offshore	4-9
5.0 SUMMARY AND CONCLUSIONS:	5-1
6.0 REFERENCES AND BIBLIOGRAPHY	6-1

LIST OF TABLES

Table 1.	Outfall Discharge Monitoring Locations and Descriptions	1-2
Table 2.	Monitoring Events Summary	3-11
Table 3.	Search Criteria for Wet Weather Worst-Case Combinations of Controlling Variables.	3-38

LIST OF FIGURES

Figure 1.	Location Map for La Jolla Storm Drains SDL-157, SDL-062 and SDL-186 in relation to ASBS 29 and ASBS 31, (from AMEC 2012).	1-3
Figure 2.	a) Period of record of San Diego rainfall and b) cumulative residual	1-5
Figure 3.	Typical wintertime Sea Surface Temperature (colors), Sea Level Pressure (contours) and surface wind stress (arrows) anomaly patterns during warm and cool phases of PDO. Red colors indicate warm, blue indicates cool.	3-2
Figure 4.	Cumulative residual of quarterly values of Southern Oscillation Index (SOI) [data from Australian Commonwealth Bureau of Meteorology].....	3-3
Figure 5.	Composite bathymetry from NOS data base and equilibrium profiles after Jenkins and Inman (2006) for wave conditions of wet weather scenario. Depth contours shown in meters mean sea level.	3-5
Figure 6.	Daily mean ocean surface salinity (a) and daily mean ocean surface temperature at La Jolla, CA; from CDIP (2012), SIO, (2010), and MBC (2012).	3-7

TABLE OF CONTENTS (Cont.)

	Page
LIST OF FIGURES (Cont.)	
Figure 7. Daily mean ocean surface salinity (a) and daily mean ocean bottom temperature at La Jolla, CA; from CDIP (2012), SIO, (2010), and MBC (2012).....	3-8
Figure 8. Controlling ocean forcing functions for La Jolla Bay: a) daily mean significant wave height, b) daily high and low water levels, c) daily maximum tidal current, d) daily mean wind speed. (data from CDIP, 2012; SIO, 2012; and NCEP, 2012).....	3-10
Figure 9. Hydrographs for storm drains SDL-062 (black) and SDL- 157 (blue) as compared against rainfall (red) during Wet Weather Event-1 , 20 November 2011 to 21 November 2011.....	3-13
Figure 10. Flux of Total Suspended Solids in a 15 minute interval (red) and Cumulative Mass Loading of Total Suspended Solids (black) for storm drain SDL-157 during Wet Weather Event-1 , 20 November 2011 to 21 November 2011.....	3-14
Figure 11. Flux of Total Suspended Solids in a 15 minute interval (red) and Cumulative Mass Loading of Total Suspended Solids (black) for storm drain SDL-062 during Wet Weather Event-1 , 20 November 2011 to 21 November 2011.....	3-15
Figure 12. Hydrographs for storm drains SDL-062 (black) and SDL- 157 (blue) as compared against rainfall (red) during Wet Weather Event-2 , 7 February 2012.....	3-16
Figure 13. Flux of Total Suspended Solids in a 15 minute interval (red) and Cumulative Mass Loading of Total Suspended Solids (black) for storm drain SDL-157 during Wet Weather Event-2 , 7 February 2012.....	3-17
Figure 14. Flux of Total Suspended Solids in a 15 minute interval (red) and Cumulative Mass Loading of Total Suspended Solids (black) for storm drain SDL-062 during Wet Weather Event-2 , 7 February 2012.....	3-18
Figure 15. Hydrographs for storm drains SDL-062 (black) and SDL- 157 (blue) as compared against rainfall (red) during Wet Weather Event-3 , 17 March 2012 to 18 March 2012.	3-19
Figure 16. Flux of Total Suspended Solids in a 15 minute interval (red) and Cumulative Mass Loading of Total Suspended Solids (black) for storm drain SDL-157 during Wet Weather Event-3 , 17 March 2012 to 18 March 2012.....	3-20

TABLE OF CONTENTS (Cont.)

	Page
LIST OF FIGURES (Cont.)	
Figure 17.	Flux of Total Suspended Solids in a 15 minute interval (red) and Cumulative Mass Loading of Total Suspended Solids (black) for storm drain SDL-062 during Wet Weather Event-3 , 17 March 2012 to 18 March 2012.....
	3-21
Figure 18.	Oceanside Littoral Cell and Torrey Pines Sub-Cell.....
	3-23
Figure 19.	Back-refraction using <i>oceanrds.for</i> with waves measured by San Clemente CDIP station during the storm of 17 January 1988 with 10m high waves at 17 second period approaching the Southern California Bight from 270 ⁰
	3-25
Figure 20.	Deep water wave data for wave forcing in Torrey Pines Sub-Cell derived from back refraction of CDIP monitoring data, 1980-2012
	3-26
Figure 21.	High resolution refraction/diffraction computation for extreme dry weather model scenario based on 0.2m deep water wave height from 210 ⁰ with 10 sec period.
	3-27
Figure 22.	High resolution refraction/diffraction computation for worst-case wet weather model scenario based on 1.8 m deep water wave height from 283 ⁰ with 14 sec period, 21 November 2011.
	3-28
Figure 23.	Statistics of composite wave record obtained by merging the CDIP archival data for 1980-2012 with the 2011-2012 ADCP wave burst measurements.....
	3-30
Figure 24.	Progressive vector plot of current field in La Jolla Bay during a neap tidal day. Vector magnitude scaled by the color bar in the upper right corner.
	3-31
Figure 25.	Progressive vector plot of current field in La Jolla Bay during a spring tidal day used in the wet weather modeling scenario. Vector magnitude scaled by the color bar in the upper right corner.
	3-32
Figure 26.	Near-bottom currents (2.4 m above seabed) at mooring location -10 m MSL at northern edge of ASBS 29 (cf. Figure 1). Measurements by Acoustic Doppler Current Profiler (ADCP), 11/14/11-11/24/12. East-west current velocity component (top); north-south velocity component (middle); total velocity amplitude (bottom).....
	3-33
Figure 27.	Histogram (probability density) and cumulative probability of near-bottom currents (2.4 m above seabed) at mooring location-10 m MSL at northern edge of ASBS 29, (cf. Figure 1); 11/14/11-11/24/12.....
	3-34
Figure 28.	Interior currents (6.4 m above seabed) at mooring location -10 m MSL at northern edge of ASBS 29 (cf. Figure 1). Measurements by Acoustic Doppler Current Profiler (ADCP), 11/14/11-11/24/12. East-west current velocity component (top); north-south velocity component (middle); total velocity amplitude (bottom).....
	3-35

TABLE OF CONTENTS (Cont.)

	Page
<hr/>	
LIST OF FIGURES (Cont.)	
<hr/>	
Figure 29.	Histogram (probability density) and cumulative probability of interior currents (6.4 m above seabed) at mooring location-10 m MSL at northern edge of ASBS 29, (cf. Figure 1); 11/14/11-11/24/12..... 3-36
Figure 30.	Depth averaged dilution for wet weather worst case due to simultaneous discharges of storm water from SDL-157, SDL-062 and SDL-186; 21 November 2011; waves: H = 1.8 m, T = 14 s, $\alpha = 283^\circ$; wind = 11 kts..... 4-2
Figure 31.	Depth averaged dilution for wet weather worst case due to isolated discharge of storm water from SDL-157; 12 November 2011; waves: H = 1.8 m, T = 14 s, $\alpha = 283^\circ$; wind = 11 kts..... 4-3
Figure 32.	Depth averaged dilution for wet weather worst case due to isolated discharge of storm water from SDL-062; 21 November 2011; waves: H = 1.8 m, T = 14 s, $\alpha = 283^\circ$; wind = 11 kts..... 4-4
Figure 33.	Depth averaged dilution for wet weather worst case due to isolated discharge of storm water from SDL-186; 21 November 2011; waves: H = 1.8 m, T = 14 s, $\alpha = 283^\circ$; wind = 11 kts..... 4-5
Figure 34.	Depth averaged concentration of total suspended solids (TSS) for wet weather worst case due to discharge of storm water from SDL-157; 21 November 2011; waves: H = 1.8 m, T = 14 s, $\alpha = 283^\circ$; wind = 11 kts..... 4-6
Figure 35.	Depth averaged concentration of total suspended solids (TSS) for wet weather worst case due to discharge of storm water from SDL-062; 21 November 2011; waves: H = 1.8 m, T = 14 s, $\alpha = 283^\circ$; wind = 11 kts..... 4-7
Figure 36.	Depth averaged concentration of total suspended solids (TSS) for wet weather worst case due to discharge of storm water from SDL-186; 21 November 2011; waves: H = 1.8 m, T = 14 s, $\alpha = 283^\circ$; wind = 11 kts..... 4-8
Figure 37.	Probability density function (red) with corresponding cumulative probability (blue line) of the minimum surfzone dilution within the ZID around storm drain SDL-157. Derived from ocean boundary conditions and forcing functions, 1980-2012, 11,688 total numbers of realizations. 4-10
Figure 38.	Probability density function (red) with corresponding cumulative probability (blue line) of the minimum surfzone dilution within the ZID around storm drain SDL-062. Derived from ocean boundary conditions and forcing functions, 1980-2012, 11,688 total numbers of realizations. 4-11
Figure 39.	Probability density function (red) with corresponding cumulative probability (blue line) of the minimum dilution on the sea surface at offshore control point in ASBS 29. Derived from ocean boundary conditions and forcing functions, 1980-2012, 11,688 total numbers of realizations. 4-12

TABLE OF CONTENTS (Cont.)

LIST OF APPENDICES

- APPENDIX A GOVERNING EQUATIONS AND CODE FOR THE TIDE_FEM CURRENT MODEL
- APPENDIX B CODE FOR THE TID_DAYS TIDAL FORCING MODEL
- APPENDIX C CODES FOR THE OCEANRDS REFRACTION/DIFFRACTION MODEL
- APPENDIX D CODE FOR THE OCEANBAT BATHYMETRY RETRIEVAL MODULE
- APPENDIX E CODE FOR THE SEDXPORT TRANSPORT MODEL
- APPENDIX F CODE FOR THE MULTINODE DILUTION MODEL
- APPENDIX G AMEC MONITORING DATA

EXECUTIVE SUMMARY

The La Jolla Shores Coastal Watershed consists of 1,639 acres, primarily residential and institutional (e.g., the University of California, San Diego [UCSD] campus) land uses. Sub-drainages within the watershed boundary drain west into two *areas of special biological significance* (ASBS): the San Diego– Scripps ASBS (ASBS 31) and the La Jolla ASBS (ASBS 29). The majority of the runoff from the watershed is conveyed through a network of storm drains before it is discharged at several locations along the beach. Hydrodynamic model analysis of the dilution and dispersion of shoreline discharges into ASBS 31 was previously done by Jenkins and Wasyl (2007) for the University of California San Diego. The present hydrodynamic analysis applies those same analysis methods in evaluating shoreline discharges of storm water into nearshore waters surrounding ASBS 29. The central and largest portion of the La Jolla watershed affecting ASBS 29 drains to only two storm drain outfalls, SDL-157 at the northern boundary of ASBS 29 and SDL-062 at Avenida de la Playa. During the 2011-2012 wet weather monitoring season (October 1, 2011 through April 30, 2012), storm water samples were collected from outfall discharge and receiving water mixing zone monitoring locations during three events (AMEC, 2012). These data were used to initialize the source loading inputs to a hydrodynamic model (*SEDXPORT*) used in the present receiving water analysis of storm water dilution and dispersion.

The *SEDXPORT* hydrodynamic modeling system was developed at Scripps Institution of Oceanography for the US Navy's *Coastal Water Clarity System* and *Littoral Remote Sensing Simulator*. This model has been peer reviewed multiple agencies and has been calibrated and validated in the Southern California Bight for six previous water quality and design projects.

Based on previous protocols established with the San Diego Regional Water Quality Control Board for storm drain dilution analysis in ASBS 31 (Jenkins and Wasyl, 2007), the numerical modeling study of the beach discharges is based on a wet weather worst-case scenario with a long-term probability assessment to bracket the envelope of the possible outcomes. Among the three wet-weather events monitored by AMEC (2012), Wet Weather Event-1 (20-21 November, 2011) comes closest to matching a computer search of marine environmental conditions for the wet-weather worst-case proxy. Analysis of the worst-case wet weather proxy was conducted over the entire coastal domain of La Jolla Bay and the Torrey Pines Littoral Sub-Cell.

The footprint of the dilution field for the wet weather worst case scenario, (involving the simultaneous discharge from storm drains SDL-157, SDL-062 and SDL-186), spreads about a kilometer seaward of the shoreline and about 2 kilometers along the shoreline, covering most of ASBS 29 and intruding into the southern portion of ASBS 31. The dilution factors of storm water in both ASBS 29 and ASBS 31 range between a minimum of 10^2 near shore to 10^7 along the seaward boundaries during the wet weather worst case. Dilution factors of 10^4 to 10^7 characterize the outer one-half of ASBS 29, while dilution factors 10^2 to 10^4 characterize the inner one-half. In the immediate neighborhood of SDL-157 and SDL-062, very near the shoreline of ASBS 29, dilution factors are as low as 40 to one.

The preponderance of the storm water discharge plume during the wet weather worst case scenario is from SDL-157 and SDL-062, while SDL-186 at Devil's Slide makes a very minor contribution. This is a fortuitous outcome in the sense that a significant amount of high-value, hard bottom marine habitat lives in the southern end of ASBS 29, and in the immediate neighborhood of SDL-186. Dilution factors of storm water discharged from SDL-186 are at most 10^3 near the shore in the nearfield of SDL-186, and more typically 10^4 to 10^5 elsewhere along the bluff-faced shoreline of the southern end of ASBS 29. The largest single contributing footprint to the combined storm water plume appears to be from SDL-062 at the end of Avendia De La Playa that produces a large patch with 10^2 minimum dilution very near the shoreline that spreads south along the shore to the La Jolla Beach and Tennis Club. The region influenced by this feature from SDL-062 is sandy, soft-bottom marine habitat. SDL-157 produces another patch with 10^2 minimum dilution, but this feature moves offshore and intrudes into the southern end of ASBS 31, where again the marine habitat is a sandy soft-bottom type.

Maximum concentrations of storm water born total suspended solids (TSS) in the receiving water due to SDL-186 storm water discharges are at most 0.001 mg/L near the shore in the nearfield of SDL-186, and more typically 0.0001 mg/L elsewhere along the bluff-faced shoreline of the southern end of ASBS 29, where significant high-value, hard bottom marine habitat resides. The highest TSS concentrations in the receiving water around SDL-062 (at the end of Avendia De La Playa), were found to be 3 mg/L in a nearshore patch that that spreads south along the shore to the La Jolla Beach and Tennis Club. Most of the shoreline impacted by SDL-157 experiences maximum TSS concentrations from storm water in the range of 0.3 mg/L to 0.03 mg/L, all of which is sandy soft- bottom marine habitat. At the northern end of ASBS 29, and extending into ASBS 31, maximum TSS concentrations in the receiving from SDL-157 are in the range of 4 mg/L to 0.4 mg/L, the highest anywhere in La Jolla Bay. These relatively higher TSS values are probably a consequence of the steep land forms that comprise the watershed of SDL-157, with portions of both developed and undeveloped coastal bluffs. Regardless, the marine habitat subjected to these TSS loadings from SDL-157 is a sandy, soft-bottom type.

Because of the disparity in length scales between dilution in the offshore region versus the surfzone, a separate analysis was performed on a nested fine scale grid covering the surf zone for a long shore reach that extended 1000 ft (305 meters) either side of the beach outfalls. The size of this grid was based on precedent already set for the definition of a zone of initial dilution (ZID) by the Regional Water Quality Control Board, San Diego. Thirty two years of receiving water variables (involving 11,688 distinct combinations) were input for daily simulations of dilution. The ZID was searched for the minimum dilution after averaging across the width of the surf zone. Source loading for these simulations were based on the discharges measured during Wet-Weather Event-1 from outfalls SDL-157, SDL-062 and SDL-186. The surfzone dilution results are then compared to minimum dilution on the sea surface at an offshore control point in ASBS 29 where local water depth is -10 m MSL.

This probability analysis procedure (based on the historic combination of 11,688 environmental variables) inevitably produces some combinations of wet weather discharges with dry weather ocean mixing conditions, and thereby results in certain worst case dilution scenarios that are more extreme, with even less dilution, than the wet weather worst case proxy derived from the monitoring program (Wet-Weather Event-1). For storm drain SDL-157, the median outcome for minimum dilution factor within the surfzone ZID is 32 to 1; however the potential range of minimum dilution goes as high as 88 to 1, and as low as 15 to 1. Low energy, dry weather ocean mixing produced the 15 to 1 minimum surfzone dilution outcome, which had a probability of occurrence of 0.13%. Altogether, 90% of the potential outcomes produce minimum dilutions in the surfzone ZID greater than 20 to 1.

Minimum surfzone dilutions in the ZID off SDL-062 are slightly less. This is due to the wave shadow found chronically in the refraction pattern of La Jolla Shores in the neighborhood of Avendia De La Playa. The minimum surfzone dilution of discharges from SDL-062 is found to be 12.6 to 1, again a low energy, dry weather ocean mixing result. The median outcome of minimum surfzone dilution for SDL-062 is 22 to 1; while the potential range of minimum dilution goes as high as 64 to 1, based on the 32-year historical sequence of receiving water variables. Ninety percent of the potential outcomes for SDL-062 produce minimum surfzone dilutions greater than 15 to 1.

For comparison, probability statistics for minimum dilution at an offshore control point in ASBS 29 (where local water depth is -10 m MSL) discovered a worst case minimum dilution of storm water of 13,200 to 1; while the median outcome is 52,000 to 1. The highest minimum dilutions of storm water at the offshore control point were found to be 4.2×10^5 . Consequently, storm water dilution is sufficiently high in the offshore regions of ASBS 29 that concentrations of storm water runoff constituents should be well below quantifiable detection limits.

Hydrodynamic Modeling of Storm Drain Discharges in the Neighborhood of ASBS 29 in La Jolla CA

By: Scott A. Jenkins, Ph. D. and Joseph Wasyl

1.0 INTRODUCTION

The La Jolla Shores Coastal Watershed consists of 1,639 acres, primarily residential and institutional (e.g., the University of California, San Diego [UCSD] campus) land uses. Sub-drainages within the watershed boundary drain west into two *areas of special biological significance* (ASBS): the San Diego– Scripps ASBS (ASBS 31) and the La Jolla ASBS (ASBS 29). The majority of the runoff from the watershed is conveyed through a network of storm drains before it is discharged at several locations along the beach. Hydrodynamic model analysis of the dilution and dispersion of shoreline discharges into ASBS 31 was previously done by Jenkins and Wasyl (2007) for the University of California San Diego. The present hydrodynamic analysis applies those same analysis methods in evaluating shoreline discharges of storm water into nearshore waters surrounding ASBS 29.

The central and largest portion of the La Jolla watershed affecting ASBS 29 drains to a single storm drain outfall that discharges at Avenida de la Playa.

Monitoring within ASBS 29 and the drainage area discharging to the ASBS has been conducted over a number of years at multiple locations. The La Jolla Shores Watershed Urban Runoff Characterization and Watershed Characterization Study (Weston Solutions, Inc., Weston, 2007) was conducted under Proposition 50 - Funding for Public Water Systems (Prop 50). The Weston (2007) study assessed data collected between 2005 and 2007 at locations within the watershed and receiving water to identify constituents of interest (COI) for ASBS 29 for future studies. Monitoring based on the Special Protections Document has been conducted since the 2008-2009 wet weather monitoring season. Monitoring activities were conducted by Weston for the wet weather monitoring seasons from fall 2008 through spring 2011 (Weston, 2009, 2010, 2011). Monitoring by Weston included a variety of sample collection programs, including pre-storm, during-storm, and post-storm sample collections. Sample collection occurred at receiving water mixing zone, outfall discharge, and reference beach locations. A summary of previous studies was published by AMEC Earth and Infrastructure, Inc. (AMEC) in a draft conceptual ASBS 29 Characterization Summary and is provided in Appendix A of AMEC (2012). During the 2011-2012 wet weather monitoring season (October 1, 2011 through April 30, 2012), storm water samples were collected from outfall discharge and receiving water mixing zone monitoring locations during three events (AMEC, 2012). Sediment samples were collected from receiving water mixing zone monitoring locations after the third monitored event. These water quality data were used to initialize the source loading inputs to the hydrodynamic model used in the present storm water dilution and dispersion analysis.

Dilution analysis of three storm drain discharges (SDL-157, SDL-062 and SDL-186) were studied in numerical simulation for wet weather extreme and average case scenarios using the **SEDXP** hydrodynamic modeling system that was developed at Scripps Institution of Oceanography for the US Navy's *Coastal Water Clarity System* and *Littoral Remote Sensing Simulator*. This model has been peer reviewed multiple times and has been calibrated and validated in the Southern California Bight for 4 previous water quality and design projects (cf. Section 2).

The locations of the monitoring locations storm drain outfalls (SDL-157, SDL-062 and SDL-186) are shown in Figure 1 and are characterized by the following locations and descriptions:

Table 1.
Outfall Discharge Monitoring Locations and Descriptions

Site ID	Pipe Diameter (in)	Number of Events / Sample Type	Latitude	Longitude	Description
SDL-062-OD	72	3 / Flow-weighted Composite	32.85384	-117.25491	Upstream of outfall at intersection of Avenida de la Playa and Paseo del Ocaso.
SDL-157-OD	48	3 / Flow-weighted Composite	32.86278	-117.25429	Upstream of outfall on east side of El Paseo Grande.
SDL-186-OD	36	2 / Time-weighted composite of 2 - 4 grab samples	32.84813	-117.26507	Upstream of outfall on Torrey Pines Road
SDL-063-OD	36	Not monitored	32.85563	-117.25818	End of Vallecitos Road
SDL-063B-OD	36	Not monitored	32.85913	-117.25608	On seawall approximately 300 feet north of northern end of Kellogg Park parking lot

Storm Drain SDL-062 – This 72-inch storm drain discharges approximately 44 % of the La Jolla Shores Coastal Watershed runoff. This percentage was revised from 49 % stated in the Work Plan based on a recalculated drainage area for the modified flow model. The SDL-062 outfall is located at the end of Avenida de la Playa and discharges to La Jolla Shores Beach. Flow-weighted composite samples were collected approximately one-quarter mile upstream of the outfall at a point where more accurate flow data could be collected. The monitoring location was within a manhole at the intersection of Avenida de la Playa and Paseo del Ocaso (Figure 1).

Storm Drain SDL-157 – This 48-inch outfall discharges directly to La Jolla Shores Beach and drains approximately 12 % of the La Jolla Shores Watershed. Flow-weighted samples were collected approximately 180 feet upstream of the outfall at a point where more accurate flow data could be collected. The monitoring location was within a manhole on the eastern side of El Paseo Grande (Figure 1).

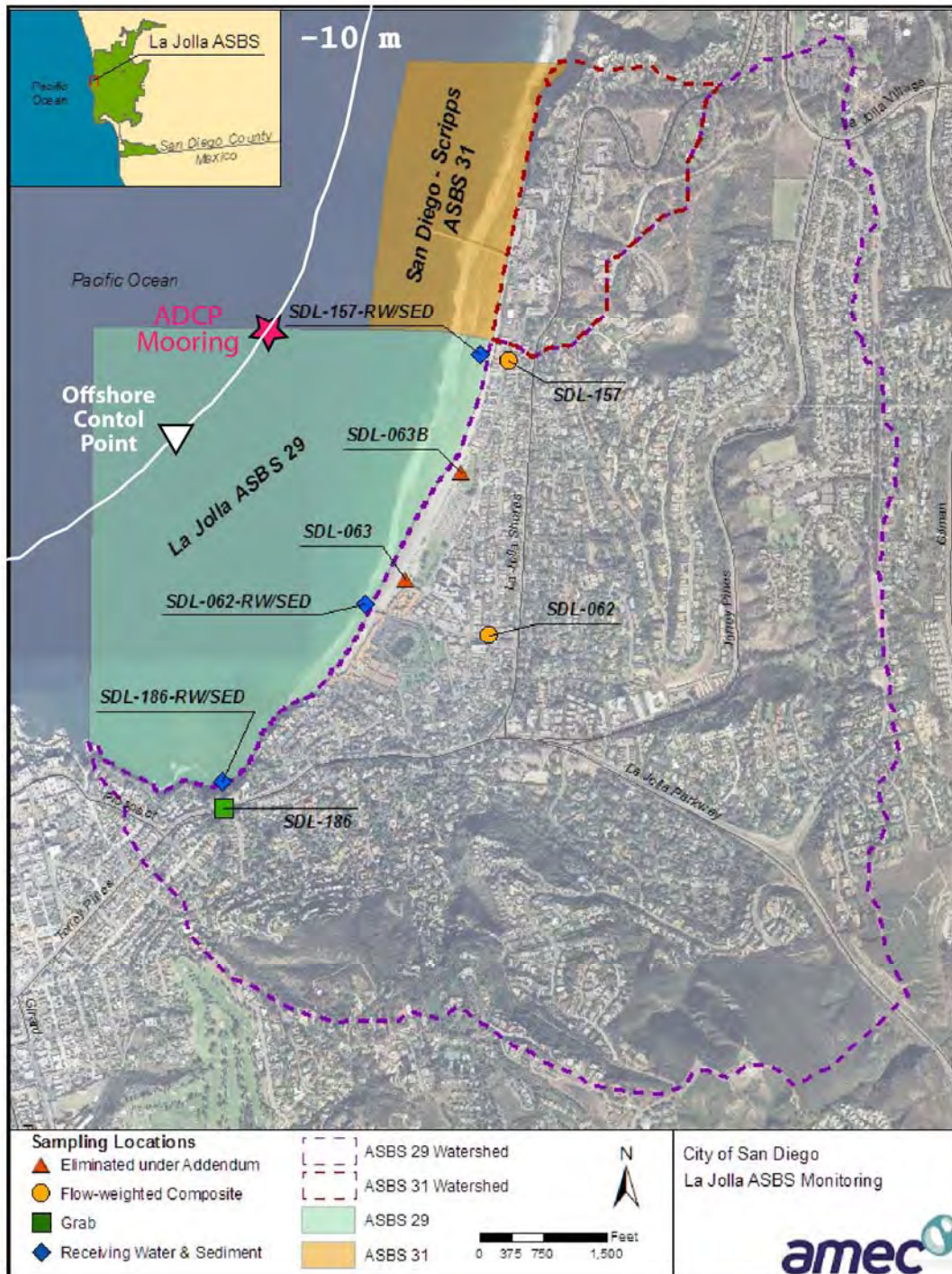


Figure 1. Location Map for La Jolla Storm Drains SDL-157, SDL-062 and SDL-186 in relation to ASBS 29 and ASBS 31, (from AMEC 2012).

Storm Drain SDL-186 – This 36-inch outfall discharges directly to the rocky intertidal area of the ASBS south of La Jolla Shores Beach, known as Devil's Slide. This outfall drains approximately 3 % of the La Jolla Shores Coastal Watershed (Figure 1). This percentage was revised from 4 % stated in the Work Plan (MACTEC. 2011a. & b.) based on a recalculated drainage area for the modified flow model. Access to this outfall is restricted during high tide conditions. Given the lack of consistent, safe access to the outfall, the storm drain upstream was sampled instead. This manhole is located on Torrey Pines Road between Prospect Place and Amalfi Street, approximately 160 feet upstream of the outfall.

The quantification of dilution requires solving the hydrodynamic transport equations for the spatial and temporal variation of dilution factor throughout the effected receiving water. The dilution factor analysis will be evaluated at two distinct worse case scenarios: 1) base flows during dry weather with low mixing rates in the receiving waters due to quiescent ocean/atmosphere conditions; and 2) storm water runoff and discharge during high energy conditions typical of a winter storm event.

It is sensible to bifurcate the model problem into these dry and wet weather scenarios based on the multi-decadal dry/ wet cycles that the regional climate undergoes. The California coast is subject to climate cycles of about 20-30 years duration known as the Pacific/ North American pattern (for atmospheric pressure) or the Pacific Decadal Oscillation (for sea surface temperature). These dry/ wet cycles are apparent in the historic rainfall record of San Diego shown in Figure 2a. A dry period extended from about 1945-1977, followed by an episodically wet period from 1978-1998 that included the occurrence of 6 strong El Niño events (Inman and Jenkins 1999; and Goddard and Graham 1997). Based on the historic duration of these cycles, 1998 was likely the end of the wet cycle of climate in California with a return to the dry climate that prevailed from 1945-1977.

To illustrate the historical evidence for these dry and wet climate cycles, the rainfall record in Figure 2a was analyzed for climate trends using the Hurst (1951, 1957) procedure that was first used for determining decadal climate effects on the storage capacity of reservoirs (Inman and Jenkins, 1999). Climate trends become apparent when the data are expressed in terms of cumulative residuals of rainfall RF_n taken as the continued cumulative sum of departures of annual values of a time series RF_i from their long term mean value RF_a such that

$$RF_n = \sum_0^n (RF_i - RF_a)$$

where n is the sequential value of the time series. When this procedure

was applied to the rainfall record in Figure 2b, dry periods are revealed by segments of the cumulative residuals having negative (downward) slopes while the wet periods have positive (upward) slopes. A dry period is found from 1945-1997, (negative slopes) while a wet period (positive slope) is shown from 1978-1998. The wet period of the climate cycle is more irregular caused by 6 strong El Niño events (water years 1978, 80, 83, 93, 95, and 98) and one 4 year period (1987-1990) of low rainfall. The analysis shows that the average annual rainfall increased by about 38% from the dry to the wet portions of the cycle. Furthermore, both the minimum and

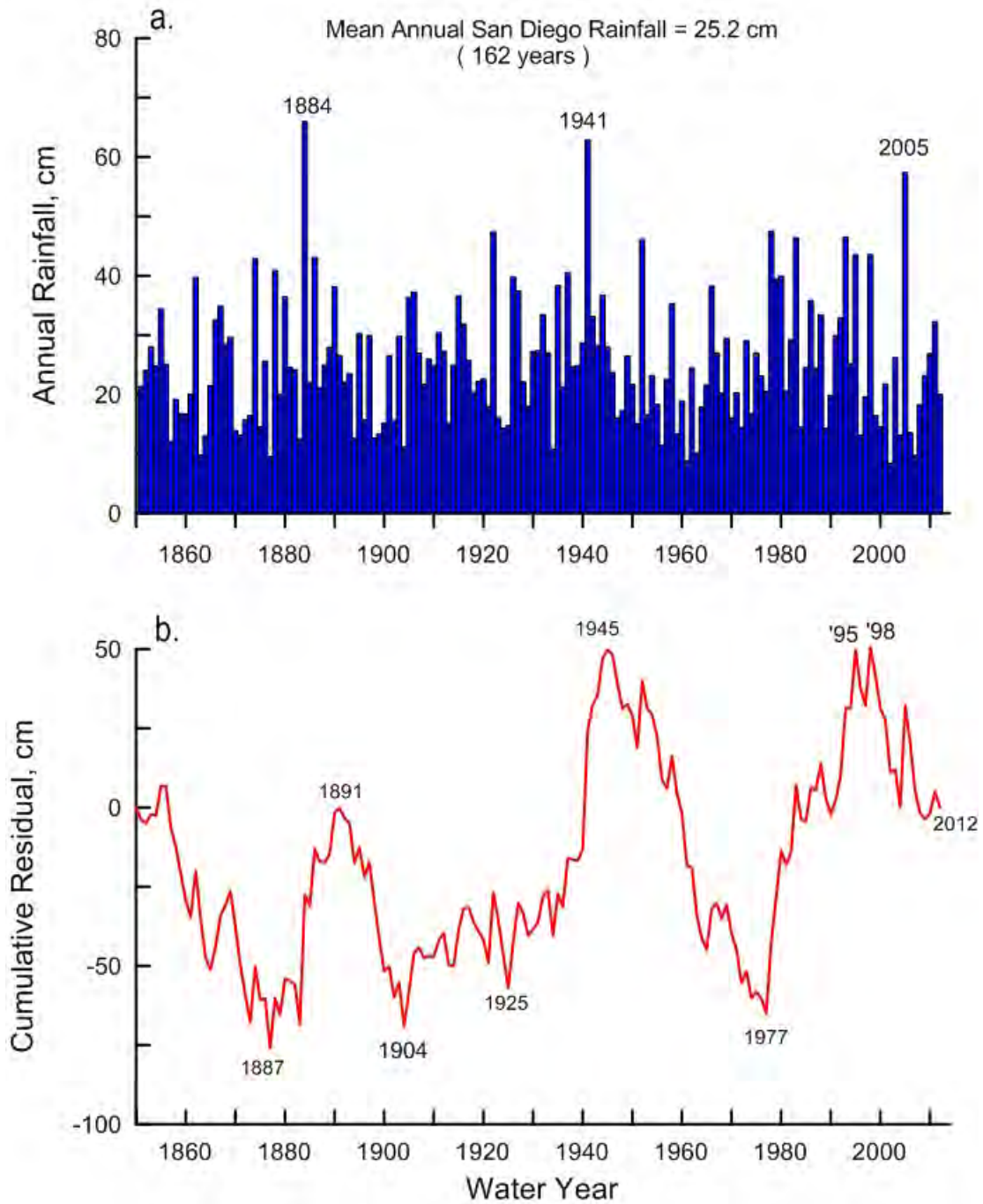


Figure 2. a) Period of record of San Diego rainfall and b) cumulative residual

maximum ranges in rainfall are higher in the wet period, while the averages of the 6 major rainfall events in 21 year periods before and after the climate change (1977/78) are about 8 to 9 inches greater during the wet period. Since 1998, Figure 2b indicates that San Diego climate appears to have regressed into a developing multi-decadal dry period. These sharp distinctions in the statistics of dry vs wet climate periods lead to posing the model problem of discharge dilution in terms of dry and wet extreme case scenarios in order to bracket the envelope of potential variability.

Altogether there are seven primary variables that enter into a solution for resolving the dispersion and dilution of shoreline discharges such as those found along Scripps and La Jolla Shores Beach and the rocky shores of the Devil's Slide area. The statistics of these seven variables all change between dry and wet climate periods. These seven variables may be organized into ***boundary conditions and forcing functions***. The boundary conditions include: ocean salinity, ocean temperature, ocean water levels and discharge flow rates. There is an additional boundary condition associated with offshore bathymetry beyond closure depth (typically greater than 12-15 m) that we will treat as constant. These boundary condition variables are developed in Section 3.1. The forcing function variables include: waves, currents, and winds and are developed in Section 3.2.

Overlapping 32 year long records containing 11,688 consecutive days between 1980 and 2012 are reconstructed in Sections 3.1 and 3.2 for each of the seven controlling variables. We search this 20.5 year period for the historical combination of these variables that give an historic extreme day in the sense of benign ocean conditions that minimize mixing and dilution rates, and a high energy day giving mixing and dilution rates typical of winter storm conditions with rainfall. We then overlay the peak discharge rates of seawater and storm water on those environmental conditions, respectively. The criteria for an extreme dry weather day was based on the simultaneous occurrence of the environmental variables having the highest combination of absolute salinity and temperature during the periods of lowest mixing and advection in the local ocean environment. These conditions coincide with the simultaneous occurrence of the lowest 5% wave, wind, currents, and ocean water levels averaged over a 24 hour period. The extreme wet weather scenarios were found by a statistical search of these records for the simultaneous occurrence of the highest 5% wave, wind, currents, and ocean water levels averaged over a 24 hour period. This procedure produced the model scenarios defined in Section 3.3. We also set up the model in Section 3.3 to solve for the minimum dilution in the surf zone for all 7523 combinations of the 7 controlling variables in order to establish the statistical properties the ***zone of initial dilution (ZID)***.

The technical approach used to evaluate these scenarios for historical extremes and average case conditions involved the use of the SEDXPORT hydrodynamic transport models. The pedigree and physics of this modeling system is described briefly in Section 2, with additional details provided in Appendices A & B. The dilution fields simulated by this model are presented in Section 4, giving results for the wet weather extreme in Section 4.1, and the long term minimum dilution in the ZID in Section 4.2. Dilution fields for an offshore control point in ASBS 29 are also given in Section 4.2.

2.0 MODEL DESCRIPTION AND CAPABILITIES

This study utilizes a coupled set of numerical tidal and wave transport models to evaluate dilution and dispersion of the discharges from the three storm drain outfalls discharging into ASBS 29 (Figure 1). The numerical model used to simulate tidal currents in the nearshore and shelf region offshore of La Jolla Shores is the finite element model **TIDE_FEM**. Wave-driven currents are computed from the shoaling wave field by a separate model, **OCEANRDS**. The dispersion and transport of concentrated seawater and storm water discharge by the wave and tidal currents is calculated by the finite element model known as **SEDXPORT**.

The finite element research model, **TIDE_FEM**, (Jenkins and Wasyl, 1990; Inman and Jenkins, 1996) was employed to evaluate the tidal currents within La Jolla Bay and in particular, the ventilation of the ASBS 29. **TIDE_FEM** was built from some well-studied and proven computational methods and numerical architecture that have done well in predicting shallow water tidal propagation in Massachusetts Bay (Connor and Wang, 1974) and along the coast of Rhode Island, (Wang, 1975), and have been reviewed in basic text books (Weiyan, 1992) and symposia on the subject, e.g., Gallagher (1981). The governing equations and a copy of the core portion of the **TIDE_FEM** FORTRAN code are found in Appendix A. **TIDE_FEM** employs a variant of the vertically integrated equations for shallow water tidal propagation after Connor and Wang (1975). These are based upon the Boussinesq approximations with Chezy friction and Manning's roughness. The finite element discretization is based upon the commonly used **Galerkin weighted residual method** to specify integral functionals that are minimized in each finite element domain using a variational scheme, see Gallagher (1981). Time integration is based upon the simple **trapezoidal rule** (Gallagher, 1981).

The computational architecture of **TIDE_FEM** is adapted from Wang (1975), whereby a transformation from a **global** coordinate system to a **natural** coordinate system based on the unit triangle is used to reduce the weighted residuals to a set of order-one ordinary differential equations with constant coefficients. These coefficients (**influence coefficients**) are posed in terms of a **shape function** derived from the natural coordinates of each nodal point in the computational grid. The resulting systems of equations are assembled and coded as banded matrices and subsequently solved by **Cholesky's method**, see Oden and Oliveira (1973) and Boas (1966). The hydrodynamic forcing used by **TIDE_FEM** is based upon inputs of the tidal constituents derived from Fourier decomposition of tide gage records. Tidal constituents are input into the module **TID_DAYS**, which resides in the hydrodynamic forcing function cluster (see Appendix B for a listing of **TID_DAYS** code). **TID_DAYS** computes the distribution of sea surface elevation variations in La Jolla Bay based on the tidal constituents derived from the Scripps Pier tide gage station (NOAA #941-0230). Forcing for **TIDE_FEM** is applied by the distribution in sea surface elevation across the deep water boundary of the computational domain.

Wave driven currents were calculated from wave measurements by Scripps SAS station at Torrey Pines (Pawka, 1982) and by the CDIP arrays and/or buoys at Scripps Pier, La Jolla Bay, Huntington Beach, San Clemente, and Oceanside, CA, see CDIP (2005). These measurements were back refracted out to deep water to correct for island sheltering effects between the monitoring sites and Scripps Beach. The waves were then forward refracted onshore to give the variation in wave heights, wave lengths and directions throughout the nearshore around Scripps Beach. The numerical refraction-diffraction code used for both the back refraction from these wave monitoring sites out to deep water, and the forward refraction to the La Jolla Shores site is **OCEANRDS** and may be found in Appendix C. This code calculates the simultaneous refraction and diffraction patterns of the swell and wind wave components propagating over bathymetry replicated by the **OCEANBAT** code found in Appendix D. **OCEANBAT** generates the associated depth fields for the computational grid networks of both **TID_FEM** and **OCEANRDS** using packed bathymetry data files derived from the National Ocean Survey (NOS) depth soundings. The structured depth files written by **OCEANBAT** are then throughput to the module **OCEANRDS**, which performs a refraction-diffraction analysis from deep water wave statistics. **OCEANRDS** computes local wave heights, wave numbers, and directions for the swell component of a two-component, rectangular spectrum.

The wave data are throughput to a wave current algorithm in **SEDXPORT** (Appendix E) which calculates the wave-driven longshore currents, $v(r)$. These currents were linearly superimposed on the tidal current. The wave-driven longshore velocity, $v(r)$, is determined from the longshore current theories of Longuet-Higgins (1970). Once the tidal and wave driven currents are resolved by **TIDE_FEM** and **OCEANRDS**, the dilution and dispersion of storm water runoff and seawater discharge is computed by the stratified transport algorithms in **SEDXPORT**. The **SEDXPORT** code is a time stepped finite element model which solves the advection-diffusion equations over a fully configurable 3-dimensional grid. The vertical dimension is treated as a two-layer ocean, with a surface mixed layer and a bottom layer separated by a pycnocline interface. The code accepts any arbitrary density and velocity contrast between the mixed layer and bottom layer that satisfies the Richardson number stability criteria and composite Froude number condition of hydraulic state.

The combined discharge of seawater and storm water from the 3 La Jolla Shores beach outfalls is represented as sources in the surface mixed layer. The source initializations for these beach discharges are handled by a companion dilution code called **MULTINODE** (Appendix F) that couples the computational nodes of **TIDE_FEM** and **OCEANRDS** with **SEDXPORT**. The codes do not time split advection and diffusion calculations, and will compute additional advective field effects arising from spatial gradients in eddy diffusivity, (the so-called “gradient eddy diffusivity velocities” after Armi, 1979). Eddy mass diffusivities are calculated from momentum diffusivities by means of a series of Peclet number corrections based upon TSS and TDS mass and upon the mixing source. Peclet number corrections for the surface and bottom boundary layers are derived from the work of Stommel (1949) with modifications after Nielsen (1979), Jensen and Carlson (1976), and Jenkins and Wasyl (1990). Peclet number correction for the wind-induced mixed layer diffusivities are calculated from algorithms developed by Martin

and Meiburg (1994), while Peclet number corrections to the interfacial shear at the pycnocline are derived from Lazara and Lasheras (1992a;1992b). The momentum diffusivities to which these Peclet number corrections are applied are due to Thorade (1914), Schmidt (1917), Durst (1924), and Newman (1952) for the wind-induced mixed layer turbulence and to Stommel (1949) and List, et al. (1990) for the current-induced turbulence.

In its most recent version, **SEDXPORT** has been integrated into the Navy's Coastal Water Clarity Model and the Littoral Remote Sensing Simulator (LRSS) (see Hammond, et al., 1995). The **SEDXPORT** code has been validated in mid-to-inner shelf waters (see Hammond, et al., 1995; Schoonmaker, et al., 1994). Validation of the **SEDXPORT** code was shown by three independent methods: 1) direct measurement of suspended particle transport and particle size distributions by means of a laser particle sizer; 2) measurements of water column optical properties; and, 3) comparison of computed stratified plume dispersion patterns with LANDSAT imagery.

Besides being validated in coastal waters of Southern California, the **SEDXPORT** modeling system has been extensively peer reviewed. Although some of the early peer review was confidential and occurred inside the Office of Naval Research and the Naval Research Laboratory, the following is a listing of 6 independent peer review episodes of **SEDXPORT** that were conducted by 8 independent experts and can be found in the public records of the State Water Resources Control Board, the California Coastal Commission and the City of Huntington Beach.

1997 – Reviewing Agency: State Water Resources Control Board

Project: NPDES 316 a/b Permit renewal, Scripps Beach, Carlsbad, CA

Reviewer: Dr. Andrew Lissner, SAIC, La Jolla, CA

1998 – Reviewing Agency: California Coastal Commission

Project: Coastal Development Permit, San Dieguito Lagoon Restoration

Reviewers: Prof. Ashish Mehta, University of Florida, Gainesville; Prof. Paul Komar, Oregon State University, Corvallis; Prof. Peter Goodwin, University of Idaho, Moscow

2000 – Reviewing Agency: California Coastal Commission

Project: Coastal Development Permit, Crystal Cove Development

Reviewers: Prof. Robert Wiegel, University of California, Berkeley; Dr. Ron Noble, Noble Engineers, Irvine, CA

2002 – Reviewing Agency: California Coastal Commission

Project: Coastal Development Permit, Dana Point Headland Reserve

Reviewers: Prof. Robert Wiegel, University of California, Berkeley; Dr. Richard Seymour, University of California, San Diego

2003 – Reviewing Agency: City of Huntington Beach

Project: EIR Certification, Poseidon Desalination Project

Reviewer: Prof. Stanley Grant, University of California, Irvine

2006 – Reviewing Agency: Regional Water Quality Control Board, San Diego Region

Project: UCSD Storm Drain Dilution Study and ASBS 31 Impacts

Reviewer: Mr. John Robertus and Dr. Charles Chen, RWQCB

SEDXPORT has been built in a modular computational architecture with a set of subroutines divided into two major clusters: 1) those which prescribe hydrodynamic forcing functions; and, 2) those which prescribe the mass sources acted upon by the hydrodynamic forcing to produce dispersion and transport. The cluster of modules for hydrodynamic forcing ultimately prescribes the velocities and diffusivities induced by wind, waves, and tidal flow for each depth increment at each node in the grid network. The subroutines **RIVXPORT** and **BOTXPORT** in **SEDXPORT** solve for the mixing and advection of the seawater and buoyant storm water discharge in response to the wave and tidal flow using an rms vorticity-based time splitting scheme. Both **BOTXPORT** and **RIVXPORT** solve the eddy gradient form of the advection diffusion equation for the water column density field:

$$\frac{\partial \rho}{\partial t} = (\bar{u} \cdot \nabla \varepsilon) \cdot \nabla \rho - \varepsilon \nabla^2 \rho + \rho_0 Q_0 \quad (1)$$

where \bar{u} is the vector velocity from a linear combination of the wave and tidal currents, ε is the mass diffusivity, ∇ is the vector gradient operator and ρ is the water mass density in the nearshore dilution field; and ρ_0 is the density of the water discharged by the outfall at a flow rate $\frac{dV_0}{dt}$. The density of the discharge is a function of the bulk density of the suspended solids ρ_s and the density of the discharge fluid ρ_f that transports those solids, or:

$$\rho_0 = \rho_s + (1 - N) \rho_f = \rho_q N + (1 - N) \rho_f \quad (2)$$

where N is the volume concentration of suspended solids equal to the ratio of suspended solids to sample volume; and $\rho_q = 2.65 \text{ g/cm}^3$ is the density of the suspended solid particles taken to be fine-grained quartz.

Both the density of the receiving water ρ and the density of the discharge fluid ρ_f is a function of temperature, T , and salinity, S , according to the equation of state expressed in terms of the specific volume, $\alpha = 1/\rho$ and $\alpha_f = 1/\rho_f$ or:

$$\frac{d\alpha}{\alpha} = \frac{1}{\alpha} \frac{\partial\alpha}{\partial T} dT + \frac{1}{\alpha} \frac{\partial\alpha}{\partial S} dS \quad (3)$$

$$\frac{d\alpha_f}{\alpha_f} = \frac{1}{\alpha_f} \frac{\partial\alpha_f}{\partial T} dT + \frac{1}{\alpha_f} \frac{\partial\alpha_f}{\partial S} dS$$

The factor $1/\alpha \partial\alpha/\partial T$, which multiplies the differential temperature changes, is known as the coefficient of thermal expansion and is typically 2×10^{-4} per $^{\circ}\text{C}$ for seawater; the factor $1/\alpha \partial\alpha/\partial S$ multiplying the differential salinity changes, is the coefficient of saline contraction and is typically 8×10^{-4} per part per thousand (ppt) where $1.0 \text{ ppt} = 1.0 \text{ g/L}$ of total dissolved solids (TDS). For a standard seawater, the specific volume has a value $\alpha = 1/\rho = 0.97264 \text{ cm}^3/\text{g}$. If the percent change in specific volume by equation (3) is less than zero, then the water mass is heavier than standard seawater, and lighter if the percent change is greater than zero.

The dilution ratio is given by the volume concentration of the discharged suspended solids in the receiving water and follows from the sediment continuity equation:

$$\frac{\partial N}{\partial t} = (\bar{u} \bullet \nabla \varepsilon) \bullet \nabla N - \varepsilon \nabla^2 N - W_0 \frac{dN}{dz} \quad (4)$$

where W_0 is the settling velocity of suspended particles. It is necessary to correct dilution ratio calculations for the loss of suspended particles due to deposition, so that loss is not included as a pseudo-dilution. The deposition flux is the net between settling and re-suspension and is found from a sub-set of solutions to (4) at the seabed as originally posed for steady flow by Krone (1962) and expanded to oscillatory flow by Jenkins and Wasyl (1990):

$$\Lambda = \frac{-K_s g N_c \left[W_0 N_c - \varepsilon \left(\frac{\partial N}{\partial z} \right)_{z=0} \right]}{(1 - N_c / N_s)} \quad (5)$$

where $K_s = 4 \times 10^{-14} \text{ sec}$ is the sedimentation coefficient after Fujita (1962); g is the acceleration of gravity; N_c is the volume concentration at the top of the wave boundary layer; and N_s is the volume concentration of the seabed sediments. If N_0 is the volume concentration of suspended solids at the point of discharge (end-of-pipe); and $N(x, y, z)$ is the volume concentration at any

location in the receiving waters, then the dilution factor at that location (corrected for deposition losses) is:

$$D(x, y, z) = \frac{N_0}{N(x, y, z)} - \frac{\Lambda}{W_0} \quad (6)$$

Hence, net deposition ($\Lambda > 0$) in the ASBS acts to increase the retention of discharged particulate, and consequently reduces the apparent dilution factor.

In (1) and (4) the term $\nabla \varepsilon$ acts much like an additional advective field in the direction of high to low eddy diffusivity. This additional "gradient eddy diffusivity velocity" is the result of local variations in current shear and wave boundary layer thickness. Both are bathymetrically controlled and the latter is associated with the refraction/diffraction pattern and is strongest in the wave shoaling region nearshore.

The settling velocity W_0 in (4) and (5) is particle size dependent. The **SEDXPOR**T code is configured to accept up to nine particle size bins which for fine-grained particulate are assigned according to the particle size distribution after Jerlov (1976):

$$N(d) = \hat{N} \left(\frac{d}{\hat{d}} \right)^\gamma \quad (7)$$

where

$$N_0 = \sum_d N(d) \quad (8)$$

Here \hat{d} is the reference grain size, typically taken as 1.0 microns; and γ is the slope of the particle size distribution on log-log scale where $\gamma \cong 2.5$ for the global average, and \hat{N} is the volume concentration of the reference grain size that is adjusted such that (8) satisfies the measure value N_0 at end-of-pipe.

Solutions for the density and concentration fields calculated by the **SEDXPOR**T codes from equations (1)-(4), (7) & (8) are through put to the dilution codes of **MULTINODE** to resolve dilution factors according to (5) & (6). These codes solve for the dilution factor (mixing ratio) for each cell in the finite element mesh of the nearshore computational domain based on a mass balance between imported exported and resident mass of that cell (see Appendix F). The diffusivity, ε , in (1) controls the strength of mixing and dilution of the seawater and storm water constituents in each cell and varies with position in the water column relative to the pycnocline interface. Vertical mixing includes two mixing mechanisms at depths above and below the pycnocline: 1) fossil turbulence from the bottom boundary layer, and 2) wind mixing in the surface mixed layer. The pycnocline depth is treated as a zone of hindered mixing and varies in

response to the wind speed and duration. Below the pycnocline, only turbulence from the bottom wave/current boundary layer contributes to the local diffusivity. Nearshore, breaking wave activity also contributes to mixing. The surf zone (zone of initial dilution) is treated as a line source of turbulent kinetic energy by the subroutine **SURXPORT** (Appendix E). This subroutine calculates seaward mixing from fossil surf zone turbulence, and seaward advection from rip currents embedded in the line source. Both the eddy diffusivity of the line source and the strength and position of the embedded rip currents are computed from the shoaling wave parameters evaluated at the breakpoint, as throughout of **OCEANRDS**.

3.0 MODEL INITIALIZATION

Uninterrupted, long-term monitoring of ocean properties has been conducted at the nearby Scripps Pier. The Scripps Pier has been the site of both a NOAA tide gage station (NOAA #941-0230) as well as a monitoring station of the Coastal Data Information Program. It has also been the site where many new monitoring techniques have been developed and validated. We will take advantage of these long term observations to develop the data bases for initializing the boundary conditions and forcing functions used in the model. Statistical searches of these data bases will be performed to extract the dry and wet weather extreme case scenarios.

These dry and wet weather model scenarios are proxies for the extremes of the long term climate variability of the region, and serve to bracket the envelope of potential discharge effects on ASBS 29. Climate variability begins with seasonal variations in Earth's exposure to the sun, producing inter-annual variations in atmospheric pressure fields which in turn cause the Earth's inter-annual seasons. Upon occasion, the typical seasonal weather cycles are abruptly and severely modified on a global scale. These intense global modifications are signaled by anomalies in the pressure fields between the tropical eastern Pacific Ocean and Australia/Malaysia known as the *El Niño Southern Oscillation*, commonly referred to as *ENSO*. The intensity of the oscillation is often measured in terms of the *Southern Oscillation Index (SOI)*, defined as the monthly mean sea level pressure anomaly in mb normalized by the standard deviation of the monthly mean pressures for the period 1951-1980 at Tahiti minus that at Darwin, Australia. (Because the SOI is a ratio of terms that all have units of atmospheric pressure, it is a non-dimensional number).

The Southern Oscillation is in turn, modulated over multi-decadal periods by the *Pacific Decadal Oscillation*, which results in alternating decades of strong and weak El Niño. The long-term variability of the Pacific Decadal Oscillation (PDO) is shown in Figure 3 and the cumulative residual of the Southern Oscillation Index, between 1882 and 1996, is plotted in Figure 4. Southern Oscillation effects give rise to enhancements and protractions of the inter-annual seasonal cycles, and their two extremes are referred to as El Niño (SOI negative) and La Niña (SOI positive). Inspection of Figures 3 and 4 reveals a number of large positive oscillations in the SOI between 1944 and 1978 corresponding to La Niña dominated climate; and a series of very large negative oscillations occurring between 1978 and 1998 which correspond with El Niño dominated climate. Along the southern California coast, a period of mild-stable weather occurred during the 30 years between the mid-1940's and mid-1970's when La Niña dominated pressure systems prevailed. The average SOI for this period was +0.1, with strong La Niña events in 1950, (SOI = +1.4); 1955/56, (+1.2); 1970/71, (+1.0); 1973/74, (+1.0); and 1975/76 (+1.4). Winters were moderate with low rainfall (see Figure 2), and winds were predominantly from the west-northwest. The principal wave energy was from Aleutian lows having storm tracks which usually did not reach southern California. Summers were mild and dry with the largest summer swells coming from very distant southern hemisphere storms.

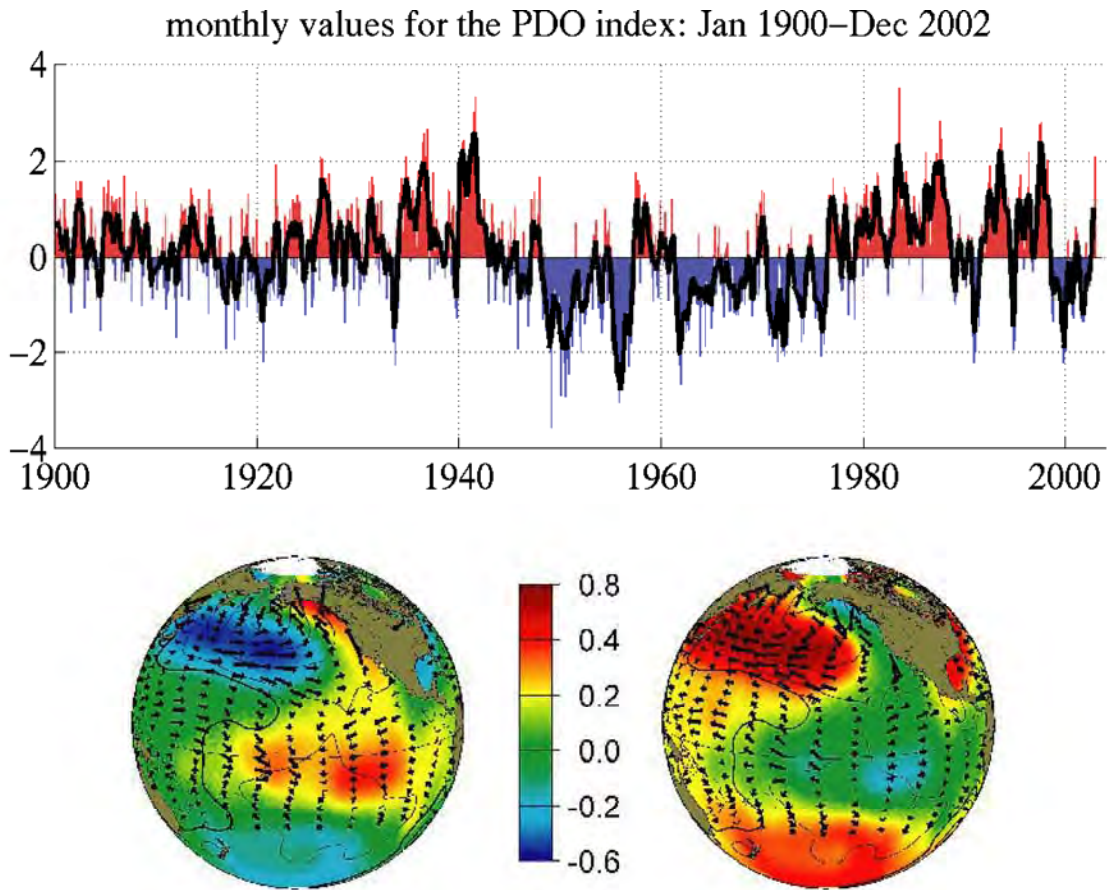


Figure 3. Typical wintertime Sea Surface Temperature (colors), Sea Level Pressure (contours) and surface wind stress (arrows) anomaly patterns during warm and cool phases of PDO. Red colors indicate warm, blue indicates cool.

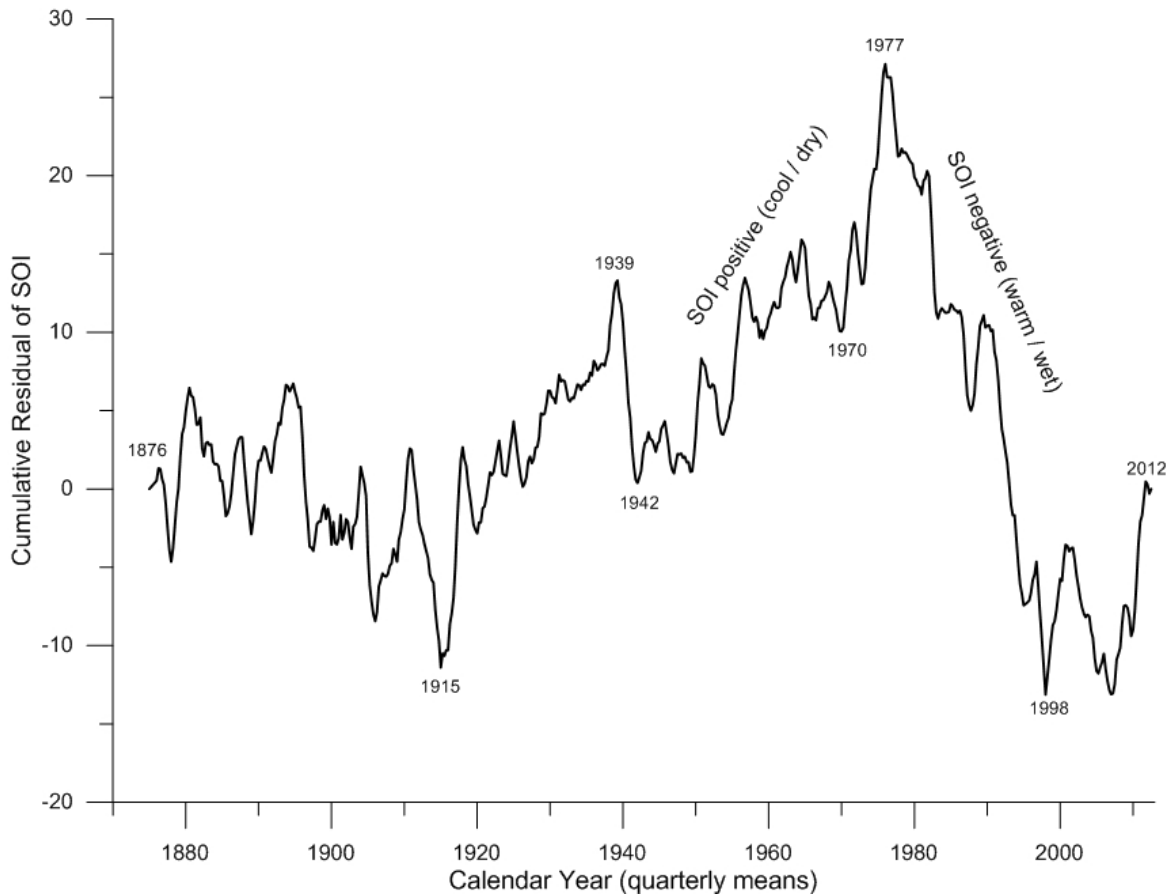


Figure 4. Cumulative residual of quarterly values of Southern Oscillation Index (SOI) [data from Australian Commonwealth Bureau of Meteorology].

Beginning in 1978, the southern California climate began transitioning into a warmer wetter period characterized by a succession of powerful El Niños, particularly those in, 1978, 1980, 1983, 1993, 1995 and 1998, [Inman & Jenkins, 1997]. The average SOI for this period was -0.5, with the 1978/79 El Niño averaging -1.2, the 1982/83 El Niño averaging a record -1.7 and the 1993/94 El Niño recording a mean of -1.0. Heavy rainfall accompanied each of these El Niño events (see Figure 2) causing flood run off to exceed many times the long term mean for all the major rivers and tributaries throughout Southern California (Inman and Jenkins, 1999). The wave climate in southern California also changed, beginning with the El Niño years of 1978/79 and extending until 1998. The prevailing northwesterly winter waves were replaced by high energy waves approaching from the west or southwest, and the previous southern hemisphere swell waves of summer have been replaced by shorter period tropical storm waves during late summer months from the more immediate waters off Central America. Other strong El Niño events of the past have also been accompanied by extreme wave events, although none of these have been as sustained as the succession of El Niños from 1978 to 1995. The 1939/42 El Niño had an average SOI of -1.3 and was associated with a series of destructive wave events in the Southern California Bight, the most intense being the 24/25 September 1939 storm which seriously

damaged the breakwater system at Long Beach, CA. The El Niño of 1904/05 had a mean SOI of -1.4 and was attended by a series of damaging west swells in March 1904 and again in March 1905 [Horrer, 1950; Marine Advisors, 1961].

A similar succession of El Niño floods also preceded the cool/dry period of 1944-77, causing major episodes of sediment yield in 1927, 1937, 1938, 1941 and 1943.

From Figures 2 - 4 it is apparent that an inter-decadal pattern of rainfall and SOI has persisted for at least the last century and a half, characterized by alternating cool/dry La Niña dominated periods with little or no sediment yield, followed by warm/wet El Niño dominated periods when heavy rainfall produces most of the total sediment runoff. This kind of inter-decadal climate variability is observed throughout the west coast of the Americas and is now known as the ***Pacific Interdecadal Oscillation (PDO)***, see Mantua et al (1997) and Zhang et al (1997). In this study we attempt to capture the potential range of PDO variability in the discharge problem by constructing the longest possible time series of the seven controlling model inputs from existing data bases, and then invoke statistical searches of those time series for the wet and dry extremes.

3.1 Boundary Conditions

A) Bathymetry: Bathymetry provides a controlling influence on all of the coastal processes at work in both the nearfield and farfield of La Jolla Shores. The bathymetry consists of two parts: 1) a stationary component in the offshore where depths are roughly invariant over time, and 2) a non-stationary component in the nearshore where depth variations do occur over time. The stationary bathymetry generally prevails at depths that exceed ***closure depth*** which is the depth at which net on/offshore transport vanishes. Closure depth is typically -15 m MSL in the Oceanside Littoral Cell, [Inman et al. 1993]. The stationary bathymetry was derived from the National Ocean Survey (NOS) digital database as plotted in Figure 5 seaward of the 15m depth contour. Gridding is by latitude and longitude with a 3 x 3 arc second grid cell resolution yielding a computational domain of 15.4 km x 18.5 km. Grid cell dimensions along the x-axis (longitude) are 77.2 meters and 92.6 meters along the y-axis (latitude). This small amount of grid distortion is converted internally to Cartesian coordinates, using a Mercator projection of the latitude-longitude grid centered on Scripps Pier. The convention for Cartesian coordinates uses x-grid spacings for longitude and y-grid spacings for latitude.

For the non-stationary bathymetry data inshore of closure depth (less than -15 m MSL) we use the equilibrium beach algorithms from Jenkins and Inman (2006). Depth contours generated from these algorithms vary with wave height, period and grain size and are plotted in Figure 5 landward of the 15m depth contour for the wave parameters of the wet weather extreme scenario (see Section 3.3).

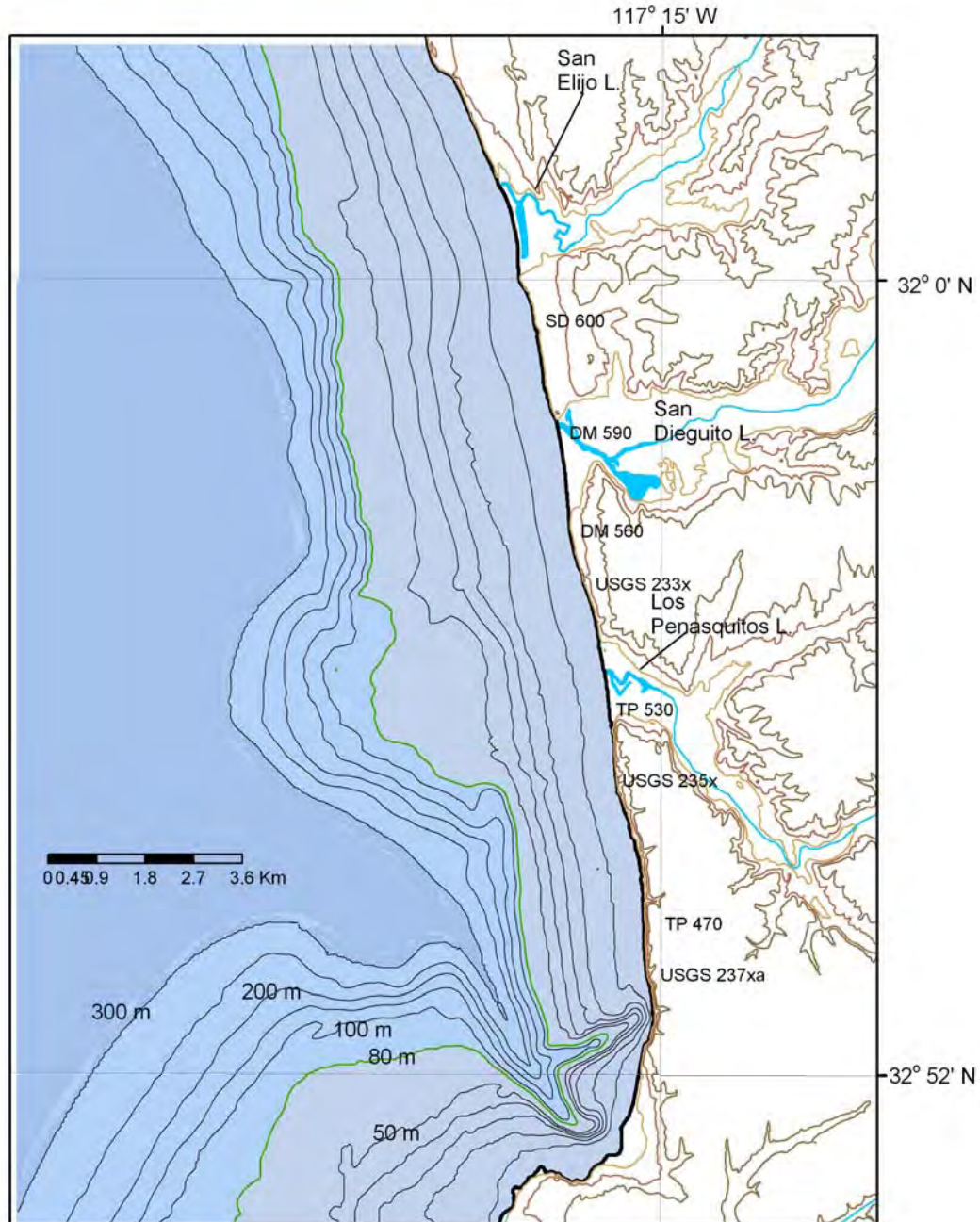


Figure 5. Composite bathymetry from NOS data base and equilibrium profiles after Jenkins and Inman (2006) for wave conditions of wet weather scenario. Depth contours shown in meters mean sea level.

B) Ocean Salinity: Since the three La Jolla Shores outfalls (SDL-157, SDL-062 and SDL-186) discharge predominantly fresh water into a surfzone, the ocean salinity variation used in equation (3) to initialize SEDXPORT is of fundamental importance to the mixing of storm water in the receiving waters. Figure 6a shows the variation in daily mean sea surface salinity in the coastal waters off La Jolla Shores while Figure 7 shows daily mean seafloor salinity, both plotted from 32 years of monitoring data derived from the archival data bases of Scripps Institution of Oceanography (Scripps Pier Shore Station, SIO, 2012) and the Coastal Data Information Program (CDIP, 2012), supplemented by site monitoring data from MBC *Applied Environmental Sciences* (MBC), MBC (2012). The period of these unbroken archival sources extends from 1980 until March 2012. In the period of record from 1980 to 2012, the ocean salinity varies naturally by 10% between summer maximums and winter minimums, with a long term average value of 33.52 parts per thousand (ppt) on the surface and 33.49 ppt on the seafloor. Average sea surface salinity is slightly higher due to evaporation. Maximum salinity was 34.3 ppt on the sea surface and seafloor during the 1998 summer El Nino when southerly winds transported high salinity water from southern Baja up into the Southern California Bight. Minimum salinity was 31.06 ppt on the sea surface and seafloor 30.4 ppt on the seafloor during the 1992 floods. The variation between maximum and minimum salinity is about 3.2 ppt to 3.9 ppt, which is about 10 % of the depth-averaged value of 33.5 ppt. The ocean salinity exceeded the 33.5 ppt average value during 3,736 days during the period of record, and was below average during 2,259 days. Therefore above average salinities are more common than below average salinities. Average salinities were observed a total of 5,022 days of the period of record, or about 46 % of the time. (These data are also confirmed by long term salinity monitoring at Scripps Pier NOAA Station #941-0230, and by 55 CalCOFI cruises in the Southern California Bight between 1984 and 1997, see SIO, 2005; Roemmich, 1989, and Bograd, et al, 2001).

C) Ocean Temperature: The ocean temperature effects the buoyancy of the storm water discharge through the absolute temperature of the discharge. This buoyancy effect is calculated by the specific volume change of the discharge relative to the ambient ocean water. The buoyancy of the plume exerts a strong effect on the mixing and rate of assimilation of the sea salts and backwash constituents by the receiving waters.

We use the average of temperature records from the archival data bases of Scripps Institution of Oceanography (Scripps Pier Shore Station, SIO, 2012) and the Coastal Data Information Program (CDIP, 2012), supplemented by site monitoring data from MBC (2012). An 11,688 point record of daily mean sea surface temperatures are plotted in Figure 6b, while daily mean seafloor temperatures are plotted in Figure 7b. These temperature data were throughput to dilution model as detailed in Section 2. A pronounced seasonal variation in these temperatures is quite evident with the maximum recorded daily mean temperature reaching 25.4 °C on the sea surface and 24.4 °C on the seafloor during the summer of the 1993 El Niño; and the minimum falling to 9.9 °C on the sea surface and 11.0 °C on the seafloor during the winter of the 1999-2000 La Niña. The mean temperature was found to be 17.7 °C on the sea surface and 17.2 °C on the seafloor. On a percentage basis, the natural variability of the temperature of coastal waters of La Jolla Bay is significantly greater than that of salinity, where temperature variability is on the order of $\Delta T = 86\%$ vs salinity variability of $\Delta S = 10\%$.

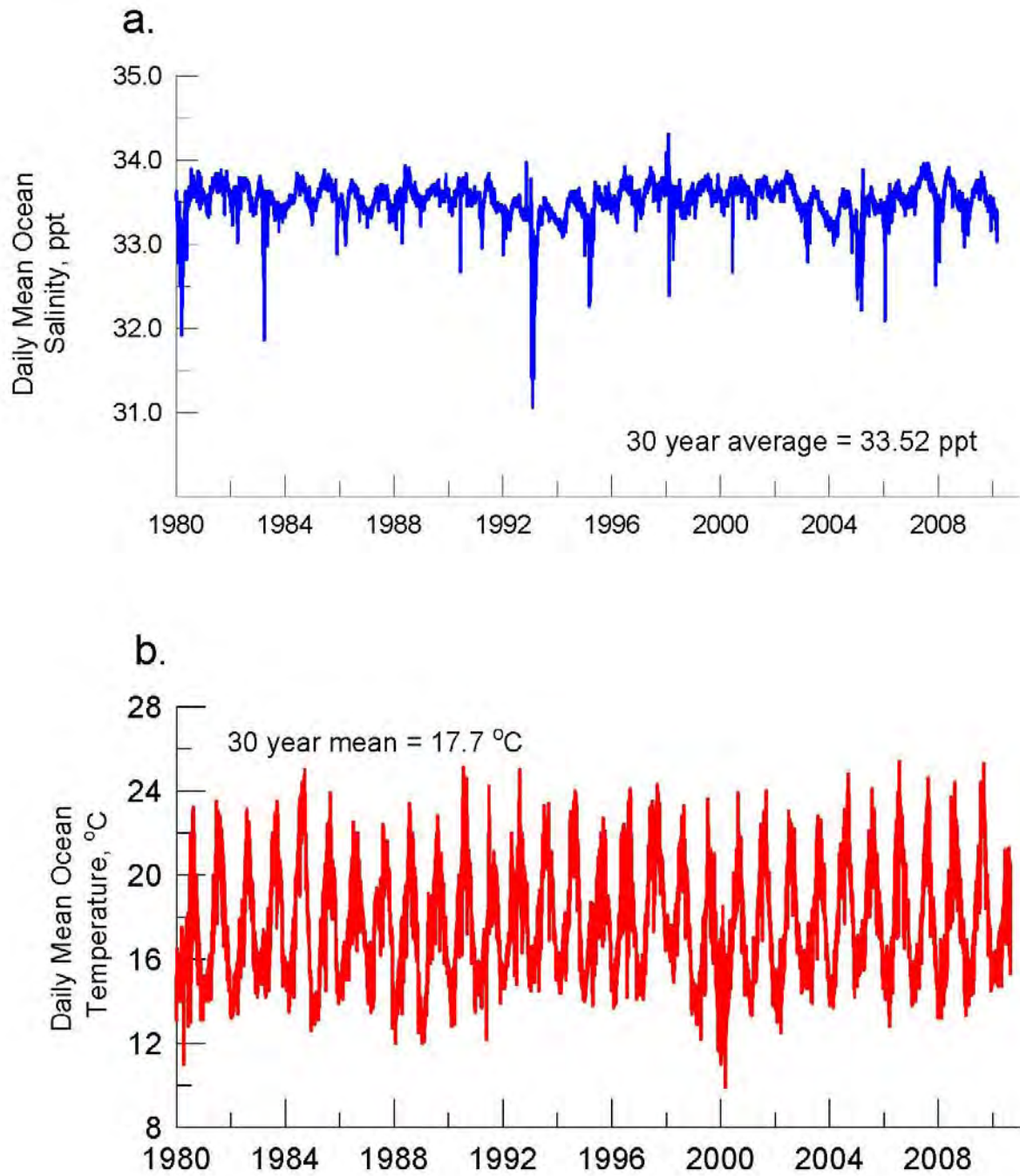


Figure 6. Daily mean ocean surface salinity (a) and daily mean ocean surface temperature at La Jolla, CA; from CDIP (2012), SIO, (2010), and MBC (2012).

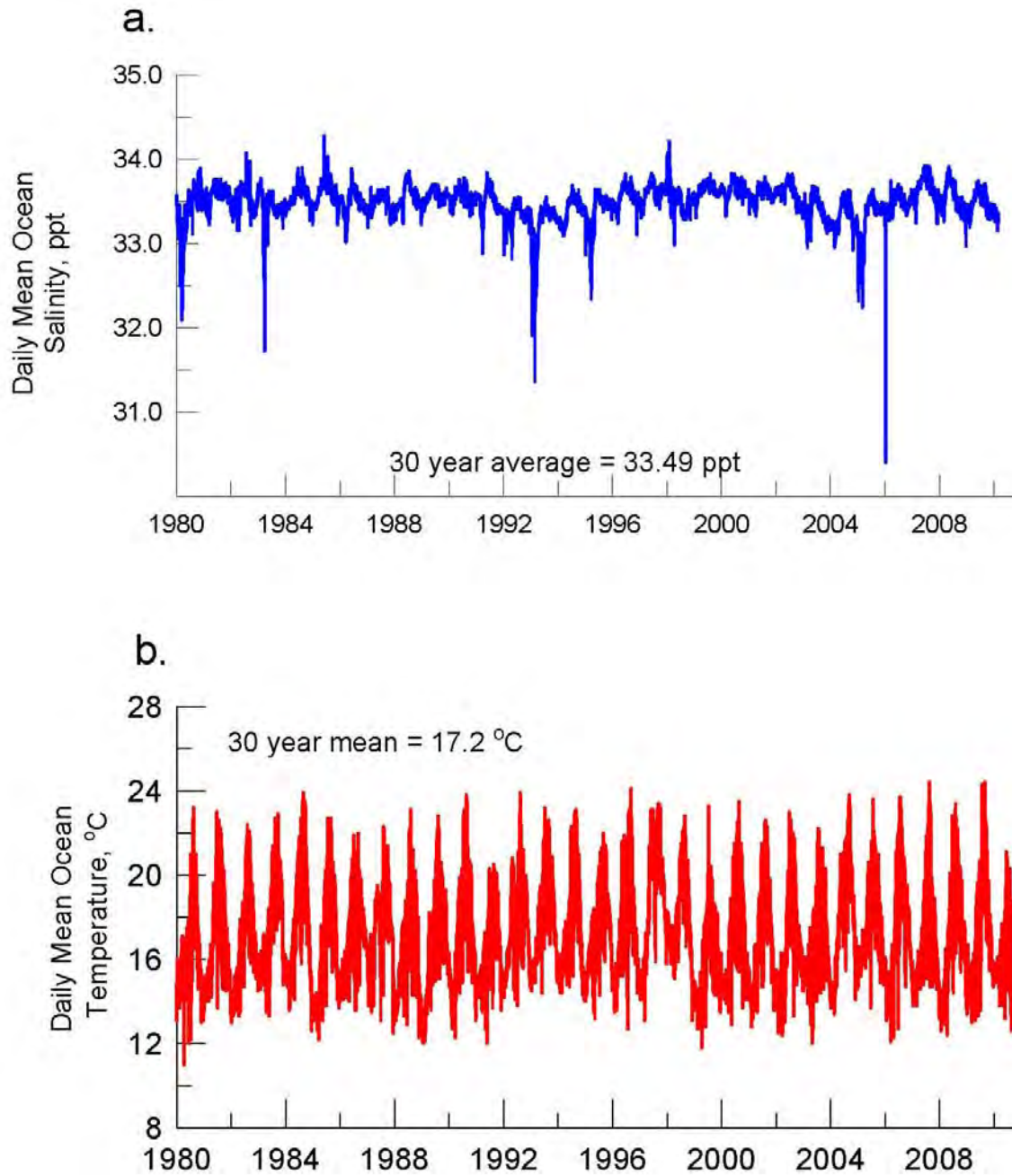


Figure 7. Daily mean ocean surface salinity (a) and daily mean ocean bottom temperature at La Jolla, CA; from CDIP (2012), SIO, (2010), and MBC (2012).

D) Ocean Water Levels: In the shallow nearshore environment off La Jolla Shores Beach, the dilution volume is limited by the time variation in ocean water level. Ocean water level varies in response to both tidal and climate oscillations such as ENSO. The ocean water level is monitored by the tide gage station located on Scripps Pier, La Jolla, CA. This tide gage (NOAA #941-0230) was last leveled using the 1983-2001 tidal epoch. Elevations of tidal datums referred to Mean Lower Low Water (MLLW), in **METERS** are as follows:

HIGHEST OBSERVED WATER LEVEL (11/13/1997) = 2.332 m

MEAN HIGHER HIGH WATER (MHHW) = 1.624 m

MEAN HIGH WATER (MHW) = 1.402 m

MEAN TIDE LEVEL (MTL) = 0.839 m

MEAN SEA LEVEL (MSL) = 0.833 m

MEAN LOW WATER (MLW) = 0.276 m

NORTH AMERICAN VERTICAL DATUM-1988 (NAVD) = 0.058 m

NGVD29 = 0.700 m

MEAN LOWER LOW WATER (MLLW) = 0.000 m

LOWEST OBSERVED WATER LEVEL (12/17/1933) = -0.874 m

Water levels measured by the Scripps Pier Tide Gage (#941-0230) have been archived by NOAA (2005) for the period of record, 1980 to 2012. Reconstruction of a water level time series was performed on the entire set of 1980-2012 NOAA measurements. The resulting time series of daily maximum and minimum ocean water levels is plotted in Panel-b of Figure 8. The positive sea level anomalies are a persistent and sustained occurrence in the observations of ocean water levels during this period of record and are another signature of El Niño. The warming of the coastal ocean during El Niño events causes thermal expansion of seawater by the second term in the equation of state, equation (3). A very significant number of diurnal tide cycles during the 32 period of record (466) have produced water level elevations well in excess of the extreme higher-high water levels (EHHW) of the astronomic tides, (where EHHW = +4.28 ft. NGVD for a perigean spring tide occurring once every 4.5 years). In the period of record shown by the blue trace in Figure 8b, the maximum ocean water level was +5.35 ft. NGVD occurring during the 1997 El Niño, 1.31 ft. higher than the astronomic tides of the tide tables. These high water levels promote initial dilution of any beach discharge because they provide additional water depth and dilution volume where these discharges enter the sea. On the other hand, the minimum ocean water level was -4.66 ft. NGVD, occurring during the 1988 winter. These low water levels shown in the green trace of Figure 8b reduce initial dilution of beach discharge.

E) Discharge Flow Rates and Constituent Mass Loads: Wet weather monitoring was performed during three storm events during the 2011-2012 wet weather monitoring season, (AMEC, 2012). Table 2 presents the dates, sites monitored, and total rainfall for each of the three significant monitored events. Appendix G gives tabular listings of the AMEC monitoring data.

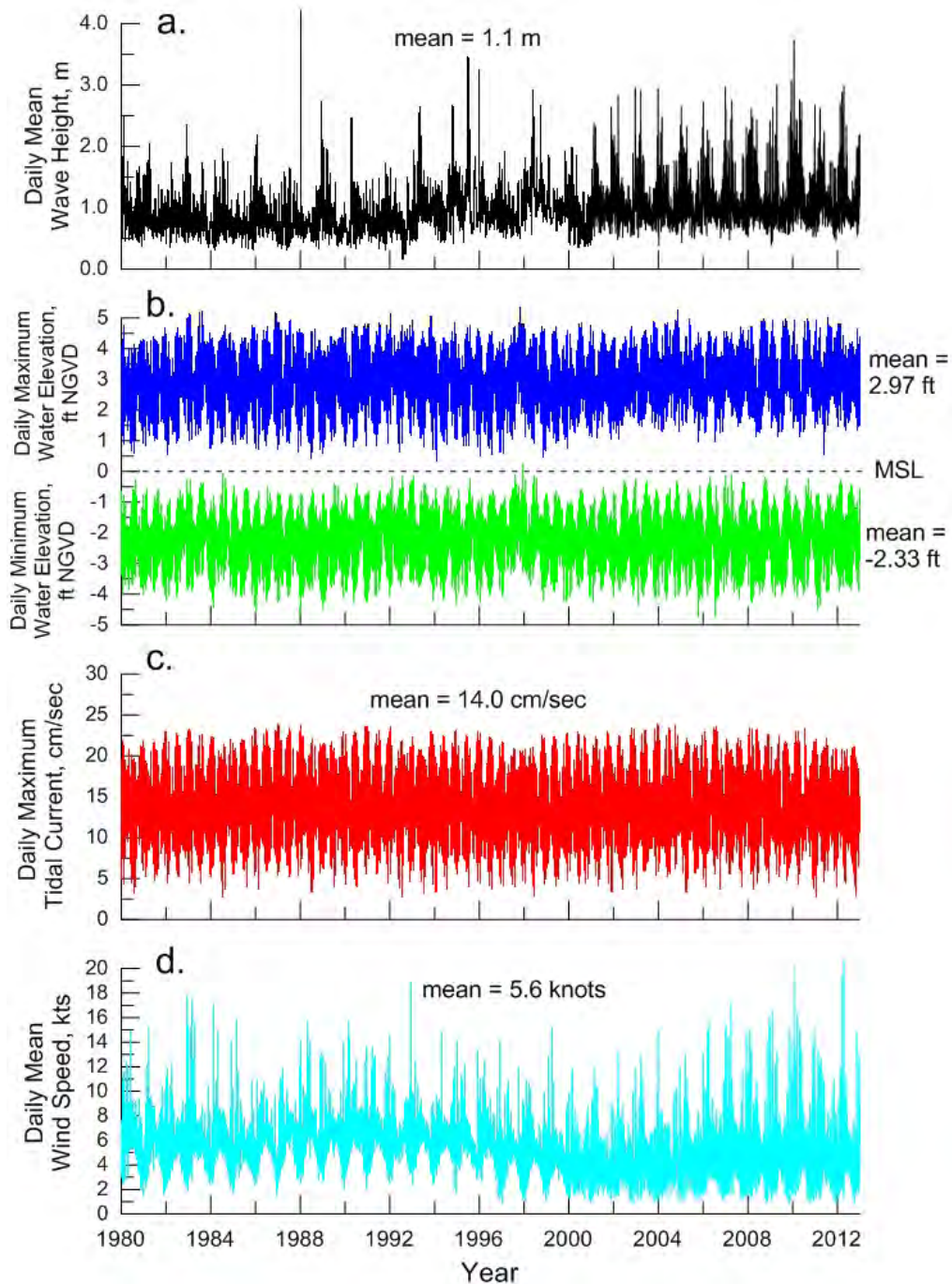


Figure 8. Controlling ocean forcing functions for La Jolla Bay: a) daily mean significant wave height, b) daily high and low water levels, c) daily maximum tidal current, d) daily mean wind speed. (data from CDIP, 2012; SIO, 2012; and NCEP, 2012).

Table 2.
Monitoring Events Summary

Event	Date	Total Rainfall (inches)	Sites Monitored
Event 1	11/20 to 21/2012	0.89	SDL-062-OD/RW SDL-157-OD/RW
Event 2	2/7/2012	0.23	SDL-062-OD/RW SDL-157-OD/RW SDL-186-OD/RW
Event 3	3/17 to 18/2012	0.54	SDL-062-OD/RW/SED SDL-157-OD/RW/SED SDL-186-OD/RW/SED

Notes:
 OD - Outfall Discharge
 RW - Receiving Water
 SED - Sediment

Per the Special Protections Document Core Discharge Monitoring program, storm water outfalls 18 inches in diameter or greater must be monitored. Of the four outfalls within the La Jolla Shores Coastal Watershed that meet these criteria, the two largest outfalls (SDL-062 and SDL-157) were monitored during three events listed in Table 2. During these wet weather events, flow-weighted composites were collected, in addition to time-weighted composites composed of two to four grab samples that were collected during two storm events at a third outfall monitoring location (SDL-186). (The remaining two outfalls (SDL-063 and SDL-063B) were not sampled). The concentrations in mass per unit volume $\rho_{0_i}(t)$ that were measured at time t for constituent i were applied to the measured flow rates $Q_j(t)$ of outfall j to obtain the flux $J_{ji}(t)$ of that constituent from outfall j , or $J_{ji}(t) = \rho_{0_i}(t)Q_j(t)$. The cumulative mass loading $M_{ji}(\Delta t)$ of constituent i from outfall j over time period Δt is simply the time integral of the fluxes $M_{ji}(\Delta t) = \int_{\Delta t} J_{ji}(t)dt$. These data are used to define the variation the wet conditions that the La

Jolla Shores storm drain discharges exert on the receiving water and ASBS 29. These data are also used to identify the maximum discharge rates and concentration of discharge constituents, with primary emphasis here on total suspended solids (TSS) and the cumulative mass loading of total suspended solids, $M_{ji}(\Delta t)$. The dilution modeling of these point sources presented herein does not consider combined effects from non-point source runoff, such as from Peñasquitos Canyon.

Wet Weather Event 1: Rainfall began at 5:01 pm on November 20, 2011 and ended at 12:21 am on November 21, 2011, totaling 0.89 inches. Flow began shortly after the onset of rainfall at both monitored locations, SDL-062 and SDL-157. Figure 9 presents the hydrographs for storm drains SDL-062 (black) and SDL- 157 (blue) as compared against rainfall (red) during Wet Weather Event-1. Peak flow rates were for storm drain SDL-157 were 3.5 cfs with a storm total flow volume of 53,425 cubic feet. Peak flow rates were on the order of 11 cubic feet per second (cfs) for storm drain SDL-062 while the storm total flow volume was 120,569 cubic feet. Figure 10 gives the flux of total suspended solids in a 15 minute interval (red) and cumulative mass loading of total suspended solids (black) for storm drain SDL-157 during Wet Weather Event-1. Peak TSS fluxes for SDL-157 were 28 kg in a 15 minute interval, or 1.9 kg/min; and the cumulative TSS mass loading from this storm drain for the entire event was 515 kg. Figure 11 gives the corresponding TSS fluxes and cumulative mass loading from storm drain SDL-062 for Wet Weather Event-1. Peak TSS fluxes for SDL-062 were significantly higher, on the order of 70 kg in a 15 minute interval, or 4.7 kg/min; and the cumulative TSS mass loading from SDL-062 gave a storm total of 888 kg. This is the highest TSS total load measured during any event or for any storm drain during the entire 2011-2012 monitoring period, as a consequence of Wet Weather Event-1 having the highest rainfall totals and representing a first-flush type of event.

Wet Weather Event 2: Rainfall began at 3:06 pm on February 7, 2012 and ended at 5:46 pm on February 7, 2012, totaling 0.23 inches. Flow began shortly after the onset of rainfall at the three monitored locations, SDL-062, SDL-157, and SDL-186. Figure 12 presents the hydrographs for storm drains SDL-062 (black) and SDL- 157 (blue) as compared against rainfall (red) during Wet Weather Event-2. Peak flow rates were for storm drain SDL-157 were 3.5 cfs with a storm total flow volume of 25,248 cubic feet. Peak flow rates were on the order of 7 cubic feet per second (cfs) for storm drain SDL-062 while the storm total flow volume was 27,052 cubic feet. Figure 13 gives the flux of total suspended solids in a 15 minute interval (red) and cumulative mass loading of total suspended solids (black) for storm drain SDL-157 during Wet Weather Event-2. Peak TSS fluxes for SDL-157 were 20 kg in a 15 minute interval, or 1.3 kg/min; and the cumulative TSS mass loading from this storm drain for the entire event was 164 kg. Figure 14 gives the corresponding TSS fluxes and cumulative mass loading from storm drain SDL-062 for Wet Weather Event-1. Peak TSS fluxes for SDL-062 were slightly greater, on the order of 22 kg in a 15 minute interval, or 1.4 kg/min; but the cumulative TSS mass loading from SDL-062 was less, about 100 kg, due to a rapid decline in TSS fluxes during the latter portion of the storm hydrograph for SDL-062 during Wet Weather Event-2.

Wet Weather Event 3: Rainfall began at 3:55 am on March 17, 2012 and ended at 7:31 pm on March 18, 2012, totaling 0.54 inches. Flow began shortly after the onset of rainfall at the three monitored locations, SDL-062, SDL-157, and SDL-186. Figure 15 presents the hydrographs for storm drains SDL-062 (black) and SDL- 157 (blue) as compared against rainfall (red) during Wet Weather Event-3. Peak flow rates were for storm drain SDL-157 were about 3.0 cfs with a storm total flow volume of 49,414 cubic feet. Peak flow rates were on the order of 7 cubic feet per second (cfs) for storm drain SDL-062 while the storm total flow volume was 89,485 cubic feet. Figure 16 gives the flux of total suspended solids in a 15 minute interval (red) and

cumulative mass loading of total suspended solids (black) for storm drain SDL-157 during Wet Weather Event-3. Peak TSS fluxes for SDL-157 were 13 kg in a 15 minute interval, or 0.9 kg/min; and the cumulative TSS mass loading from this storm drain for the entire event was 238 kg. Figure 17 gives the corresponding TSS fluxes and cumulative mass loading from storm drain SDL-062 for Wet Weather Event-3. Peak TSS fluxes for SDL-062 were slightly greater, on the order of 15 kg in a 15 minute interval, or 1.0 kg/min; but the cumulative TSS mass loading from SDL-062 was less, about 205 kg; again due to a rapid decline in TSS fluxes during the latter portion of the storm hydrograph for SDL-062 during Wet Weather Event-3.

Discharge from storm drain SDL-186 was not measured during the monitoring program, but was modeled in AMEC (2012). For the purposes of initializing SDL-186 in the SEDXPORT model in the present study, we use these modeled discharges. For Wet Weather Event-1, flow volume for SDL-186 was taken as 28,237 cubic feet. For Wet Weather Event-2, flow volume for SDL-186 was taken as 4,525 cubic feet. For Wet Weather Event-3, flow volume for SDL-186 was taken as 12,137 cubic feet.

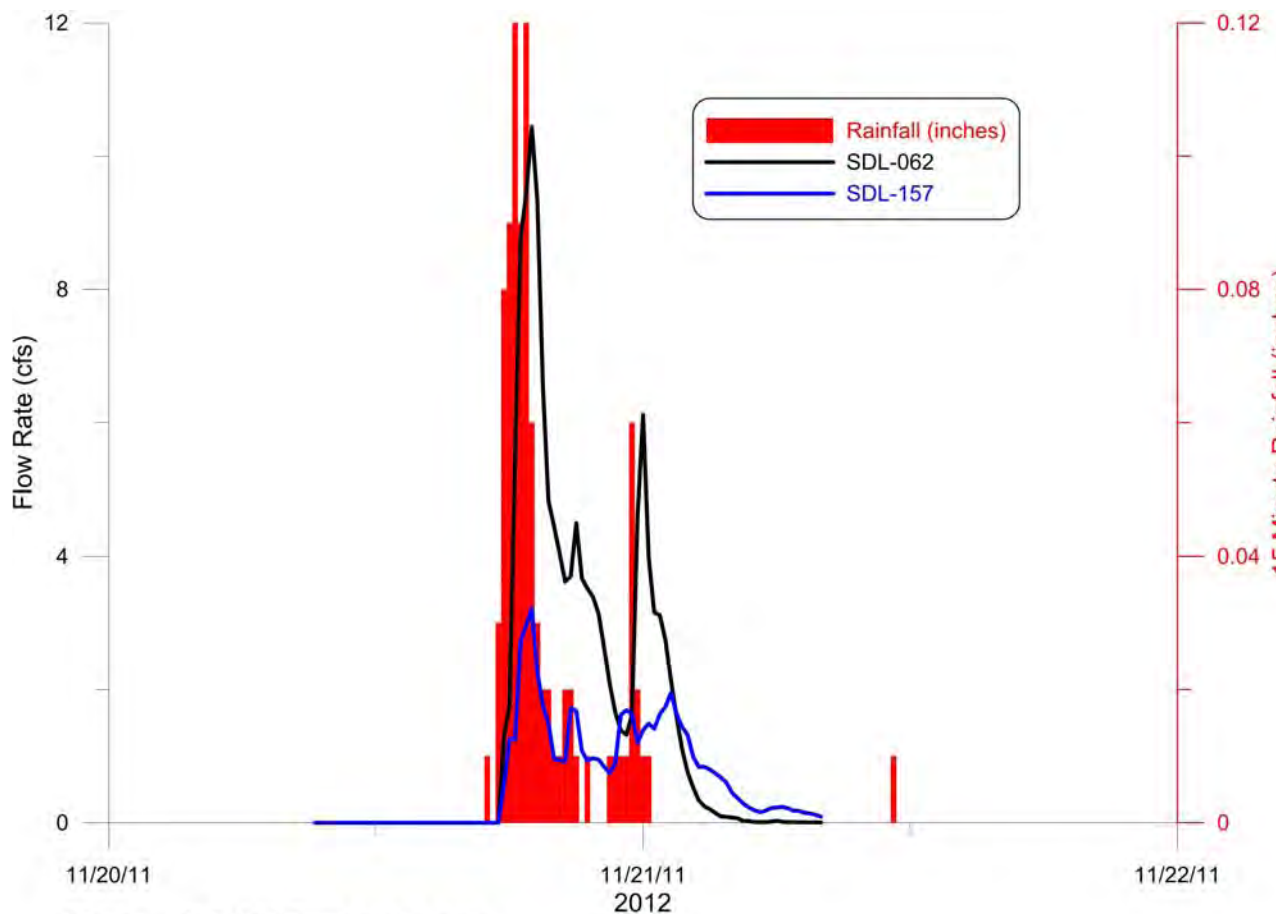


Figure 9. Hydrographs for storm drains SDL-062 (black) and SDL- 157 (blue) as compared against rainfall (red) during Wet Weather Event-1 , 20 November 2011 to 21 November 2011.

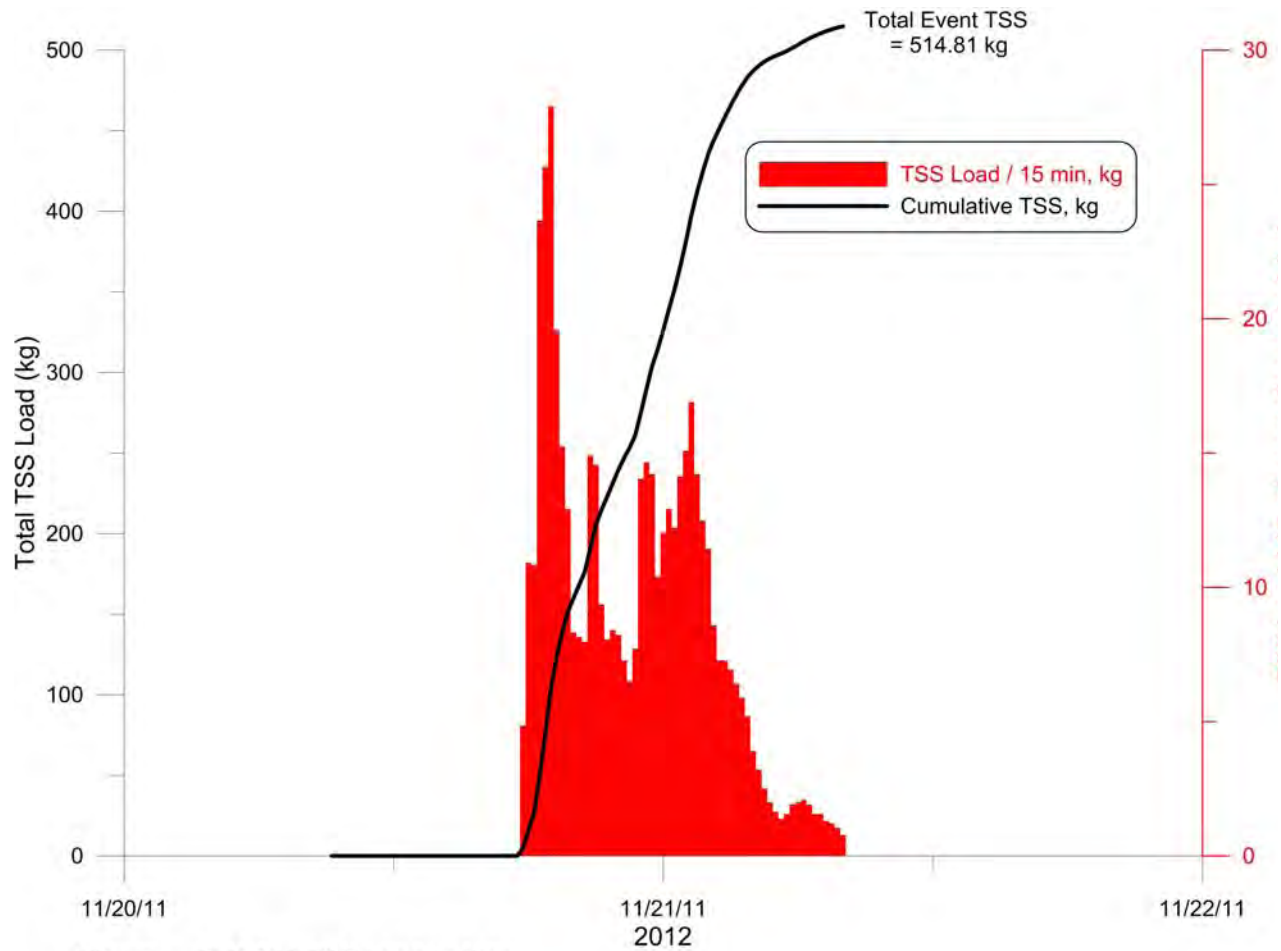
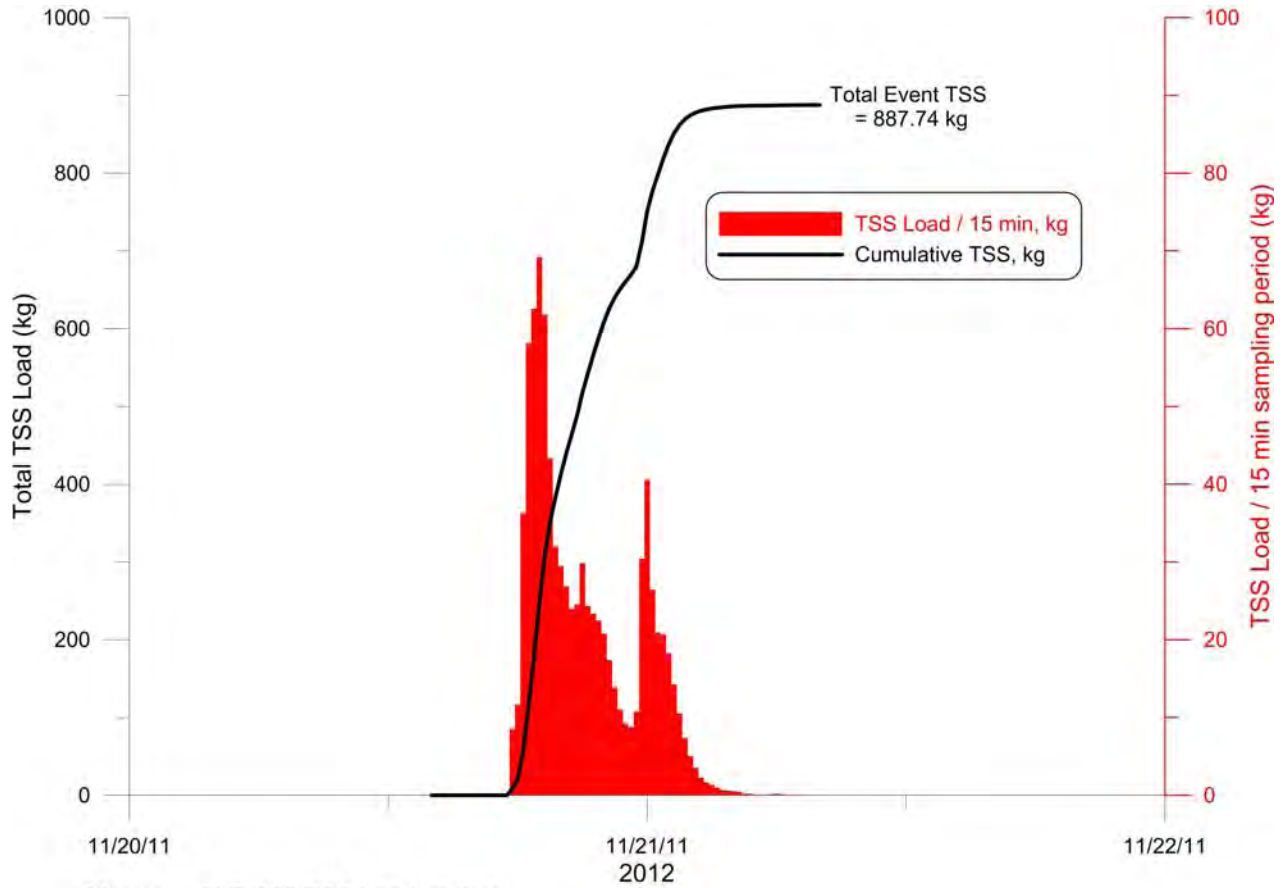


Figure 10. Flux of Total Suspended Solids in a 15 minute interval (red) and Cumulative Mass Loading of Total Suspended Solids (black) for storm drain SDL-157 during Wet Weather Event-1 , 20 November 2011 to 21 November 2011.



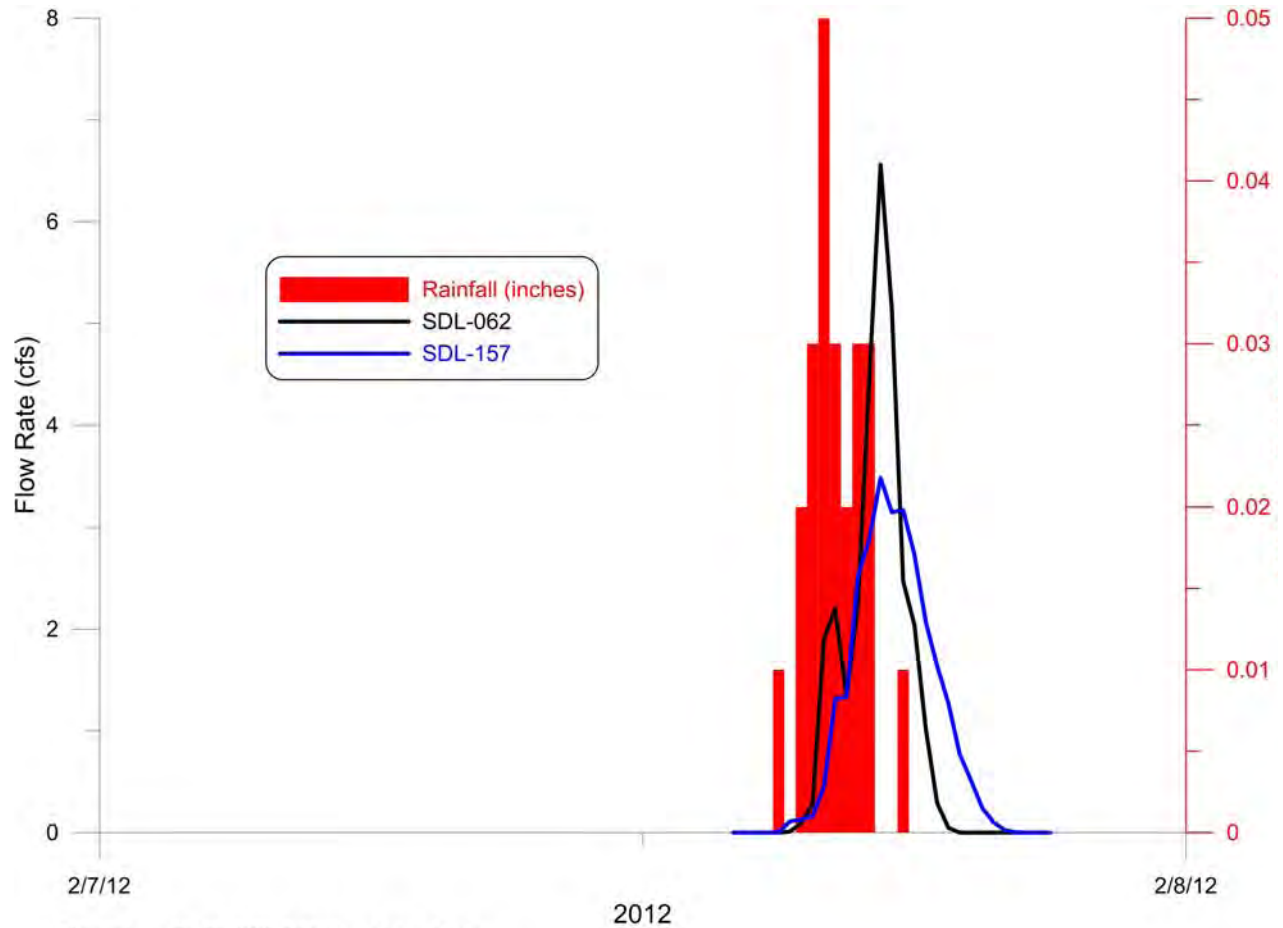


Figure 12. Hydrographs for storm drains SDL-062 (black) and SDL- 157 (blue) as compared against rainfall (red) during Wet Weather Event-2 , 7 February 2012.

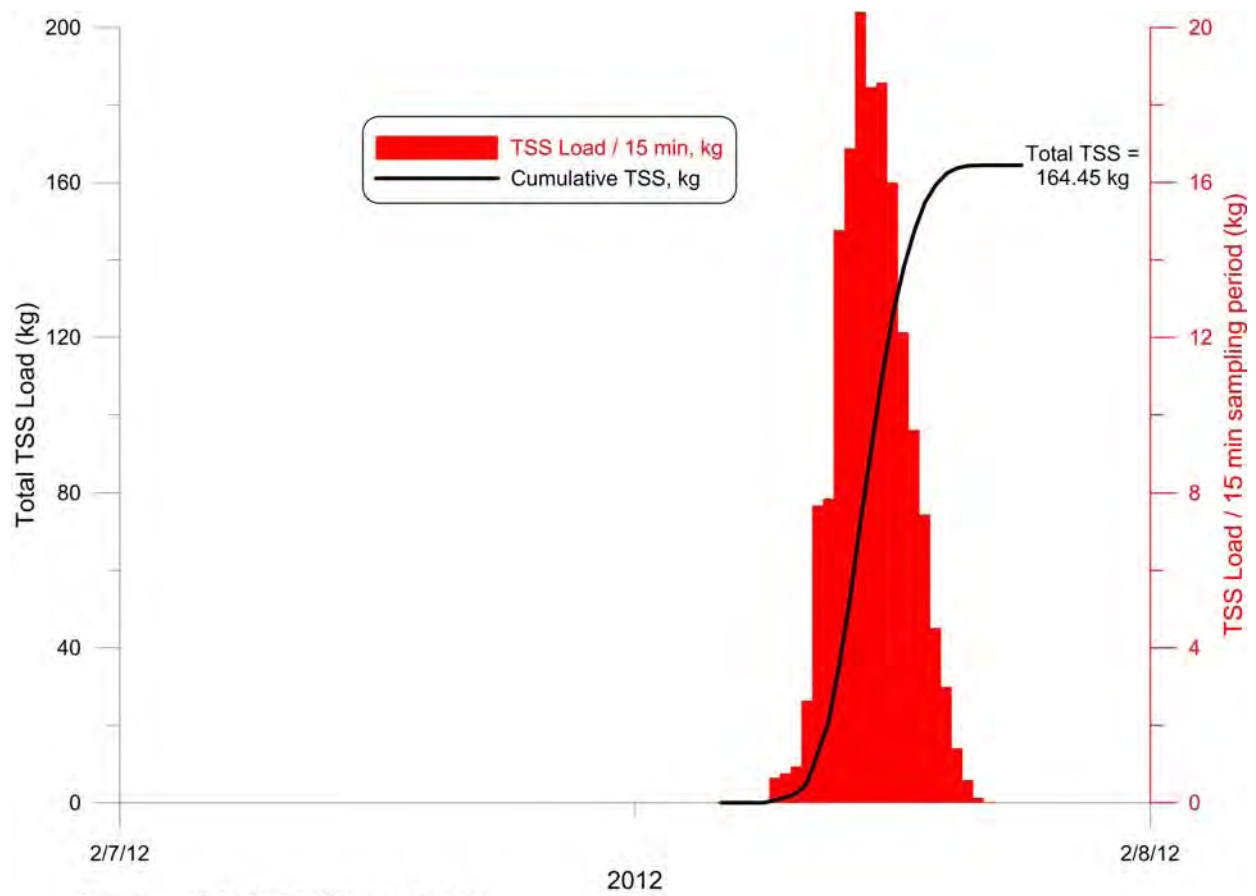


Figure 13. Flux of Total Suspended Solids in a 15 minute interval (red) and Cumulative Mass Loading of Total Suspended Solids (black) for storm drain SDL-157 during Wet Weather Event-2 , 7 February 2012.

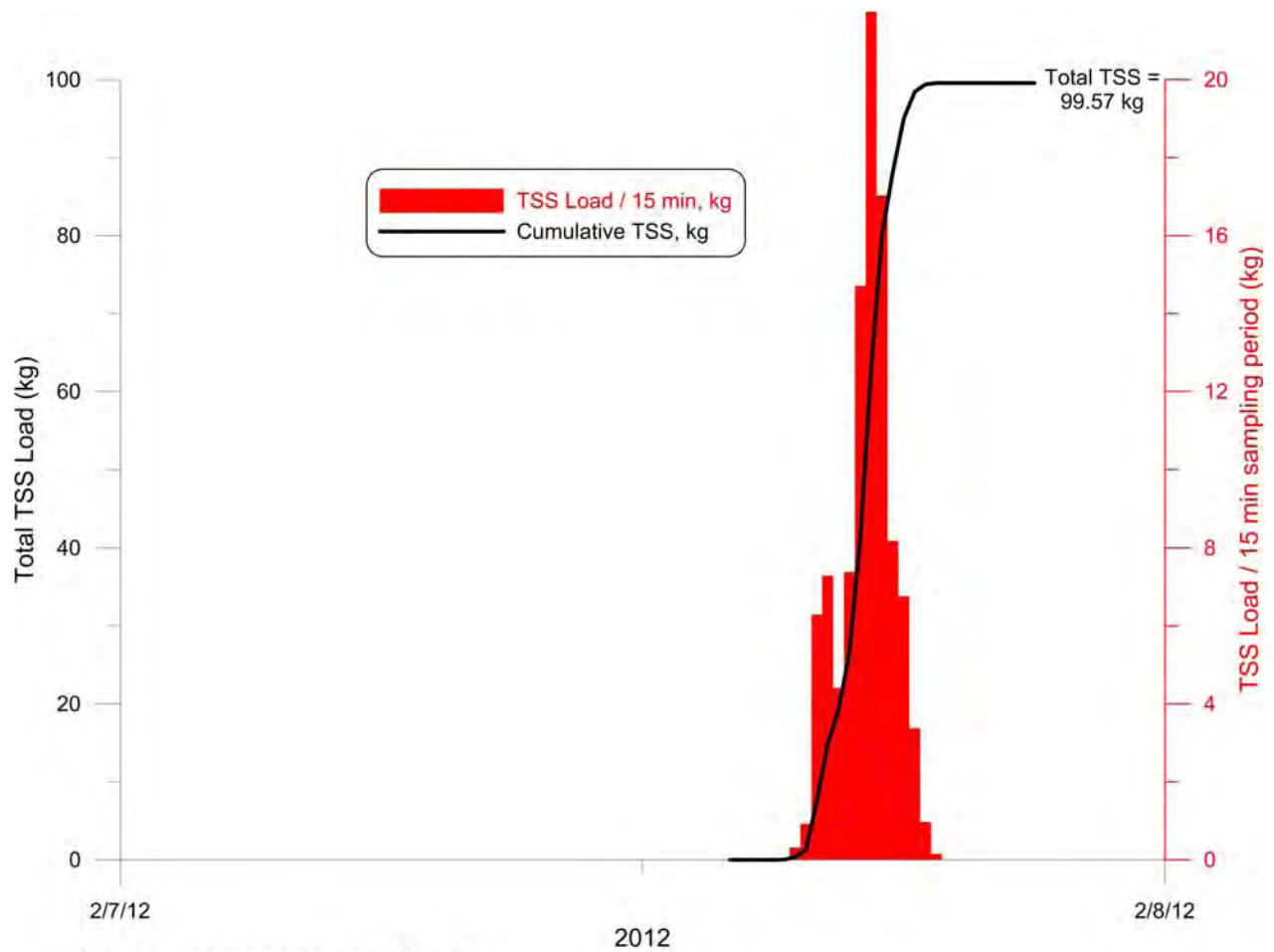


Figure 14. Flux of Total Suspended Solids in a 15 minute interval (red) and Cumulative Mass Loading of Total Suspended Solids (black) for storm drain SDL-062 during Wet Weather Event-2 , 7 February 2012.

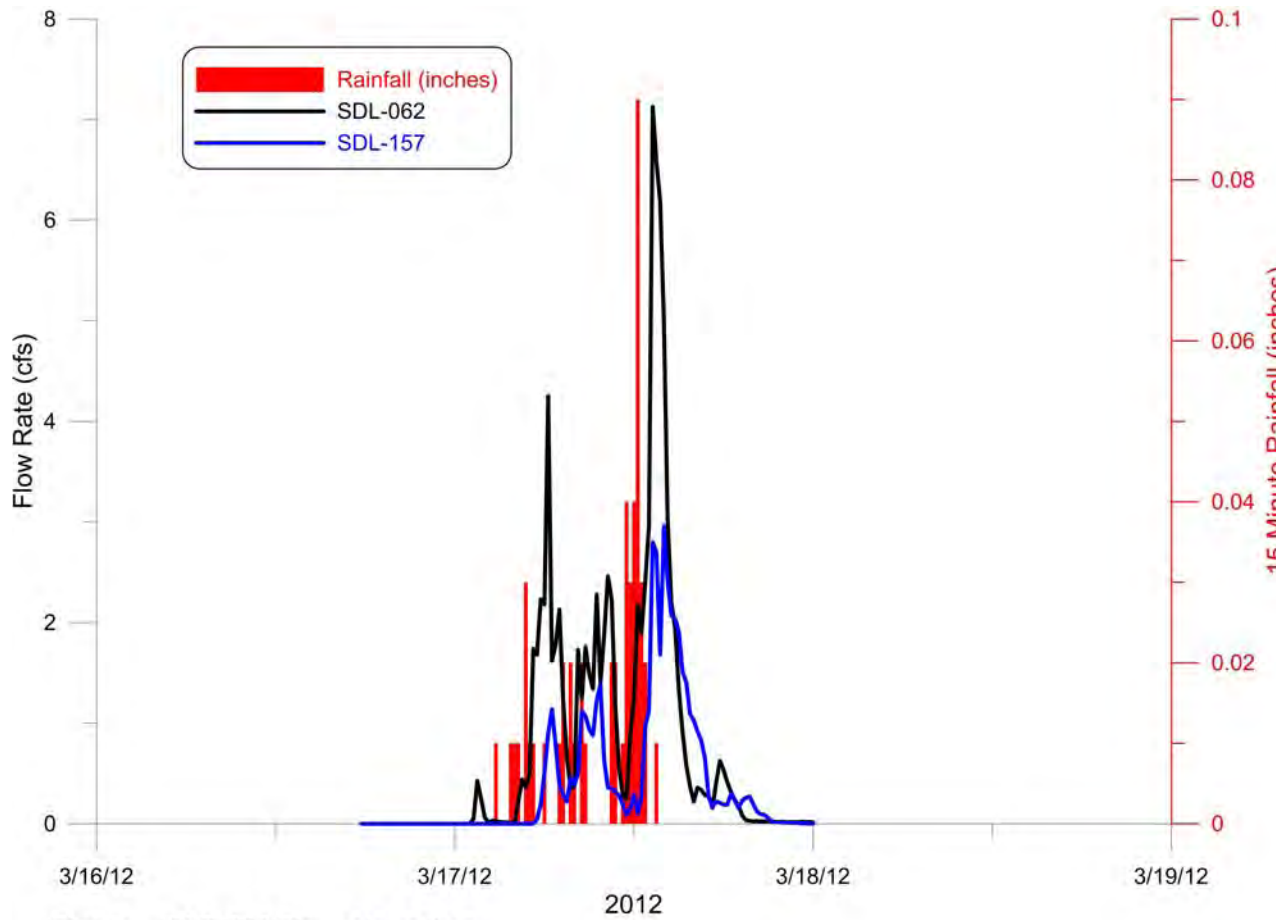


Figure 15. Hydrographs for storm drains SDL-062 (black) and SDL- 157 (blue) as compared against rainfall (red) during Wet Weather Event-3 , 17 March 2012 to 18 March 2012.

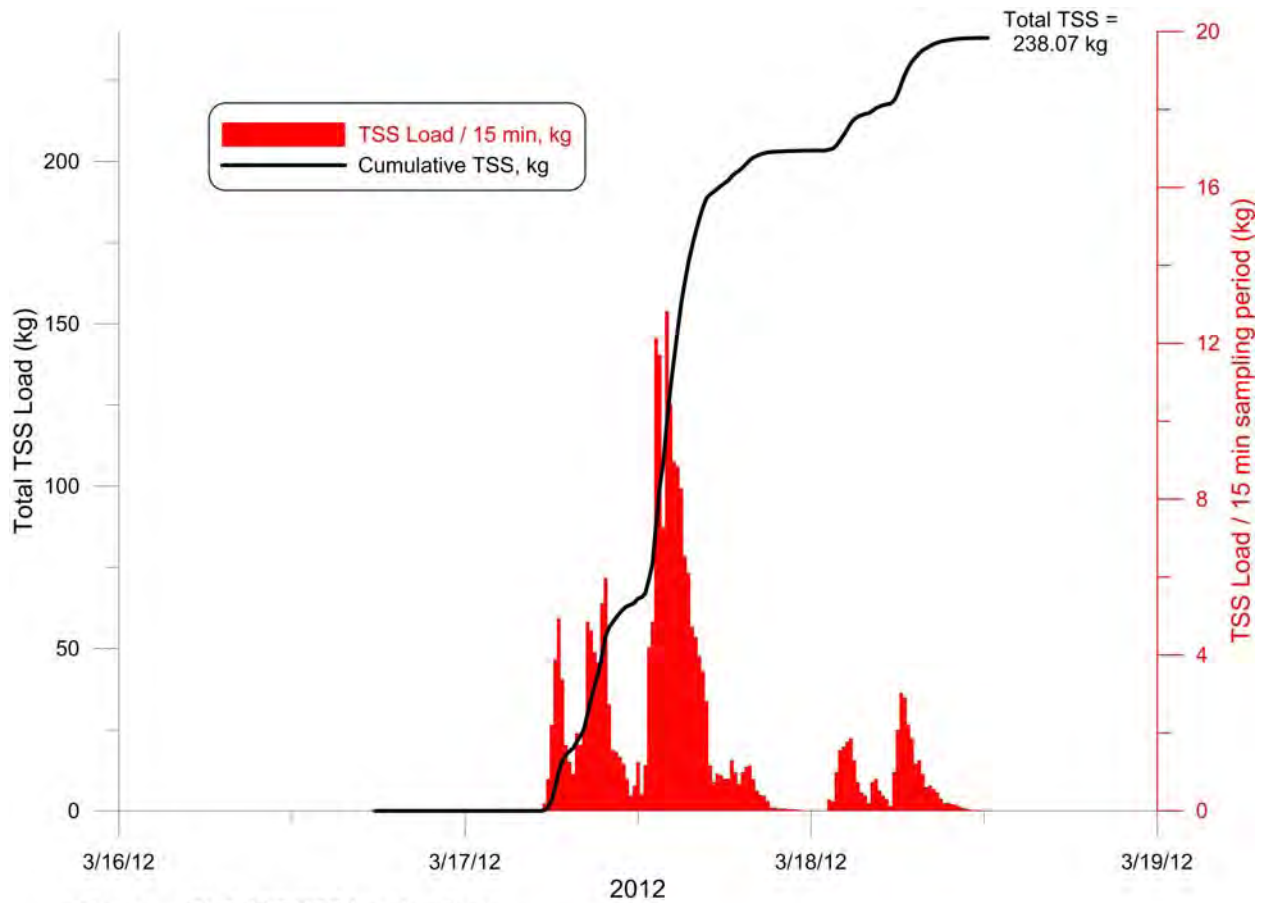


Figure 16. Flux of Total Suspended Solids in a 15 minute interval (red) and Cumulative Mass Loading of Total Suspended Solids (black) for storm drain SDL-157 during Wet Weather Event-3 , 17 March 2012 to 18 March 2012.

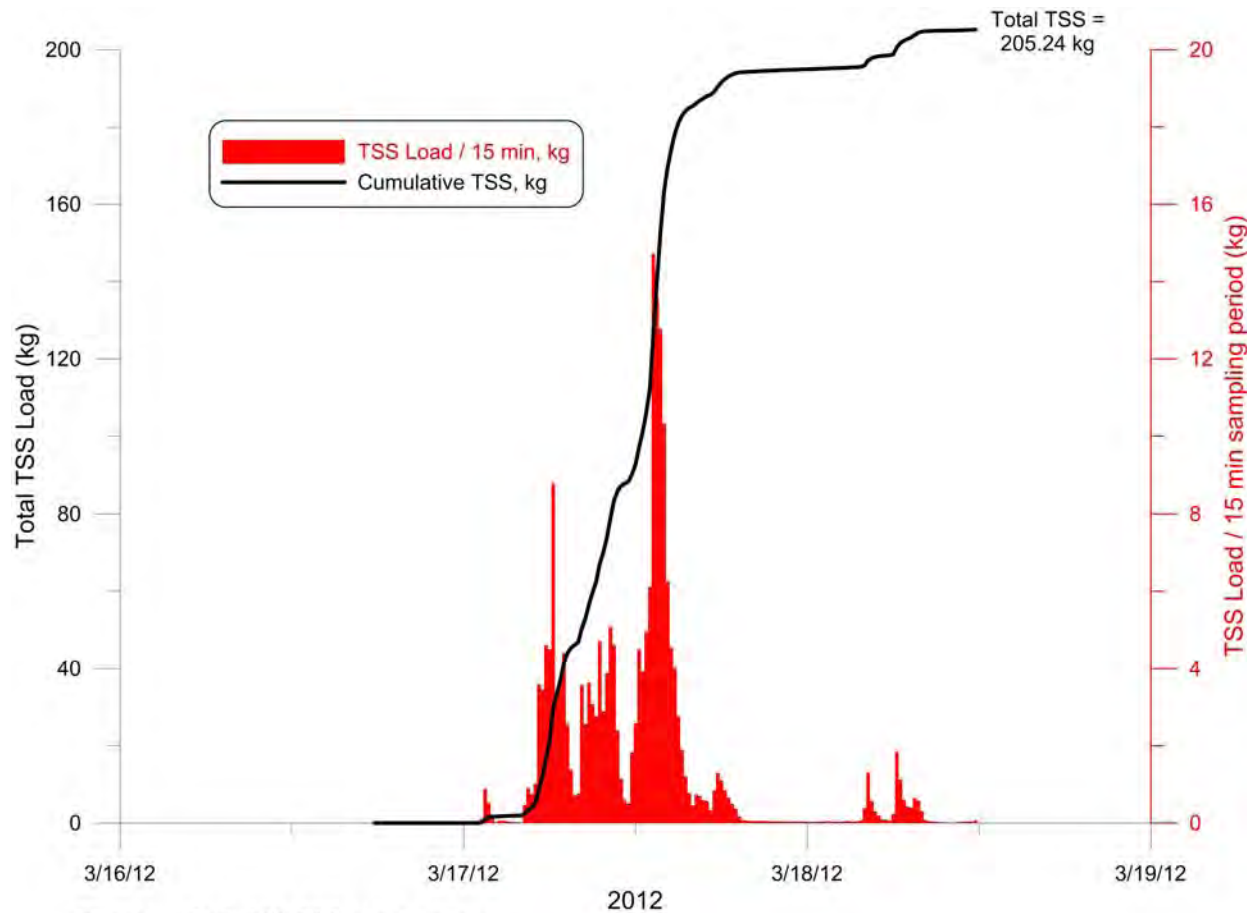


Figure 17. Flux of Total Suspended Solids in a 15 minute interval (red) and Cumulative Mass Loading of Total Suspended Solids (black) for storm drain SDL-062 during Wet Weather Event-3 , 17 March 2012 to 18 March 2012.

3.2 Forcing Functions

A) Waves: Because the combined discharges of storm water from the La Jolla Shores storm drains are discharged into the surfzone, the wave climate exerts leading order control on the initial dilution and dispersion of TSS as well as the copper or TCDD constituents adsorbed on the surfaces of the fine grained sediments that make up the suspended solids loading. The wave forcing records are derived from measurements during the Coastal Data Information Program, (CDIP). This program routinely monitored waves at several locations in the lower Southern California Bight since 1980. The nearest CDIP *directional* wave monitoring sites for the Oceanside Littoral Cell and Torrey Pines Sub-Cell (Figure 18) are:

- a. Oceanside Array
 - Station ID: 00401
 - Location:

- 33 11.4⁰ North, 117 23.4⁰ West
- 500 feet SW of pier
- Water Depth (m): 10
- Instrument Description:
 - Underwater Directional Array
- Measured Parameters:
 - Wave Energy
 - Wave Direction
- b. San Clemente
- Station ID: 05201
- Location:
 - 33 25.2⁰ North, 117 37.8⁰ West
 - 1000 ft NW of San Clemente Pier
- Water Depth (m): 10
- Instrument Description:
 - Underwater Directional Array
- c. Measured Parameters:
 - Wave Energy
 - Wave Direction
- d. Huntington Beach Array
- Station ID: 07201
- Location:
 - 33 37.9⁰ North, 117 58.7⁰ West
 - Approximately 1 mile west of lifeguard headquarters at Huntington Beach, CA
- Water Depth (m): 10
- Instrument Description:
 - Underwater Directional Array
- Measured Parameters:
 - Wave Energy
 - Wave Direction

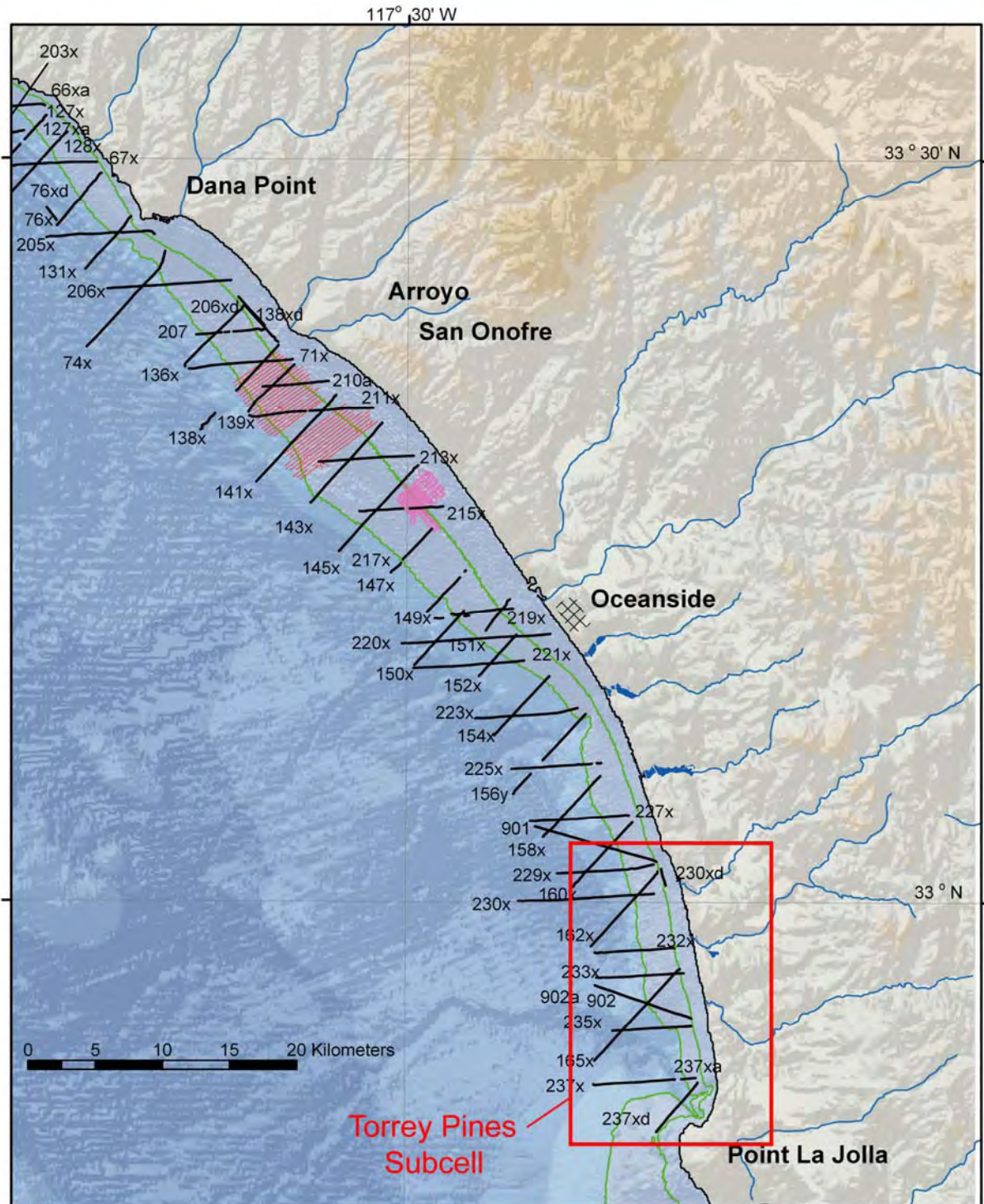


Figure 18. Oceanside Littoral Cell and Torrey Pines Sub-Cell.

Data for these CDIP wave monitoring sites is available beginning January 1980 through March 2012 [CDIP, 2012]. In addition to the CDIP sites, waves have been monitored at Torrey Pines Beach from 1972 until 1984 by the SAS Stations deployed by Scripps Institution of Oceanography, (SIO), Pawka (1982). The ensemble of data from the CDIP and SAS monitoring stations were pieced together into a continuous record from 1980-2012 and entered into a structured preliminary data file.

The data in the preliminary file represent partially shoaled wave data specific to the local bathymetry around Oceanside, San Clemente or Huntington Beach. To correct these data to the Torrey Pine Sub-Cell in which the dilution modeling is performed, the data are entered into a refraction/diffraction numerical code, back-refracted out into deep water, and subsequently brought onshore into the immediate neighborhood of the Torrey Pines Sub Cell (as delineated in Figure 5 and 18). CDIP wave data are shoaled into Scripps Beach and the neighboring beaches of the Torrey Pines Sub-Cell using the **OCEANRDS** refraction-diffraction computer codes. The primitive equations for this code are lengthy, listings of the FORTRAN codes of **OCEANRDS** appear in Appendix C. These codes calculate the simultaneous refraction and diffraction patterns propagating over a Cartesian depth grid. "OCEANRDS" uses the parabolic equation method (PEM), Radder (1979), applied to the mild-slope equation, Berkhoff (1972). To account for very wide-angle refraction and diffraction relative to the principle wave direction, "OCEANRDS" also incorporates the high order PEM Pade approximate corrections modified from those developed by Kirby (1986a-c). Unlike the recently developed REF/DIF model due to Dalrymple et al (1984), the Pade approximates in "OCEANRDS" are written in tesseral harmonics, per Jenkins and Inman (1985); in some instances improving resolution of diffraction patterns associated with steep, highly variable bathymetry along the shelf break. These refinements allow calculation of the evolution and propagation of directional modes from a single incident wave direction; which is a distinct advantage over the more conventional directionally integrated ray methods that are prone to caustics (crossing rays) and other singularities in the solution domain where bathymetry varies rapidly over several wavelengths.

An example of a reconstruction of the back-refracted wave field throughout the Bight is shown in Figure 19 using the CDIP data from the San Clemente array. Wave heights are contoured in meters according to the color bar scale and represent 6 hour averages, not an instantaneous snapshot of the sea surface elevation. Note how the sheltering effects of Catalina and San Clemente Islands have induced longshore variations in wave height throughout the Southern California Bight. These variations (referred to as shadows and bright spots) induce longshore transport away from areas of high waves (bright spots, red) and toward areas of low waves (shadows, dark blue). Figure 20 shows the deep water significant wave heights, periods and directions resulting from the series of back-refraction calculations for the complete CDIP and SIO data set at $\Delta t = 6$ hour intervals over the 1980-2012 period of record. The data in Figure 20 are the values used as the deep water boundary conditions of the forward refraction computations into the Torrey Pines Sub Cell (Figure 18). The deep water wave angles are plotted with respect to the direction (relative to true north) from which the waves are propagating at the deep water boundary of Figure 18. Inspection of Figure 20 reveals that a number of large swells lined up with the wave windows open to the Torrey Pine Sub-Cell during the El Niño's of 1980-83, 1986-

88, 1992-95, and 1997-98. The largest of these swell events was the 18 January 1988 storm, producing 4.5 m deep water swells off Scripps Beach (see event #6 in Figure 20).

Figure 21 gives an example of the forward refraction calculation over the Torrey Pines Sub-Cell and La Jolla Bay region for the low energy waves that characterize the low mixing conditions of the dry weather modeling scenario. These particular waves were observed on 22 August 2011, and had a daily mean wave height of only 0.2 m, approaching La Jolla Shores from 210° with 10 sec period. In contrast, the refraction/diffraction pattern for a wet weather scenario is shown in Figure 22 for 1.8 m high storm swells shoaling onto La Jolla Shores from 283° with 14 sec period during 21 November 2011 (Wet-Weather Event-1). The longer period northwest swells of the stormy wet weather scenario produce a pronounced pattern of shadows (regions of locally smaller waves) and bright spots (regions of locally higher waves). Wave driven nearshore currents flow away from bright spots and converge on shadows. Inspection of Figure 22 reveals that the Avenedia de La Playa storm drain SDL-062 is in a shadow zone flanked by bright spots to the north near storm drain SDL-157. Consequently the zone of initial dilution for the SDL-062 storm drain is located in a region of converging longshore currents during the wet weather scenario. Such a convergence of drift results in rip currents and offshore flow, acting to disperse the beach discharges into deep water.

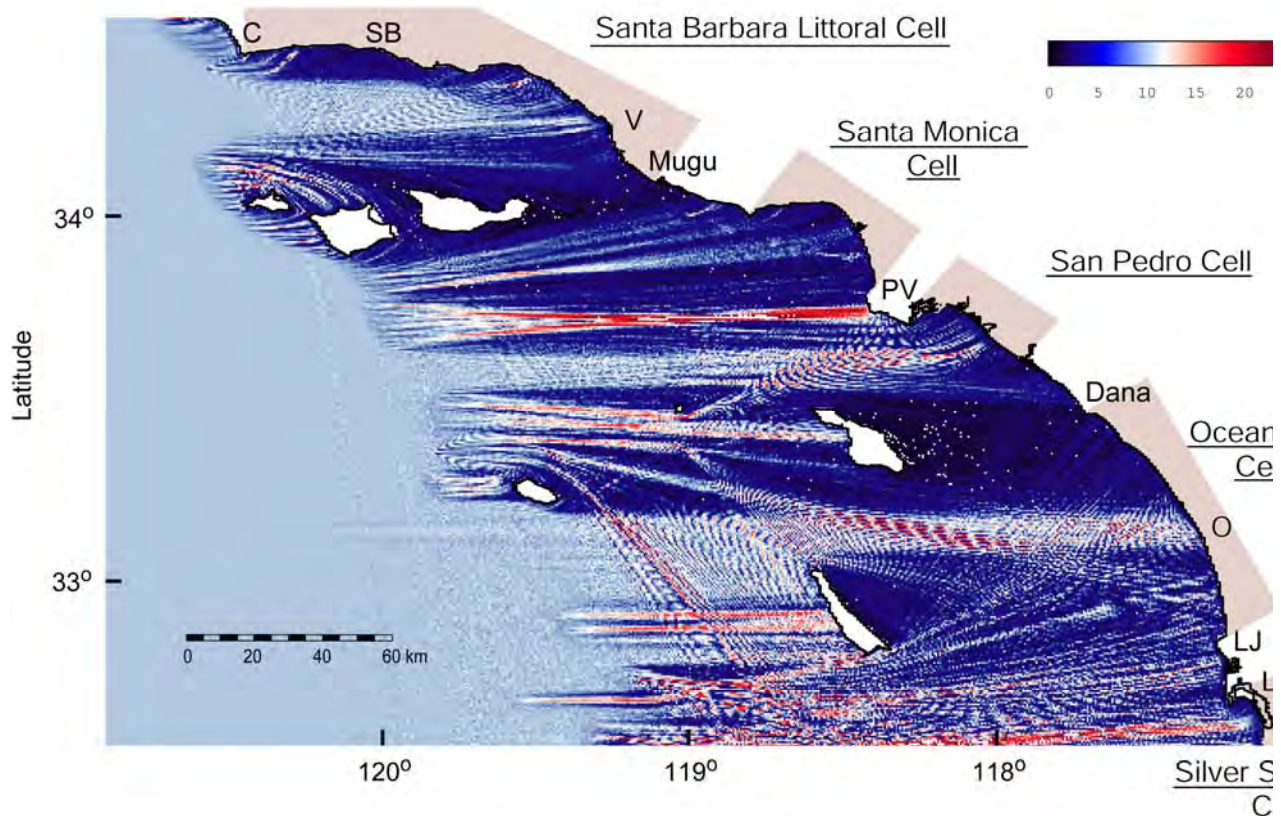


Figure 19. Back-refraction using *oceanrds.for* with waves measured by San Clemente CDIP station during the storm of 17 January 1988 with 10m high waves at 17 second period approaching the Southern California Bight from 270°

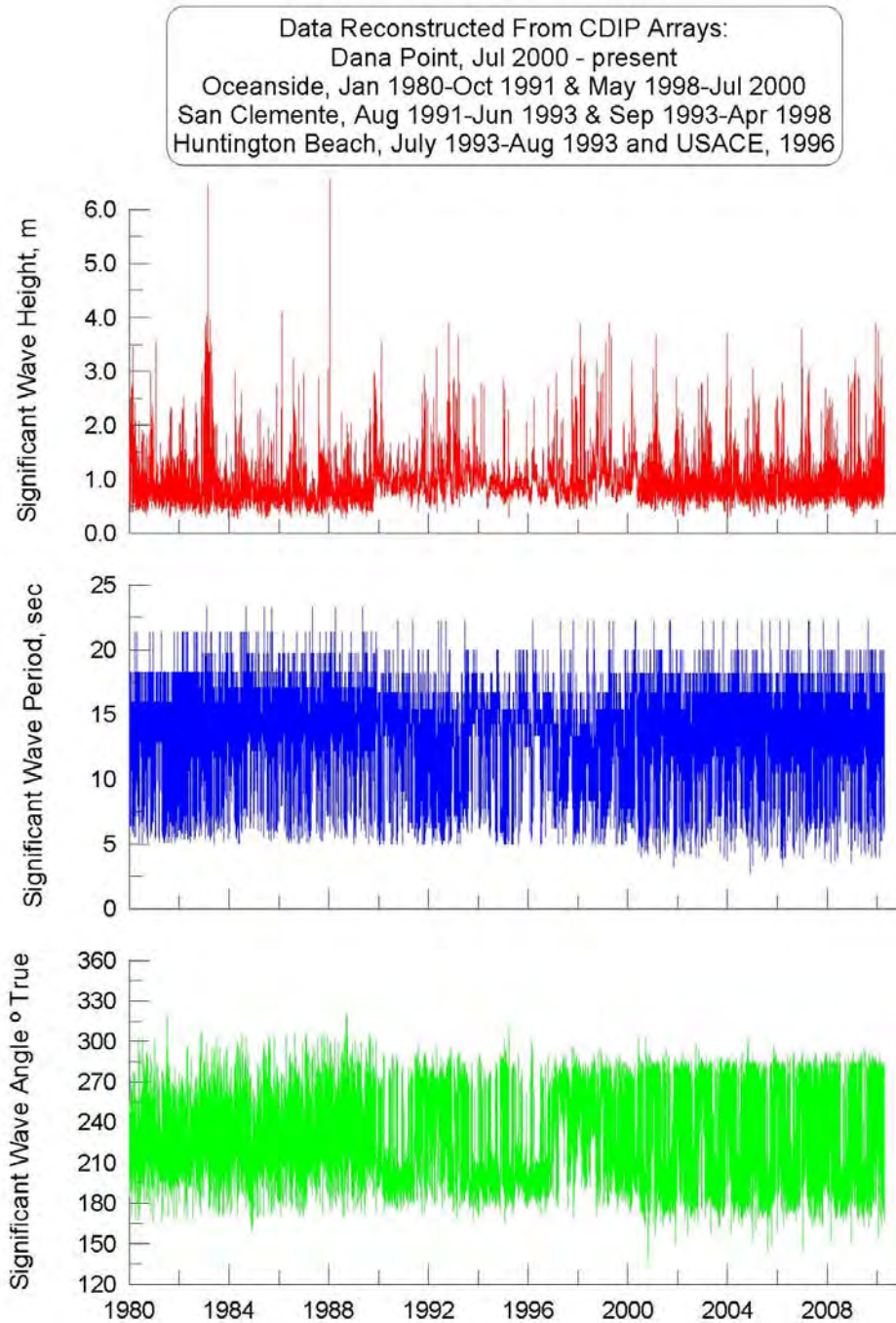


Figure 20. Deep water wave data for wave forcing in Torrey Pines Sub-Cell derived from back refraction of CDIP monitoring data, 1980-2012

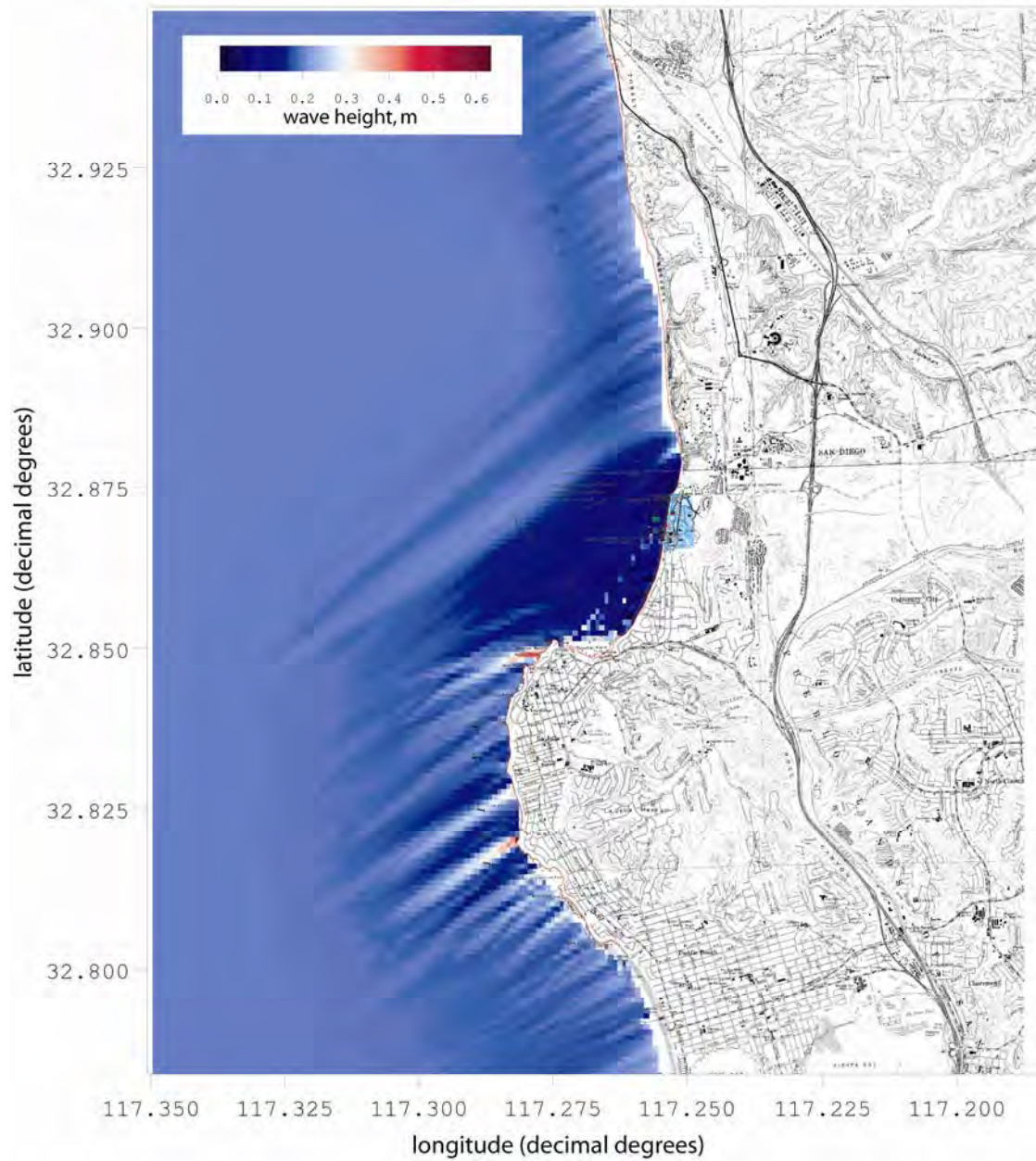


Figure 21. High resolution refraction/diffraction computation for extreme dry weather model scenario based on 0.2m deep water wave height from 210° with 10 sec period.

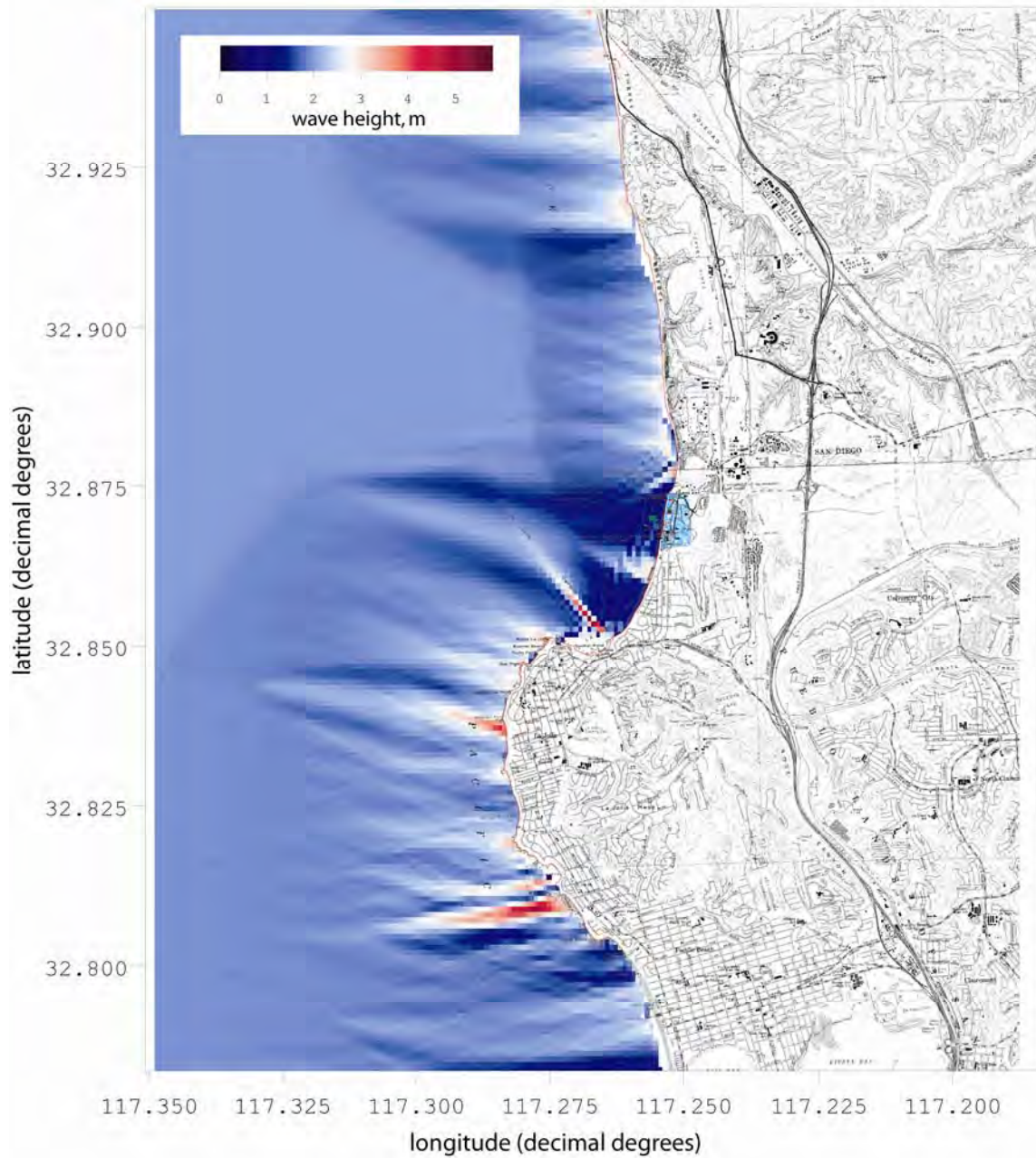


Figure 22. High resolution refraction/diffraction computation for worst-case wet weather model scenario based on 1.8 m deep water wave height from 283° with 14 sec period, 21 November 2011.

The directional dependence of the shoaling waves on La Jolla Shores that is shown in the refraction analysis of the examples in Figures 21 and 22 has been decomposed into a set of probability density functions in Figure 23, used to characterize the long-term wave mixing in the zone of initial dilution of storm drains SDL-062 and SDL-157. This figure reveals that the waves that influence dilution and dispersion of surf zone discharges of storm water at La Jolla Shores are *bi-modal* in character, meaning there are two primary directional modes: waves that approach the La Jolla Shores from the *northwest*, and waves that approach from the *southwest*. At lowest order, this bi-modality reflects seasonal wave climate cycles. The waves from the northwest are typically wet weather winter storm waves from Gulf of Alaska frontal-cyclones, and have typically higher significant wave heights (3m) and shorter wave periods (11 sec.). The southwest approaching waves are typically dry weather summer swells from distant Mexican tropical cyclones or southern hemisphere storms with lesser significant wave heights (1m - 2m) and longer wave periods (16 sec).

Southern Oscillation climate effects give rise to enhancements and protractions of the seasonal wave climate cycles, and their two extremes are referred to as El Niño (SOI negative) and La Niña (SOI positive). The wave climate in southern California changed, beginning with the El Niño years of 1978/79 and extending at least until the present. The average SOI for this period was -0.5, with the 1978/79 El Niño averaging -1.2, the 1982/83 El Niño averaging a record -1.7 and the 1993/94 El Niño recording a mean of -1.0. The prevailing northwesterly winter waves were replaced by high energy waves approaching from the west or southwest, and the previous southern hemisphere swell waves of summer have been replaced by shorter period tropical storm waves during late summer months from the more immediate waters off Central America. The net result appears to be a decrease in the southward component of the wave-induced longshore currents and the net littoral drift that had otherwise prevailed during the preceding thirty years (Jenkins and Wasyl, 2005, Inman and Jenkins, 1999). The wave statistics in Figure 23 seem to confirm this theory; whereby, despite the lesser intensity, there were 140,830 realizations of waves approaching from the southwest (El Niño dominant direction), as compared against only 61,508 realizations of waves approaching La Jolla Shores and the Torrey Pines Sub-cell from the northwest (La Niña dominant direction).

B) Currents: While waves dominate the initial dilution and dispersion of storm water and seawater discharges in the inshore domain, the tidal currents control dilution and dispersion in the offshore domain, particularly over most of the ASBS 29 footprint. A general southward net tidal drift is produced by the daily average of all the potential combinations of standing and progressive mixed tides. This net southward drift is an indication that the tidal transport in this region is *ebb dominated*. The strength of the net drift varies with the spring-neap cycle, with the strongest southward drift produced on the spring tides. In the La Jolla Bay portion of the Torrey Pines Sub-Cell, the southward drift is deflected by Pt La Jolla, producing a complex eddy structure in La Jolla Bay with a jet of converging flow immediately to the South of Pt La Jolla. The La Jolla Bay eddy is of particular interest because it often exerts sufficient entrainment near shore to cause ventilation of the ASBS by currents.

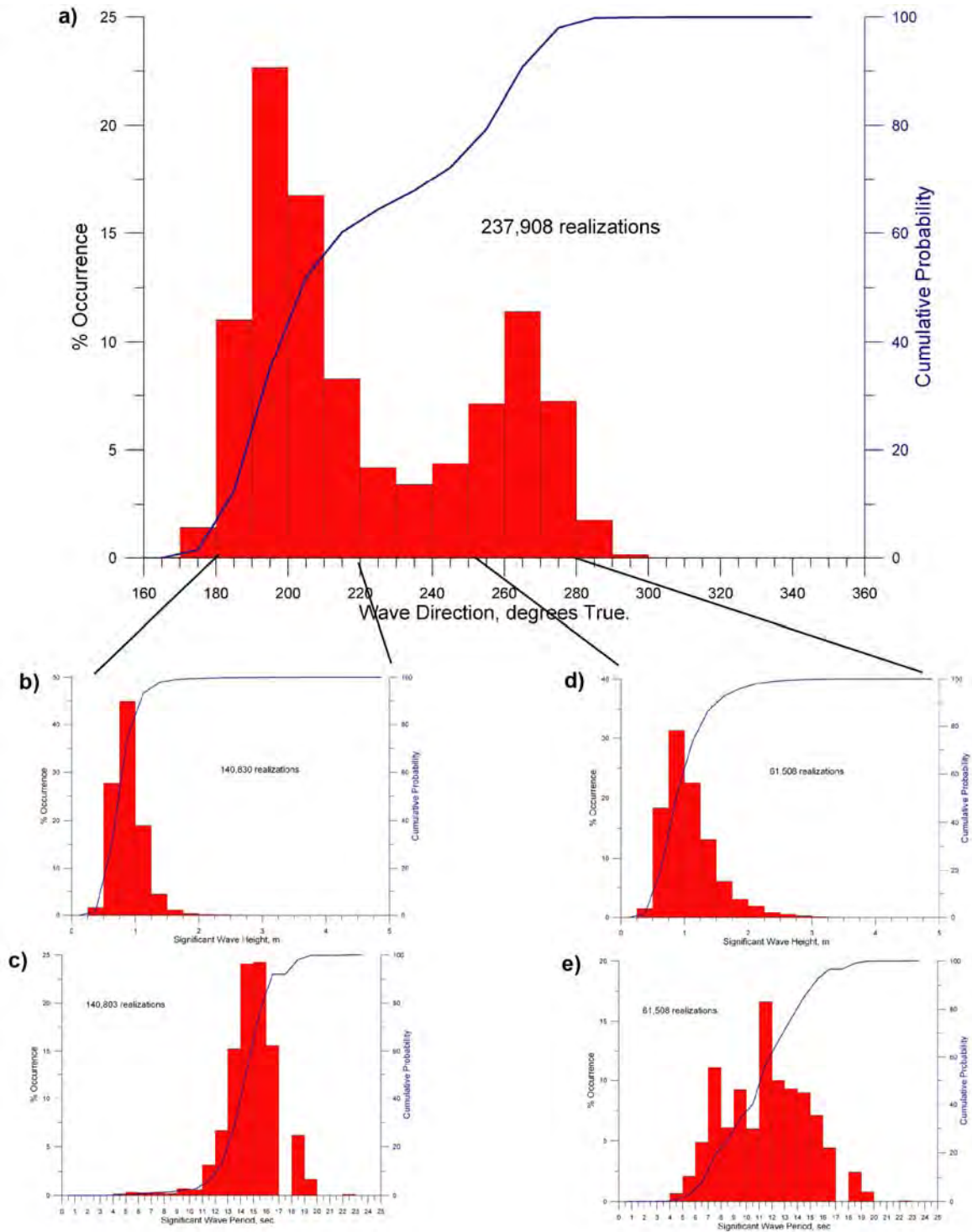


Figure 23. Statistics of composite wave record obtained by merging the CDIP archival data for 1980-2012 with the 2011-2012 ADCP wave burst measurements.

Figure 24 shows a progressive vector plot of the net tidal drift in La Jolla Bay during a neap tidal day, 22 August 2011. This current field is used to represent the minimal offshore mixing and advection conditions of the dry weather conditions. It can be seen from the vector field in Figure 24 that the La Jolla Bay eddy entrainment during neap tide does not extend close enough to shore to cause any appreciable ventilation of La Jolla Shores Beach or ASBS 29. The tidal drift ranges from nil to at most 5 cm/sec along the offshore boundary of the ASBS 29. The core of the La Jolla Bay eddy remains several kilometers offshore and its convergence with the broad field drift produces a 25 cm/sec jet flowing to the south near Marine Street in La Jolla. Given these features, the neap tidal drift used in the dry weather modeling scenario would appear to provide minimal dispersion of the beach discharges at La Jolla Shores Beach or the Devil's Slide area.

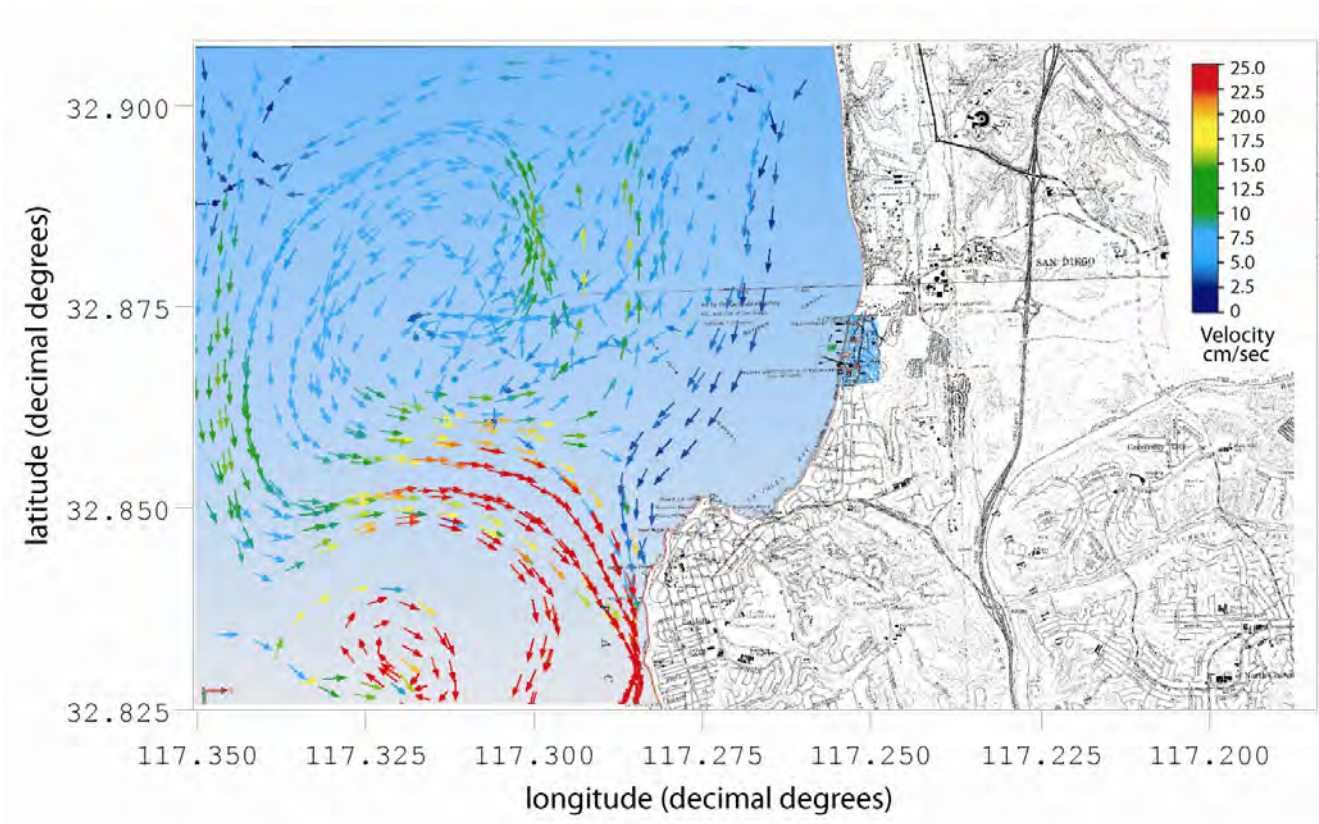


Figure 24. Progressive vector plot of current field in La Jolla Bay during a neap tidal day. Vector magnitude scaled by the color bar in the upper right corner.

By contrast, Figure 25 gives a progressive vector plot of the net tidal drift in La Jolla Bay during the spring tidal day concurrent with the wave conditions in Figure 22 during Wet Weather Event-1. This current field is used to represent the offshore mixing and advection conditions of the wet weather modeling scenario. In this case the La Jolla Bay eddy has moved closer to shore and has become paired with a system of counter rotating eddies off Pt La Jolla. The eddy entrainment currents off La Jolla Shores and through ASBS 29 are typically 9-15 cm/sec flowing toward the

south, following the shoreline contours along La Jolla Shores and subsequently feeding an eddy pair off Pt La Jolla. This eddy pair in turn discharges a jet flowing 45 cm/sec into deeper waters several kilometers west of Pt La Jolla. In total, the eddy system in the La Jolla Bay region during spring tides forms a very efficient conveyor for transporting near shore discharges at La Jolla Shores Beach and Devil's Slide into deep water off shore with significant intervening vorticity and eddy mixing to promote dilution.

Figures 26-29 confirms these model results with ADCP current measurements taken at the northern edge of ASBS 29 (Figure 1) where local water depth is -10 m MSL. Figure 26 gives near bottom currents from profile cell #1 (2.4 m above seabed) during the site monitoring period 11/14/11-11/24/12 for the east-west current velocity component (a); north-south velocity component (b); total velocity amplitude (c). Figure 27 decomposes the near-bottom total velocity amplitudes into probability densities (red bars) and cumulative probability (blue). Over this one-year current monitoring effort, we occasionally find rather large maximum near bottom currents on the order of 50 cm/sec (~1.0 kt) at the northern

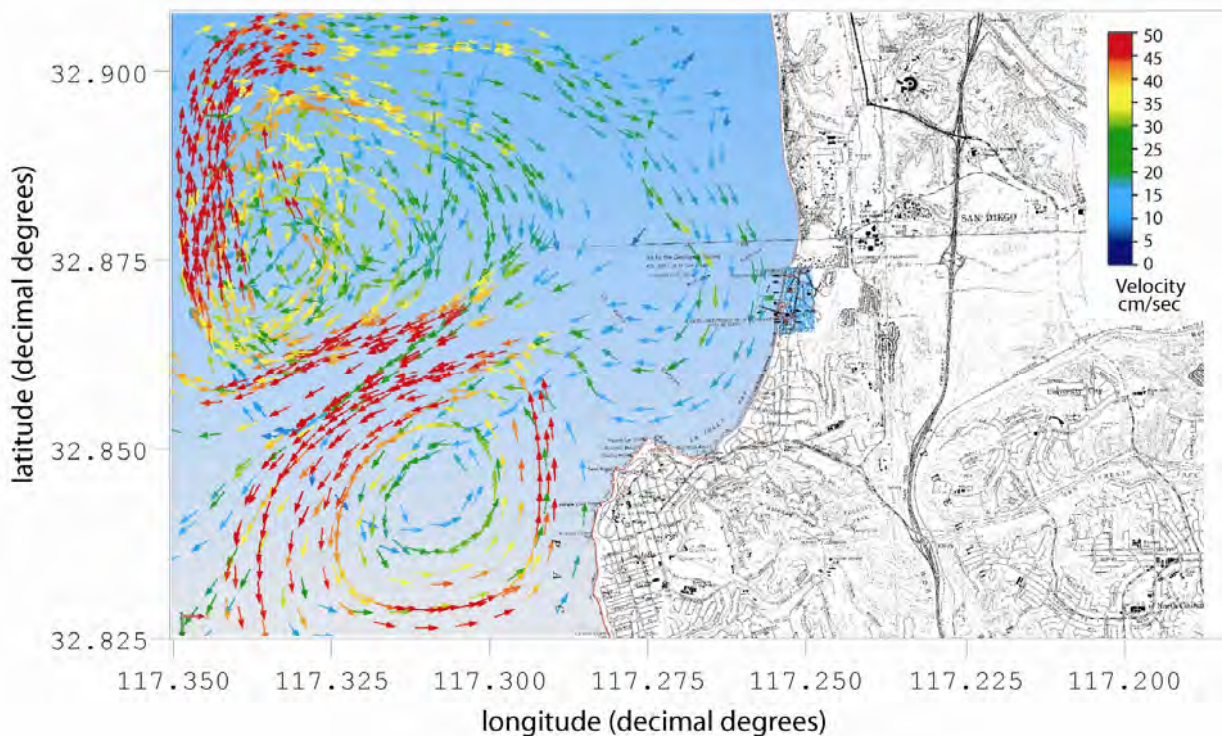


Figure 25. Progressive vector plot of current field in La Jolla Bay during a spring tidal day used in the wet weather modeling scenario. Vector magnitude scaled by the color bar in the upper right corner.

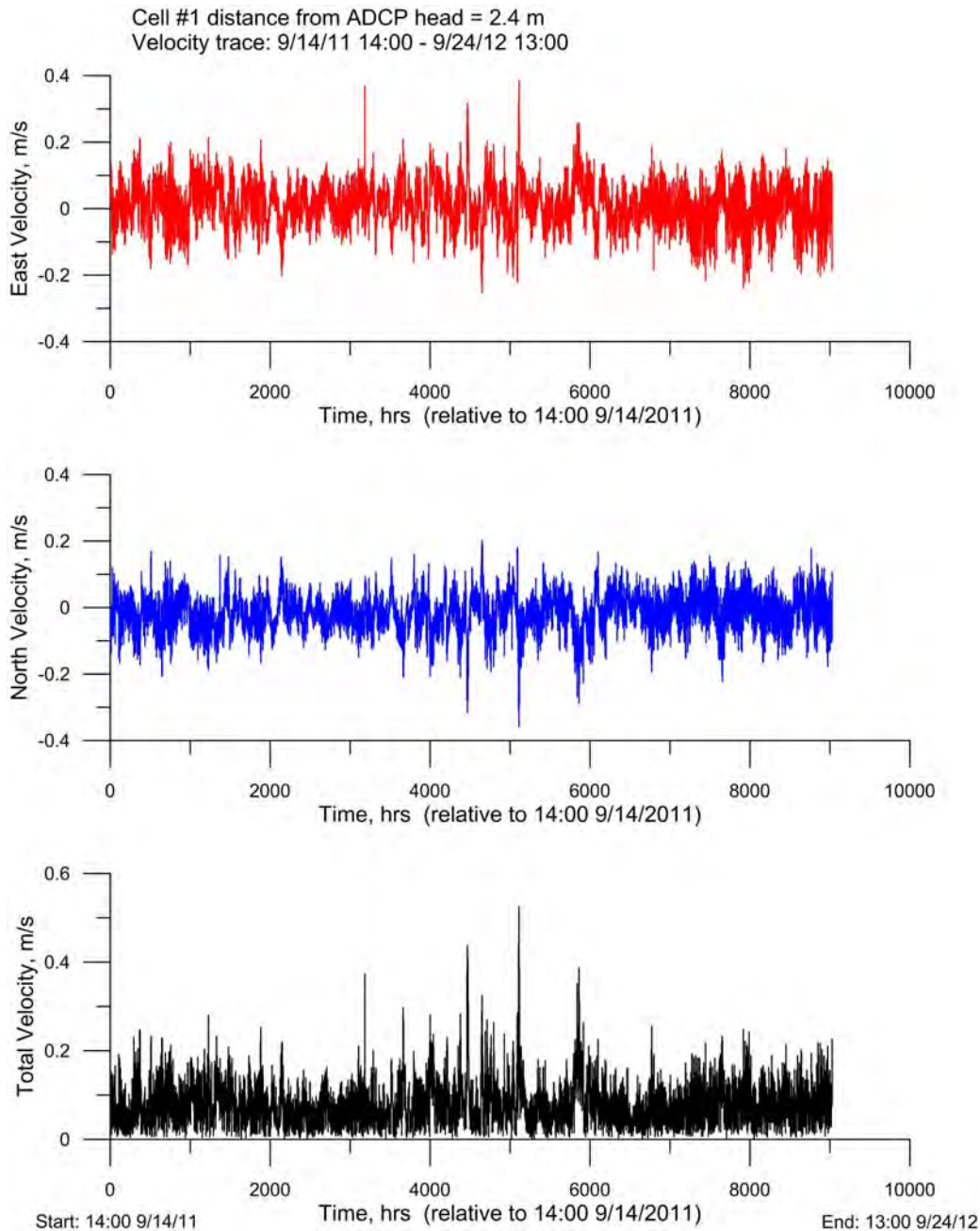


Figure 26. Near-bottom currents (2.4 m above seabed) at mooring location -10 m MSL at northern edge of ASBS 29 (cf. Figure 1). Measurements by Acoustic Doppler Current Profiler (ADCP), 11/14/11-11/24/12. East-west current velocity component (top); north-south velocity component (middle); total velocity amplitude (bottom).

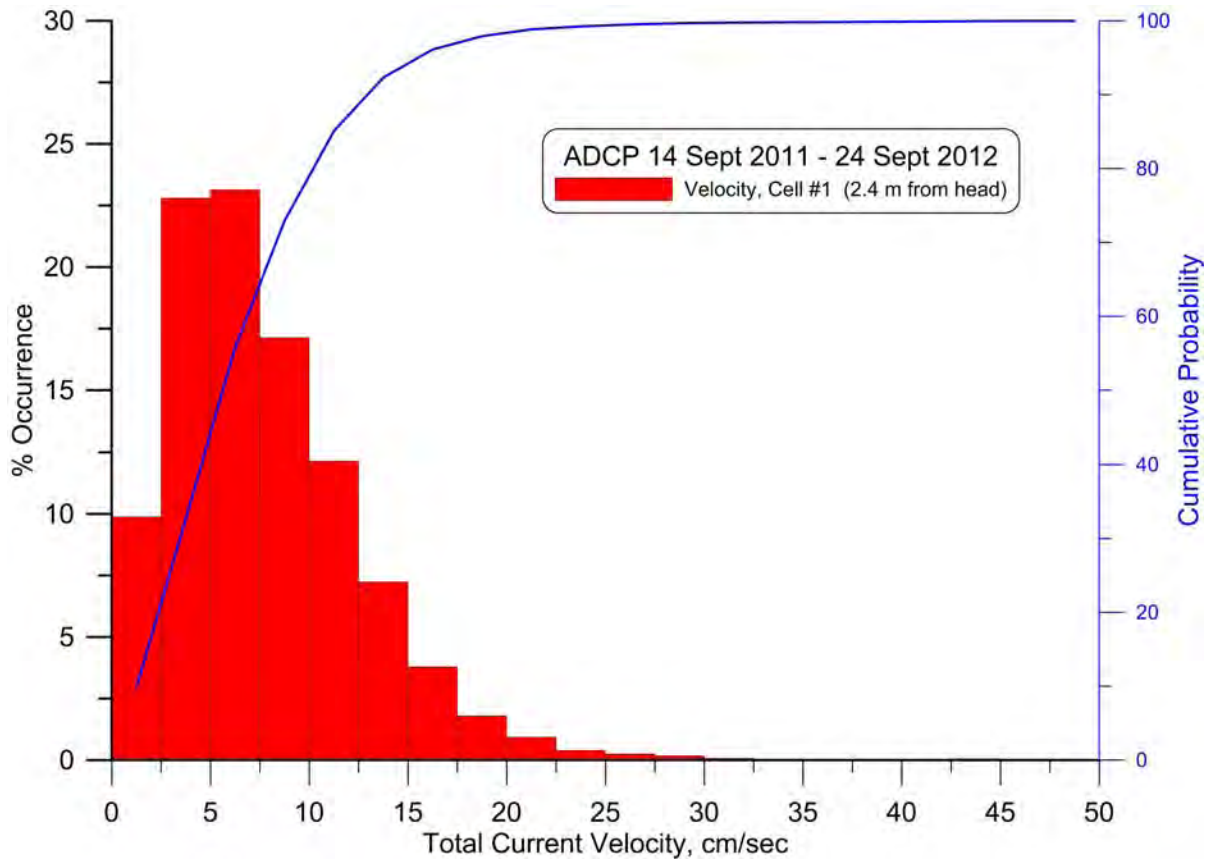


Figure 27. Histogram (probability density) and cumulative probability of near-bottom currents (2.4 m above seabed) at mooring location-10 m MSL at northern edge of ASBS 29, (cf. Figure 1); 11/14/11-11/24/12.

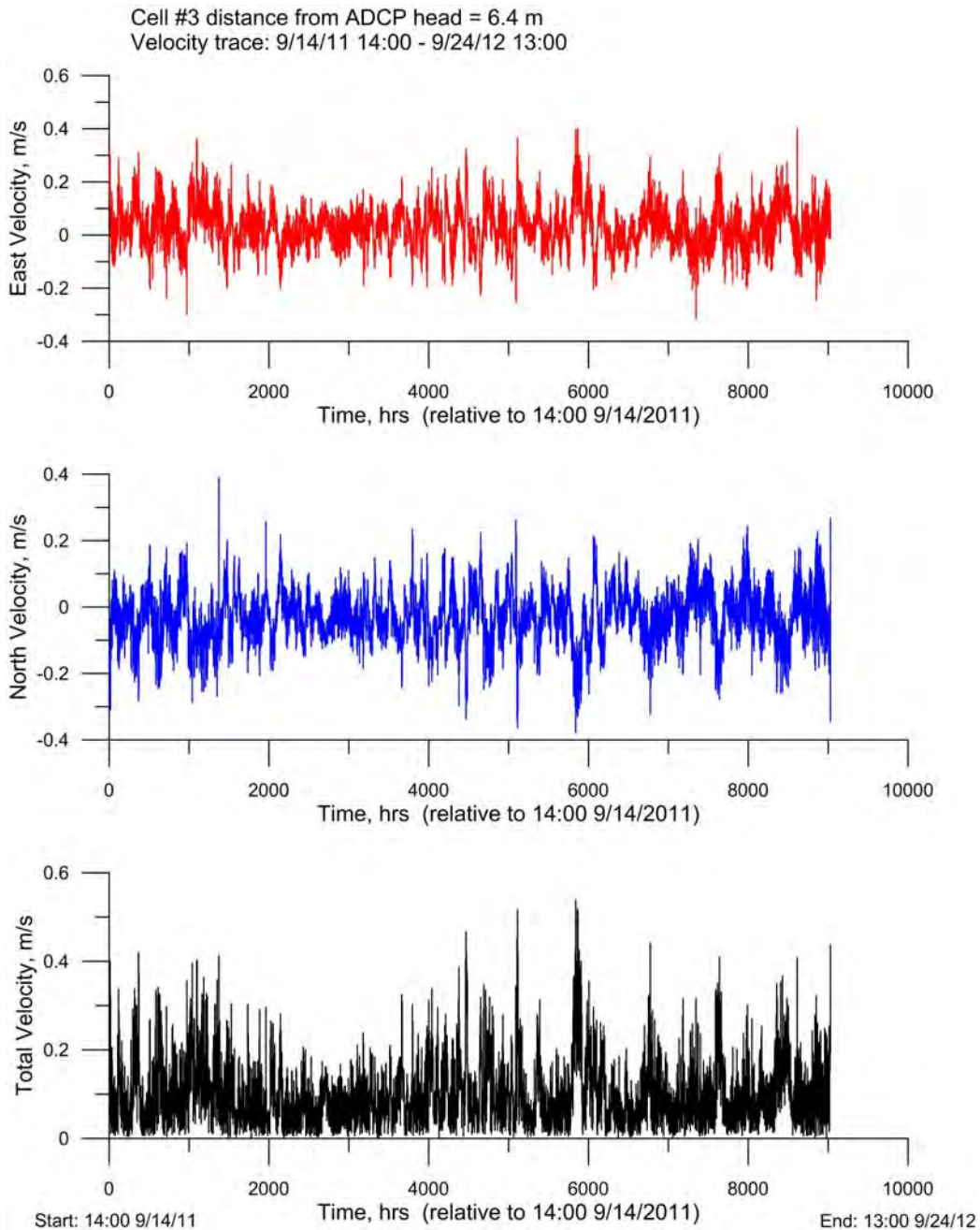


Figure 28. Interior currents (6.4 m above seabed) at mooring location -10 m MSL at northern edge of ASBS 29 (cf. Figure 1). Measurements by Acoustic Doppler Current Profiler (ADCP), 11/14/11-11/24/12. East-west current velocity component (top); north-south velocity component (middle); total velocity amplitude (bottom).

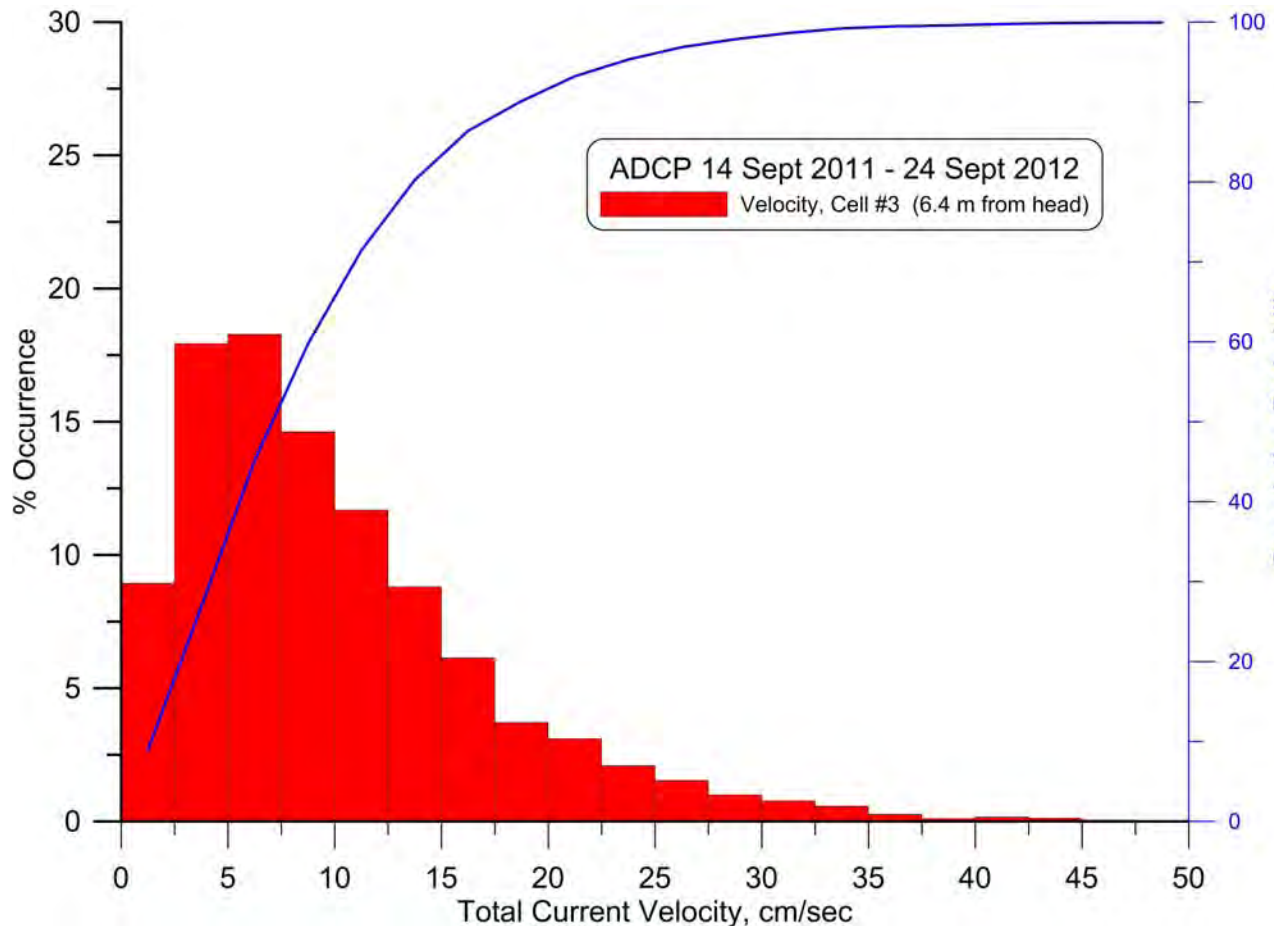


Figure 29. Histogram (probability density) and cumulative probability of interior currents (6.4 m above seabed) at mooring location-10 m MSL at northern edge of ASBS 29, (cf. Figure 1); 11/14/11-11/24/12.

edge of ASBS 29, while average near bottom currents are considerably less, on the order of only 5cm/sec. Further up into the water column, ADCP currents from profile cell #3 (6.4 m above seabed) in Figure 28 somewhat higher current amplitudes with more instances of maximum currents on the order of 50 cm/sec to 55 cm/sec during the site monitoring period 11/14/11-11/24/12. Accordingly, the probability densities (red bars) and cumulative probability (blue) of the interior currents in Figure 29 reveal higher average total current amplitudes, with average amplitudes of 8 cm/sec to 10 cm/sec, consistent with model results in Figures 24 & 25. These are favorable findings with respect to brine dilution rates of storm water in ASBS 29 where persistent currents are found at water column elevations close to the surface mixing layer of buoyant storm water.

C) Wind: Daily mean winds from the Scripps Pier Shore Station (SIO, 2001) and the Scripps Pier CDIP station (CDIP, 2002) were compiled over the 32 year period from January 1980 thru March 2012. This wind record is plotted in Panel-d of Figure 8. Because the lower Southern

California Bight is a “wind drought” region due to orographic blocking by the Peninsular Range, the 32 year mean wind speed is only 5.6 knots. However, El Niño storms and North Pacific cold fronts episodically increase daily wind speeds with the maximum sustained 24 hour mean wind speed reaching 19.6 knots during the 1997 El Niño storms. The minimum daily mean wind speed is 0 knots. In general the coastal winds in the nearshore of La Jolla Shores and Scripps Beach are benign, thereby limiting the degree of wind mixing of the surface water mass.

3.3 Model Scenarios

Based on discussions held in November 2004 with the San Diego Regional Water Quality Control Board, it was decided that the numerical modeling study of the beach discharges should be based on a wet weather worst-case scenario with a long-term probability assessment to bracket the envelope of the possible outcomes. The analysis of the multi-decadal rainfall variability of the San Diego found at the start of Section 3 provides justification for this approach.

A) Search Criteria for Wet Weather Worst Case Conditions: The 32 year long records of the boundary condition and variables in Figures 6-8 and the forcing function variables in Figure 20 were subjected to a joint probability analysis for the simultaneous recurrence of the combination of these variables for the *wet weather worst case* combination. Table 3 provides the search criteria that were applied to these records to establish the wet weather worst case combination of model inputs. The principle requirement of the wet weather worst-case is to maximize the combined discharges of storm water, while using ocean mixing variables that are characteristic, yet minimal for wet weather conditions. Because wet weather conditions occur during the passage of Pacific storms over the Southern California Bight, the worst case criteria of minimal ocean mixing tends to be mutually exclusive with the occurrence of storm water runoff. Wet weather worst case conditions for the receiving water involve storm minimums with respect to winds, waves and currents. To find such conditional minimums from among the 11,688 combinations found in Figures 6-8, and 20, the computer search criteria solved for the minimum of the largest 10% of the wind, waves and current combinations. Because the storm water discharge is predominately fresh water that is warmer than ocean water, the search criteria seeks salinity maximums and temperature minimums in the receiving water concurrent with the storm minimums of waves, winds and currents. In this way the maximum possible density contrast is achieved between the storm drain discharges and receiving water to retard the dilution rates of the discharge as much as possible under wet weather conditions.

Table 3.
Search Criteria for Wet Weather Worst-Case Combinations of Controlling Variables.

Variable	Search Criteria	Physical Significance
Discharge Rate	Maximize	Higher storm water and seawater discharge flow rates lead to higher source loading
Waves	Minimize Highest 10%	Smaller waves result in less mixing in surfzone and less inshore dilution
Currents	Minimize Highest 10%	Weaker currents result in less advection and less offshore dilution
Winds	Minimize Highest 10%	Weaker winds result in less surface mixing and less dilution in both the inshore and offshore
Ocean Water Level	Minimize	Lower water level results in less dilution volume in receiving water
Ocean Salinity	Maximize	Higher salinity leads to greater density contrast between discharge and receiving water
Ocean Temperature	Minimize	Higher temperature leads to density contrast between discharge and receiving water

B) Wet Weather Worst-Case Assignments: Among the three events monitored by AMEC (2012), Wet Weather Event-1 comes closest to matching the search conditions in Table-3 for the wet-weather worst-case proxy. The daily combination of receiving water variables that were recovered from the search criteria in Table 3 was represented best by the conditions on 21 November 2011. This day was post frontal with moderate, winds, waves, and currents. Ocean salinity was 33.11 ppt, depressed about 0.4 ppt by the run off from storms in the previous days while the ocean temperature was 14.5° C, about 4° C below the annual mean. Wave heights were 1.8 m, approaching La Jolla Bay from the northwest at 283° with a 14 sec period. The refraction/diffraction pattern of these storm swells are shown in Figure 22. Winds were post-frontal northwest winds at 10-12 knots from at 290°. The maximum tidal currents in ASBS 29 were 9-15 cm/sec flowing toward the south, (Figure 25), with a weak inshore counter current immediately outside the surf zone following the shoreline contours northward along La Jolla Shores. The tidal current was due to a moderate ebbing spring tide with a minimum water level of -3.63 ft NGVD. With this combination of receiving water variables the model overlaid the storm drain discharges from Wet Weather Event-1 from the monitoring program. Discharges for storm drain outfalls SDL-062 and SDL-157 were initialized according to Figures 9-11. For the purposes of initializing SDL-186 for the worst-case wet weather proxy, we use these modeled discharges from AMEC (2012). For Wet Weather Event-1, flow volume for SDL-186 was taken as 28,237 cubic feet. TSS fluxes for SDL-186 were taken as 70 kg in a 15 minute interval, or 4.7 kg/min, or equivalent to peak TSS fluxes from the neighboring SDL-062 storm drain.

C) Long-Term Simulations of Zone of Initial Dilution: The historic boundary conditions from Figures 6-8 and the forcing functions from Figure 20 were sequentially input into the model, producing daily solutions for the dilution field due to the peak flow event during the monitoring period (Wet Weather Event-1). This procedure inevitably produces some combinations of wet weather discharges with dry weather ocean mixing conditions, and thereby results in certain worst case dilution scenarios that are more extreme, with even less dilution, than the wet weather worst case proxy derived from the monitoring program (Wet-Weather Event-1). The input stream of seven controlling variables from Figures 6-8 & 20 produced 11,688 daily solutions for the dilution field in the zone of initial dilution (ZID) taken as the surfzone. A numerical scan of each of these daily solutions searched for the minimum dilution averaged between the wave break point and the shoreline along the inshore boundary of ASBS 29. Based on the ZID definition contained in the NPDES permit issued by the RWQCB, San Diego Region, for beach discharges at Encina Generating Station, Carlsbad, CA, the search for the minimum dilution was taken longshore to a distance of 1000 ft (305 meters) away from the discharge points in all directions, (although the minimum dilution was found without exception to be within 150m of the discharge points). The solution scans searched for minimum dilution in both the water column and along the sea floor. For each search, the minimum dilution found in any direction away from the outfall was entered into a histogram bin for ultimately assembling a probability density function and cumulative probability from the 11,688 outcomes. These results provided a statistical basis for assessing long term variability of dilution in the ZID. For comparison, a similar procedure of searching the solution space for minimum dilution was repeated at an offshore control point near the interior of ASBS 29, where local water depth was -10m MSL, see Figure-1.

3.4 Calibration

The coupled sets of wave, current and dilution/dispersion models were calibrated for end-to-end simulations of known dye dispersion events measured off Scripps Beach by Inman et al. (1971). Initializations for the model were derived from the measured forcing functions reported in that publication. Free parameters in the subroutines of the **SEDXPORT** for dilution/dispersion model were adjusted iteratively until a best fit was achieved between the measured and simulated dye concentrations and dilution factors.

The subroutines of **SEDXPORT**.for contain seven free parameters which are selected by a calibration data set specific to the coastal type for which the hindcast calibration simulation is run. These parameters are as follows according to subroutine:

BOTXPORTAf

- *ak2 - stretching factor for vertical eddy diffusivity
- *ak - adjusts mixing lengths for outfalls

NULLPOINTAf

*ak7 - adjusts the asymmetry of the bedform distribution curve

SURXPORTAf

*aks - adjusts the surf zone suspended load efficiency, K_s

ak4 - stretching factor for the horizontal eddy diffusivity_x

RIVXPORTAf

*ak3_1 - adjusts the jetty mixing length and outfall mixing lengths

*ak3 - stretching factor for the horizontal eddy diffusivity of the river plume_H

The set of calibration values for these parameters was used without variation or modification for all model scenarios.

4.0 RESULTS

The model scenarios defined in Section 3.3 are run in simulations of one tidal day using the numerical codes described in Section 2 and listed in Appendices A-F. The dilution fields are then depth averaged, and averaged over the simulation period. In the sections that follow, dilution fields are contoured in base -10 log according to the color bar scale in the lower right-hand corner of each plot, with a scale range that covers dilution factors between 10^0 and 10^7 . Two separate perspectives of the worst-case results are given: 1) a composite dilution field when storm drains SDL-062, SDL-157 and SDL-186 are discharging simultaneously (Figure 30); and 2) the dilution field associated with each individual storm drain discharging in isolation under worst-case conditions (Figures 31-33). These dilution results are then applied to the peak TSS discharge fluxes to give TSS concentrations in the receiving water in mg/L in Figures 34-36.

4.1 Wet Weather Worst Case Dilution Results

Figure 30 shows the broad-scale view of the footprint of the dilution field for the wet weather worst case scenario (Wet-Weather Event-1) involving the simultaneous discharge from storm drains SDL-157, SDL-062 and SDL-186. In the broad-scale view, the dilution field of storm water spreads about a kilometer seaward of the shoreline due to vigorous cross shore mixing and advection from the storm winds and shoaling swells of the wet weather receiving water scenario. The dilution field of storm water from all three storm drains spreads about 2 kilometers along the shoreline, covering most of ASBS 29 and intruding into ASBS 31 under the advective influence of the longshore transport of rip current cells near the shoreline, while the tidal drift dominates the longshore spreading of the dilution field offshore, (cf. Figures 22 and 25). The dilution factors for the combined discharges from SDL-157, SDL-062 and SDL-186 in both ASBS 29 and ASBS 31 range between a minimum of 10^2 near shore to 10^7 along the seaward boundaries during the wet weather worst case. Dilution factors of 10^4 to 10^7 characterize the outer one-half of ASBS 29, while dilution factors 10^2 to 10^4 characterize the inner one-half. In the immediate neighborhood of SDL-157 and SDL-062, very near the shoreline of ASBS 29, dilution factors are as low as 40 to one.

Figures 31-33 allow us to examine the individual contributions to the combined storm water plume from each storm drain during the wet weather worst case from the monitoring program. It is clear from Figures 31 and 32 that the preponderance of the discharge plume is from SDL-157 and SDL-062, while SDL-186 at Devil's Slide (Figure 33) makes a very minor contribution. This is a fortuitous outcome in the sense that a significant amount of high-value, hard bottom marine habitat lives in the southern end of ASBS 29, and in the immediate neighborhood of SDL-186. Dilution factors of storm water discharged from SDL-186 are at most 10^3 near the shore in the nearfield of SDL-186 (Figure 33) and more typically 10^4 to 10^5 elsewhere along the bluff-faced shoreline of the southern end of ASBS 29. The largest single contributing footprint to the combined storm water plume appears to be from SDL-062 at the end of Avendia De La Playa (Figure 32) that produces a large patch with 10^2 minimum dilution very near the shoreline that spreads south along the shore to the La Jolla Beach and Tennis Club. The region influenced by

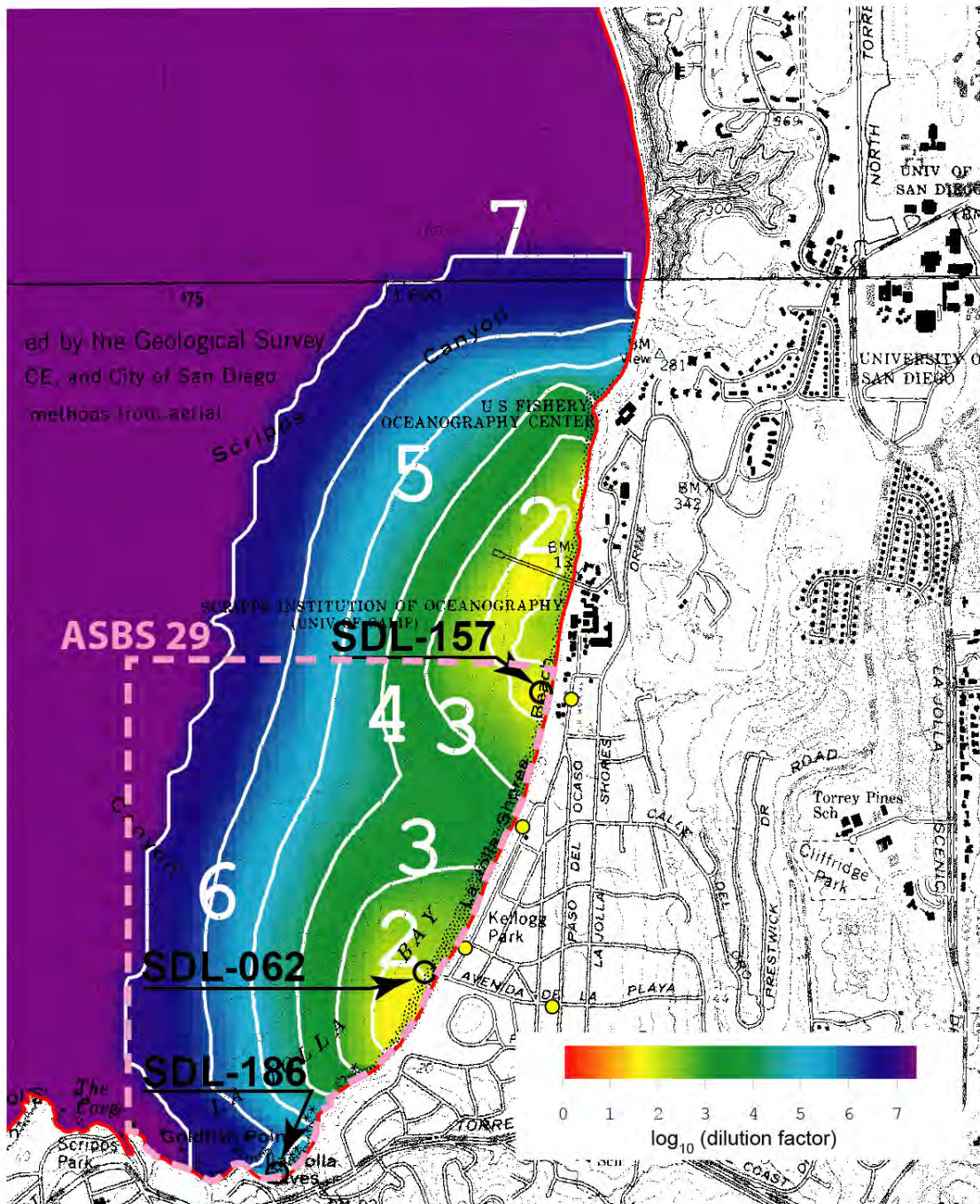


Figure 30. Depth averaged dilution for wet weather worst case due to simultaneous discharges of storm water from SDL-157, SDL-062 and SDL-186; 21 November 2011; waves: $H = 1.8$ m, $T = 14$ s, $\alpha = 283^\circ$; wind = 11 kts.

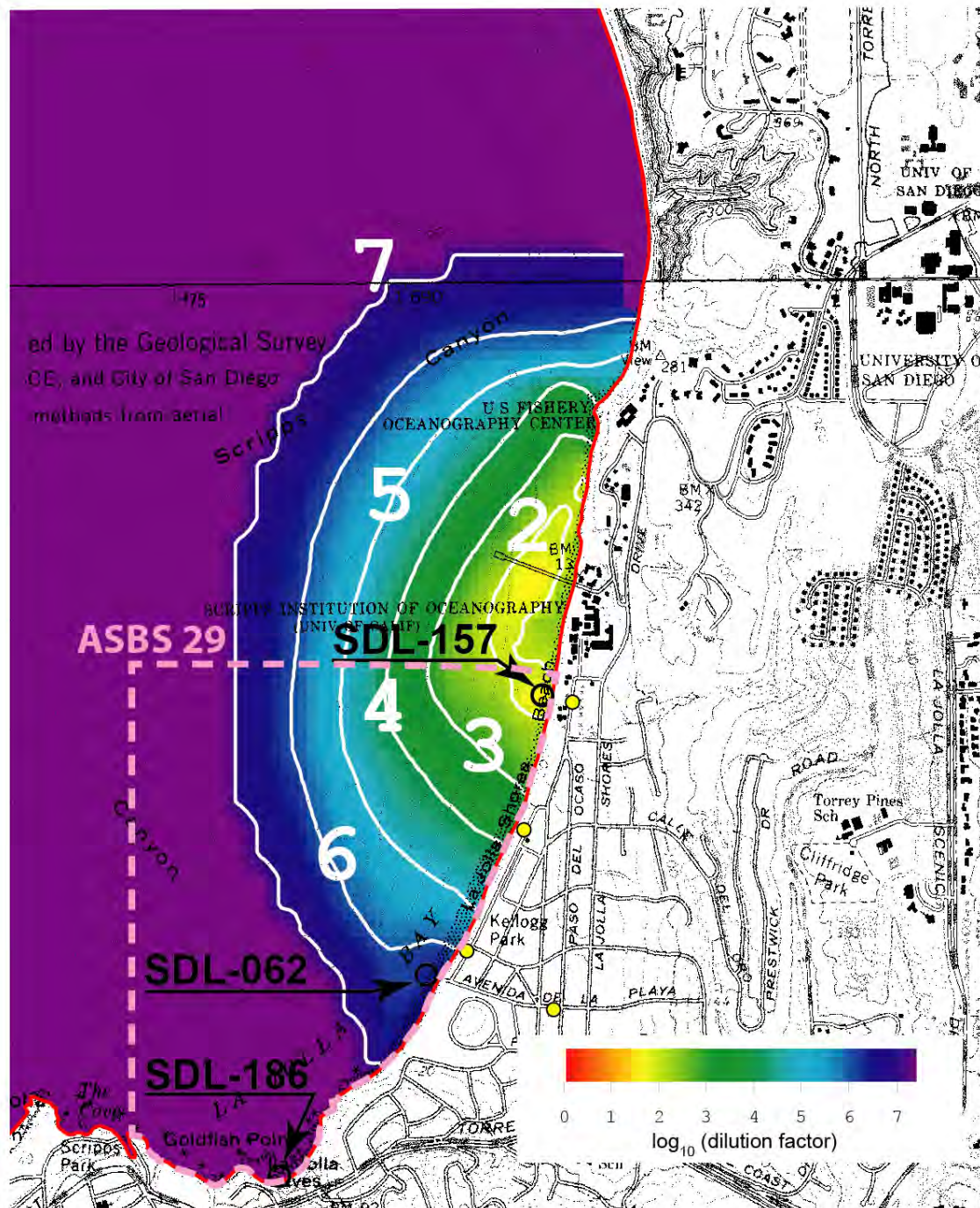


Figure 31. Depth averaged dilution for wet weather worst case due to isolated discharge of storm water from SDL-157; 12 November 2011; waves: $H = 1.8$ m, $T = 14$ s, $\alpha = 283^\circ$; wind = 11 kts.

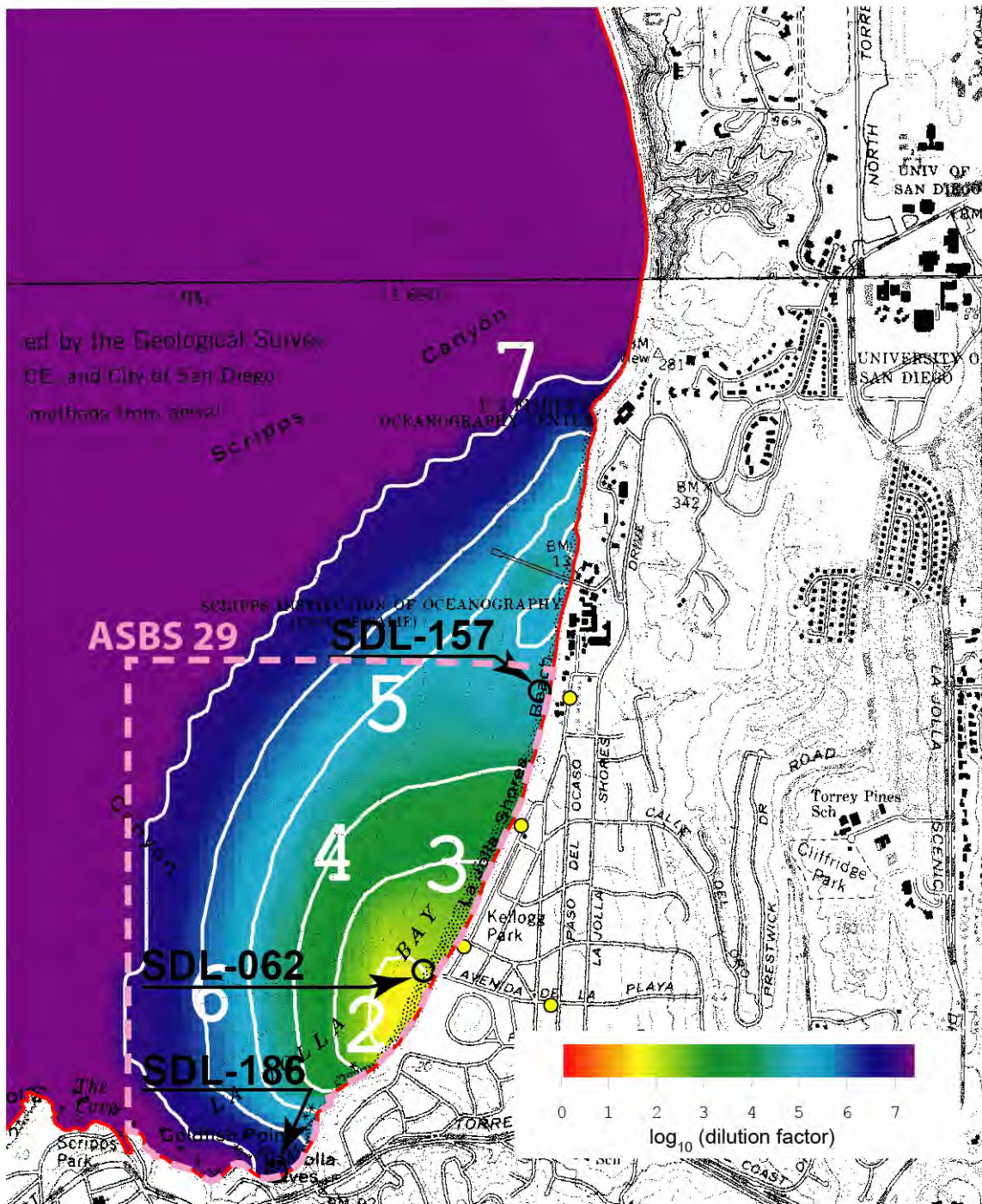


Figure 32. Depth averaged dilution for wet weather worst case due to isolated discharge of storm water from SDL-062; 21 November 2011; waves: $H = 1.8$ m, $T = 14$ s, $\alpha = 283^\circ$; wind = 11 kts.

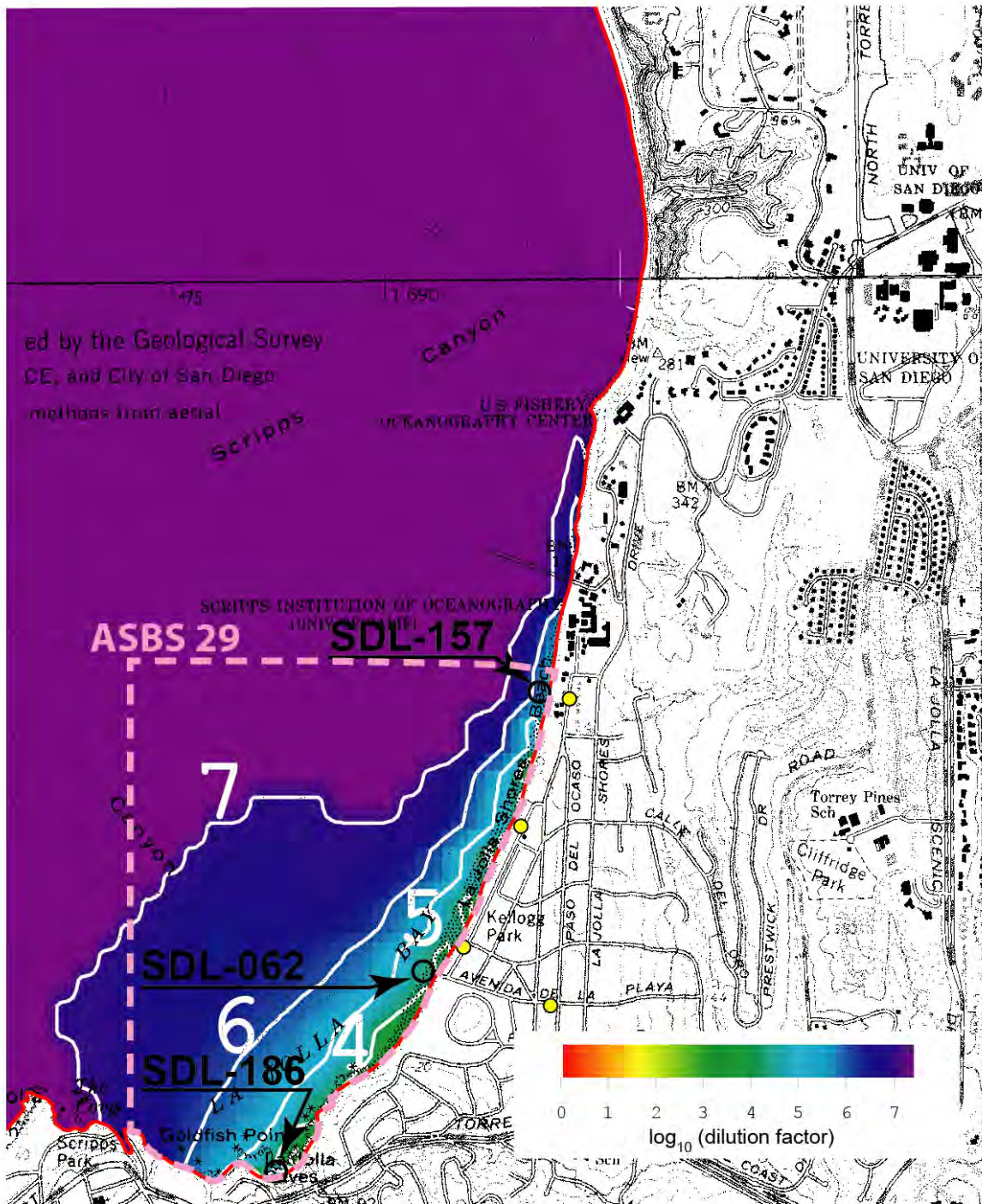


Figure 33. Depth averaged dilution for wet weather worst case due to isolated discharge of storm water from SDL-186; 21 November 2011; waves: $H = 1.8$ m, $T = 14$ s, $\alpha = 283^\circ$; wind = 11 kts.

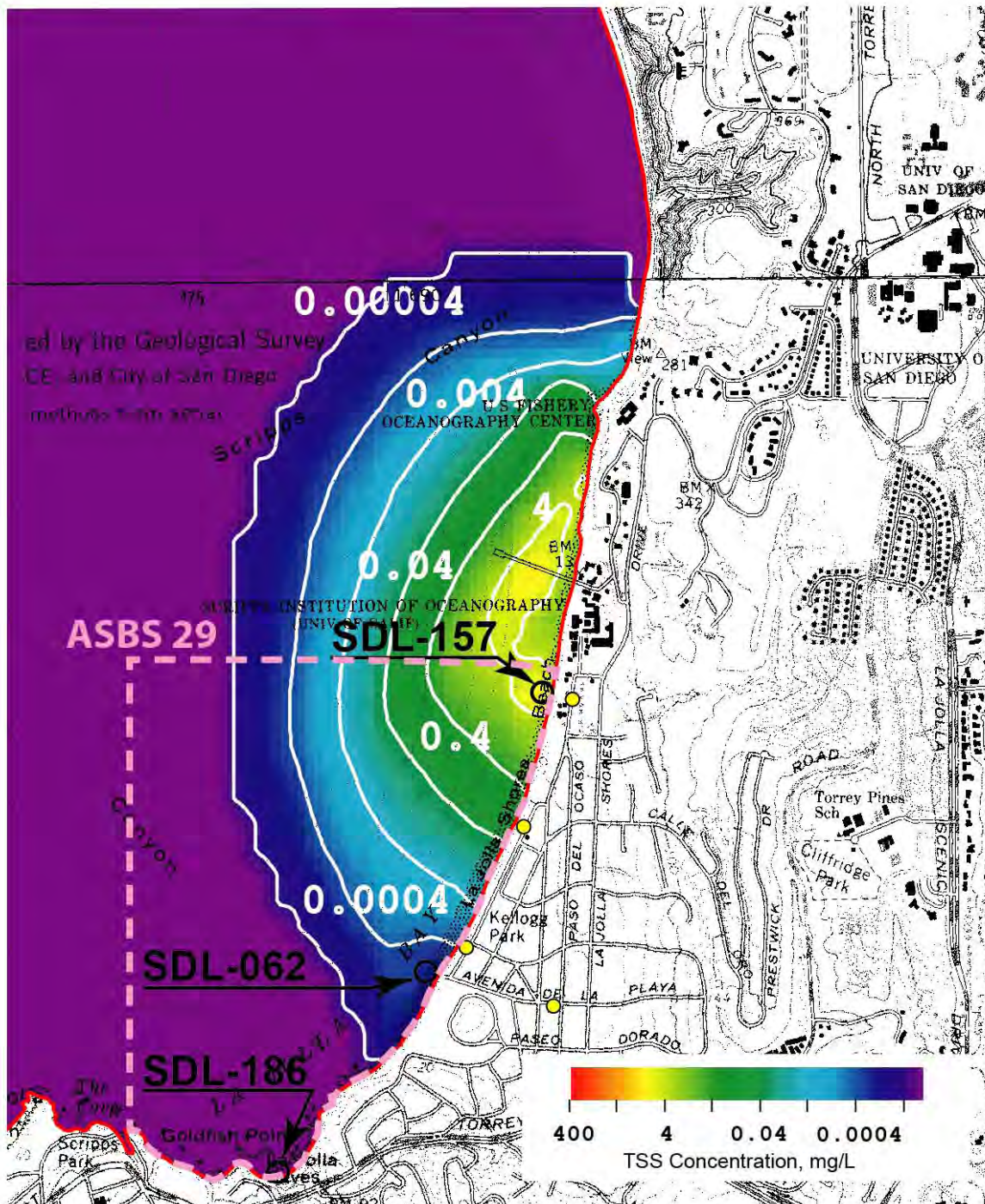


Figure 34. Depth averaged concentration of total suspended solids (TSS) for wet weather worst case due to discharge of storm water from SDL-157; 21 November 2011; waves: $H = 1.8$ m, $T = 14$ s, $\alpha = 283^\circ$; wind = 11 kts.

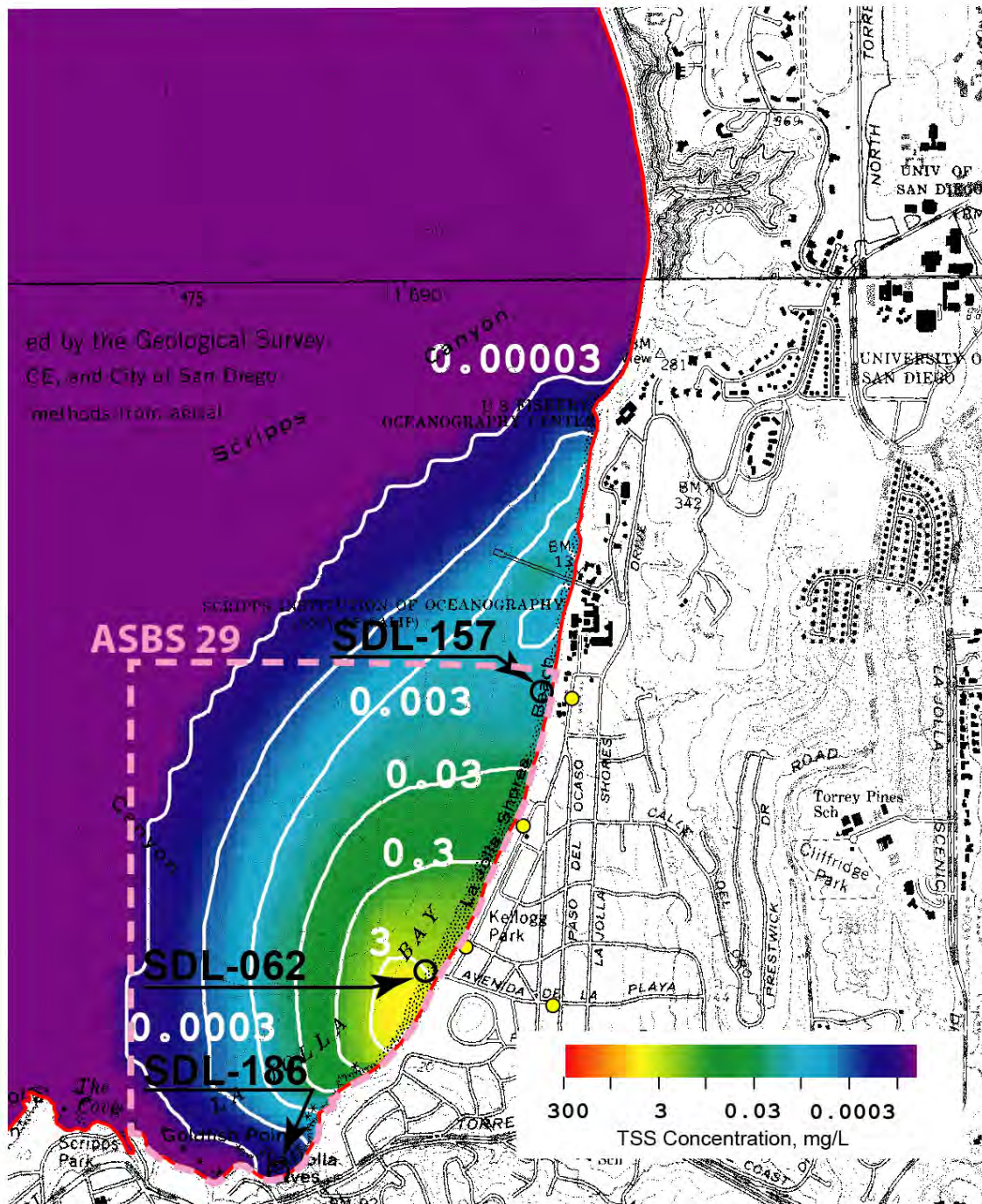


Figure 35. Depth averaged concentration of total suspended solids (TSS) for wet weather worst case due to discharge of storm water from SDL-062; 21 November 2011; waves: $H = 1.8$ m, $T = 14$ s, $\alpha = 283^\circ$; wind = 11 kts.

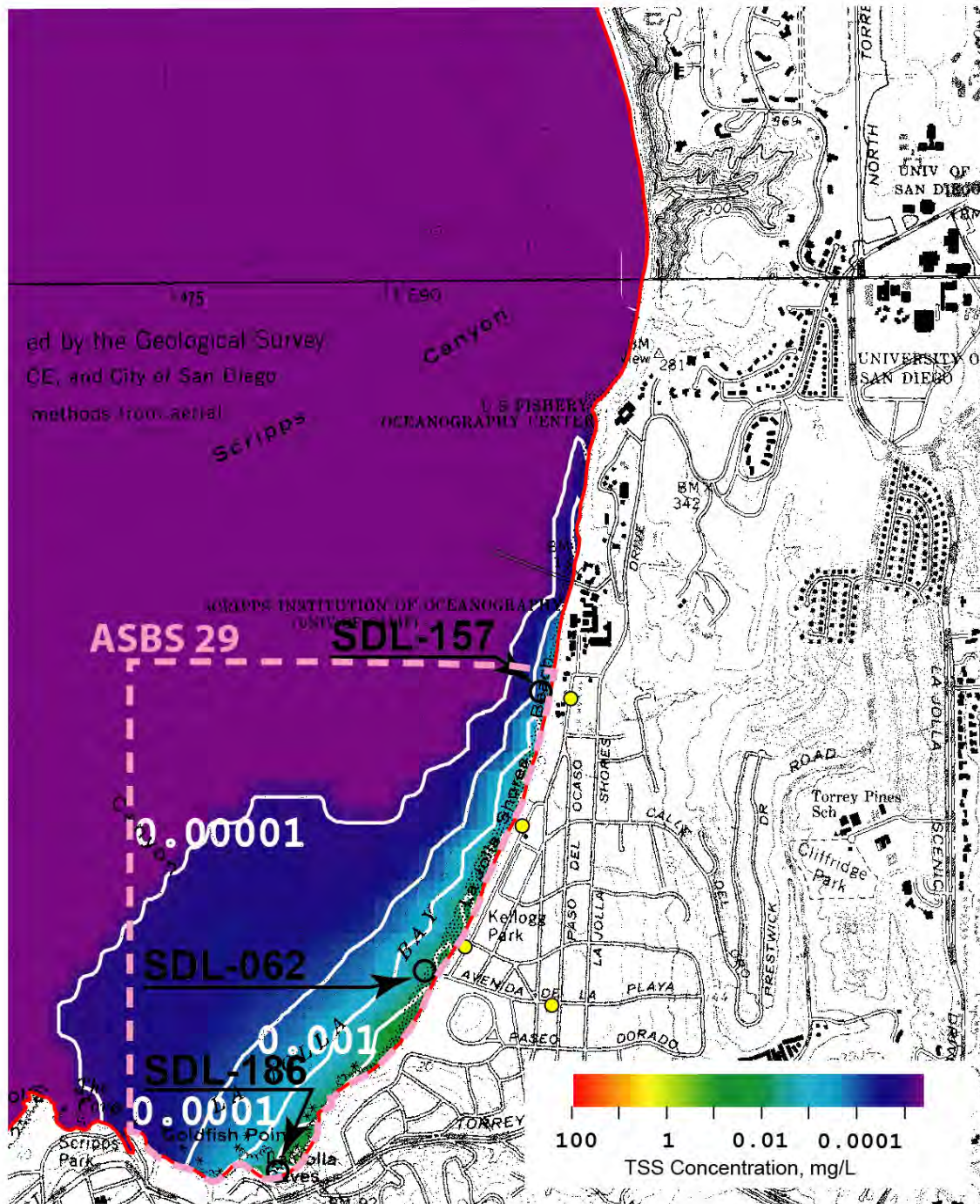


Figure 36. Depth averaged concentration of total suspended solids (TSS) for wet weather worst case due to discharge of storm water from SDL-186; 21 November 2011; waves: $H = 1.8$ m, $T = 14$ s, $\alpha = 283^\circ$; wind = 11 kts.

this feature from SDL-062 is sandy, soft-bottom marine habitat. SDL-157 produces another patch with 10^2 minimum dilution, but this feature moves offshore and intrudes into the southern end of ASBS 31 (Figure-31), where again the marine habitat is a sandy soft-bottom type.

Figures 34-36 the corresponding concentrations of total suspended solids (TSS) in the storm water plumes discharged by the individual storm drains during the wet weather worst case from the monitoring program. Maximum TSS concentrations in the receiving water due to SDL-186 storm water discharges are at most 0.001 mg/L near the shore in the nearfield of SDL-186 (Figure 36) and more typically 0.0001 mg/L elsewhere along the bluff-faced shoreline of the southern end of ASBS 29, where significant high-value, hard bottom marine habitat resides. The highest TSS concentrations in the receiving water around SDL-062 (at the end of Avendia De La Playa, see Figure 35), were found to be 3 mg/L in a nearshore patch that that spreads south along the shore to the La Jolla Beach and Tennis Club. Most of the shoreline impacted by SDL-157 experiences maximum TSS concentrations from storm water in the range of 0.3 mg/L to 0.03 mg/L, all of which is sandy soft- bottom marine habitat. At the northern end of ASBS 29, and extending into ASBS 31, maximum TSS concentrations in the receiving from SDL-157 are in the range of 4 mg/L to 0.4 mg/L, the highest anywhere in La Jolla Bay. These relatively higher TSS values are probably a consequence of the steep land forms that comprise the watershed of SDL-157, with portions of both developed and undeveloped coastal bluffs. Regardless, the marine habitat subjected to these TSS loadings from SDL-157 is sandy, soft-bottom habitat type.

4.2 Long Term Minimum Dilution in the Surf Zone and Offshore

Because of the disparity in length scales between dilution in the offshore region versus the surfzone, a separate analysis was performed on a nested fine scale grid covering the surf zone for a long shore reach that extended 1000 ft (305 meters) either side of the beach outfalls. The size of this grid was based on precedent already set for the definition of a zone of initial dilution (ZID) by the Regional Water Quality Control Board, San Diego. All 11,688 combinations of receiving water variables from Figures 6 and 20 were input for daily simulations of dilution using the numerical codes described in Section 2 and listed in Appendices A-F. The ZID was searched for the minimum dilution after averaging across the width of the surf zone. Source loading for these simulations were based on the discharges measured during Wet-Weather Event-1 from outfalls SDI-157, SDL-062 and SDL-186. The surfzone dilution results are then compared to minimum dilution on the sea surface at an offshore control point in ASBS 29 where local water depth is -10 m MSL (Figure-1).

Figure 37 presents a probability density function (red histogram) with corresponding cumulative probability (blue line) of the minimum surfzone dilution within the ZID for storm drain SDL-157 for an ensemble of 11,688 daily outcomes (32 years). The median outcome is a minimum dilution factor of 32 to 1 based on the historical sequence of receiving water variables found in Figures 6-8 and 20. However the potential range of minimum dilution within the ZID goes as high as 88 to 1, and as low as 15 to 1. Low energy, dry weather ocean mixing produced the 15 to 1 minimum dilution outcome, which had a probability of occurrence of 0.13%. Altogether, 90% of the potential outcomes produce minimum dilutions in the ZID greater than 20 to 1.

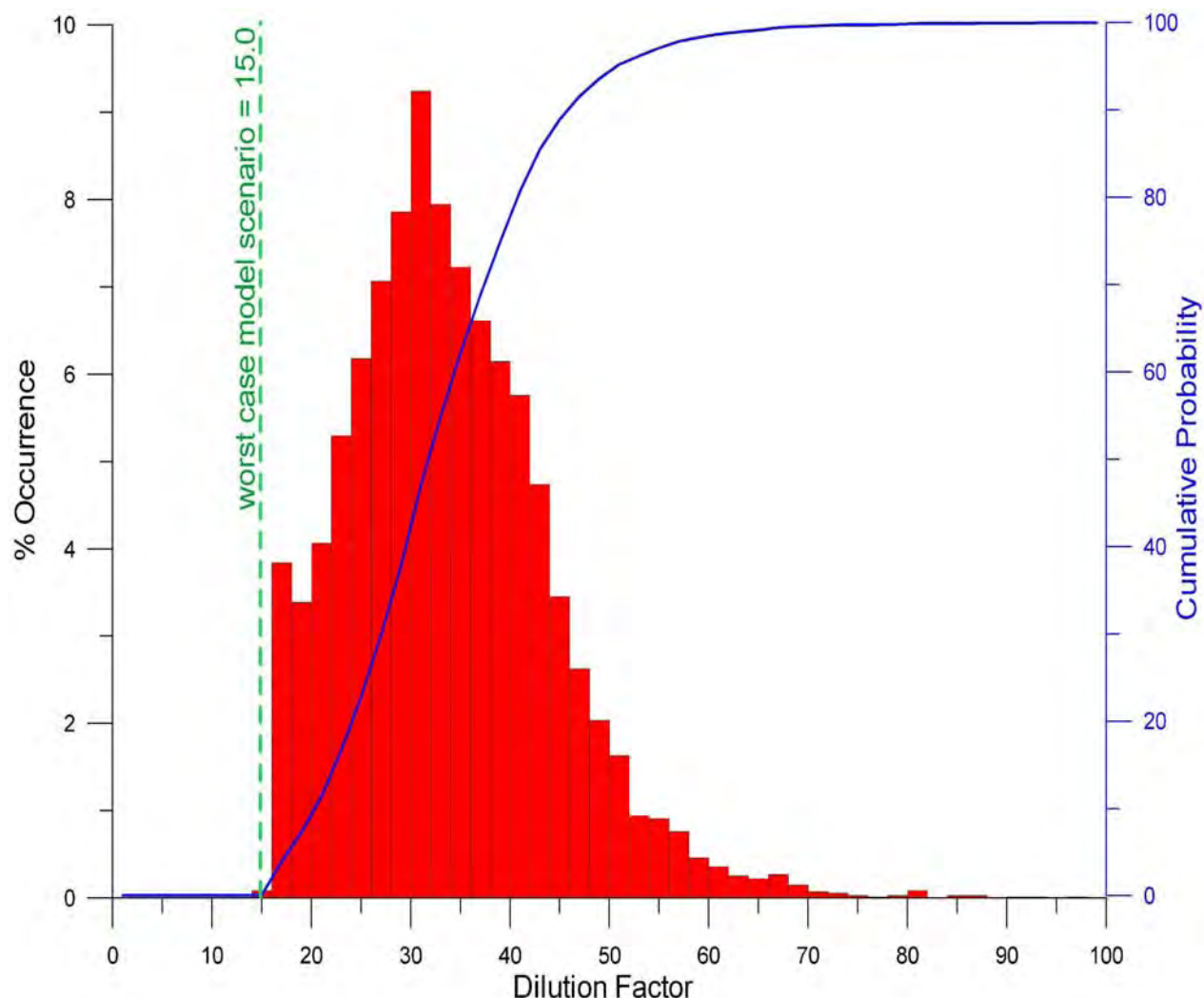


Figure 37. Probability density function (red) with corresponding cumulative probability (blue line) of the minimum surfzone dilution within the ZID around storm drain SDL-157. Derived from ocean boundary conditions and forcing functions, 1980-2012, 11,688 total numbers of realizations.

Minimum surfzone dilutions in the ZID off SDL-062 in Figure 38 are slightly less. This is due to the wave shadow found chronically in the refraction pattern of La Jolla Shores in the neighborhood of Avendia De La Playa (Figures 21 & 22). The minimum surfzone dilution of discharges from SDL-062 is found in Figure 38 to be 12.6 to 1, again a low energy, dry weather ocean mixing result. The median outcome of minimum surfzone dilution for SDL-062 is 22 to 1; while the potential range of minimum dilution goes as high as 64 to 1, based on the historical sequence of receiving water variables found in Figures 6-8 and 20. Ninety percent of the potential outcomes for SDL-062 produce minimum surfzone dilutions greater than 15 to 1.

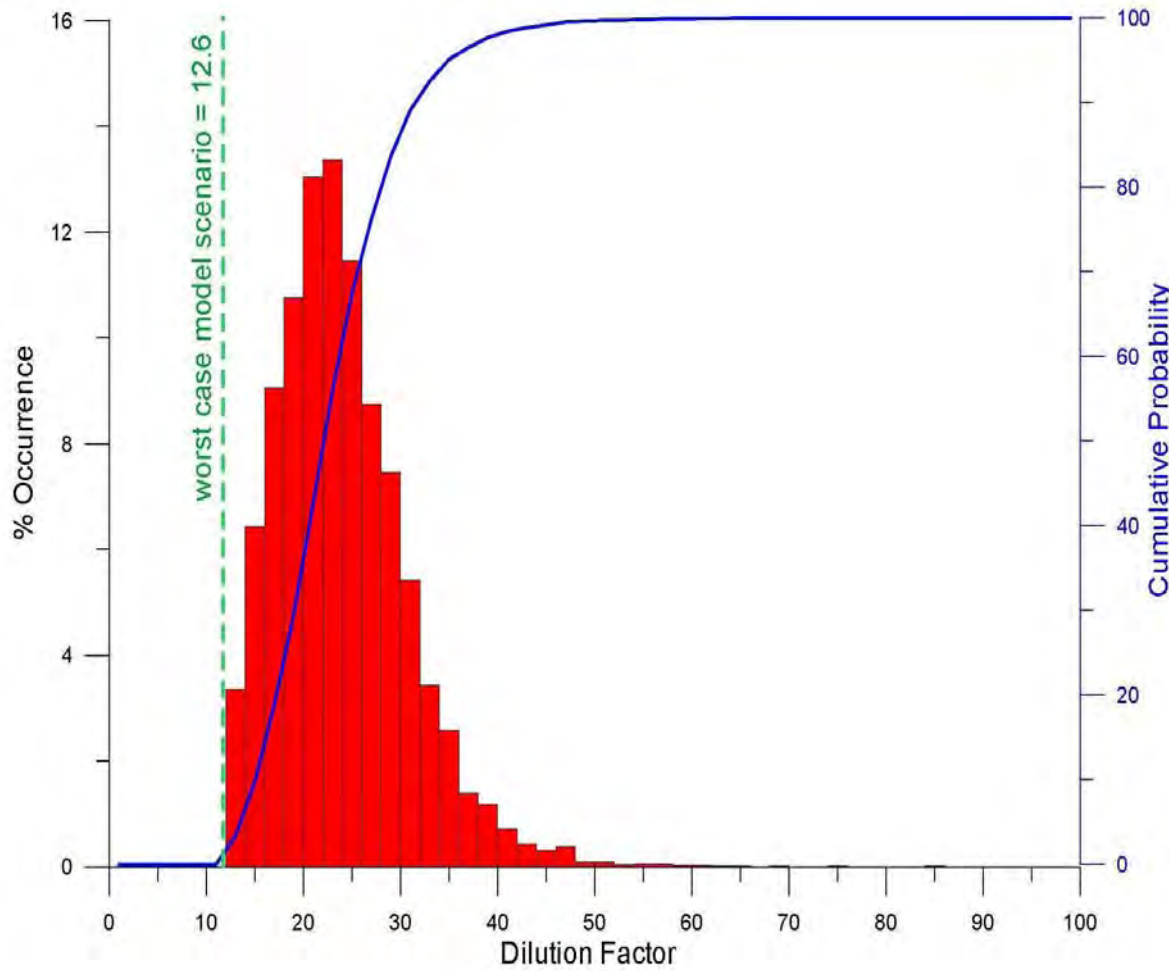


Figure 38. Probability density function (red) with corresponding cumulative probability (blue line) of the minimum surfzone dilution within the ZID around storm drain SDL-062. Derived from ocean boundary conditions and forcing functions, 1980-2012, 11,688 total numbers of realizations.

For comparison, probability statistics for minimum dilution are presented in Figure 39 at an offshore control point in ASBS 29 where local water depth is -10 m MSL (Figure-1). Here worst case minimum dilution of storm water is 13,200 to 1 while the median outcome from 11,688 model solutions is 52,000 to 1. The highest minimum dilutions of storm water at the offshore control point were found to be 4.2×10^5 . Consequently, storm water dilution is sufficiently high in the offshore regions of ASBS 29 that concentrations of storm water runoff constituents should be well below quantifiable detection limits.

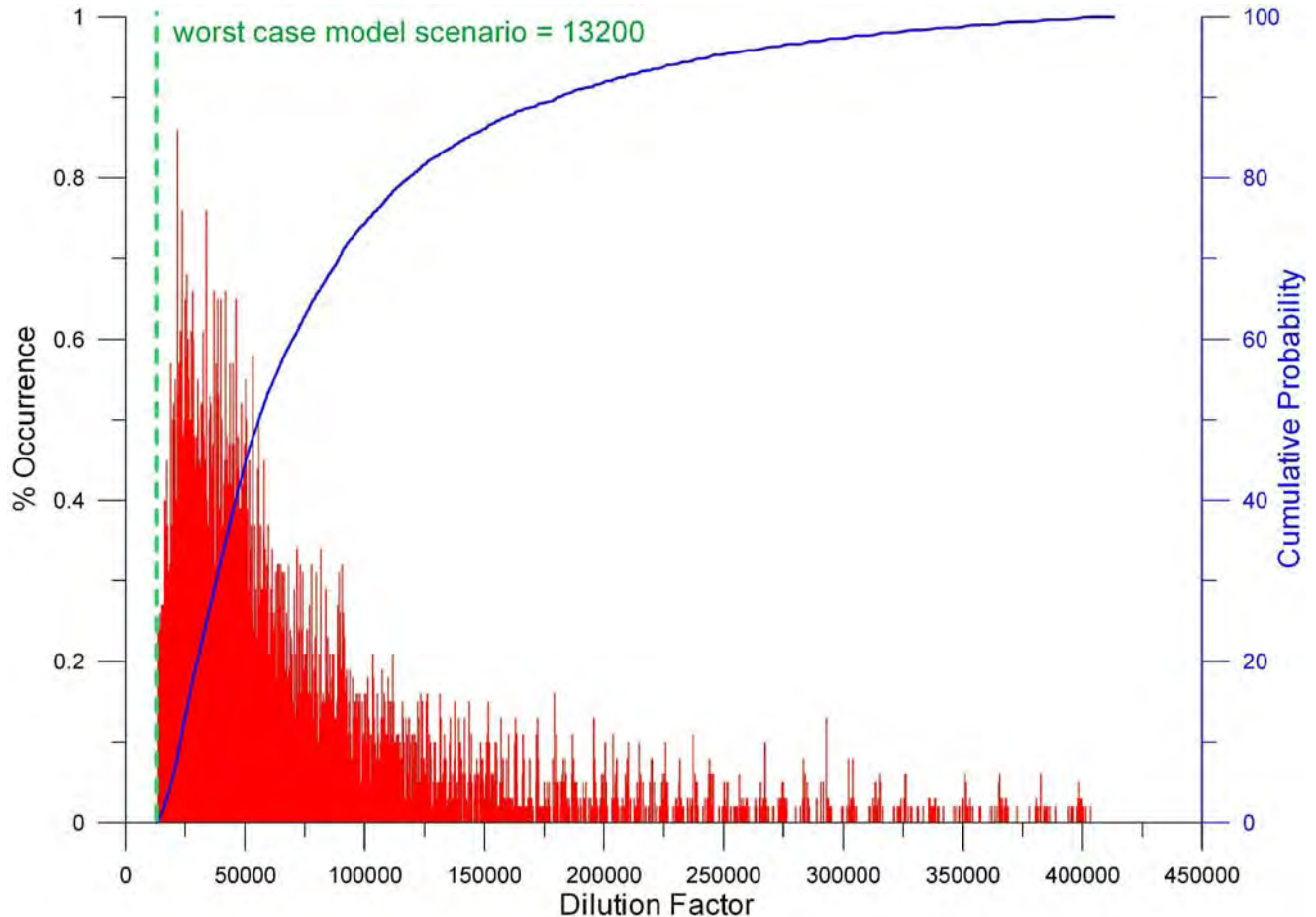


Figure 39. Probability density function (red) with corresponding cumulative probability (blue line) of the minimum dilution on the sea surface at offshore control point in ASBS 29. Derived from ocean boundary conditions and forcing functions, 1980-2012, 11,688 total numbers of realizations.

5.0 SUMMARY AND CONCLUSIONS:

During the 2011-2012 wet weather monitoring season (October 1, 2011 through April 30, 2012), storm water samples were collected from outfall discharge and receiving water mixing zone monitoring locations during three events (AMEC, 2012). These data were used to initialize the source loading inputs to a hydrodynamic model (*SEDXPORT*) used in the present receiving water analysis of storm water dilution and dispersion.

The *SEDXPORT* hydrodynamic modeling system was developed at Scripps Institution of Oceanography for the US Navy's *Coastal Water Clarity System* and *Littoral Remote Sensing Simulator*. This model has been peer reviewed multiple times and has been calibrated and validated in the Southern California Bight for six previous water quality and design projects.

Based on previous protocols established with the San Diego Regional Water Quality Control Board for storm drain dilution analysis in ASBS 31 (Jenkins and Wasyl, 2007), the numerical modeling study of the beach discharges is based on a wet weather worst-case scenario with a long-term probability assessment to bracket the envelope of the possible outcomes. Among the three wet-weather events monitored by AMEC (2012), Wet Weather Event-1 (20-21 November, 2011) comes closest to matching a computer search of marine environmental conditions for the wet-weather worst-case proxy. Analysis of the worst-case wet weather proxy was conducted over the entire coastal domain of La Jolla Bay and the Torrey Pines Littoral Sub-Cell.

The footprint of the dilution field for the wet weather worst case scenario, (involving the simultaneous discharge from storm drains SDL-157, SDL-062 and SDL-186), spreads about a kilometer seaward of the shoreline and about 2 kilometers along the shoreline, covering most of ASBS 29 and intruding into the southern portion of ASBS 31. The dilution factors of storm water in both ASBS 29 and ASBS 31 range between a minimum of 10^2 near shore to 10^7 along the seaward boundaries during the wet weather worst case. Dilution factors of 10^4 to 10^7 characterize the outer one-half of ASBS 29, while dilution factors 10^2 to 10^4 characterize the inner one-half. In the immediate neighborhood of SDL-157 and SDL-062, very near the shoreline of ASBS 29, dilution factors are as low as 40 to one.

The preponderance of the storm water discharge plume during the wet weather worst case scenario is from SDL-157 and SDL-062, while SDL-186 at Devil's Slide makes a very minor contribution. This is a fortuitous outcome in the sense that a significant amount of high-value, hard bottom marine habitat lives in the southern end of ASBS 29, and in the immediate neighborhood of SDL-186. Dilution factors of storm water discharged from SDL-186 are at most 10^3 near the shore in the nearfield of SDL-186, and more typically 10^4 to 10^5 elsewhere along the bluff-faced shoreline of the southern end of ASBS 29. The largest single contributing footprint to the combined storm water plume appears to be from SDL-062 at the end of Avenida De La Playa that produces a large patch with 10^2 minimum dilution very near the shoreline that spreads south along the shore to the La Jolla Beach and Tennis Club. The region influenced by this feature from SDL-062 is sandy, soft-bottom marine habitat. SDL-157 produces another patch with 10^2

minimum dilution, but this feature moves offshore and intrudes into the southern end of ASBS 31, where again the marine habitat is a sandy soft-bottom type.

Maximum concentrations of storm water born total suspended solids (TSS) in the receiving water due to SDL-186 storm water discharges are at most 0.001 mg/L near the shore in the nearfield of SDL-186, and more typically 0.0001 mg/L elsewhere along the bluff-faced shoreline of the southern end of ASBS 29, where significant high-value, hard bottom marine habitat resides. The highest TSS concentrations in the receiving water around SDL-062 (at the end of Avendia De La Playa), were found to be 3 mg/L in a nearshore patch that that spreads south along the shore to the La Jolla Beach and Tennis Club. Most of the shoreline impacted by SDL-157 experiences maximum TSS concentrations from storm water in the range of 0.3 mg/L to 0.03 mg/L, all of which is sandy soft-bottom marine habitat. At the northern end of ASBS 29, and extending into ASBS 31, maximum TSS concentrations in the receiving from SDL-157 are in the range of 4 mg/L to 0.4 mg/L, the highest anywhere in La Jolla Bay. These relatively higher TSS values are probably a consequence of the steep land forms that comprise the watershed of SDL-157, with portions of both developed and undeveloped coastal bluffs. Regardless, the marine habitat subjected to these TSS loadings from SDL-157 is a sandy, soft-bottom type.

Because of the disparity in length scales between dilution in the offshore region versus the surfzone, a separate analysis was performed on a nested fine scale grid covering the surf zone for a long shore reach that extended 1000 ft (305 meters) either side of the beach outfalls. The size of this grid was based on precedent already set for the definition of a zone of initial dilution (ZID) by the Regional Water Quality Control Board, San Diego. Thirty two years of receiving water variables (involving 11,688 distinct combinations) were input for daily simulations of dilution. The ZID was searched for the minimum dilution after averaging across the width of the surf zone. Source loading for these simulations were based on the discharges measured during Wet-Weather Event-1 from outfalls SDI-157, SDL-062 and SDL-186. The surfzone dilution results are then compared to minimum dilution on the sea surface at an offshore control point in ASBS 29 where local water depth is -10 m MSL.

This probability analysis procedure (based 11,688 historic combination of environmental variables) inevitably produces some combinations of wet weather discharges with dry weather ocean mixing conditions, and thereby results in certain worst case dilution scenarios that are more extreme, with even less dilution, than the wet weather worst case proxy derived from the monitoring program (Wet-Weather Event-1). For storm drain SDL-157, the median outcome for minimum dilution factor within the surfzone ZID is 32 to 1; however the potential range of minimum dilution goes as high as 88 to 1, and as low as 15 to 1. Low energy, dry weather ocean mixing produced the 15 to 1 minimum surfzone dilution outcome, which had a probability of occurrence of 0.13%. Altogether, 90% of the potential outcomes produce minimum dilutions in the surfzone ZID greater than 20 to 1.

Minimum surfzone dilutions in the ZID off SDL-062 are slightly less. This is due to the wave shadow found chronically in the refraction pattern of La Jolla Shores in the neighborhood of Avendia De La Playa. The minimum surfzone dilution of discharges from SDL-062 is found to be 12.6 to 1, again a low energy, dry weather ocean mixing result. The median outcome of minimum surfzone dilution for SDL-062 is 22 to 1; while the potential range of minimum dilution goes as high as 64 to 1, based on the 32-year historical sequence of receiving water variables. Ninety percent of the potential outcomes for SDL-062 produce minimum surfzone dilutions greater than 15 to 1.

For comparison, probability statistics for minimum dilution at an offshore control point in ASBS 29 (where local water depth is -10 m MSL) discovered a worst case minimum dilution of storm water of 13,200 to 1; while the median outcome is 52,000 to 1. The highest minimum dilutions of storm water at the offshore control point were found to be 4.2×10^5 . Consequently, storm water dilution is sufficiently high in the offshore regions of ASBS 29 that concentrations of storm water runoff constituents should be well below quantifiable detection limits.

6.0 REFERENCES AND BIBLIOGRAPHY

- Armi, L. A. (1979). *Effects of variations in eddy diffusivity on property distributions in the oceans*, Jour. of Mar. Res., v. 37, n. 3, p. 515-530.
- Berkoff, J. C. W. (1972). *Computation of combined refraction-diffraction*, Proc. 13th Coastal Eng. Conf., p. 471-490.
- Boas, M. L. (1966). *Mathematical Methods in the Physical Sciences*, John Wiley & Sons, Inc., New York, 778 pp.
- Coastal data information program (CDIP) (2001). University of California, San Diego (UCSD) Scripps Institution of Oceanography (SIO) Reference Series, 01-20 and <http://cdip.ucsd.edu>.
- Connor, J. J. and Wang, J.D. (1973). *Finite element modeling of two-dimensional hydrodynamic circulation*, MIT Tech Rpt., #MITSG 74-4, p. 1-57.
- Conte, S. D. and DeBoor, C. (1972). *Elementary Numerical Analysis*, Second Edition, McGraw-Hill Book Co., New York.
- Cox, R. A., and N. D. Smith (1959). *The specific heat of sea water*, Proc. Roy. Soc., A, 252, 51-62.
- Dalrymple, R. A., Kirby, J.T. and Hwang, P.A. (1984). *Wave diffraction due to areas of energy dissipation*, Jour. Waterway Port, Coast, and Ocean Engineering, v. 110, p. 67-79.
- DeGroot, S. R. and Mazur, P. (1984). *Non-Equilibrium Thermodynamics*, Dover Pub., Inc., New York, 510 pp.
- Durst, C. S. (1924). *The relationship between current and wind*, Quart. J. R. Met. Soc., v. 50, p. 113 (London).
- Finlayson, B. A. (1972). *The Method of Weighted Residuals and Variational Principles*, Academic Press.
- Flick, R.E. and Sterrett, E.H. (1994). *The San Diego Shoreline, Shoreline Erosion Assessment and Atlas of the San Diego Region*, Vol. 1, California Department of Boating and Waterways, 135 pp.
- Fujita, H. (1962). *Mathematical Theory of Sedimentation Analysis*. York: Academic, 315pp.
- Gallagher, R. H. (1981). *Finite Elements in Fluids*, John Wiley & Sons, New York, 290 pp.
- Goddard, L. and Graham, N.E. (1997). *El Niño in the 1990's*, Jour. Geophysical Res., v. 102, n. C5, p. 10,423-36.

- Inman, D. L., Nordstorm, C. E. and Flick, R. E. (1976). *Currents in submarine canyons: an air-sea-land interaction*, p. 275-310 in M. Van Dyke, et al (eds.), *Annual Review of Fluid Mechanics*, v. 8, 418 pp.
- Inman, D. L., Nordstorm, C. E. and Tait, R. J. (1971). *Mixing in the surf zone* Jour. Geophys. Res., v.76, no. 15, pp 3493-3514.
- Inman, D. L., Flick, R. E. and Guza, R. T. (1981). *Elevation and velocity measurements of laboratory shoaling waves*, J. Geophys. Res., 86(C5), 4149-4160.
- Inman, D. L. and Masters, P. M. (1991a). *Coastal sediment transport concepts and mechanisms*, Chapter 5 (43 pp.) in *State of the Coast Report, San Diego Region, Coast of California Storm and Tidal waves Study*, U. S. Army Corps of Engineers, Los Angeles District Chapters 1-10, Appen. A-I, 2 v.
- Inman, D. L. and Masters, P. M., (1991b). *Budget of sediment and prediction of the future state of the coast*, Chapter 9 (105 pp.) in *State of the Coast Report, San Diego Region, Coast of California Storm and Tidal Waves Study*, U. S. Army Corps of Engineers, Los Angeles District, Chapters 1-10, Appen. A-I; 2 v.
- Inman D. L. and Jenkins, S. A. (2006). *Thermodynamic solutions for equilibrium beach profiles*, Jour. Geophys. Res., v.3, C02003, doi:10.1029, 21pp.
- Inman, D. L. and Jenkins, S. A. (1999). *Climate change and the episodicity of sediment flux of small California rivers*, Jour. Geology, v. 107, p. 251–270. <http://repositories.cdlib.org/sio/cmng/2/>
- Inman, D. L. and Jenkins, S. A. (1997). *Changing wave climate and littoral drift along the California coast*, p. 538-49 in O. T. Magoon et al., eds., *California and the World Ocean '97*, American Society of Civil Engineers (ASCE), Reston, VA, 1756 pp.
- Inman, D. L. and Jenkins, S. A. (1996). *A chronology of ground mine studies and scour modeling in the vicinity of La Jolla*, UCSD SIO Reference Series 96-13, 26 pp.
- Inman, D. L. and Jenkins, S. A. (1985). *Erosion and accretion waves from Oceanside Harbor*, p. 591-3 in *Oceans 85: Ocean Engineering and the Environment*, Marine Technological Society & IEEE, v. 1, 674 pp.
- Inman D. L. and Jenkins, S. A. (1985). *On a submerged sphere in a viscous fluid excited by small amplitude periodic motion*, Jour. Fluid Mech., v. 157, p. 199-124.
- Inman, D. L., Jenkins, S. A. and Elwany, M. H. S. (1996). *Wave climate cycles and coastal engineering practice*, Coastal Engineering, 1996, Proc. 25th Int. Conf., (Orlando), ASCE, New York, v. 1, Ch 25, p. 314-27.

- Inman, D. L., Jenkins, S. A. and Elwany, M. H. S. (1993). *Shorerise and bar-berm profiles on ocean beaches*, Jour. Geophys. Res., 98(C10), p. 18, 181-199.
- Inman, D. L., Jenkins, S. A. and Van Dorn, W. G. (1981). *Evaluation of sediment management procedures*, UCSD SIO Reference Series No. 81-22, 212 pp.
- Inman D. L., Jenkins, S. A., Wasyl, J., Richardson, M. D., Wever, T.F. (2007). *Scour and burial mechanics of objects in the nearshore*, IEEE Jour.Oc.Eng, vol. 32, no. 1, pp 78-90.
- Inman D. L. and Komar, P. D. (1970). *Longshore sand transport of beaches*, Jour. Geophys. Res., v. 75, n. 30, p. 5914-5927.
- Inman, D. L., Pawka, S. S., Lowe, R. L., and Holmes, L. (1976). *Wave climate at Torrey Pines Beach, California*, U. S. Army Corps of Engineers, Coastal Engineering Research Center, Tech Paper 76-5, 372 pp.
- Jenkins, S. A., Paduan, J., Roberts, P., Schlenk, D., and Weis, J. (2012). *Management of Brine Discharges to Coastal Waters; Recommendations of a Science Advisory Panel*, submitted at the request of the California Water Resources Control Board, 56 pp. + App.
- Jenkins, S. A. and Skelly, D. W. (1989). *An evaluation of the coastal data base pertaining to seawater diversions at Encina Power Plant*, UCSD SIO Reference Series, #89-4, 52 pp.
- Jenkins, S. A. and Wasyl, J. (2007). *Hydrodynamic Modeling of Shoreline Discharges of Laboratory Seawater and Storm Water at Scripps Beach, CA*, submitted to UCSD Facilities Design and Construction, 266 pp.
- Jenkins, S. A. and Wasyl, J. (2005). *Coastal evolution model*, UCSD SIO Tech. Rpt. No. 58, 179 pp + appendices. <http://repositories.cdlib.org/sio/techreport/58/>
- Jenkins, S. A. and Wasyl, J. (1990). *Resuspension of estuarial sediments by tethered wings*, Jour. of Coastal Res., v. 6, n. 4, p. 961-980.
- Jenkins, S. A., Wasyl, J. and Aijaz, S. (1992). *Transport of fine sediment by hydrostatic jets*, Coastal and Estuarine Studies, American Geophysical Union, v. 42, p. 331-47.
- Jenkins, S. A., Wasyl, J. and Jenkins, S. A. (1989). *Dispersion and momentum flux study of the cooling water outfall at Agua Hedionda*, UCSD SIO Reference Series, #89-17, 36 pp.
- Jenkins, S. A., Wasyl, J., Cleveland, J. S., Talcott, J.C., Health, A.L., Goosby, S.G., Schmitt, K.F., and Leven, L.A. (1995). *Coastal water clarity modeling*, Science Applications International Corporation (SAIC), Tech. Rpt. 01-1349-03-4841-000, 491 pp.
- Jerlov, N.G. (1976). *Marine Optics*, Elsevier, Amsterdam, 231 pp.

- Kirby, J. T. (1986a). *Higher-order approximations in the parabolic equation method for water waves*, Jour. Geophys. Res., v. 91, C1, p. 933-952.
- Kirby, J. T. (1986b). *Rational approximations in the parabolic equation method for water waves*, Coastal Engineering, 10, p. 355-378.
- Kirby, J. T. (1986c). *Open boundary condition in the parabolic equation method*, Jour. Waterway, Port, Coastal, and Ocean Eng., 112(3), p. 460-465.
- Krone, R.B. (1962). *Flume Studies of the Transport of Sediment in Estuarial Shoaling Processes*, University of California, Berkeley Press, 69 pp.
- Lazara, B. J. and Lasheras, J. C. (1992a). *Particle dispersion in a developing free shear layer, Part 1, Unforced flow*, Jour. Fluid Mech. 235, p. 143-178.
- Lazara, B. J. and Lasheras, J. C. (1992b). *Particle dispersion in a developing free shear layer, Part 2, Forced Flow*, Jour. Fluid Mech., 235, p. 179-221.
- LePage, S. and Ware, R. (2001). *Assessment of biological impacts of the Agua Hedionda jetty restoration project*, Tech. Rpt. Submitted to Cabrillo Power 1LLC.
- List, E. J., Gartrell, G. and Winant, C. D. (1990). *Diffusion and dispersion in coastal waters*, Jour. Hydraulic Eng., v. 116, n. 10, p. 1158-79.
- Longuet-Higgins, M. S. (1970). *Longshore currents generated by obliquely incident waves*, Jour. Geophys. Res., v. 75, n. 33, p. 6778-6789.
- MACTEC. (2011a). *La Jolla Shores Area of Special Biological Significance (ASBS) Compliance Monitoring Work Plan*. October 2011. Prepared for the City of San Diego
- MACTEC. (2011b). *La Jolla Shores Area of Special Biological Significance (ASBS) Compliance Monitoring Work Plan Addendum*. November 2011. Prepared for the City of San Diego
- Martin, J. E. and Meiberg, E. (1994). *The accumulation and dispersion of heavy particles in forced two-dimensional mixing layers, 1: The fundamental and subharmonic cases*, Phys. Fluids, A-6, p. 1116-1132.
- National Oceanic and Atmospheric Administration (NOAA) (2000). *Verified/Historical Water Level Data*, http://www.opsd.nos.noaa.gov/data_res.html
- Neumann, G. (1952). *Ober die komplexe Natur des Seeganges, Teil 1 and 2*, Deut. Hydrogr. Zeit., v. 5, n. 2/3, p. 95-110, n. 5/6, p. 252-277.
- Neumann, G., Pierson, Jr., W. J. (1966). *Principles of Physical Oceanography*, Prentice-Hall, Inc., Englewood Cliffs, NJ, 545 pp.

- Nielsen, P. (1979). *Some basic concepts of wave sediment transport*, Series Paper No. 20, Institute of Hydrodyn. and Hydro. Eng., Tech. Univ. of Denmark.
- Oden, J. T. and Oliveira, E. R. A. (1973). *Lectures on Finite Element Methods in Continuum Mechanics*, The University of Alabama Press.
- Pawka, S. S. (1982). *Wave directional characteristics on a partially sheltered coast*, PhD dissertation, UCSD, 246 pp.
- PBS&J (2005). UCSD/SIO seawater separation and discharge” Appendix C of Jacobs and Associates design submission to UCSD Facilities, Design and Construction May 20, 2005, 10 pp + figs.
- Radder, A. C. (1979). *On the parabolic equation method for water-wave propagation*, J. Fluid Mech., 95, part 1, p. 159-176.
- Schmidt, W. (1917). *Wirkungen der ungeordneten Bewegungen im Wasser der Meere und Seen*, Ann. D. Hydr. u. Marit. Meteorol., vol. 45, p. 367-381.
- Schoonmaker, J. S., Hammond, R. R., Heath, A. L., and Cleveland, J. S. (1994). *A numerical model for prediction of sub-littoral optical visibility*, SPIE Ocean Optics XII, 18 pp.
- Scripps Institution of Oceanography (SIO) (2001). *SIO shore station, Scripps Pier*, <http://www-mrlrg.ucsd.edu/shoresta/mnSIOMain/siomain.htm>
- Stommel, H. (1949). *Horizontal diffusion due to oceanic turbulence*, Journal of Marine Research, v. VIII, n. 3, p. 199-225.
- Thorade, H. (1914). *Die Geschwindigkeit von Triftstormungen und die Ekman'sche Theorie*, Ann. D Hydr. u. Marit. Meteorol., v. 42, p. 379.
- University of California, San Diego (UCSD) (2005a). *Quarterly (January – March, 2005) Monitoring Report - Attachment C*, Discharge Order No. R9-2005-0008, NPDES Permit No. CA0107239. UCSD SIO. June 1, 2005.
- UCSD (2005b). *Quarterly (April – June, 2005) Monitoring Report - Attachment C*, Discharge Order No. R9-2005-0008, NPDES Permit No. CA0107239. UCSD SIO. Volume I. September 1, 2005.
- UCSD, (2005c). *Quarterly (January – March, 2005) Monitoring Report - Attachment B*, Discharge Order No. R9-2005-0008, NPDES Permit No. CA0107239. UCSD SIO. June 1, 2005.

- UCSD, (2005d). *Quarterly (April – June, 2005) Monitoring Report - Attachment B*, Discharge Order No. R9-2005-0008, NPDES Permit No. CA0107239. UCSD SIO. Volume I. September 1, 2005.
- UCSD, (2005e). *Semi-Annual (January – June, 2005) Monitoring Report*, Discharge Order No. R9-2005-0008, NPDES Permit No. CA0107239. UCSD SIO. Volume II. September 1, 2005.
- Weston Solutions, Inc. (2011). *La Jolla Shores Area of Special Biological Significance Regional Compliance Monitoring, 2010-2011, Final Report*. June, 2011. Prepared for the City of San Diego.
- Weston Solutions, Inc. (2010). *La Jolla Shores Area of Special Biological Significance Regional Compliance Monitoring, 2009-2010, Final Report*. June, 2010. Prepared for the City of San Diego.
- Weston Solutions, Inc. (2009). *La Jolla Shores ASBS Regional Compliance Monitoring, 2008-2009, Final Report*. June, 2009. Prepared for the City of San Diego.
- Weston Solutions, Inc. (2007). *La Jolla Shores Watershed Urban Runoff Characterization and Watershed Characterization Study, Final Report*. July, 2007. Prepared for the City of San Diego.
- Wang, H. P. (1975). *Modeling an ocean pond: a two-dimensional, finite element hydrodynamic model of Ninigret Pond, Charleston, Rhode Island*, Univ. of Rhode Island, Marine Tech. Rpt., #40, p. 1-58.
- Weiyan, T. (1992). *Shallow Water Hydrodynamics*, Water & Power Press, Hong Kong, 434 pp.
- White, W. B. and Cayan, D.R. (1998). *Quasi-periodicity and global symmetries in interdecadal upper ocean temperature variability*, Jour. Geophysical Res., v. 103, n. C10, p. 21,335-54.
- Winant, C. D. (1974). *Internal surges in coastal waters*, Jour. Geophys. Res., v. 79, n. 30, p. 4523-26.

AMEC, Environment & Infrastructure, Inc.
Hydrodynamic Modeling of Storm Drain Discharges in
the Neighborhood of ASBS 29 in La Jolla, California
Revised: 13 March 2013

APPENDIX A

GOVERNING EQUATIONS AND CODE FOR THE TIDE_FEM CURRENT MODEL

Appendix A: Governing Equations and Code for the TIDE_FEM Current Model

A finite element approach was adapted in preference to more common finite difference shallow water tidal models, e.g., Leendertse (1970), Abbott et al (1973), etc. Finite difference models employ rectangular grids which would be difficult to adapt to the complex geometry of the La Jolla Bay. It is believed that large errors would accumulate from attempting to approximate the irregular boundaries of the La Jolla Bay system with orthogonal segments. On the other hand, finite element methods allow the computational problem to be contained within a domain bounded by a continuous contour surface, such as the S_f contours stored within the *bathy* bathymetry file.

A finite element tidal hydraulics model, **TIDE_FEM**, [Inman and Jenkins, 1996] was employed to evaluate the tidal hydraulics of the La Jolla Bay (containing ASBS 31). **TIDE_FEM** was built from some well-studied and proven computational methods and numerical architecture that have done well in predicting shallow water tidal propagation in Massachusetts Bay [Connor and Wang, 1974] and estuaries in Rhode Island, [Wang, 1975], and have been reviewed in basic text books [Weiyan, 1992] and symposia on the subject, e.g., Gallagher (1981).

TIDE_FEM employs a variant of the vertically integrated equations for shallow water tidal propagation after Connor and Wang (1975). These are based upon the Boussinesq approximations with Chezy friction and Manning's roughness. The finite element discretization is based upon the commonly used *Galerkin weighted residual method* to specify integral functionals that are minimized in each finite element domain using a variational scheme, see Gallagher (1981). Time integration is based upon the simple *trapezoidal rule* [Gallagher, 1981]. The computational architecture of **TIDE_FEM** is adapted from Wang (1975), whereby a transformation from a **global** coordinate system to a **natural** coordinate system based on the unit triangle (see Figure A-1) is used to reduce the weighted residuals to a set of order-one ordinary differential equations with constant coefficients. These coefficients (*influence coefficients*) are posed in terms of a *shape function* derived from the natural coordinates of each nodal point. The resulting systems of equations are assembled and coded as banded matrices and subsequently solved by *Cholesky's method*, see Oden and Oliveira (1973 and Boas (1966).

Specifying the Shape Function $\langle N \rangle$ for any 3-Node Triangular Element

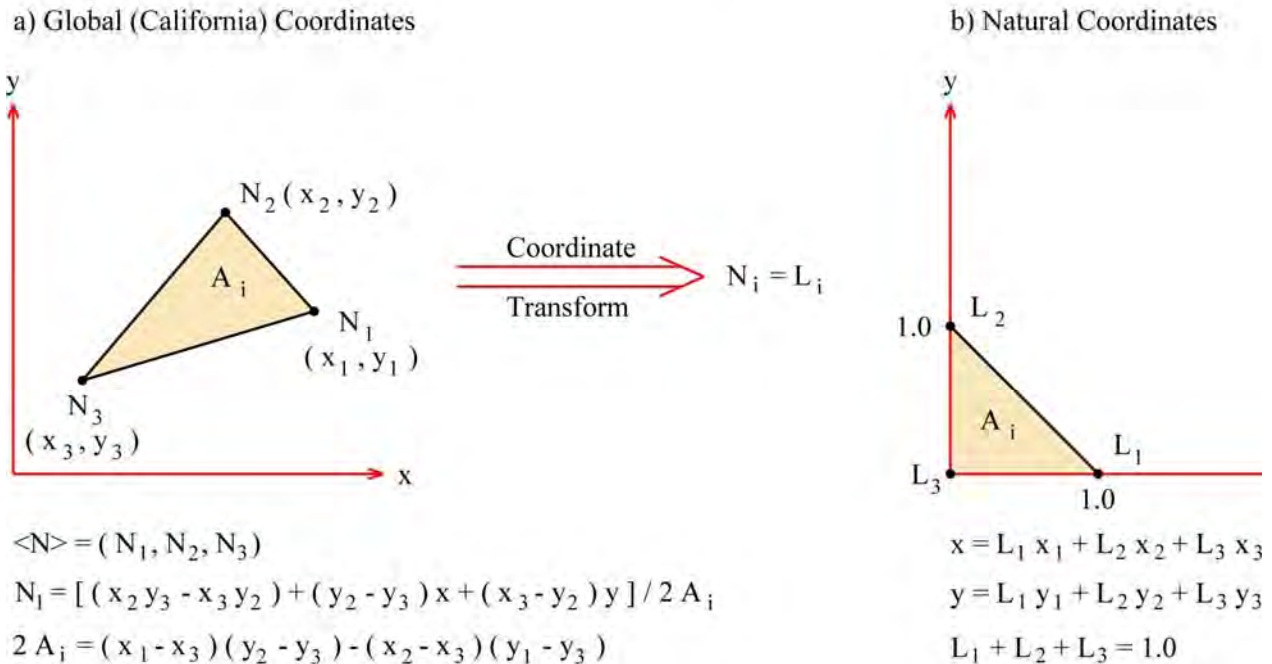


Figure A-1. Shape function polynomial and transform to natural coordinates for a generalized 3-node triangular element in the cross-shore plane

We adapt the California coordinates as our **global** coordinate system (x, y) to which the nodes in the computational mesh are referenced, with x (easting) and y (northing). The vertical coordinate z is fixed at 0.0 ft NGVD and is positive upward. The local depth relative to 0.0 ft NGVD is h and the mean surface elevation about 0.0 ft NGVD is η . The total depth of water at any node is $H = h + \eta$. The vertically averaged xy -components of velocity are (\bar{u}, \bar{v}) . The continuity and momentum equations may be written from Connor and Wang, (1974), as:

$$\begin{aligned}
 \frac{\partial}{\partial t} \rho H + \frac{\partial}{\partial x} q_x + \frac{\partial}{\partial y} q_y &= 0 \\
 \frac{\partial}{\partial t} q_x + \frac{\partial}{\partial x} \bar{u} q_x + \frac{\partial}{\partial y} \bar{u} q_y &= B_x + \frac{\partial}{\partial x} (F_{xx} - F_p) + \frac{\partial}{\partial x} F_{yx} \\
 \frac{\partial}{\partial t} q_y + \frac{\partial}{\partial x} \bar{v} q_x + \frac{\partial}{\partial y} \bar{v} q_y &= B_y + \frac{\partial}{\partial y} (F_{yy} - F_p) + \frac{\partial}{\partial x} F_{xy}
 \end{aligned}
 \tag{A2}$$

Here \mathbf{q}_x , \mathbf{q}_y are mass flux components

$$q_x = \rho \int_{-h}^{\eta} \bar{u} dz \quad (\text{A3})$$

$$q_y = \rho \int_{-h}^{\eta} \bar{v} dz \quad (\text{A4})$$

and \mathbf{q}_I is the mass flux through the ocean inlet due to water surface elevation changes in the estuary:

$$q_I = \rho \frac{\partial}{\partial t} \left(\frac{\partial s}{\partial \eta} \right) \quad (\text{A5})$$

\mathbf{F}_p is the pressure force resultant and \mathbf{F}_{xx} , \mathbf{F}_{xy} , \mathbf{F}_{yy} are "equivalent" internal stress resultants due to turbulent and dispersive momentum fluxes

$$\begin{aligned} F_p &= \int_{-h}^{\eta} p dz = \frac{\rho g H^2}{2} \\ F_{xx} &= 2\varepsilon \frac{\partial}{\partial x} q_x \\ F_{yy} &= 2\varepsilon \frac{\partial}{\partial y} q_y \\ F_{yx} = F_{xy} &= \varepsilon \left(\frac{\partial}{\partial y} q_y + \frac{\partial}{\partial x} q_x \right) \end{aligned} \quad (\text{A6})$$

and ε is the eddy viscosity. \mathbf{B}_x and \mathbf{B}_y are the bottom stress components

$$\begin{aligned} B_x &= \tau_x + \rho g H \frac{\partial h}{\partial x} \\ B_y &= \tau_y + \rho g H \frac{\partial h}{\partial y} \end{aligned} \quad (\text{A7})$$

In Equation (A7), τ_x and τ_y are the bottom shear stress components that are quasi-linearized by Chezy-based friction using Manning's roughness factor, \mathbf{n}_0 :

$$\begin{aligned}\tau_x &= -\frac{g}{\rho H^2 C_z^2} q_x (q_x^2 + q_y^2)^{1/2} \\ \tau_y &= -\frac{g}{\rho H^2 C_z^2} q_y (q_x^2 + q_y^2)^{1/2}\end{aligned}\tag{A8}$$

where C_z is the Chezy coefficient calculated as:

$$C_z = \frac{1.49}{n_0} H^{1/6}\tag{A9}$$

Boundary conditions are imposed at the locus of possible land/water boundaries, S_f in the *bathym* file and at the shoreline, S_0 . Flux quantities normal to these contours are denoted with "n" subscripts and tangential fluxes are given "s" subscripts. At any point along a boundary contour, the normal and tangential mass fluxes are:

$$\begin{aligned}q_n &= \int_{-h}^{\eta} \rho u_n dz = \alpha_{nx} q_x + \alpha_{ny} q_y \\ q_s &= \int_{-h}^{\eta} \rho u_s dz = -\alpha_{nx} q_x + \alpha_{ny} q_y \\ \alpha_{nx} &= \cos(n, x) \\ \alpha_{ny} &= \cos(n, y)\end{aligned}\tag{A10}$$

Components of momentum fluxes across a boundary are equivalent to internal force resultants according to:

$$\begin{aligned}F_{nx} &= \alpha_{nx} (F_{xx} - F_p) + \alpha_{ny} F_{yx} \\ F_{ny} &= \alpha_{ny} (F_{yy} - F_p) + \alpha_{nx} F_{xy}\end{aligned}\tag{A11}$$

On land boundary contours, the flux components are prescribed

$$q_n = q_s = 0 \quad \text{on land}\tag{A12}$$

On the deep water ocean boundary, the normal boundary forces (due to sea surface elevation) are continuous with ocean values, and the mass exchange is limited by the storage capacity of the estuary. Hence

$$F_{nm} = \bar{F}_{nm} \quad \text{and} \quad q_{nm} = q_l \quad \text{ocean boundary} \quad (\text{A13})$$

In the problem at hand \bar{F}_{nm} is prescribed on the shoreline by the ocean tidal elevation, η_0 , and the local depth, h_0 according to

$$\bar{F}_{nm} = \frac{\rho g}{2} (\eta_0 + h_0)^2 \quad \text{on } S_0 \quad (\text{A14})$$

Ocean *tidal forcing functions* η_0 were developed in Section 3.1. The ocean boundary condition as specified by Equation (A13) places a dynamic boundary condition on the momentum equations and a kinematic boundary condition on the continuity equation that is constrained by the storage rating curve. Solutions are possible by specifying only the dynamic boundary condition, but then mass exchanges are controlled by the wetting and drying of individual grid cells with associated discretization and interpolation errors which threaten mass conservation. The technique of over specifying the ocean boundary condition with both a dynamic and kinematic condition is discussed in the book by Weiyan (1992).

The governing equations (A2-A9) and the boundary conditions (A10-A13) are cast as a set of integral functionals in a variational scheme, [Boas, 1966]. Within the domain of each element of the mesh, A_i the unknown solution to the governing equations is simulated by a set of *trial functions* (\hat{H}, \hat{q}) having adjustable coefficients. The trial functions are substituted into the governing equations to form *residuals*, $(\mathbf{R}_H, \mathbf{R}_q)$. The residuals are modified by *weighting functions*, $(\Delta H, \Delta q)$. The coefficients of the trial functions are adjusted until the weighted residuals vanish. The solution condition on the weighted residuals then becomes:

$$\iint_{A_i} R_H \Delta H dA = 0$$

$$\iint_{A_i} R_q \Delta q dA = 0$$

By the Galerkin method of weighted residuals, [Finlaysen, 1972], the weighting functions are set equal to nodal *shape functions*, $\langle \mathbf{N} \rangle$, or:

$$\begin{aligned}\Delta H &\sim N_i \\ \Delta q &\sim N_j\end{aligned}$$

The shape function, $\langle \mathbf{N} \rangle$, is a polynomial of degree which must be at least equivalent to the order of the highest derivative in the governing equations. The shape function also provides the mechanism to discretize the governing equations. Figure A-1 gives the shape function polynomial in terms of *global (California)* coordinates for the first nodal point, \mathbf{N}_1 of a generalized 3-node triangular element of area \mathbf{A}_i . Wang (1975) obtained significant numerical efficiency in computing the weighted residuals when the shape functions of each nodal point, \mathbf{N}_i , are transformed to a system of *natural* coordinates based upon the unit triangle, giving $\mathbf{N}_i \rightarrow \mathbf{L}_i$ as detailed in Figure A-1. The shape functions also permit semi-discretization of the governing equations when the trial functions are posed in the form:

$$\begin{aligned}\hat{H}(x, y, t) &= \sum_i H_i(t) N_i(x, y) \\ \hat{q}(x, y, t) &= \sum_j q_j(t) N_j(x, y)\end{aligned}\tag{A15}$$

Discretization using the weighting and trial functions expressed in terms of the nodal shape functions allows the *distribution* of dependent variables over each element to be obtained from the values of the independent variables at discrete nodal points. However, the shape function at any given nodal point, say \mathbf{N}_1 , is a function of the independent variables of the two other nodal points which make up that particular 3-node triangular element, see Figure A-1. Consequently, the computations of the weighted residuals lead to a series of influence coefficient matrices defined by

$$\begin{aligned}
a_{ij} &= \frac{1}{A_i} \iint N_i N_j dA \\
s_{ij} &= \frac{1}{A_i} \iint N_i \frac{\partial N_j}{\partial x} dA \\
t_{ij} &= \frac{1}{A_i} \iint N_i \frac{\partial N_j}{\partial y} dA \\
g_{ijk} &= \frac{1}{A_i} \iint N_i N_j \frac{\partial N_k}{\partial x} dA \\
h_{ijk} &= \frac{1}{A_i} \iint N_i N_j \frac{\partial N_k}{\partial y} dA
\end{aligned} \tag{A16}$$

The influence coefficient matrices given by equation (A16) are evaluated in both global and natural coordinates. Once the influence coefficients have been calculated for each 3-node element, the weighted residuals reduce to a set of order-one ordinary differential with constant coefficients. The continuity equation becomes:

$$\begin{aligned}
\sum \left(a_{ij} \frac{dH_i}{dt} \right) &= - \sum_i \sum_k [g_{ijk} (H_i q_{xk} + H_k q_{xi}) + h_{ijk} (H_i q_{yk} + H_k q_{yi})] \\
\sum \left(a_{ij} \frac{dq_{xj}}{dt} \right) &= - \sum_j \sum_k [g_{ijk} (q_{xk} q_{xj}) + h_{ijk} (q_{yj} q_{xk})] + N_i \sum_j N_j S_{jj} + g \sum_i s_{ij} H_i \\
\sum \left(a_{ij} \frac{dq_{yj}}{dt} \right) &= - \sum_j \sum_k [g_{ijk} (q_{xj} q_{yk}) + h_{ijk} (q_{yj} q_{xk})] + N_i \sum_j N_j S_{jj} + g \sum_i t_{ij} H_i
\end{aligned} \tag{A17}$$

Equations (A17) are essentially simple oscillator equations forced by the collection of algebraic terms appearing on the right hand side; and are therefore easily integrated over time. The time integration scheme used over each time step of the tidal forcing function is based upon the *trapezoidal rule*, see Gallagher 1981) or Conte and deBoor (1972). This scheme was chosen because it is known to be unconditionally stable, and in tidal propagation problems has not been known to introduce spurious phase differences or damping. It replaces time derivatives between two successive times, $\Delta t = t_{n+1} - t_n$, with a truncated Taylor series. For the water depth it would take on the form:

$$\begin{aligned}\frac{dH}{dt} &= \eta(t) \\ H_{n+1} - H_n &= \frac{\Delta t}{2}(\eta_{n+1} + \eta_n) + E\Delta t \\ E &= \frac{1}{12}(\Delta t)^2 \left| \frac{d^2\eta}{dt^2} \right|\end{aligned}\tag{A18}$$

To solve equation (A18), iteration is required involving successive forward and backward substitutions.

Of particular interest are the *hydraulic friction slope coefficients*, S_{ff} , appearing as damping terms on the right hand side of equation (A17). Two separate formulations are used. One is given for the 3-node triangular elements situated in the interior of La Jolla Bay which do not experience successive wetting and drying during each tide cycle. The other formulation is used for the hydraulic friction slope coefficients for the elements situated along the wet and dry boundaries of the shoreline. These have been formulated as 3-node triangular elements with one curved side based upon the cubic-spline matrices developed by Weiyan (1992). The wet-dry boundary coordinates of the curved side, (x=, y=), are linearly interpolated for any given water elevation from the contours stored in the *bathym* file.

The influence and friction slope coefficient matrices together with the trapezoidal rule reduce equations (A16) and (A17) to a system of algebraic equations [Grotkop, 1973] which are solved by Cholesky's method per a numerical coding scheme by Wang (1975). For more details, refer to the TIDE_FEM code below, and Gallagher (1981) or Oden and Oliveira (1973).

Bathymetry errors are the most common cause of modeling errors. Other sources of errors include:

ELEMENT INTERPOLATION ERROR: Due to the degree of the polynomial used to specify shape function, N_i .

DISCRETIZATION ERRORS: Due to mesh coarseness and approximating the curved wet/dry boundary side of an element with a quadratic spline.

QUADRATURE ERRORS: Due to reducing the weighted residual integral with the influence coefficient matrices.

ITERATION ERRORS: Due to solving the system of algebraic equations reduced from the Galerkin Equations.

ROUND OFF ERRORS: Due to time integration by the trapezoidal rule.

SEA LEVEL ANOMALIES: Due to discrepancies between the astronomic tides and the actual observed water levels in the ocean.

INSUFFICIENT CALIBRATION DATA: Due to limitations in the period of record

The following is a listing of the TIDE_FEM code:

C..tide_fem.f

c..Finite element tidal hydraulics model using the Galerkin weighted
c..residual process to implement the finite element scheme
c..with Chezy based friction terms.
c..Adapted from Wang (1975) by Scott Jenkins and Joseph Wasyl.
c..7/16/04

c

```
dimension X(500), Y(500), H(500),B1(1000,100),B2(500,50),  
& U(500), V(500), ETA(500), UVP(500), EP(500),MEXT(500),  
& MINT(500), R1(1000),R2(500),A(20,1000),Q(1000),MB(500),  
& CMAN(1000),CHEZ(1000),AREA(1000),N1(1000),N2(1000),N3(1000),  
& MH(10),MLE(200),ANG(200),tide(500),time(500)  
character*12 tidein, bathym, nodes, datout, temp
```

c

```
open(20,file='tide_fem.inp',status='old')  
read(20,'(a12)')tidein  
read(20,'(a12)')bathym  
read(20,'(a12)')nodes  
read(20,'(a12)')temp  
read(20,'(a12)')datout
```

c

C..READ COMPUTATIONAL PARAMETERS

```
READ(20,280) NN,NM,NW  
280 FORMAT(3I10)  
READ(20,281) T,TLIM,DT,WW  
281 FORMAT(4F10.0)  
READ(20,282) ATTD,HA,WX,WY  
282 FORMAT(4F10.1)  
READ(20,283) STEP0,PUNCH  
283 FORMAT(2F10.0)  
READ(20,284) UNIT,UNAR  
284 FORMAT(2F10.0)  
READ(20,285) SILL  
285 FORMAT(F10.3)
```

C

```
open(21,file=bathym,status='old')  
open(22,file=nodes,status='old')  
open(23,file=tidein,status='old')  
open(24,file=datout,status='unknown')  
open(16,file=temp,status='unknown')
```

```
c
C..READ GLOBAL COORDINATE OF EACH NODE
  WRITE(16,298)
298  FORMAT(1H,' NODE NUMBER',5X,'X',9X,'Y',9X,'DEPTH',/)
  DO 205 I=1,NN
    READ(21,300)MEXT(I),MB(I),X(I),Y(I),H(I)
300  FORMAT(I4,I1,2F10.5,F3.1)
205  MINT(MEXT(I)=I
    WRITE(16,301)MEXT(I),I,MB(I),X(I),Y(I),H(I),I=1,NN
301  FORMAT(2(3I5,3F10.3))
C
C..READ ELEMENT DATA
C
  READ(22,302)N1(I),N2(I),N3(I),I=1,NM)
302  FORMAT(3I3)
  WRITE(16,303)
303  FORMAT(1H,' THE ELEMENT CONNECTIONS ',/)
  WRITE(16,304) (I,N1(I),N2(I),N3(I),I=1,NM)
304  FORMAT(5(I7,2X,3I4))
C
C..READ OPEN AND LAND BOUNDARY
C
  READ(22,306)MHNO,(MH(I),I=1,MHNO)
  READ(22,306)MLNO,(MLE(I),I=1,MLNO)
306  FORMAT(16I5)
  WRITE(16,307)MHNO
307  FORMAT(1H,'THERE ARE',I5,'NODES ON THE OPEN BOUNDARY')
  WRITE(16,309) (MH(I),I=1,MHNO)
  WRITE(16,308)MLNO
308  FORMAT(1H,'THERE ARE',I5,'NODES ON THE OPEN BOUNDARY')
  WRITE(16,309) (MLE(I),I=1,MLNO)
309  FORMAT(3X,15I5)
  READ(22,310)(ANG(I),I=1,MLNO)
310  FORMAT(8F10.4)
  WRITE(16,311)
311  FORMAT(1H,' THE OUTWARD DIRECTIONS ',/)
  WRITE(16,312)(MLE(I),ANG(I),I=1,MLNO)
312  FORMAT(5(I8,F10.4))
  STEBC=1.e10
  NBAND=0
  CRHO=0.00114
  G=32.174
  CDRAG=0.0025
```

```
F=3.141592/21600.0*SIN(ATTD/180.0*3.141592)
NWN=2*NW-1
NN1=NN*2
NW1=NW*2+1
CCX=CDRAG*CRHO*ABS(WX)*WX
CCY=CDRAG*CRHO*ABS(WY)*WY
C1=1.0/3.0
C2=1.0/3.0
C3=1.0/3.0
C4=1.0/12.0
C5=1.0/12.0
C6=1.0/12.0
C7=1.0/6.0
C8=1.0/6.0
C9=1.0/6.0
DO 201 I=1,NN
X(I)=X(I)*UNIT
201 Y(I)=Y(I)*UNIT
DO 202 I=1,MLNO
202 ANG(I)=ANG(I)*DATAN(6.1001)/45.0
DO 204 I=1,NN1
DO 204 J=1,NWN1
204 B1(I,J)=0.0
DO 203 I=1,NN
DO 203 J=1,NWN
203 B2(I,J)=0.0
C
C
DO 10 I=1,NM
N1(I)=MINT(N1(I))
N2(I)=MINT(N2(I))
N3(I)=MINT(N3(I))
L1=IABS(N1(I)-N2(I))+1
L2=IABS(N2(I)-N3(I))+1
L3=IABS(N3(I)-N1(I))+1
IF(NBAND.LT.L1) NBAND=L1
IF(NBAND.LT.L2) NBAND=L2
IF(NBAND.LT.L3) NBAND=L3
C
C..TRANSFER TO LOCAL COORDINATE
C
XP1=(2.0*X(N1(I))-X(N2(I))-X(N3(I)))/3.0
XP2=(2.0*X(N2(I))-X(N1(I))-X(N3(I)))/3.0
```

```

XP3=(2.0*X(N3(I))-X(N1(I))-X(N2(I)))/3.0
YP1=(2.0*Y(N1(I))-Y(N2(I))-Y(N3(I)))/3.0
YP2=(2.0*Y(N2(I))-Y(N1(I))-Y(N3(I)))/3.0
YP3=(2.0*Y(N3(I))-Y(N1(I))-Y(N2(I)))/3.0
C
C..CALCULATE ELEMENT AREA
C
  AREA=0.5*(XP2*YP3+XP1*YP2+XP3*YP1-XP2*YP1-XP3*YP2-XP1*YP3)
C
C..CALCULATE MANNING FACTOR
C
  CMAN(I)=0.03
C
C..CALCULATE COEFFICIENTS OF SHAPE FUNCTION
C
  A(1,I)=(XP2*YP3-XP3*YP2)/2.0*AREA(I)
  A(2,I)=(YP2-YP3)/2.0*AREA(I)
  A(3,I)=(XP3-XP2)/2.0*AREA(I)
  A(4,I)=(XP3*YP1-XP1*YP3)/2.0*AREA(I)
  A(5,I)=(YP3-YP1)/2.0*AREA(I)
  A(6,I)=(XP1-XP3)/2.0*AREA(I)
  A(7,I)=(XP1*YP2-XP2*YP1)/2.0*AREA(I)
  A(8,I)=(YP1-YP2)/2.0*AREA(I)
  A(9,I)=(XP2-XP1)/2.0*AREA(I)
C
C
  AREA(I)=AREA(I)*UNAR
  DIS1=SQRT((X(N1(I))-X(N2(I)))**2+(Y(N1(I))-Y(N2(I)))**2)
  DIS2=SQRT((X(N2(I))-X(N3(I)))**2+(Y(N2(I))-Y(N3(I)))**2)
  DIS3=SQRT((X(N3(I))-X(N1(I)))**2+(Y(N3(I))-Y(N1(I)))**2)
  DH1A=DIS1/SQRT(G*H(N1(I)))
  DH1B=DIS1/SQRT(G*H(N2(I)))
  DH2A=DIS2/SQRT(G*H(N2(I)))
  DH2B=DIS2/SQRT(G*H(N3(I)))
  DH3A=DIS3/SQRT(G*H(N3(I)))
  DH3B=DIS3/SQRT(G*H(N1(I)))
  IF(STEBC.GT.DH1A) STEBC=DH1A
  IF(STEBC.GT.DH1B) STEBC=DH1B
  IF(STEBC.GT.DH2A) STEBC=DH2A
  IF(STEBC.GT.DH2B) STEBC=DH2B
  IF(STEBC.GT.DH3A) STEBC=DH3A
  IF(STEBC.GT.DH3B) STEBC=DH3B
C

```

C..FORM THE GLOBAL MATRIX

C

```

  II=N1(I)
  JJ=N2(I)
  KK=N3(I)
  II1=NW
  JJ1=JJ-(II-NW)
  KK1=KK-(II-NW)
  B2(II,II1)=B2(II,II1)+C7*AREA(I)
  B2(II,JJ1)=B2(II,JJ1)+C4*AREA(I)
  B2(II,KK1)=B2(II,KK1)+C6*AREA(I)
  II1=II-(JJ-NW)
  JJ1=NW
  KK1=KK-(JJ-NW)
  B2(JJ,II1)=B2(JJ,II1)+C4*AREA(I)
  B2(JJ,JJ1)=B2(JJ,JJ1)+C8*AREA(I)
  B2(JJ,KK1)=B2(JJ,KK1)+C5*AREA(I)
  II1=II-(KK-NW)
  JJ1=JJ-(KK-NW)
  KK1=KK-NW
  B2(KK,II1)=B2(KK,II1)+C6*AREA(I)
  B2(KK,JJ1)=B2(KK,JJ1)+C5*AREA(I)
  B2(KK,KK1)=B2(KK,KK1)+C9*AREA(I)
10  CONTINUE
  WRITE(16,320) NBAND,STEBBC,UNAR
320  FORMAT(1H0,' THE BANDWIDTH = ',I5,' THE SMALLEST L/SQRT(GH) ='
    & ',F10.0,/,1H,' ELEMENT AREA (UNIT',F10.2,' SQRT FEET)')
  WRITE(16,321)(I,AREA(I),I=1,MN)
321  FORMAT(5(I6,F12.4))
  DO 12 I=1,NN
  DO 12 J=1,NWN
  B1(2*I-1,2*J)=B2(I,J)
12  B1(2*I,2*J)=B1(2*I-1,2*J)

```

C

C..ROTATE COORDINATE ON THE BOUNDARY

```

  LB1=NWN-1
  LB2=(NN1-NW1+2)/2
  DO 13 NI=1,MLNO
  I=MINT(MLE(NI))
  NMB=MB(I)
  GO TO (14,13,14,13),NMB
14  CALL ROTB1(B1,ANG(NI),NN1,NW1,NWN1,NW,I,LB1,LB2)
13  CONTINUE

```

```
      DO 23 NI=1,MLNO
      I=MINT(MLE(NI))
      NMB=MB(I)
      GO TO (15,23,15,21),NMB
15   DO 16 J=1,NWN1
16   B1(2*I-1,J)=0.0
      B1(2*I-1,NW1)=1.0
      GO TO 23
21   DO 22 J=1,NWN1
      B1(2*I-1,J)=0.0
22   B1(2*I,J)=0.0
      B1(2*I,NW1)=1.0
      B1(2*I-1,NW1)=1.0
23   CONTINUE
C
C..L U DECOMPOSE MATRIX
C
      CALL MATRIX(B1,NN1,NW1,NWN1)
      DO 17 NI=1,MHNO
      I=MINT(MH(NI))
      DO 18 J=1,NWN
18   B2(I,J)=0.0
      B2(I,NW)=1.0
17   CONTINUE
      CALL MATRIX(B2,NN,NW,NWN)
C
C
C..SET INITIAL VALUES
C
      READ(23,318)(I,TIDE(I),U(I),V(I),I=1,NN)
      DO 9 I=1,NN
      if(TIDE(I).GT.sill)THEN
      ETA(I)=TIDE(I)
      ELSE
      ETA(I)=SILL+0.00001
      ENDIF
      Q(2*I-1)=U(I)*(ETA(I)+H(I))
9   Q(2*I)=V(I)*ETA(I)+H(I)
C
      KL=0
      ML=0
      MLL=1
C
```

```

C..START SEMI-IMPLICIT METHOD
C
  IF(KL.EQ.ML*STEP0) GO TO 27
  GO TO 28
27  ML=ML+1
    TIM=T/60.0
    WRITE(16,315)TIM
315  FORMAT(/,' TIME='F10.2)
    WRITE(16,316)
316  FORMAT(2X,'ELEMENT TIDE  U VELOCITY V VELOCITY')
    WRITE(16,317)(I,MEXT(I),ETA(I),U(I),V(I),I=1,NN)
317  FORMAT(3(2I4,3F10.3))
28  IF(KL.EQ.MLL*PUNCH) GO TO 34
    GO TO 36
34  MLL=MLL+1
    WRITE(24,318)(I,ETA(I),U(I),V(I),I=1,NN)
318  FORMAT(I5,3F1.4,I5,3F11.4)
36  CALL WH(T,HH,WW,HA)
    DO 38 NI=1,MHNO
      I=MINT(MH(NI))
      ETA(I)=HH
38  CONTINUE
39  DO 40 I=1,NN
    R1(2*I-1)=0.0
40  R1(2*i)=0.0
    DO 42 I=1,NM
      UU=Q(2*N1(I)-1)**2+Q(N*N2(I)-1)**2+Q(2*N3(I)-1)**2
      VV=Q(2*N1(I))**2+Q(N*N2(I))**2+Q(2*N3(I))**2
      AVEG=((UU+VV)/3.0)**0.5
      HE1=H(N1(I))+ETA(N1(I))
      HE2=H(N2(I))+ETA(N2(I))
      HE3=H(N3(I))+ETA(N3(I))
      AVEG=((HE1+HE2+HE3)/3.0)**2
      CHEZ(I)=1.49/CMAN(I)*((HE1+HE2+HE3)/3.0)**(1.0/6.0)
      C746E=C7*ETA(N1(I))+C4*H(N2(I))+C6*ETA(N3(I))
      C485E=C4*ETA(N1(I))+C8*H(N2(I))+C5*ETA(N3(I))
      C659E=C6*ETA(N1(I))+C5*H(N2(I))+C9*ETA(N3(I))
      C746H=C7*H(N1(I))+C4*H(N2(I))+C6*H(N3(I))
      C485H=C4*H(N1(I))+C8*H(N2(I))+C5*H(N3(I))
      C659H=C6*H(N1(I))+C5*H(N2(I))+C9*H(N3(I))
      A258E=A(2,I)*ETA(N1(I))+A(5,1)*ETA(N2(I))+A(8,1)*ETA(N3(I))
      A369E=A(3,I)*ETA(N1(I))+A(6,1)*ETA(N2(I))+A(9,1)*ETA(N3(I))
      PREX1=G*(C746H+C746E)*A258E

```

$PREX2=G*(C485H+C485E)*A258E$
 $PREX3=G*(C659H+C659E)*A258E$
 $PREY1=G*(C746H+C746E)*A369E$
 $PREY2=G*(C485H+C485E)*A369E$
 $PREY3=G*(C659H+C659E)*A369E$
 $C746U=C7*Q(2*N1(I)-1)+C4*Q(2*N2(I)-1)+C6*Q(2*N3(I)-1)$
 $C485U=C4*Q(2*N1(I)-1)+C8*Q(2*N2(I)-1)+C5*Q(2*N3(I)-1)$
 $C659U=C6*Q(2*N1(I)-1)+C5*Q(2*N2(I)-1)+C9*Q(2*N3(I)-1)$
 $C746V=C7*Q(2*N1(I))+C4*Q(2*N2(I))+C6*Q(2*N3(I))$
 $C485V=C4*Q(2*N1(I))+C8*Q(2*N2(I))+C5*Q(2*N3(I))$
 $C659V=C6*Q(2*N1(I))+C5*Q(2*N2(I))+C9*Q(2*N3(I))$
 $QXX1=Q(2*N1(I)-1)**2/HE1$
 $QXX2=Q(2*N2(I)-1)**2/HE2$
 $QXX3=Q(2*N3(I)-1)**2/HE3$
 $QYY1=Q(2*N1(I))**2/HE1$
 $QYY2=Q(2*N2(I))**2/HE2$
 $QYY3=Q(2*N3(I))**2/HE3$
 $QXY1=Q(2*N1(I)-1)*Q(2*N1(I))/HE1$
 $QXY2=Q(2*N2(I)-1)*Q(2*N2(I))/HE2$
 $QXY3=Q(2*N3(I)-1)*Q(2*N3(I))/HE3$
 $CONU=(A(2,I)*QXX1+A(5,I)*QXX2+A(8,1)*QXX3+$
 $\&A(3,I)*QXY1+A(6,I)*QXY2+A(9,I)*QXY3)/3.0$
 $CONV=(A(2,I)*QXY1+A(5,I)*QXY2+A(8,1)*QXY3+$
 $\&A(3,I)*QYY1+A(6,I)*QYY2+A(9,I)*QYY3)/3.0$
 $GACA=G*AVEG/(CHEZ(I)**2)/AVEGH$
 $FRU1=GACA*C746U$
 $FRV1=GACA*C746V$
 $FRU2=GACA*C485U$
 $FRV2=GACA*C485V$
 $FRU3=GACA*C659U$
 $FRV3=GACA*C659V$
 $UK1=(CONU+PREX1-F*C746V-CCX+FRU1)*AREA(I)$
 $UK2=(CONU+PREX2-F*C485V-CCX+FRU2)*AREA(I)$
 $UK3=(CONU+PREX3-F*C659V-CCX+FRU3)*AREA(I)$
 $VK1=(CONV+PREY1-F*C746V-CCX+FRU1)*AREA(I)$
 $VK2=(CONV+PREY2-F*C485V-CCX+FRU2)*AREA(I)$
 $VK3=(CONV+PREY3-F*C659V-CCX+FRU3)*AREA(I)$
 $II=N1(I)$
 $JJ=N2(I)$
 $KK=N3(I)$
 $R1(II*2-1)=R1(II*2-1)-UK1$
 $R1(JJ*2-1)=R1(JJ*2-1)-UK2$
 $R1(KK*2-1)=R1(KK*2-1)-UK3$

```
      R1(II*2)=R1(II*2)-VK1
      R1(JJ*2)=R1(JJ*2)-VK2
42   R1(KK*2)=R1(KK*2)-VK3
      C
      T=T+DT/2.0
      DO 50 NI=1,MLNO
      I=MINT(MLE(NI))
      NMB=MB(I)
      GO TO (49,50,49,52),NMB
52   R1(2*I-1)=0.0
      R1(2*I)=0.0
      GO TO 50
49   CALL ROTUV(R1(2*I-1),R1(2*I),ANG(NI))
      R1(2*I-1)=0.0
50   CONTINUE
      CALL SOLVE(B1,R1,UEVP,NN1,NW1,NWN1)
      DO 53 NI=1,MLNO
      I=MINT(MLE(NI))
      NMB=MB(I)
      GO TO (54,53,54,53),NMB
54   CALL ROTUV(UEVP(2*I-1)+DT*UEVP(2*I),-ANG(NI))
53   CONTINUE
      DO 56 I=1,NN
      Q(2*I-1)=Q(2*I-1)+DT*UEVP(2*I-1)
56   Q(2*I)=Q(2*I)+DT*UEVP(2*I)
      DO 62 I=1,NN
      HE=H(I)+ETA(I)
      U(I)=Q(2*I-1)/HE
      V(I)=Q(2*I)/HE
62   R2(I)=0.0
      DO 64 I=1,NM
      EK=(A(2,1)*Q(2*(N1(I))-1)+A(5,1)*Q(2*(N2(I))-1)+
&   A(8,1)*Q(2*(N3(I))-1)+A(3,1)*Q(2*(N1(I))-1)
&   A(6,1)*Q(2*(N2(I)))+A(9,1)*Q(2*(N3(I))))/3.0*AREA(I)
      II=N1(I)
      JJ=N2(I)
      KK=N3(I)
      R2(II)=R2(II)-EK
      R2(JJ)=R2(JJ)-EK
64   R2(KK)=R2(KK)-EK
      T=T+DT/2.0
      CALL WHP(T,HP,WW,HA)
      DO 66 NI=1,NHNO
```

```
      I=MINT(MH(NI))
      EP(I)=HP
      R2(I)=EP(I)
66  CONTINUE
      CALL SOLVE(B2,R2,EP,NN,NW,NWN)
      DO 68 I=1,NN
68  ETA(I)=ETA(I)+DT*EP(I)
      KL=KL+1
      IF(T-TLIM) 25,25,70
70  STOP
      END
C
      SUBROUTINE WH(T,HH,WW,HA)
      HH=COS(2.0*3.141592*T/WW)*HA
      RETURN
      END
C
      SUBROUTINE WHP(T,HP,WW,HA)
      HP=-2.0*3.141592/WW*SIN(2.0*3.141592*(T/WW))*HA
      RETURN
      END
C
C..LU DECOMPOSITION
C
      SUBROUTINE MATRIX(A,N,NW,NWN)
      DIMENSION A(N,NWN)
      M=N-1
      DO 30 K=1,M
      I1=K+1
      NW1=NW+K-1
      IF(NW1.le.N) GO TO 20
      NW1=N
20  DO 30 I=I1,NW1
      NI=NW-1+I1
      Y=A(I,NI-1)/A(K,NW)
      A(I,NI-1)=Y
      NW11=NI+NW-2
45  DO 30 J=NI,NW11
      A(I,J)=A(I,J)-Y*A(K,J+I-K)
30  CONTINUE
      RETURN
      END
C
```

```
      SUBROUTINE SOLVE(A,B,X,N,NW,NWN)
      DIMENSION A(N,NWN),B(N),X(N)
      X(1)=B(1)
      K1=NW-1
      DO 60 K=2,N
      SUM=0.0
      NW2=NW-K+1
      IF(K.LE.NW) GO TO 54
      NW2=1
54   DO 55 J=NW2,K1
55   SUM=SUM+A(K,J)*X(J-NW+K)
60   X(K)=B(K)-SUM
      X(N)=X(N)/A(N,NW)
      K=N
      NW4=NW+1
62   SUM=0.0
      K=K-1
      NW3=NW+N-K
      IF(NW3.LT.NWN) GO TO 64
      NW3=NWN
64   DO 65 J=NW4,NW3
65   SUM=SUM+A(K,J)*X(J-NW+K)
      X(K)=(X(K)-SUM)/A(K,NW)
      IF(K.EQ.1) GO TO 80
      GO TO 62
80   RETURN
      END
C
C..COORDINATE POSITION
C
      SUBROUTINE ROTB1(B1,ANGLE,NN1,NWN1,NWNI,LB1,LB2)
      DIMENSION B1(NN1,NWN1)
      NWM=NW-1
      IF(I.LE.NW) GO TO 20
      LB=LB1
9    DO 10 J=NW,LB
      II=I-J+NW-1
      CALL ROTSM(B1(2*II-1,2*J+2),B1(2*II-1,2*J+3),B1(2*II,2*J+1),
      &B1(2*II,2*J+2),ANGLE)
      NWJ=4*NW-2*J
      B1(2*I,NWJ-2)=B1(2*II-1,2*J+2)
      B1(2*I,NWJ-3)=B1(2*II-1,2*J+3)
      B1(2*I-1,NWJ-1)=B1(2*II,2*J+1)
```

```
      B1(2*I-1,NWJ-2)=B1(2*II,2*J+2)
10  CONTINUE
      GO TO 30
20  IF(I.EQ.1)GO TO 30
      LB=I+NW-2
      GO TO 9
30  IF(I.GT.LB2 GO TO 60
      LB=1
50  DO 70 J=LB,NWM
      II=I-J+NW
      CALL ROTSM(B1(2*II-1,2*J),B1(2*II-1,2*J+1),B1(2*II,2*J-1),
&B1(2*II,2*J),ANGLE)
      NWJ=4*NW-2*J
      B1(2*I,NWJ)=B1(2*II-1,2*J)
      B1(2*I,NWJ-1)=B1(2*II-1,2*J)
      B1(2*I-1,NWJ+1)=B1(2*II-1,2*J-1)
      B1(2*I-1,NWJ)=B1(2*II,2*J)
70  CONTINUE
      GO TO 90
60  IF(I.EQ.NN1/2)GO TO 90
      LB=1+(I-LB2)
90  RETURN
      END
C
      SUBROUTINE ROTSM(SM1,SM2,SM3,SM4,ANGLE)
      SM1P=SM1*COS(ANGLE)+SM2*SIN(ANGLE)
      SM2=SM1*SIN(ANGLE)+SM2*COS(ANGLE)
      SM3P=SM3*COS(ANGLE)+SM4*SIN(ANGLE)
      SM4=SM3*SIN(ANGLE)+SM4*COS(ANGLE)
      SM1=SM1P
      SM3=SM3P
      RETURN
      END
C
      SUBROUTINE ROTUV(A,B,ANGLE)
      AP=A*COS(ANGLE)+B*SIN(ANGLE)
      B=A*SIN(ANGLE)+B*COS(ANGLE)
      A=AP
      RETURN
      END
C
```

AMEC, Environment & Infrastructure, Inc.
Hydrodynamic Modeling of Storm Drain Discharges in
the Neighborhood of ASBS 29 in La Jolla, California
Revised: 13 March 2013

APPENDIX B

CODE FOR THE TID_DAYS TIDAL FORCING MODEL

Appendix B:
Code for the TID_DAYS Tidal Forcing Model

```

c: Tidal Forcing Model TID_DAYS.FOR
c      Sep 23, 2004
c..only does 1 month at user selected interval TIMER
c..modified STORX and u2 arrays to 50000
c..outputs in feet NGVD
c....6 minute
C This program outputs the predicted tidal amplitudes at 1 hr
C intervals for a 24 hr period beginning at local time 00:00 of
C January of the year selected in the input file. The input file
C must contain the amplitude and phase of the local tidal constituents
C (up to 37 constituents).
C Uses Long's code for the prediction of tides using harmonic
C equations from U.S. Dept of Commerce SP #98 1988
C by Scott A. Jenkins & Joseph Wasyl
c
C*****
      character nameref*60,ifile*60
      LOGICAL      MKTABLE
      INTEGER      STARTDATE(3), BEGIN_DAY(12), END_DAY(12)
      INTEGER      MO(12)
      DIMENSION    A(37),   AMP(37),   PHASE(37)
      DIMENSION    SPD(37),  AMPA(37),  EPOCH(37)
      DIMENSION    STORX(50000)
      DIMENSION    YODE(37),  YVPU(37)
      DIMENSION    JDAYF(12), JDAYL(12), JWKDA(12)
C
C Tidal constituent speeds in degrees per hour
C
c Tidal constituents speed, amplitude, phase angle read from data
c file tideconst.dat (degrees/hr, feet, degrees)
c
c
      DATA      MO/ 1, 2, 3, 4, 5, 6, 7, 8, 9, 10, 11, 12 /
C
      DATA BEGIN_DAY/ 1, 1, 1, 1, 1, 1, 1, 1, 1, 1, 1, 1 /
C
      DATA END_DAY/ 31, 28, 31, 30, 31, 30, 31, 31, 30, 31, 30, 31 /
C
      COMMON /AC1/  SPD,   EPOCH,   AMPA
      COMMON /AC2/  STORX,   MO,  BEGIN_DAY,  END_DAY,

```

```
&      NUMCON, MKTABLE,      JP,  LPYR,
&      TIMER,  NOHRS
C
C PRELIMINARY CONSTANTS
C
  MKTABLE=.TRUE.           !MAKE A TABLE
  CON=2048./90.           !UNITS/DEG, DISCRETE COS LOOP
  NUMCON=37               !# OF TIDAL CONSTITUANTS
c* read from input file   TIMER=1. !# OF PREDICTIONS/HOUR
  NUM_MONTHS=12          !# OF MONTHS TO RUN
c
c
  open(25,file='tides1mo.inp',status='old')
c
  read(25,*)IYR
  read(25,*)IMO
  read(25,*)TIMER
  read(25,'(a)')nameref
  close(25)
c
  JP=IMO
c
  write(ifile,1000)nameref(1:LSTGDCCHR(nameref))
c
1000  format(a)
c
c.....tidal constituents from file name in input file 'tide_1yr.inp'
c
  open(26,file=ifile,status='old')
c
  do 49 ic=1,numcon
  read(26,*)A(ic),AMP(ic),PHASE(ic)
49  continue
c
  read(26,*)c1
  close(26)
c
  M2=AMP(1)
c
C COMPUTE INDEX OF THE WEEKDAY OF 1 JAN OF COMPUTATION YEAR
C (1=SUNDAY, 2=MONDAY, ... , 7=SATURDAY)
C
```

```

    IDAY11=1+MOD((IYR-1+INT(FLOAT(IYR-1)/4.)),7)
C
C CHECK FOR AND DEAL WITH LEAP YEAR
C
    LPYR=0
    NDAYS=365
    IF(MOD(IYR,4).EQ.0) THEN
        LPYR=1
        END_DAY(2)=29
        NDAYS=366
    END IF
C
C SET STARTING DATE
C
    STARTDATE(1)=IYR        !YEAR
    STARTDATE(2)=1         !MONTH
    STARTDATE(3)=1         !DAY
C
C SET EQUILIBRIUM ARGUMENTS (?)
C
    CALL EQU(NUMCON,STARTDATE,NDAYS,YODE,YVPU)
C
C OUTPUT CONTENTS OF YODE AND YVPU (COMMENT OUT IF NOT NEEDED)
C
C OPEN(11,FILE='EQUOUT.DAT',STATUS='UNKNOWN',FORM='FORMATTED')
C WRITE(11,'(1X," YODE(J)",7X," YVPU(J)",/)' )
C DO 10 J=1,NUMCON
C   WRITE(11,'(1X,F8.3," ----- ",F8.3)' ) YODE(J),YVPU(J)
C 10 CONTINUE
C CLOSE(11)
C
    WRITE(*,'(1X,/,1X,"Calculating tide predictions.",1X,/)' )
C
C CREATE OPERATING ARRAYS: AMPA, EPOCH, SPD
C
    DO 20 J=1,NUMCON
        AMPA(J)=AMP(J)*YODE(J)
        TEMX=YVPU(J)-PHASE(J)
        IF(TEMX .LT. 0.) TEMX=TEMX+360.
        EPOCH(J)=TEMX*CON
        SPD(J)=A(J)*CON/TIMER
    20 CONTINUE
C

```

```
C COMPUTE JULIAN START AND END DAYS AND WEEK DAY OF 1ST OF
C EACH MONTH BASED ON END_DAY ARRAY AND IDAY11
C
  JDAYF(1)=1
  JDAYL(1)=END_DAY(1)
  JWKDA(1)=IDAY11
  DO 25 N=2,12
    JDAYF(N)=JDAYL(N-1)+1
    JDAYL(N)=JDAYL(N-1)+END_DAY(N)
    JWKDA(N)=1+MOD( (JDAYF(N)+IDAY11-2) ,7)
  25 CONTINUE
C
C CALL ROUTINES TO DO TIDAL PREDICTION CALCULATIONS
C
C*****Only calculate month from input file*****
c..... DO 30 JP=1,NUM_MONTHS
  CALL CTIDE
  CALL TIDEOUT(M2,c1,IYR,IMO,IDAY,JDAYF(JP),JDAYL(JP),JWKDA(JP))
c..... 30 CONTINUE
C
  WRITE(*,'(1X,/,1X,"Tide calculations complete.")')
C
  END
C
C
C
C
  SUBROUTINE CTIDE
C
C COMPUTES TIMER PREDICTIONS PER HOUR OF THE TIDES AND
C STORES THE RESULT IN ARRAY STORX.
C NUMCON = MAX NUMBER OF TIDAL CONSTITUENTS
C MKTABLE = LOGICAL FLAG; WHEN .TRUE. IT MAKES A TABLE
C OF 8193 COSINES (SAVED IN ARRAY XCOS) THAT
C REPRESENT 360 DEGREES FOR A TABLE LOOK-UP OF
C THE TIDAL COSINE FUNCTION
C TABHR = HOURS TO THE BEGINNING OF EACH MONTH, OFFSET
C BY 24. FIRST 12 ELEMENTS FOR A NORMAL YEAR;
C SECOND 12 FOR LEAP YEAR.
C
  LOGICAL MKTABLE
  INTEGER BEGIN_DAY(12), END_DAY(12), MO(12)
  DIMENSION XCOS(8193), ARG(37)
```

```

    DIMENSION    SPD(37), EPOCH(37), AMPA(37)
    DIMENSION    TABHR(24), STORX(50000)
    DOUBLE PRECISION    H
C
    COMMON /AC1/    SPD,    EPOCH,    AMPA
    COMMON /AC2/    STORX,    MO, BEGIN_DAY,
&    END_DAY,    NUMCON, MKTABLE,
&    JP,    LPYR,    TIMER,
&    NOHRS
C
    DATA TABHR/ -24., 720., 1392., 2136., 2856., 3600.,
&    4320., 5064., 5808., 6528., 7272., 7992.,
&    -24., 720., 1416., 2160., 2880., 3624.,
&    4344., 5088., 5832., 6552., 7296., 8016./
C
    IF(MKTABLE) THEN
        H=8.D0*DATAN(1.D0)/8192.D0
        DO 10 I=1,8193
            XCOS(I)=SNGL(DCOS(DFLOAT(I-1)*H))
10    CONTINUE
        MKTABLE=.FALSE.
    END IF
C
C SET DATES AND TIMES
C
    NOD=END_DAY(JP)-BEGIN_DAY(JP)+1    !# OF DAYS
    NOHRS=(NOD*24)*NINT(TIMER)+1    !# OF SAMPLES
    NOHRS=NOHRS+24*NINT(TIMER)    !ADD 12 HRS AT ENDS
c.....NOHRS is the total number of tidal realizations
C
C FIRST = # OF ESTIMATION POINTS (HOURS*TIMER), COUNTING
C FROM 0000 1 JAN OF PREDICTION YEAR, OF FIRST PREDICTION
C
    FIRST=(TABHR(MO(JP))+12*LPYR)+24.*BEGIN_DAY(JP)*TIMER
    FIRST=FIRST-12.*TIMER    !START @ 1200, DAY 0
C
C*****
C START MAIN COMPUTATION LOOP    *
C*****
C
    DO 30 K=1,NOHRS
C
C SET NUMCON VALUES OF ARG(J)

```

```

C
  IF(K.EQ.1) THEN
    DO 40 J=1,NUMCON
      ARGU=SPD(J)*FIRST+EPOCH(J)
      ARG(J)=AMOD(ARGU,8192.)
      IF(ARG(J).LT.0.) ARG(J)=ARG(J)+8192.
40    CONTINUE
    ELSE
      DO 50 J=1,NUMCON
        ARG(J)=ARG(J)+SPD(J)
        IF(ARG(J).GE.8192.) ARG(J)=ARG(J)-8192.
50    CONTINUE
    END IF
C
C SUM NUMCON CONSTITUENT CONTRIBUTIONS FOR ONE TIDAL ELEVATION
C
  TIDE=0.
  DO 60 J=1,NUMCON
    NP=INT(ARG(J)+1.5)
    TIDE=TIDE+AMPA(J)*XCOS(NP)
60  CONTINUE
C
C SET FINAL OUTPUT
C
  STORX(K)=(TIDE+0.26)c..convert from feet MSL to feet NGVD C
30 CONTINUE
C
C*****
C END OF MAIN COMPUTATION LOOP          *
C*****
C
  RETURN
  END
C
C
C
C
  SUBROUTINE TIDEOUT(M2,c1,IYR,IMO,IDAY,JDAYB,JDAYE,JDAYW)
C
C WRITES TIDAL PREDICTION ARRAY AND COMPUTED TIME TO AN
C OUTPUT FILE.  JDAYB AND JDAYE ARE BEGINNING AND ENDING
C JULIAN DAYS OF THE JP'TH MONTH.  JDAYW IS THE WEEKDAY OF
C THE 1ST OF THE MONTH (1 = SUNDAY, 2 = MONDAY, ... ,

```

```

C 7 = SATURDAY)
C
  LOGICAL      MKTABLE
  CHARACTER*2   CYR
  CHARACTER*3   MONAME(12)
  CHARACTER*10  FNAME
  INTEGER      BEGIN_DAY(12), END_DAY(12), MO(12)
  DIMENSION    STORX(50000), u0(50000)
C
  COMMON /AC2/  STORX,      MO, BEGIN_DAY,
&             END_DAY,   NUMCON, MKTABLE,
&             JP,      LPYR,  TIMER,
&             NOHRS
C
  DATA MONAME/ 'Jan','Feb','Mar','Apr','May','Jun',
&             'Jul','Aug','Sep','Oct','Nov','Dec'/
C
C CORRECTION MINUTES, HOURS AND DAYS FOR OFFSET START TIME
C
  IMNOFF=0
  IHROFF=0
  IDAOFF=0
C
C NAME OUTPUT FILE
C
  WRITE(CYR,'(I2)') MOD(IYR,100)
  FNAME=MONAME(JP)//CYR//'.DAT'
  WRITE(*,*) ' Writing to ', FNAME
C
  OPEN(10,FILE=FNAME,STATUS='UNKNOWN',FORM='FORMATTED')
C
c*****comment out the bullshit headers*****
c  WRITE(10,'(2X,"Tides for ",A3," ",I4)') MONAME(JP), IYR
c  WRITE(10,'(2X,"Julian days ",I3," to ",I3)') JDAYB, JDAYE
c  WRITE(10,'(2X,I1," = weekday of ",A3," 1st",/)' ) JDAYW,
c  & MONAME(JP)
c  WRITE(10,'(2X," date/time",3X,"m (NGVD)",/)' )
C
  PLUSTIME=60./TIMER
  IMN=-PLUSTIME + IMNOFF      !START @ 0 MIN + FIX
  IHR=12 + IHROFF           !START @ NOON + FIX
  IDA=BEGIN_DAY(JP) - 1 + IDAOFF  !START @ DAY 0 + FIX
C

```

c*****only write out 00:00 day1 - 23:00 day 30,31,28,29)*****

TIMER12=TIMER*12
 NOHRS12T=NOHRS-12*NINT(TIMER)-1

c

DO 10 I=1,NOHRS
 IMN=IMN+PLUSTIME
 IF(IMN.GE.60) THEN
 IHR=IHR+1
 IMN=IMN-60
 END IF
 IF(IHR.GE.24) THEN
 IDA=IDA+1
 IHR=IHR-24
 END IF
 ITIME=100*IHR+IMN
 if(I.LE.TIMER12)go to 1111
 if(I.GT.NOHRS12T)go to 1111

c

Im1=I-1

c*****tide current module*****

eldif=(STORX(I)-STORX(Im1))
 u0(I)=(2.04*9.8*ABS(eldif)*M2/c1)**0.5
 if(eldif.LT.0)dir=0
 if(eldif.GE.0)dir=180

c*****

c

chrs=1.0*(I-TIMER12-1)/TIMER WRITE(10,'(F10.2,F10.4)')
 & chrs,STORX(I)
 1111 continue
 10 CONTINUE

C

CLOSE(10)

C

RETURN
 END

C

C

C

C

SUBROUTINE EQU(NSPED,IDT,LENGTH,FFF,VAU)

C

C CALCULATE TIDAL EQUILIBRIUM ARGUMENTS (VAU) AND NODE

C FACTORS (FFF). DEVELOPERS: E.E. LONG, B.B. PARKER,

C L. HICKMAN AND G. FRENCH. NOTES: VAU IS CALCULATED
C FOR THE BEGINNING OF THE SERIES; FFF IS ADJUSTED TO
C THE MIDPOINT OF THE YEAR BEING CALCULATED

C
CHARACTER*10 LNAME, LABEL(37)
DIMENSION NODAYS(12), FFF(37), VAU(37), IDT(3)
DIMENSION CXX(30), OEX(5)
DOUBLE PRECISION SPEED, SPD(37)

C
COMMON /LOCAT/ TM, GONL
COMMON /COSTX/ CXX, OEX
COMMON /FAD/ IPICK
COMMON /VEE/ TML, CON, U, Q, UI
COMMON /BOXA/ S, XL, PM, PL, SL, PS,
& PLM, SKYN, VI, V, XI, VPP
COMMON /BOXB/ VP, P, AUL, AUM, CRA, CQA
COMMON /BOXS/ AW, AI, AE, AE1, ASP

C
DATA NODAYS/ 31, 28, 31, 30, 31, 30, 31, 31, 30, 31, 30, 31 /

C
DATA LABEL/
& 'M(2) ', 'S(2) ', 'N(2) ', 'K(1) ',
& 'M(4) ', 'O(1) ', 'M(6) ', 'MK(3) ',
& 'S(4) ', 'MN(4) ', 'Nu(2) ', 'S(6) ',
& 'Mu(2) ', '2N(2) ', 'OO(1) ', 'Lambda(2) ',
& 'S(1) ', 'M(1) ', 'J(1) ', 'Mm ',
& 'Ssa ', 'Sa ', 'Msf ', 'Mf ',
& 'Rho(1) ', 'Q(1) ', 'T(2) ', 'R(2) ',
& '2Q(1) ', 'P(1) ', '2SM(2) ', 'M(3) ',
& 'L(2) ', '2MK(3) ', 'K(2) ', 'M(8) ',
& 'MS(4) ' /

C
C SET SOME VARIABLES:
C NSPED = NUMBER OF CONSTITUENTS TO BE CALCULATED
C MONTH = MONTH OF FIRST DATA POINT
C IDAY = DAY OF FIRST DATA POINT
C IYER = YEAR OF FIRST DATA POINT
C LENGTH = LENGTH (IN DAYS) OF SERIES TO BE GENERATED
C
IYER=IDT(1)
DAYB=0.0
GRBS=0.0

C

C DEAL WITH LEAP YEAR FEBRUARY, DAYS/YEAR AND MIDDLE DAY/TIME

C

IF(MOD(IYER,4) .EQ. 0) THEN

 NODAYS(2)=29

 NDAY=366

 DAYM=184.0

 GRMS=0.0

ELSE

 NODAYS(2)=28

 NDAY=365

 DAYM=183.0

 GRMS=12.0

END IF

C

 XYER=FLOAT(IYER)

C

C CALL ROUTINE TO COMPUTE BASIC ASTRONOMICAL CONSTANTS

C

 CALL ASTRO(XYER,DAYB,DAYM,GRBS,GRMS)

C

C MORE CONSTANTS FOR COMMON BLOCKS

C

 TM=0.0

 GONL=0.0

 TML=0.0

 JUDAY=IDT(3)

C

C LOOK UP CONSTITUENT PARAMETERS BY NAME MATCHING

C

 DO 10 J=1,NSPED

 LNAME=LABEL(J)

 SPEED=0.D0

 CALL NAME(SPEED,LNAME,ISUB,INUM,2)

 SPD(J)=SPEED

 CALL VANDUF(SPEED,E,F,1)

 FFF(J)=F

 VAU(J)=E

 10 CONTINUE

C

C ROUND NODE TO 3 DECIMAL PLACES, VO+U TO 1 DECIMAL PLACE

C

 DO 30 J=1,NSPED

 FFF(J)=ANINT(FFF(J)*1000.)*0.001

```
      VAU(J)=ANINT(VAU(J)*10.)*0.1
30 CONTINUE
C
  RETURN
  END
C
C
C
C
  SUBROUTINE ASTRO(XYER,DAYB,DAYM,GRBS,GRMS)
C
C COMPUTES ASTRONOMICAL CONSTANTS FOR THE YEAR BEGINNING
C DAY (DAYB) AND HOUR (GRBS) AND FOR THE YEAR MIDDLE DAY
C (DAYM) AND HOUR (GRMS)
C
  DIMENSION CXX(30), OEX(5)
C
  COMMON /LOCAT/  TM, GONL
  COMMON /COSTX/  CXX, OEX
  COMMON /VEE/    TML, CON, U, Q, UI
  COMMON /BOXA/   S, XL, PM, PL, SL, PS, PLM,
&               SKYN, VI, V, XI, VPP
  COMMON /BOXB/   VP, P, AUL, AUM, CRA, CQA
  COMMON /BOXS/   AW, AI, AE, AE1, ASP
  COMMON /BOXXS/  VIB, VB, XIB, VPB, VPPB, CXSB, CXPB,
&               CXHB, CXP1B
C
  PINV = 57.29578          !degrees/radian
C
C ORBIT SETS LUNAR AND SOLAR MEAN LATITUDES FOR THE BEGINNING OF
C THE CENTURY CONTAINING THE TIDE YEAR XYER (FROM TABLE 1 IN
C S.P. 98)
C
  CALL ORBIT(XCEN,XSX,XPX,XHX,XP1X,XNX,OEX,T,XYER,5)
C
C FROM TABLE 1 IN S.P. 98:
C
C XW = OBLIQUITY OF THE ECLIPTIC = MAX DECLINATION OF THE SUN
C      (w) (DEGREES)
C XI = INCLINATION OF THE MOON'S ORBIT TO PLANE OF THE ECLIPTIC
C      (i) (DEGREES)
C AW = XW IN RADIANS
C AI = XI IN RADIANS
```

```

C AE = ECCENTRICITY OF MOON'S ORBIT (e)
C AE1 = ECCENTRICITY OF EARTH'S ORBIT (e1)
C ASP = SOLAR FACTOR (S')
C
  XW=23.4522944+T*(-0.0130125+T*(-0.00000164+T*(0.000000503)))
  XI = 5.14537628
  AW = 0.0174533*XW           !w
  AI = 0.0174533*XI           !I
  AE = 0.0548997             !e
  AE1 = 0.01675104+T*(-0.0000418+T*(-0.000000126)) !e1
  ASP = 0.46022931           !S'
C
  DO 30 NOE=1,30
    CXX(NOE) = 0.0
  30 CONTINUE
C
C This next section must have something to do with the 1/4 day per
C year difference between the Common Year and the Julian Year
C
  IF(DAYB.GT.0.0) DAYB = DAYB-1.    !reduce beginning day by 1
  IF(DAYM.GT.0.0) DAYM = DAYM-1.    !reduce middle day by 1
  AMIT = 0.0                        !initialize correction
  AMI = XYER-XCEN                    !years into current century
  CPLEX = XCEN/400.+0.0001           !century/400 + epsilon
  DICF = CPLEX-AINT(CPLEX)          !remainder after century/400
  IF(AMI .EQ. 0.) GO TO 40           !skip if exact century year
  XCET = XCEN+1.                    !century year + 1
  CDIF = XYER-XCET                  !years into century - 1
  DOBY = CDIF/4.+0.0001             !(yrs in cent - 1)/4 + eps
  AMIT = AINT(DOBY)                 !truncate (yrs in cent - 1)/4
  IF(DICF .LT. 0.001) AMIT = AMIT+1.0 !add 1 if 1600's or 2000's
  40 CONTINUE
C
  DBMT = DAYB+AMIT                  !fix for 1/4 day/(year in cent)
  DMMT = DAYM+AMIT                  ! ditto
C
C FROM TABLE 1, S.P. 98, BOX 4, CXX(1-8) ARE RATES OF CHANGE OF
C MEAN LATITUDE OF:
C
C CXX(1) = MOON TO BEGINNING DAY AND BEGINNING HOUR
C CXX(2) = LUNAR PERIGEE TO BEGINNING DAY AND HOUR
C CXX(3) = SUN TO BEGINNING DAY AND HOUR
C CXX(4) = SOLAR PERIGEE TO BEGINNING DAY AND HOUR

```

```

C   CXX(5) = LUNAR PERIGEE TO MIDDLE DAY AND HOUR
C   CXX(6) = MOON'S NODE TO MIDDLE DAY AND HOUR
C   CXX(7) = LUNAR PERIGEE TO MIDDLE DAY AND BEGINNING HOUR
C   CXX(8) = MOON'S NODE TO BEGINNING DAY AND HOUR
C
CXX(1)=XSX+ 129.384820*AMI+ 13.1763968*DBMT+0.549016532*GRBS
CXX(2)=XPX+ 40.6624658*AMI+ 0.111404016*DBMT+0.004641834*GRBS
CXX(3)=XHX- 0.238724988*AMI+ 0.985647329*DBMT+0.041068639*GRBS
CXX(4)=XP1X+ 0.01717836*AMI+ 0.000047064*DBMT+0.000001961*GRBS
CXX(5)=XPX+ 40.6624658*AMI+ 0.111404016*DMMT+0.004641834*GRMS
CXX(6)=XNX- 19.3281858*AMI- 0.052953934*DMMT-0.002206414*GRMS
CXX(7)=XPX+ 40.6624658*AMI+ 0.111404016*DMMT+0.004641834*GRBS
CXX(8)=XNX-19.328185764*AMI-0.0529539336*DBMT-0.002206414*GRBS
C
C Round CXX(1-8) to nearest 0.01 deg and, if negative, increment
C by 360 deg (essentially modulo 360 arithmetic)
C
DO 50 J=1,8
  ZAT = CXX(J)/360.                !# of loops + fraction
  IF(ZAT.LT. 0.) THEN              !if negative angle
    CXX(J) = ((ZAT-AINT(ZAT))+1.)*360.    !360 + fraction*360
  ELSE                               !if positive angle
    CXX(J) = (ZAT-AINT(ZAT))*360.        !fraction*360
  END IF
  CXX(J) = FLOAT(IFIX(CXX(J)*100.+0.5))*0.01 !nearest 0.01 deg
50 CONTINUE
C
C Use latitude of moon's node (N) at beginning day and hour
C
  ANG = CXX(8)
C
C Set astronomical constants at beginning day and hour
C
  CALL TABLE6(VIB,VB,XIB,VPB,VPPB,XX,XX,XX,XX,XX,ANG,ANB,ATB)
C
CXX(26) = VIB    !I at beginning day and hour
CXX(27) = VB     !nu at      "
CXX(28) = XIB    !zi at      "
CXX(29) = VPB    !nu' at     "
CXX(30) = VPPB   !2*nu" at   "
C
CXXSB = CXX(1)   !s at beginning day and hour
CXPB = CXX(2)    !p      "

```

```

    CXHB = CXX(3)    !h      "
    CXP1B = CXX(4)    !p1    "
C
C Use latitude of moon's node (N) at middle day and hour
C
    ANG = CXX(6)
C
C Set astronomical constants at middle day and hour
C
    CALL TABLE6(VI,V,XI,VP,VPP,CIG,CVX,CEX,PVC,PVCP,ANG,AN,AT)
C
    CXX(9) = VI      !I at middle day and hour
    CXX(10) = V      !nu at      "
    CXX(11) = XI     !zi at      "
    CXX(12) = VP     !nu' at     "
    CXX(13) = VPP    !2*nu" at   "
C
C Round CXX(9-13) to nearest 0.01 deg
C
    DO 60 J=9,13
        CXX(J) = FLOAT(IFIX(CXX(J)*100.+0.5))*0.01
    60 CONTINUE
C
C Define P = p - zi following Eq. 191, para. 122.
C
    PGX = FLOAT(IFIX((CXX(5)-CXX(11))*100.+0.5))*0.01 !define P to 0.01 deg
    ZAT = PGX/360.                                !modulo 360 math
    IF(ZAT .LT. 0.) THEN
        PGX = ((ZAT-AINT(ZAT))+1.)*360.           !360+fraction*360
    ELSE
        PGX = (ZAT-AINT(ZAT))*360.                !fraction*360
    END IF
    XPG = PGX*0.0174533                            !P in radians
    CXX(14) = PGX
C
C For argument of constituent L2, compute R of Eq. 214, para. 129 (which
C info. is also tabulated in Table 8 of S.P. 98):
C
    RAXE = sin(2P)
    RAXN = -cos(2P) + 1/6 [cot(I/2)]**2
    R = arctan(RAXE/RAXN)
C
    RAXE = SIN(2.*XPG)

```

```

RAXN = -COS(2.*XPG)+1./(6.*(TAN(0.5*AT)**2))
RXX = 0.
IF(RAXE .EQ. 0. .OR. RAXN .EQ. 0.) GO TO 70
RAX = RAXE/RAXN                !tan(R)
IF(RAX .GT. 3450.) GO TO 70
RXX = ATAN(RAX)*PINV           !R in degrees
CXX(22) = RXX
70 CONTINUE

```

C
 C For amplitude of constituent L2, compute 1/Ra with Eq. 213 of
 C para. 129 [for which Table 7 lists log(Ra)]:

```

C 1/Ra = Sqrt[ 1 - 12 tan^2(I/2) cos(2P) + 36 tan^4(I/2) ]
C
CRA = SQRT( 1.
&      -12. * ( TAN(0.5*AT)**2 ) * COS(2.*XPG)
&      +36. * ( TAN(0.5*AT)**4 ) )

```

C
 C Find constant terms in cosine argument of Eq. 212, para. 129.

```

C
UM2 = 2.*(CXX(11)-CXX(10))      !2(zi-nu)
CXX(21) = UM2                    !2(zi-nu)
CXX(24) = CRA                    !1/Ra
U12 = UM2-RXX                    !2(zi-nu)-R
U12 = U12+180.                  !2(zi-nu)-R+180
CXX(15) = U12

```

C
 C Compute Q of Eq. 202, para. 123:

```

C
C      Q = arctan[(5 cos I - 1)*tan P / (7 cos I + 1)]
C
ZES = (5.*COS(AW)-1.) * SIN(XPG)
ZEC = (7.*COS(AW)+1.) * COS(XPG)
CALL FITAN(ZES,ZEC,QXX,SPXX,2)
CXX(23) = QXX                    !Q in proper quadrant

```

C
 C For constant terms in cosine argument of Eq. 201, para. 123.
 C Note: sign on 90 is opposite to that given in S.P. 98

```

C
CRAV = 0.5*UM2+QXX+90.          !zi-nu+Q+90
CXX(16) = CRAV

```

C
 C For 1/Qa of Eq. 195, para. 122 for M1 tide:

```

C Note: changed AW to AT to be consistent with S.P. 98!!!
C
C -> OLD TERM:  CQA = SQRT( 0.25
C &      +1.50 * COS(2.*XPG) * COS(AW) / (COS(0.5*AW)**2)
C &      +2.25 * (COS(AW)**2) / (COS(0.5*AW)**4)  )
C
CQA = SQRT( 0.25
&      +1.50 * COS(2.*XPG) * COS(AT) / (COS(0.5*AT)**2)
&      +2.25 * (COS(AT)**2) / (COS(0.5*AT)**4)  )
C
CXX(25) = CQA
C
C Round CXX(14-23) to nearest 0.01 deg
C
DO 80 J=14,23
  CXX(J) = FLOAT( IFIX( CXX(J)*100.+0.5 ) )/0.01
80 CONTINUE
C
C Give names to some of the array elements
C
PM = CXX(1)      !s (beginning day)
PL = CXX(2)      !p  "
SL = CXX(3)      !h  "
PS = CXX(4)      !p1 "
PLM = CXX(5)     !p (middle day)
SKYN = CXX(6)    !N  "
VI = CXX(9)      !I  "
V = CXX(10)      !nu "
XI = CXX(11)     !zi "
VP = CXX(12)     !nu' "
VPP = CXX(13)    !2*nu" "
P = CXX(14)      !P  "
AUL = CXX(15)    !2zi-2nu-R+180 (middle)
AUM = CXX(16)    !zi-nu+Q+90  "
CRA = CXX(24)    !1/Ra
CQA = CXX(25)    !1/Qa
C
U = V*0.0174533 !nu in radians
Q = P*0.0174533 !P  in radians
UI = VI*0.0174533 !I  in radians
C
RETURN
END

```

C
C
C
C

SUBROUTINE FITAN(AUS,AUC,RTA,SPDX,JMAP)

C*****
C THIS APPEARS TO BE A FORM OF THE FUNCTION ATAN2, BUT *
C WITH SOME ADDITIONAL STUFF. *
C*****

```
IF(AUC .EQ. 0.) THEN
  IF(AUS .LT. 0.) THEN
    RTA = 270.
  ELSE IF(AUS .EQ. 0.) THEN
    RTA = 0.
  ELSE
    RTA = 90.
  END IF
ELSE
  RTA = 57.2957795*ATAN(AUS/AUC)
  IF(JMAP .EQ. 2) THEN
    IF(AUS .LE. 0.) THEN
      IF(AUC .LT. 0.) THEN
        RTA = RTA+180.
      ELSE IF(AUC .EQ. 0.) THEN
        RTA = 0.
      ELSE
        RTA = RTA+360.
      END IF
    ELSE
      IF(AUC .LT. 0.) THEN
        RTA = RTA+180.
      ELSE IF(AUC .EQ. 0.) THEN
        RTA = 90.
      END IF
    END IF
  END IF
END IF
```

C
SPDX = 0.
C
RETURN
END

C

C
C
C

SUBROUTINE ORBIT(XCEN,XSX,XPX,XHX,XP1X,XNX,OEX,T,
& XYER,NNN)

C

C Computes fundamental astronomical variables from Table 1 in

C S.P. 98 (1988 ed.)

C

C S = rate of change of mean longitude of the moon per solar day

C P = rate of change of mean longitude of lunar perigee/solar day

C XH = rate of change of mean longitude of the sun per solar day

C P1 = rate of change of mean longitude of solar perigee/solar day

C XN = rate of change of mean longitude of moon's node/solar day

C T = number of Julian centuries (36525 days) reckoned from

C Greenwich mean noon, 31 December 1899

C YR = number of days and half days to correct astronomical

C constants to 0000 hrs, 1 January of proper century, starting

C with the year 1600 (correction is 0.5 days for 20th century,

C i.e., noon on 31 December 1899 to 0000 hrs, 1 January 1900)

C GAT = the century (XCEN) in which the year XYER resides

C OEX = array of (NNN => 5 elements, redundantly returned with the

C mean latitudes listed below as of 0000 hrs, 1 January of

C the proper century:

C

C XSX = OEX(1) = mean longitude of moon (s)

C XPX = OEX(2) = mean longitude of lunar perigee (p)

C XHX = OEX(3) = mean longitude of sun (h)

C XP1X = OEX(4) = mean longitude of solar perigee (p1)

C XNX = OEX(5) = mean longitude of moon's node (N)

C

DIMENSION OEX(NNN)

C

S = 13.1763968

P = 0.1114040

XH = 0.9856473

P1 = 0.0000471

XN = -0.0529539

XCAN = XYER*0.01+0.001

XCEN = AINT(XCAN)*100.

T = -3.0

YR = 2.5

GAT = 1600.

C

```
DO 10 JK=1,30
  GP = GAT/400.+0.00001
  COL = GP-AINT(GP)
  IF(COL .LT. 0.01) THEN
    IF(GAT .EQ. XCEN) GO TO 12
  ELSE
    IF(GAT .EQ. XCEN) GO TO 12
    YR = YR-1.
  END IF
  GAT = GAT+100.
10 CONTINUE
12 CONTINUE
```

C

```
T = (GAT-1900.)*0.01
```

C

```
OEX(1) = 270.437422 + T*( 307.892 + T*( 0.002525
& + T*( 0.00000189))) + YR*S
OEX(2) = 334.328019 + T*( 109.032206 + T*(-0.01034444
& + T*(-0.0000125))) + YR*P
OEX(3) = 279.696678 + T*( 0.768925 + T*( 0.0003205))
& + YR*XH
OEX(4) = 281.220833 + T*( 1.719175 + T*( 0.0004528
& + T*( 0.00000333))) + YR*P1
OEX(5) = 259.182533 + T*(-134.142397 + T*( 0.00210556
& + T*( 0.00000222))) + YR*XN
```

C

```
DO 100 I=1,5
  ZAT = OEX(I)/360.
  IF(ZAT .LT. 0.) THEN
    OEX(I) = ((ZAT-AINT(ZAT))+1.)*360.
  ELSE
    OEX(I) = (ZAT-AINT(ZAT))*360.
  END IF
  OEX(I) = FLOAT(IFIX(OEX(I)*100.+0.5))*0.01
100 CONTINUE
```

C

```
XSX = OEX(1)
XPX = OEX(2)
XHX = OEX(3)
XP1X = OEX(4)
XNX = OEX(5)
```

C

RETURN

END

C

C

C

C

SUBROUTINE VANDUF(SPEED,E,F,ITYPE)

C

C Computes phases and node factors for tidal constituents.

C

C References:

C

C S.P. 98 = US Dept of Commerce, Coast and Geodetic Survey,

C "Manual of Harmonic Analysis and Prediction

C of Tides," 1988 Ed.

C A.M. = British Admiralty, "Admiralty Manual of Tides,"

C 1941 Ed.

C

C Common block variables have the following meanings (as

C best I can tell):

C

C /LOCAT/ TM and GONL are 0.0 in main program, not defined,

C but may be related to meridian differences of

C local time and Greenwich time per Eq. 318, para.

C 223 in S.P. 98

C

C /FAD/ IPICK is defined in this routine as constituent

C index based on matching SPEED with array of SPD

C in NAMES common block

C

C /VEE/ TML = not defined (may relate to TM in /LOCAT/)

C CON = defined in this routine

C U = nu for middle day in radians

C Q = P "

C UI = I "

C

C /BOXA/ S = not defined

C XL = not defined

C PM = s for beginning day in degrees

C PL = p "

C SL = h "

C PS = p1 "

C PLM = p for middle day in degrees

```

C   SKYN = N           "
C   VI = I            "
C   V = nu           "
C   XI = zi          "
C   VPP = nu"        "
C
C /BOXB/  VP = nu' for middle day in degrees
C   P = P           "
C   AUL = 2*zi - 2*nu - R + 180 , middle day, deg
C   AUM = zi - nu + Q + 90 , middle day, deg
C   CRA = 1/Ra for L(2) constituent
C   CQA = 1/Qa for M(1) constituent
C
C /BOXS/  AW = w  obliquity of ecliptic (max. declination of Sun)
C   AI = i  inclination of Moon's orbit to ecliptic plane
C   AE = e  eccentricity of Moon's orbit
C   AE1 = e1 eccentricity of Earth's orbit
C   ASP = S' Solar factor
C
C Order of constituents is same as in NAMES common.
C
C NOTE: Constituents marked with * have phases shifted
C by 180 deg from what is given in S.P. 98. These are coded
C with the option of adding 180 deg by setting ISHIFT = 1.
C Original code is retained by setting ISHIFT = 0.
C
DOUBLE PRECISION  SPEED, SPD(37)
DIMENSION        MS(37)
C
COMMON /LOCAT/  TM, GONL
COMMON /FAD/  IPICK
COMMON /VEE/  TML, CON, U, Q, UI
COMMON /BOXA/  S, XL, PM, PL, SL, PS, PLM,
&             SKYN, VI, V, XI, VPP
COMMON /BOXB/  VP, P, AUL, AUM, CRA, CQA
COMMON /BOXS/  AW, AI, AE, AE1, ASP
COMMON /SPEEDS/  SPD
COMMON /MMSS/  MS
C
ISHIFT=0          ! if 1, flips *'d constituents by 180 deg
C
CON = SL+TML      ! h, beginning day + TML
C5AW = COS(0.5*AW) ! cos(w/2)

```

C5AI = COS(0.5*AI) ! cos(i/2)
 C5UI = COS(0.5*UI) ! cos(I/2)
 SAW = SIN(AW) ! sin w
 SAI = SIN(AI) ! sin i
 SUI = SIN(UI) ! sin I

C

DO 600 J=1,37
 IPICK = J
 IF(SPEED .EQ. SPD(J)) GO TO 610

600 CONTINUE

WRITE(*,'(2X,"SPEED MATCH NOT FOUND IN VANDUF -> QUIT")')
 WRITE(*,'(2X,"SPEED = ",F12.7)') SPEED
 STOP

610 CONTINUE

C

GO TO (1, 2, 3, 4, 5, 6, 7, 8, 9, 10,
 & 11, 12, 13, 14, 15, 16, 17, 18, 19, 20,
 & 21, 22, 23, 24, 25, 26, 27, 28, 29, 30,
 & 31, 32, 33, 34, 35, 36, 37), IPICK

C*****

C CONSTITUENT CALCULATION CODES

C*****

C

C M(2): term A39, p. 22 and Eq. 70, 78, S.P. 98

C

1 E = 2.*(CON-PM+XI-V)
 F = (C5AW**4)*(C5AI**4)/(C5UI**4)
 GO TO 800

C

C N(2): term A40, p. 22 and Eq. 70, 78, S.P. 98

C

2 E = 2.*(CON+XI-V)-3.*PM+PL
 F = (C5AW**4)*(C5AI**4)/(C5UI**4)
 GO TO 800

C

C S(2): p. 39, S.P. 98

C

3 E = 2.*TML
 F = 1.
 GO TO 800

C

C *O(1): term A14, p. 21 and Eq. 67, 75, S.P. 98

C

4 E = CON-V-2.*(PM-XI)-90.+ISHIFT*180.
F = SAW*(C5AW**2)*(C5AI**4)/(SUI*(C5UI**2))
GO TO 800

C

C *K(1): Eq. 222 and 227, p. 45, S.P. 98

C

5 E = CON-VP+90.+ISHIFT*180.
F = SQRT(0.8965*(SIN(2.*UI)**2)+0.6001*SIN(2.*UI)*COS(U)
& +0.1006)
F = 1./F
GO TO 800

C

C K(2): Eq. 230 and 235, p. 46, S.P. 98

C

6 E = 2.*CON-VPP
F = SQRT(19.0444*(SUI**4)+2.7702*(SUI**2)*COS(2.*U)+0.0981)
F = 1./F
GO TO 800

C

C L(2): Term A41, p. 22, Eq. 212, p. 44, and Eq. 70, 78, and 215,
S.P. 98

C

7 E = 2.*CON-PM-PL+AUL
F = (C5AW**4)*(C5AI**4)/(CRA*(C5UI**4))
GO TO 800

C

C 2N(2): Term A42, p. 22, and Eq. 70, 78, S.P. 98

C

8 E = 2.*(CON+XI-V+PL)-4.*PM
F = (C5AW**4)*(C5AI**4)/(C5UI**4)
GO TO 800

C

C R(2): Term B47, p. 39, and para. 118, p. 40, S.P. 98

C

9 E = SL-PS+180.+2.*TML
F = 1.
GO TO 800

C

C T(2): Term B40, p. 39, and para. 118, p. 40, S.P. 98

C

10 E = 2.*TML-(SL-PS)
F = 1.
GO TO 800

C

C Lambda(2): Term A44, p. 22, and Eq. 70, 78, S.P. 98

C

$$11 E = 2. * (CON + XI - V - SL) - PM + PL + 180.$$

$$F = (C5AW^{**4}) * (C5AI^{**4}) / (C5UI^{**4})$$

GO TO 800

C

C Mu(2): Term A45, p. 22, and Eq. 70, 78, S.P. 98

C

$$12 E = 2. * (CON + XI - V + SL) - 4. * PM$$

$$F = (C5AW^{**4}) * (C5AI^{**4}) / (C5UI^{**4})$$

GO TO 800

C

C Nu(2): Term A43, p. 22, and Eq. 70, 78, S.P. 98

C

$$13 E = 2. * (CON + XI - V + SL) - 3. * PM - PL$$

$$F = (C5AW^{**4}) * (C5AI^{**4}) / (C5UI^{**4})$$

GO TO 800

C

C *J(1): Term A24, p. 22, and Eq. 68, 76, S.P. 98

C

$$14 E = CON + PM - PL - V + 90. + ISHIFT * 180.$$

$$F = SIN(2. * AW) * (1. - 1.5 * (SAI^{**2})) / SIN(2. * UI)$$

GO TO 800

C

C *M(1): Eq. 201, p. 42, and Eq. 206, p. 43, S.P. 98

C

$$15 E = CON - PM + AUM + ISHIFT * 180.$$

$$F = SAW * (C5AW^{**2}) * (C5AI^{**4}) / (CQA * SUI * (C5UI^{**2}))$$

GO TO 800

C

C *OO(1): Term A31, p. 22, and Eq. 69, 77, S.P. 98

C

$$16 E = CON - V + 2. * (PM - XI) + 90. + ISHIFT * 180.$$

$$F = SAW * (SIN(0.5 * AW)^{**2}) * (C5AI^{**4}) / (SUI * (SIN(0.5 * UI)^{**2}))$$

GO TO 800

C

C P(1): Term B14, p. 39, and para. 118, p. 40, S.P. 98

C

$$17 E = TML + 270. - SL$$

$$F = 1.$$

GO TO 800

C

C *Q(1): Term A15, p. 21, and Eq. 67, 75, S.P. 98

C

18 E = CON-V-3.*PM+2.*XI+PL-90.+ISHIFT*180.
F = SAW*(C5AW**2)*(C5AI**4)/(SUI*(C5UI**2))
GO TO 800

C

C *2Q(1): Term A17, p. 21, and Eq. 67, 75, S.P. 98

C

19 E = CON-V-4.*PM+2.*XI+2.*PL-90.+ISHIFT*180.
F = SAW*(C5AW**2)*(C5AI**4)/(SUI*(C5UI**2))
GO TO 800

C

C *Rho(1): Term A18, p. 21, and Eq. 67, 75, S.P. 98

C

20 E = CON-V-3.*PM+2.*XI-PL+2.*SL-90.+ISHIFT*180.
F = SAW*(C5AW**2)*(C5AI**4)/(SUI*(C5UI**2))
GO TO 800

C

C M(4): para. 139, p. 47, S.P. 98

C

21 E = 4.*(CON-PM+XI-V)
F = ((C5AW**4)*(C5AI**4)/(C5UI**4))**2
GO TO 800

C

C M(6): para. 139, p. 47, S.P. 98

C

22 E = 6.*(CON-PM+XI-V)
F = ((C5AW**4)*(C5AI**4)/(C5UI**4))**3
GO TO 800

C

C M(8): para. 139, p. 47, S.P. 98

C

23 E = 8.*(CON-PM+XI-V)
F = ((C5AW**4)*(C5AI**4)/(C5UI**4))**4
GO TO 800

C

C S(4): para. 139, p. 47, S.P. 98

C

24 E = 4.*TML
F = 1.
GO TO 800

C

C S(6): para. 139, p. 47, S.P. 98

C

$$25 E = 6.*TML$$

$$F = 1.$$

GO TO 800

C

C *M(3): Term A82, p. 35, and para. 106, p. 35, S.P. 98

C

$$26 E = 3.*(CON-PM+XI-V)+180.+ISHIFT*180.$$

$$F = (C5AW**6)*(C5AI**6)/(C5UI**6)$$

GO TO 800

C

C *S(1): para. 119, p. 40, S.P. 98

C

$$27 E = TML+180.+ISHIFT*180.$$

$$F = 1.$$

GO TO 800

C

C *MK(3): p. 68, A.M., M(2)+K(1) interaction

C

$$28 E = 2.*(CON-PM+XI-V)+(CON-VP+90.)+ISHIFT*180.$$

$$F = ((C5AW**4)*(C5AI**4)/(C5UI**4))$$

$$F = F/SQRT(0.8965*(SIN(2.*UI)**2)+0.6001*SIN(2.*UI)*COS(U)$$

$$\& \quad \quad \quad +0.1006)$$

GO TO 800

C

C *2MK(3): p. 68, A.M., assume M(4)-K(1) interaction, sign is unsure

C

$$29 E = 4.*(CON-PM+XI-V)-(CON-VP+90.)+ISHIFT*180.$$

$$F = ((C5AW**4)*(C5AI**4)/(C5UI**4))**2$$

$$F = F/SQRT(0.8965*(SIN(2.*UI)**2)+0.6001*SIN(2.*UI)*COS(U)$$

$$\& \quad \quad \quad +0.1006)$$

GO TO 800

C

C MN(4): p. 68, A.M., M(2)+N(2) interaction

C

$$30 E = 4.*(CON+XI-V)+PL-5.*PM$$

$$F = ((C5AW**4)*(C5AI**4)/(C5UI**4))**2$$

GO TO 800

C

C MS(4): p. 67, A.M., M(2)+S(2) interaction

C

$$31 E = 2.*(CON-PM+XI-V)+2.*TML$$

$F = (C5AW^{**4}) * (C5AI^{**4}) / (C5UI^{**4})$
GO TO 800

C

C 2SM(2): p. 68, A.M., 2M(2)-S(2) interaction

C

32 E = 4.*TML-2.*(CON-PM+XI-V)
 $F = (C5AW^{**4}) * (C5AI^{**4}) / (C5UI^{**4})$
GO TO 800

C

C Mf: Term A6, p. 21, and Eq. 66, 74, S.P. 98

C

33 E = 2.*(PM-XI)
 $F = (SAW^{**2}) * (C5AI^{**4}) / (SUI^{**2})$
GO TO 800

C

C MSf: Term A5, p. 21, and Eq. 65, 73, S.P. 98; p. 67, A.M.,

C S(2)-M(2) interaction

C Note: F was redefined to be consistent with S.P. 98,

C old F is commented out...

C

34 E = 2.*TML-2.*(CON-PM+XI-V)
C $F = (C5AW^{**4}) * (C5AI^{**4}) / (C5UI^{**4})$
 $F = ((2./3.-(SAW^{**2})) * (1.-1.5*(SAI^{**2}))) / (2./3.-(SUI^{**2}))$
GO TO 800

C

C Mm: Term A2, p. 21, and Eq. 65, 73, S.P. 98

C

35 E = PM-PL
 $F = ((2./3.-(SAW^{**2})) * (1.-1.5*(SAI^{**2}))) / (2./3.-(SUI^{**2}))$
GO TO 800

C

C Sa: para. 119, p. 40, S.P. 98

C

36 E = SL
F = 1.
GO TO 800

C

C Ssa: Term B6, p. 39, S.P. 98

C

37 E = 2.*SL
F = 1.
GO TO 800

C*****

C END OF CONSTITUENT CALCULATION CODES

C*****

C

800 CONTINUE

C

IF(ITYPE .EQ. 2) THEN

E = E + FLOAT(MS(IPICK))*GONL-SPD(IPICK)*TM/15.

ELSE IF(ITYPE .EQ. 1) THEN

ZAT = E/360. !# OF CIRCLES

IF(ZAT.LT.0.) THEN

E = (ZAT-AINT(ZAT)+1.)*360. !360 + MOD(E,360)

ELSE

E = (ZAT-AINT(ZAT))*360. !MOD(E,360)

END IF

END IF

C

F = 1./F

C

RETURN

END

C

C

C

C

SUBROUTINE TABLE6(VI,V,XI,VP,VPP,CIG,CVX,CEX,PVC,
 & PVC,ANG,AN,AT)

C

C Using as input the longitude of the moon's node N (here
 C called ANG) and the astronomical constants w, i, e, e1
 C and S' (here called AW, AI, AE, AE1 and ASP, respectively,
 C and input through the common block BOXS) from the beginning
 C of subroutine ASTRO, computes the 5 astronomical entities
 C listed in Table 6 of S.P. 98 and used for tidal computations,
 C specifically:

C

C VI = inclination of moon's orbit to celestial equator (I)
 C in degrees to nearest 0.01 deg

C V = right ascension or longitude in celestial equator of
 C moon's orbit (nu) in degrees to nearest 0.01 deg

C XI = longitude in moon's orbit of the lunar intersection
 C (zi) to nearest 0.01 deg

C VP = nu' of Eq. 224 in S.P. 98 in degrees

C VPP = 2*nu'' of Eq. 232 in S.P. 98 in degrees

C

C Also returned are:

C

C CIG = VI (I) in radians

C CVX = V (nu) in radians

C CEX = XI (zi) in radians

C PVC = VP (nu') in radians

C PVCP = VPP (2*nu") in radians

C AN = ANG (N) in radians

C AT = CIG identically, i.e., redundancy

C

COMMON /BOXS/ AW, AI, AE, AE1, ASP

C

PI = 4.*ATAN(1.) !YOU KNOW, PI
 DTR = 180./PI !DEG./RAD., 57.295780
 RTD = PI/180. !RAD./DEG., 0.0174533

C

C Initialize returned values

C

V = 0.0 !nu, right ascension
 XI = 0.0 !zi, long. in moon's orbit of intersection
 VP = 0.0 !nu' of Eq. 224
 VPP = 0.0 !2*nu" of Eq. 232
 AN = ANG*RTD !N in radians

C

AX = ANG !redundant replacement
 EYE = COS(AI)*COS(AW)-SIN(AI)*SIN(AW)*COS(AN) !cos(I)
 C9 = DTR*ACOS(EYE) !I in deg
 VI = FLOAT(IFIX(C9*100.+0.5))*0.01 !I to nearest 0.01 deg
 CIG = RTD*VI !VI in radians
 AT = CIG !redundant CIG

C

C Special condition checks

C

IF(CIG .EQ. 0.) GO TO 230
 IF(AX .EQ. 0.) GO TO 230
 IF(AX .EQ. 180.) GO TO 230

C

C Spherical trigonometry to get nu (Fig. 1, Pg. 6, S.P. 98)

C

VXXE = SIN(AI)*SIN(AN)
 VXXN = COS(AI)*SIN(AW)+SIN(AI)*COS(AW)*COS(AN)
 IF(VXXE .EQ. 0.) GO TO 201

```

    IF( VXXN .EQ. 0. ) GO TO 201
    VXX = VXXE/VXXN                !tan(nu)
    C10 = DTR*ATAN(VXX)            !nu in deg.
    V = FLOAT(IFIX(C10*100.+0.5))*0.01    !nu to 0.01 deg
    IF( V .GT. 0. .AND. AX .GT. 180. ) V = -V    !- for 180 < N < 360
  C
  201 CONTINUE
  C
    CVX = RTD*V                    !nu in radians
  C
  C Spherical trigonometry to get zi (Fig. 1, Pg. 6, S.P. 98)
  C
    TERM = SIN(AI)*COS(AW)/SIN(AW)
    EXX = TERM*SIN(AN)/COS(AN) + (COS(AI)-1.)*SIN(AN)
    EZZ = TERM+COS(AI)*COS(AN) + (SIN(AN)**2)/COS(AN)
    IF( EXX .EQ. 0. ) GO TO 202
    IF( EZZ .EQ. 0. ) GO TO 202
    EXEZ = EXX/EZZ                !tan(zi)
    IF( EXEZ .GT. 3450. ) GO TO 202
    C11 = DTR*ATAN(EXEZ)          !zi in deg.
    XI = FLOAT(IFIX(C11*100.+0.5))*0.01    !zi to 0.01 deg
    IF( XI .GT. 0. .AND. AX .GT. 180. ) XI = -XI    !- if 180 < N < 360
  C
  202 CONTINUE
  C
    CEX = RTD*XI                  !zi in radians
  C
  C From paragraph 133 of S.P. 98 to find nu':
  C
    A22 = (0.5+0.75*(AE**2))*SIN(2.*CIG)    !lunar coeff. A of Eq. 216
    B22 = (0.5+0.75*(AE1**2))*ASP*SIN(2.*AW) !solar coeff. B of Eq. 217
    VPXE = A22*SIN(CVX)                    !numerator in Eq. 224
    VPXN = A22*COS(CVX)+B22                !denominator in Eq. 224
    IF( VPXE .EQ. 0. ) GO TO 203
    IF( VPXN .EQ. 0. ) GO TO 203
    VPX = VPXE/VPXN                       !tan(nu')
    IF( VPX .GT. 3450. ) GO TO 203
    VP = DTR*ATAN(VPX)                    !nu' in degrees
    IF( VP .GT. 0. .AND. AX .GT. 180. ) VP = -VP    !- if 180 < N < 360
  C
  203 CONTINUE
  C
    PVC = RTD*VP                    !nu' in radians
  
```



```

C*****
  CHARACTER*10  LABLE(37), ITAG
  DIMENSION     IP(37)
  DOUBLE PRECISION  SPD(37), SPDD
C
  COMMON /MMSS/  IP
  COMMON /SPEEDS/  SPD
  COMMON /NAMES/ LABLE
C
  1 FORMAT(10X,'Speed constituent ',F12.7,' not in list')
  2 FORMAT(10X,'Constituent named ',A10,' not in list')
  3 FORMAT(10X,'Constituent number ',I4,' not in list')
C
  IF(ICODE.EQ.1) THEN          !SEARCH BY SPEED
    DO 100 J=1,37
      IF(SPDD.NE.SPD(J)) THEN
        GO TO 100
      ELSE
        ITAG=LABLE(J)
        ISUB=IP(J)
        INUM=J
        GO TO 400
      END IF
    100 CONTINUE
    WRITE(*,1) SPDD
C
  ELSE IF(ICODE.EQ.2) THEN     !SEARCH BY NAME
    DO 200 I=1,37
      IF(ITAG.NE.LABLE(I)) THEN
        GO TO 200
      ELSE
        SPDD=SPD(I)
        ISUB=IP(I)
        INUM=I
        GO TO 400
      END IF
    200 CONTINUE
    WRITE(*,2) ITAG
C
  ELSE IF(ICODE.EQ.3) THEN     !SEARCH BY NUMBER
    K=INUM
    IF(K.GT.0 .AND. K.LE.37) THEN
      ITAG=LABLE(K)
  
```

```

      SPDD=SPD(K)
      ISUB=IP(K)
      GO TO 400
    END IF
    WRITE(*,3) INUM
  END IF
C
  WRITE(*,('*****EXECUTION STOPPED IN SUBROUTINE NAME*****'))
  STOP
C
  400 CONTINUE
C
  RETURN
  END
C
C
C
C
  BLOCK DATA CONSTS
C*****
C 37 CONSTITUENT ELEMENTS IS NOAA STANDARD AS OF PEARL *
C HARBOR DAY 1987 *
C*****
  CHARACTER*10 LABEL(37)
  INTEGER MS(37)
  DOUBLE PRECISION SPD(37)
C
  COMMON /SPEEDS/ SPD
  COMMON /NAMES/ LABEL
  COMMON /MMSS/ MS
C
C Tidal constituent speeds in degrees per hour
C
  DATA SPD/
& 28.9841042D0, 28.4397295D0, 30.0000000D0, 13.9430356D0,
& 15.0410686D0, 30.0821373D0, 29.5284789D0, 27.8953548D0,
& 30.0410667D0, 29.9589333D0, 29.4556253D0, 27.9682084D0,
& 28.5125831D0, 15.5854433D0, 14.4966939D0, 16.1391017D0,
& 14.9589314D0, 13.3986609D0, 12.8542862D0, 13.4715145D0,
& 57.9682084D0, 86.9523127D0, 115.9364169D0, 60.0000000D0,
& 90.0000000D0, 43.4761563D0, 15.0000000D0, 44.0251729D0,
& 42.9271398D0, 57.4238337D0, 58.9841042D0, 31.0158958D0,
& 1.0980331D0, 1.0158958D0, 0.5443747D0, 0.0410686D0,

```

```

& 0.0821373D0/
C
C Constituent subscripts
C
  DATA      MS/
&      2,      2,      2,      1,
&      1,      2,      2,      2,
&      2,      2,      2,      2,
&      2,      1,      1,      1,
&      1,      1,      1,      1,
&      4,      6,      8,      4,
&      6,      3,      1,      3,
&      3,      4,      4,      2,
&      0,      0,      0,      0,
&      0/
C
C Constituent names
C
  DATA      LABEL/
& 'M(2)  ', 'N(2)  ', 'S(2)  ', 'O(1)  ',
& 'K(1)  ', 'K(2)  ', 'L(2)  ', '2N(2)  ',
& 'R(2)  ', 'T(2)  ', 'Lambda(2) ', 'Mu(2)  ',
& 'Nu(2) ', 'J(1)  ', 'M(1)  ', 'OO(1)  ',
& 'P(1)  ', 'Q(1)  ', '2Q(1) ', 'Rho(1) ',
& 'M(4)  ', 'M(6)  ', 'M(8)  ', 'S(4)  ',
& 'S(6)  ', 'M(3)  ', 'S(1)  ', 'MK(3)  ',
& '2MK(3) ', 'MN(4) ', 'MS(4) ', '2SM(2) ',
& 'Mf    ', 'Msf   ', 'Mm    ', 'Sa    ',
& 'Ssa   '/
C
  END
c*****
  INTEGER FUNCTION LSTGDCHR(NAMESUB)
c
  CHARACTER*(*) NAMESUB
  INTEGER II,CLEN,INDEX
c
  CLEN = LEN(NAMESUB)
  DO 100 II = CLEN,1,-1
100 IF( ICHAR(NAMESUB(II:II)) .GT. 60 .AND.
  1 ICHAR(NAMESUB(II:II)) .LT. 127 )GOTO 101
101 INDEX=II
c

```

AMEC, Environment & Infrastructure, Inc.
Hydrodynamic Modeling of Storm Drain Discharges in
the Neighborhood of ASBS 29 in La Jolla, California
Revised: 13 March 2013

LSTGDCHR = INDEX
RETURN

c

END

AMEC, Environment & Infrastructure, Inc.
Hydrodynamic Modeling of Storm Drain Discharges in
the Neighborhood of ASBS 29 in La Jolla, California
Revised: 13 March 2013

APPENDIX C

CODES FOR THE OCEANRDS REFRACTION/DIFFRACTION MODEL

Appendix C: Codes for the OCEANRDS Refraction/Diffraction Model

There is a family of OCEANRDS codes, with each specific to particular grid domains. For the back refraction problems and other far field applications the **oceanrds_socal.for** version is used on a 2,405 x 4,644 raster formatted grid that encompasses the entire Southern California Bight. The input parameters output files which are required by **oceanrds_socal.for** are

graham_m.grd * * (name.grd) bathymetry input file
-1.0 * (gis) if data is parsed GIS data gis= -1.0, if NOS data gis=1.0
1 * wave exposure 1=west, 2=north, 3=east, 4=south (icoast)
0.0 * sea level adjustment MSL meters (sealev) (+ = deeper water)
77.5 * outer grid dimensions in meters perpendicular to coast (sx)
92.6 * outer grid dimensions in meters parallel to coast (sy)
4644 * number of grid cells in from deep water perpendicular to coast raster
(nx)
2405 * number of grid cells along coast from top edge (ny)
17.0 * wave period in seconds (persw)
270.0 * wave direction degress clockwise from true north (asw)
10.0 * wave height meters (hsw)

```
C*****
C
C   Ocean refraction - diffraction module oceanrds_socal.for
C
C   programmed to run on full socal elevation data (graham_m.grd)
C   extracted from GIS grid by read_graham_bathy_full.for
C       10 oct, 2002
C
C*****
C   This program is the first program in a 2 program series to treat
C   the distribution of wave heights, angles, wave numbers from the
C   combined effect of a wave field containing two distinct periods
C   and/or directions. The second program (windwave.f) must also be run
C   in order for the ultimate output file to be properly name for use
C   by the other modules even if there is 0 energy in the second band.
C   It solves a parabolic approximation to the mild slope equation
C   for the transmitted field of a linear wave.  Outputs wave height,
C   wave number, and wave angle for each grid point in a 2405 x 4644
C   grid array with 3 second x 3 second spacing.  Bathymetry is read from
C   a formatted 2405 x 4644 real number array called 'ifile'.grd,
C   created by the oceanbat.f module, where 'ifile' corresponds to
C   the inputted site name.  Program uses "oceanrd.inp" input file.
C   All output files are named 'ifile' with different extensions,
C   ie. 'ifile'.wh1.
C*****
C*****
C
C       parameter (max=10000000)
C       character name*8,ifile*12
C       character ofile1*12,ofile2*12,ofile3*12,ofile4*12
C       character ofile5*12,ofile6*12,ofile7*12
C       dimension ccg(max),di(max),hab(max),rlb(max),dib(max),ih(max)
C       dimension depth(4644,4644),wht(4644,4644)
C       dimension ang(4644,4644)
C       dimension depthold(4644,4644)
C       real kbar(2,max),kave
C
C       complex aa(max),bb(max),cc(max),dd(max),uu(max),aprev(max)
C       complex c3,t1,t2,t3,f,alast(max),aphys(max),mim,mip
C
C       common /grid/ ny,sy,sx,dely,delx,ndely,freq,dcon,ify,ifx,tide
C       common /cut/ dc
C
```

```
    pi=acos(-1.)
c
c  open parameter input file, return error message if missing
c
c
c
    open(2,file='oceanrds_socal.inp',status='old',err=900)
    read(2,'(a)') name
    read(2,*) gis
    read(2,*) icoast
    read(2,*) tide_elev
    read(2,*) sx
    read(2,*) sy
    read(2,*) nx
    read(2,*) ny
    read(2,*) persw
    read(2,*) asw
    read(2,*) hsw
c
    tide=tide_elev
    amp=hsw
    dir=asw
    per=persw
c
    freq=1/per
c
c... change to proper rotation frame, flag if theta not between +/- 45
c
    IF (icoast .EQ. 1) coast=270.0
    IF (icoast .EQ. 2) coast=90.0
    IF (icoast .EQ. 3) coast=0.0
    IF (icoast .EQ. 4) coast=180.0
c
    theta=coast-dir
c
c... set some variables to constant values
c
c    dcon = 1. for nuwave version
    dcon=1.
c
c    cutoff depth (dc) -5.0 meters
    dc=-5.0
c
```

```
c   breaking wave switch (ibreak) (1=on, 0=off)
    ibreak=1
c
c   breaking criteria (bc) 0.5 for wave height = (bc)*depth
    bc=0.5
c
c   lateral b.c.: ibc=(0) transmitting, ibc=(1) reflective
    ibc=0
c   if trans: (isn=0) straight snell, isn=(1) kirby's improved
    isn=1
c   idf=(0) small angle diff, idf=(1) large angle dif
    idf=1
c
c
    write(*,'(5(/),10x,a)')
    &' KIRBY HIGHER ORDER REFRACTION-DIFFRACTION PROGRAM '
    write(*,'(/,10x,a)')
    &'- based on the parabolic equation method (PEM) of solving'
    write(*,'(10x,a,5(/)')
    &' the mild-slope equation. '
c
    nn=8
    do 3 m=8,1,-1
3   if(name(m:m).eq.' ') nn=m-1
c
c
c... open grid file
c
    write(ifile,'(a,a)') name(:nn),'.grd'
    open(20,file=ifile,status='old',err=900)
c
c
c... open breaker ix,iy,wave height, wave angle, depth file
    write(ofile7,'(a,a)') name(:nn),'.bra'
    open(39,file=ofile7)
c
c
c... open sea level corrected ascii bathymetry file
    write(ofile1,'(a,a)') name(:nn),'.dep'
    open(31,file=ofile1)
c
c
c... open ascii wave number file
```

```
        write(ofile2,'(a,a)') name(:nn),'.wvn'  
        open(32,file=ofile2)  
c  
c  
c  
c... open ascii wave height file  
        write(ofile3,'(a,a)') name(:nn),'.wh1'  
        open(33,file=ofile3)  
c  
c  
c  
c... open ascii wave angle file  
        write(ofile4,'(a,a)') name(:nn),'.an1'  
        open(34,file=ofile4)  
c  
c  
c  
c.... create depth array  
c  
        do 111 j=ny,1,-1  
            read(20,*) (depthold(j,i),i=1,nx)  
111    continue  
        rewind(20)  
c  
c 10oct02 *****correct for sea level and change sign if GIS data  
        do 711 i=1,nx  
            do 811 j=1,ny  
                depthold(j,i)=(gis*depthold(j,i))+sealev  
811    continue  
711    continue  
c  
c.....write rotated ascii depth file for internal use in ref/dif  
165    format(2405f12.2)  
        DO 101 i=1,nx  
            WRITE(31,165)(depthold(j,i),j=1,ny)  
101    CONTINUE  
        rewind(31)  
c  
c  
        do 119 i=1,nx  
            read(31,*) (depth(i,j),j=1,ny)  
119    continue  
        rewind(31)
```

```
c
c
c... read first depth to initialize offshore boundary
c
      read(31,*) (di(m),m=1,ny)
      ridep=di(ny/2)
      rewind(31)

c.... would like a grid step size on the order of 1/5 wavelength

      call getkcg(10.,wk,cg0)
      wl=2*pi/wk
      ifx=1+sx/(.2*wl)
      ify=1+sy/(.2*wl)
c
      nmx=ifx
      nmy=ify
c
      amp=amp/2.
c
c... calculate dimensions of interpolated grid
c
      dely=sy/ify
      delx=sx/ifx
      ndely=(ny-1)*ify
      ndelx=(nx-1)*ifx
c
c
      call getkcg(ridep,wk0,cg0)
c wave length (m)
      wl=2*pi/wk0
c wave frequency (rad/sec)
      sig=2*pi/per
c radder's correction factor
      do 33 j=1,ndely+1
33   ccg(j)=sqrt(sig*cg0/wk0)
c
c
      ltype=2
c... open binary wave height file
      write(ofile5,'(a,a)' name(:nn),'.bw1'
      open(9,file=ofile5,form='unformatted')
c
```

```
c... open binary wave angle file
      write(ofile6,'(a,a)') name(:nn),'.bal'
      open(11,file=ofile6,form='unformatted')
c
c.. initialize depth array
      do 555 nn=1,ndely+1
        hab(nn)=0.
        ih(nn)=0
555    continue
c
c enter initial condition at x=0
c
      call inbc(amp,wk0,theta,ndely,dely,alast)
c
      do 202 j=1,ndely+1
        kbar(1,j)=wk
202    kbar(2,j)=wk
c
c scale alast as in radder(1978)
      do 32 j=1,ndely+1
        alast(j)=alast(j)*ccg(j)
32    continue
c
c      call wwave(alast,ndely,nmy,dely,kbar)
c
c solution of the parabolic eqn. by the crank-nicholson formulation
c
c start x increments
c
      c2=1./2./dely**2
      c3=2.*(0,1)/delx
c
c-----
c increments in x-direction
c
      ikount=0
      do 100 l=1,ndelx
c
c... write every 10th step to the screen
c
      if(10*((l+1)/10).eq.l+1) then
        print *, ' column ',l+1,' of ',ndelx+1
      endif
```

```

c
  lm=1
c
  call intkcg(lm,kbar,ccg,di,ikount)
c
c correction factor
  do 34 j=1,ndely+1
    ccg(j)=sqrt(sig*ccg(j)/kbar(2,j))
34  continue
c-----
c increments in y-direction - 1st. round
  do 200 j=2,ndely
c
  kave=(kbar(2,j)+kbar(1,j))/2.
c  kave=kbar(2,j)
c
  if(idf.eq.0) then
c small angle diffraction approximation
c
  t1=c2
  t3=c3*kave
  f=2*kave*(kave-wk)+c3/2*(kbar(2,j)-kbar(1,j))
c
  aa(j-1)=t1
  bb(j-1)=t3-2.*t1+f/2.
  cc(j-1)=t1
  dd(j-1)=-t1*alast(j+1)+(t3+2*t1-f/2)*alast(j)-t1*alast(j-1)
c
  endif
c
  if(idf.eq.1) then
c large angle diffraction approximation
c
  t1=c2/2.*(3.-wk/kave)
  t2=c2*c3/4./kave
  t3=c3*kave
  f=2*kave*(kave-wk)+c3/2*(kbar(2,j)-kbar(1,j))
c
  aa(j-1)=t1+t2
  bb(j-1)=t3-2.*(t1+t2)+f/2.
  cc(j-1)=t1+t2
  dd(j-1)=(t2-t1)*(alast(j+1)+alast(j-1))+(t3-2*(t2-t1)-f/2)
&  *alast(j)

```

```
endif
c
  if(j.eq.2) then
c   if(IBC.EQ.1) CC(1)=AA(1)+CC(1)
c reflective b.c. : a1=a3
    if(IBC.EQ.1) BB(1)=AA(1)+BB(1)
c reflective b.c. : a1=a2
    if(IBC.EQ.0) then
c transmitting b.c.
c
    if(ISN.EQ.0) then
c straight snell
      mip= (0.,1.)*wk*sin(theta)/2.
      mip=(1./dely-mip)/(1./dely+mip)
    else
c kirby's improved
      mip=(alast(2)-alast(1))/(alast(2)+alast(1))
      mip=(1.-mip)/(1.+mip)
    endif
c
    bb(1)=bb(1)+mip*aa(1)
    endif
    aa(j-1)=(0.,0.)
c
  endif
c
  if(j.eq.ndely) then
c   if(IBC.EQ.1) aa(j-1)=aa(j-1)+cc(j-1)
c reflective b.c. : an=an-2
    if(IBC.EQ.1) bb(j-1)=bb(j-1)+cc(j-1)
c reflective b.c. : an=an-1
    if(IBC.EQ.0) then
c transmitting b.c.
c
    if(ISN.EQ.0) then
c straight snell
      mim= (0.,1.)*wk*sin(theta)/2.
      mim=(1./dely+mim)/(1./dely-mim)
    else
c kirby's improved
      mim=(alast(j+1)-alast(j))/(alast(j+1)+alast(j))
      mim=(1.+mim)/(1.-mim)
    endif
```

```
c
  bb(j-1)=bb(j-1)+mim*cc(j-1)
  endif
  cc(j-1)=(0.,0.)
  endif

c
200  continue

c-----
c
c          *****  compute the solution  *****
c
c      neqs=ndely-1
c
c      call tridag(aa,bb,cc,dd,uu,neqs)
c
c      do 143 j=2,ndely
143  alast(j)=uu(j-1)
c load alast(j)
c
c      if(IBC.EQ.1) then
c      alast(1)=alast(3)
c reflective b.c.: a1=a3
c      alast(ndely+1)=alast(ndely-1)
c          : an=an-2
c      alast(1)=alast(2)
c reflective b.c.: a1=a2
c      alast(ndely+1)=alast(ndely)
c          : an=an-1
c      endif
c
c      if(IBC.EQ.0) then
c transmitting b.c.
c
c      alast(1)= mip*alast(2)
c      alast(ndely+1)= mim*alast(ndely)
c
c      endif
c
c transform back into phys. height
  do 37 j=1,ndely+1
37  aphys(j)=2.*alast(j)/ccg(j)
c
c          *****  check for breaking  *****
```

```

c
    if(ibreak.eq.1) then
    do 54 j=1,ndely+1
    hb=bc*di(j)
    rat=hb/cabs(aphys(j))
    if(di(j).lt.0) rat=0.
    if(rat.lt.1) then
c save point just before wave first breaks
    if(ih(j).eq.0) then
        hab(j)=cabs(aprev(j))
        rlb(j)=(lm-1)/real(ifx)
c calculate direction before breaking
        if(j.eq.ndely+1.or.ih(j+1).eq.1) then
            xx=aimag((aprev(j)-aprev(j-1))/(dely*kbar(1,j)*aprev(j)))
            if(xx.gt.1) xx=1.
            if(xx.lt.-1.) xx=-1.
            dib(j)=asin(xx)
        else
            xx=aimag((aprev(j+1)-aprev(j))/(dely*kbar(1,j)*aprev(j)))
            if(xx.gt.1) xx=1.
            if(xx.lt.-1.) xx=-1.
            dib(j)=asin(xx)
        endif
        dib(j)=270.-dib(j)*57.296-rot
        if(dib(j).lt.0) dib(j)=360+dib(j)
        ih(j)=1
    endif
    aphys(j)=rat*aphys(j)
    alast(j)=rat*alast(j)
    endif
54 continue
endif

c
c *****
c
c... writing wave field
    if(nmx*(lm/nmx).eq.lm.or.lm.eq.1) then
    call wwave(aphys,ndely,nmy,dely,kbar)
    endif

c
    do 55 nn=1,ndely+1
    aprev(nn)=aphys(nn)
55 continue

```

```
c
100  continue
c
c... output prebreak heights and directions
      open(24,file='break.dat')
      write(24,'(/,18x,a)') '      REFRACTION - DIFFRACTION      '
      write(24,'(/,18x,a)') ' WAVE HEIGHT AND DIRECTION BEFORE BREAKING'
      write(24,'(/,15x,a,a,a,f5.1,a,f4.1)')
& ' site: ',name,' direction: ',dir,' period: ',per
      write(24,'(/,20x,a,6x,a,6x,a,9x,a,/)')
&'row',' H (m) ','col','dir'
      m=1
      write(24,'(18x,i4,f12.2,f12.1,f12.1)') m,hab(m),rlb(m),dib(m)
      alphab=dib(m)-shor
      irlb=NINT(rlb(m))+1
      breakd=(5.0/4.0)*hab(m)
***rasterisze break point file m.....ixbra
      ixbra=2405-m
      write(39,'(18x,i4,i4,f12.3,f12.1,f12.3)') ixbra,irlb,hab(m),
&alphab,breakd
      if(nmy.eq.1) then
      is=2
      else
      is=nmy
      endif
      mm=1
      do 888 m=is,ndely,nmy
      mm=mm+1
      write(24,'(18x,i4,f12.2,f12.1,f12.1)') mm,hab(m),rlb(m),dib(m)
      alphab=dib(m)-shor
      irlb=NINT(rlb(m))+1
      breakd=(5.0/4.0)*hab(m)
      ixbra=2405-mm
      write(39,'(18x,i4,i4,f12.3,f12.1,f12.3)')ixbra,irlb,hab(m),
&alphab,breakd
888  continue
c
c
      rewind (9)
      rewind (11)
c
c.....create wave height and wave angle arrays
      do 114 i=1,nx
```

```

        read(9) (wht(i,j),j=1,ny)
        read(11) (ang(i,j),j=1,ny)
114  continue
c
c.... write array values to:
c.... ascii depth, wave number, wave angle, wave height grid files
c
c
c2002  format(4644f12.2)
c
cccc Comment out old way of writing arrays
cccccccc do 134 i=1,nx
cccccccc write(33,2002) (wht(i,j),j=1,ny)
cccccccc write(34,2002) (ang(i,j),j=1,ny)
cccccccc134  continue
c
CCCCCC Raster way of writing arrays!!!!!!!!!!!!!!
    DO 176 j=ny,1,-1
        write(33,6666) (wht(i,j),i=1,nx)
        write(34,6666) (ang(i,j),i=1,nx)
    176 CONTINUE
6666  format(4644f12.2)
6667  format(4644f12.6)
c
c
    go to 901
900  write(*,'(20x,a,a,a)') '***** error ***** 'ifile,' missing'
        write(*,'(20x,a)') ' press any key to continue '
        read(*,'(a)') idum
901  continue
        stop
        end
c
c-----
c
    subroutine tridag(a,b,c,r,u,n)
c
    parameter (nmax=250002)
    complex gam(nmax),a(n),b(n),c(n),r(n),u(n),bet
c
    bet=b(1)
    u(1)=r(1)/bet
    do 11 j=2,n

```

```

    gam(j)=c(j-1)/bet
    bet=b(j)-a(j)*gam(j)
    if(bet.eq.0)pause
    u(j)=(r(j)-a(j)*u(j-1))/bet
11  continue
    do 12 j=n-1,1,-1
    u(j)=u(j)-gam(j+1)*u(j+1)
12  continue
    return
    end
c
c-----
c
    subroutine wwave(aphys,ndely,nmy,dely,kbar)
c
c compute & write wave height and direction, initial breaking point
c imax= max grid size nmax=max no. of steps
c
    parameter (nmax=45000000,imax=4500000)
    dimension amod(nmax),alfa(nmax)
    real kbar(2,nmax)
    complex aphys(nmax)
c
    nky=0
    do 350 j=1,ndely+1
    if(nmy*(j/nmy).eq.j.or.j.eq.1) then
    nky=nky+1
c
    amod(nky)=cabs(aphys(j))
    if(amod(nky).gt..05) then
    if(j.eq.ndely+1) then
    xx=aimag((aphys(j)-aphys(j-1))/(dely*kbar(2,j)*aphys(j)))
    if(xx.gt.1) xx=1.
    if(xx.lt.-1.) xx=-1.
    alfa(nky)=asin(xx)
    else
    xx=aimag((aphys(j+1)-aphys(j))/(dely*kbar(2,j)*aphys(j)))
    if(xx.gt.1) xx=1.
    if(xx.lt.-1.) xx=-1.
    alfa(nky)=asin(xx)
    endif
    else
    alfa(nky)=0

```



```

common /grid/ ny,sy,sx,dely,delx,ndely,f,dcon,ify,ifx,tide
data tpi/6.2831853/
c
sig=tpi*f
a=d*sig*sig/9.81
if(a.ge.1) then
  yhat=a*(1+1.26*exp((-1.84)*a))
  t=exp((-2)*yhat)
  aka=a*(1+2*t*(1+t))
else
  aka=sqrt(a)*(1+a/6.*(1+a/5.))
endif
k=aka/d
x=2*k*d
cg=tpi*(f/k)*.5*(1+x/sinh(x))
return
end
c
c*****
c
c      subroutine intkcg(lm,kbar,ccg,di,ikount)
c
c      parameter(max=45000002)
c      real kbar(2,max)
c      dimension ccg(max),d(2,max),di(max)
c
c      save d
c      common /cut/ dc
c      common /grid/ ny,sy,sx,dely,delx,ndely,f,dcon,ify,ifx,tide
c      data  istart,ncol,eps/1,0,.0000001/
c
c... if this is the first call, load first two columns
c
c      go to (1,3) istart
1      istart=2
c... read in first 2 columns
      do 777 i=1,2
777      read(31,*) (d(i,j),j=1,ny)
      ncol=1
c... interpolate grid points for first row
      do 2 i=1,ndely
2      y=1+real(i-1)/real(ify)+eps
      ym=amod(y,1.)

```

```

    iy=int(y)
    di(i)=d(1,iy)+ym*(d(1,iy+1)-d(1,iy))+tide
    call getkcg(di(i)*dcon,rk,cg)
    ccg(i)=cg
2    kbar(2,i)=rk
c
c... figure out which bathymetry grid columns should be used
c
3    icol=1+real(lm)/real(ifx)+eps
    if(icol.ne.ncol) then
        do 5 i=1,ny
5        d(1,i)=d(2,i)
        read(31,*,end=999) (d(2,j),j=1,ny)
999    ncol=icol
        endif
        dd1=d(1,100)
c
c... bilinear interpolate depths for new column of k and cg
c
15    x=1+real(lm)/real(ifx)+eps
        xm=amod(x,1.)
        do 20 i=1,ndely
            y=1+real(i-1)/real(ify)+eps
            ym=amod(y,1.)
            iy=int(y)
            di(i)=d(1,iy)+xm*(d(2,iy)-d(1,iy))+ym*(d(1,iy+1)-d(1,iy))+
& xm*ym*(d(2,iy+1)-d(1,iy+1)-d(2,iy)+d(1,iy))+tide
            if(di(i).le.01) then
                di(i)=.01
            endif
c
c... shift k and ccg col 2 to 1 and calculate new 2's
c
        if(di(i).lt.dc) di(i)=dc
        kbar(1,i)=kbar(2,i)
        call getkcg(di(i)*dcon,rk,cg)
        kbar(2,i)=rk
20    ccg(i)=cg
        kbar(1,ndely+1)=kbar(1,ndely)
        kbar(2,ndely+1)=kbar(2,ndely)
        ccg(ndely+1)=ccg(ndely)
        di(ndely+1)=di(ndely)
c

```

AMEC, Environment & Infrastructure, Inc.
Hydrodynamic Modeling of Storm Drain Discharges in
the Neighborhood of ASBS 29 in La Jolla, California
Revised: 13 March 2013

return
end

For high resolution local refraction/diffraction calculations within the Torrey Pines Sub-Cell, we use the **oceanrds_tp.for** codes on a 441 x 236 raster formatted grid found in Appendix D. The input parameters output files which are required by **oceanrds_tp.for** are:

subbot50.grd.....*bathymetry input file
1.0*(gis) if water values are negative gis= -1.0, if positive gis=1.0
1* wave exposure 1=west, 2=north, 3=east, 4=south (icoast)
0.0* sea level adjustment MSL meters (sealev) (+ = deeper water)
50.0* inner grid dimensions in meters perpendicular to coast (sx)
50.0* inner grid dimensions in meters parallel to coast (sy)
236* number of grid cells in from deep water perpendicular to coast raster
(nx)
441* number of grid cells along coast from top edge (ny)
15.0* wave period in seconds (persw)
285.0* wave direction degress clockwise from true north (asw)
2.0* wave height meters (hsw)

```
C*****
C
C   Ocean refraction - diffraction module oceanrds_tp.for
C
C   programmed to run on gis elevation data (tp_subbot50_grd.txt subbot50.grd)
C   extracted from GIS grid by gis_ascii_utm-xyz.for
C           14 sep, 2004
C
C*****
C Bathymetry is read from
C a formatted 441 (row) x 236 (col) real number array called 'ifile'.grd,
C created by gis_ascii_utm-xyz.for, where'ifile' corresponds to
C the inputted site name. Program uses "oceanrd_tp.inp" input file.
C All output files are named 'ifile' with different extensions,
C ie. 'ifile'.wh1.
C*****
C*****
C
C       parameter (max=10000000)
C       character name*8,ifile*12
C       character ofile1*12,ofile2*12,ofile3*12,ofile4*12
C       character ofile5*12,ofile6*12,ofile7*12
C       dimension ccg(max),di(max),hab(max),rlb(max),dib(max),ih(max)
C       dimension depth(4644,4644),wht(4644,4644)
C       dimension ang(4644,4644)
C       dimension depthold(4644,4644)
C       real kbar(2,max),kave
C
C       complex aa(max),bb(max),cc(max),dd(max),uu(max),aprev(max)
C       complex c3,t1,t2,t3,f,alast(max),aphys(max),mim,mip
C
C       common /grid/ ny,sy,sx,dely,delx,ndely,freq,dcon,ify,ifx,tide
C           common /cut/ dc
C
C       pi=acos(-1.)
C
C   open parameter input file, return error message if missing
C
C
C
C       open(2,file='oceanrds_tp.inp',status='old',err=900)
C       read(2,'(a)') name
C           read(2,*) gis
```

```
read(2,*) icoast
  read(2,*) tide_elev
  read(2,*) sx
read(2,*) sy
  read(2,*) nx
read(2,*) ny
  read(2,*) persw
  read(2,*) asw
  read(2,*) hsw
c
  tide=tide_elev
  amp=hsw
  dir=asw
  per=persw
c
  freq=1/per
c
c... change to proper rotation frame, flag if theta not between +/- 45
c
  IF (icoast .EQ. 1) coast=270.0
  IF (icoast .EQ. 2) coast=90.0
  IF (icoast .EQ. 3) coast=0.0
  IF (icoast .EQ. 4) coast=180.0
c
  theta=coast-dir
c
c... set some variables to constant values
c
c  dcon = 1. for nuwave version
c  dcon=1.
c
c  cutoff depth (dc) -5.0 meters
c  dc=-5.0
c
c  breaking wave switch (ibreak) (1=on, 0=off)
c  ibreak=1
c
c  breaking criteria (bc) 0.5 for wave height = (bc)*depth
c  bc=0.5
c
c  lateral b.c.: ibc=(0) transmitting, ibc=(1) reflective
c  ibc=0
c  if trans: (isn=0) straight snell, isn=(1) kirby's improved
```

```
      isn=1
c      idf=(0) small angle diff, idf=(1) large angle dif
      idf=1
c
c
      write(*,'(5(/),10x,a)')
&' KIRBY HIGHER ORDER REFRACTION-DIFFRACTION PROGRAM '
      write(*,'(/,10x,a)')
&'- based on the parabolic equation method (PEM) of solving'
      write(*,'(10x,a,5(/)')
&' the mild-slope equation. '
c
      nn=8
      do 3 m=8,1,-1
3      if(name(m:m).eq.' ') nn=m-1
c
c
c... open grid file
c
      write(ifile,'(a,a)') name(:nn),'.grd'
      open(20,file=ifile,status='old',err=900)
c
c
c... open breaker ix,iy,wave height, wave angle, depth file
      write(ofile7,'(a,a)') name(:nn),'.bra'
      open(39,file=ofile7)
c
c
c... open sea level corrected ascii bathymetry file
      write(ofile1,'(a,a)') name(:nn),'.dep'
      open(31,file=ofile1)
c
c
c... open ascii wave number file
      write(ofile2,'(a,a)') name(:nn),'.wvn'
      open(32,file=ofile2)
c
c
c
c... open ascii wave height file
      write(ofile3,'(a,a)') name(:nn),'.wh1'
      open(33,file=ofile3)
c
```

```
c
c
c... open ascii wave angle file
      write(ofile4,'(a,a)') name(:nn),'.an1'
      open(34,file=ofile4)
c
c
c
c.... create depth array
c
      do 111 j=ny,1,-1
      read(20,*) (depthold(j,i),i=1,nx)
111  continue
      rewind(20)
c
c 10oct02 *****correct for sea level and change sign if GIS data
      do 711 i=1,nx
      do 811 j=1,ny
      depthold(j,i)=(gis*depthold(j,i))+sealev
811  continue
711  continue
c
c.....write rotated ascii depth file for internal use in ref/dif
165  format(2405f12.2)
      DO 101 i=1,nx
      WRITE(31,165)(depthold(j,i),j=1,ny)
101  CONTINUE
      rewind(31)
c
c
      do 119 i=1,nx
      read(31,*) (depth(i,j),j=1,ny)
119  continue
      rewind(31)
c
c
c... read first depth to initialize offshore boundary
c
      read(31,*) (di(m),m=1,ny)
      ridep=di(ny/2)
      rewind(31)

c.... would like a grid step size on the order of 1/5 wavelength
```

```
      call getkcg(10.,wk,cg0)
      wl=2*pi/wk
      ifx=1+sx/(.2*wl)
      ify=1+sy/(.2*wl)
c
      nmX=ifx
      nmY=ify
c
      amp=amp/2.
c
c... calculate dimensions of interpolated grid
c
      dely=sy/ify
      delx=sx/ifx
      ndely=(ny-1)*ify
      ndelx=(nx-1)*ifx
c
c
      call getkcg(ridep,wk0,cg0)
c wave length (m)
      wl=2*pi/wk0
c wave frequency (rad/sec)
      sig=2*pi/per
c radder's correction factor
      do 33 j=1,ndely+1
33   ccg(j)=sqrt(sig*cg0/wk0)
c
c
      ltype=2
c... open binary wave height file
      write(ofile5,'(a,a)') name(:nn),'.bw1'
      open(9,file=ofile5,form='unformatted')
c
c... open binary wave angle file
      write(ofile6,'(a,a)') name(:nn),'.ba1'
      open(11,file=ofile6,form='unformatted')
c
c.. initialize depth array
      do 555 nn=1,ndely+1
      hab(nn)=0.
      ih(nn)=0
555   continue
```

```
c
c  enter initial condition at x=0
c
c      call inbc(amp,wk0,theta,ndely,dely,alast)
c
c      do 202 j=1,ndely+1
c      kbar(1,j)=wk
202  kbar(2,j)=wk
c
c  scale alast as in radder(1978)
c      do 32 j=1,ndely+1
c      alast(j)=alast(j)*ccg(j)
32  continue
c
c      call wwave(alast,ndely,nmy,dely,kbar)
c
c  solution of the parabolic eqn. by the crank-nicholson formulation
c
c  start x increments
c
c      c2=1./2./dely**2
c      c3=2.*(0,1)/delx
c
c-----
c increments in x-direction
c
c      ikount=0
c      do 100 l=1,ndelx
c
c... write every 10th step to the screen
c
c      if(10*((l+1)/10).eq.l+1) then
c      print *, ' column ',l+1,' of ',ndelx+1
c      endif
c
c      lm=l
c
c      call intkcg(lm,kbar,ccg,di,ikount)
c
c  correction factor
c      do 34 j=1,ndely+1
c      ccg(j)=sqrt(sig*ccg(j)/kbar(2,j))
34  continue
```

```

c-----
c increments in y-direction - 1st. round
  do 200 j=2,ndely
c
  kave=(kbar(2,j)+kbar(1,j))/2.
c  kave=kbar(2,j)
c
  if(idf.eq.0) then
c small angle diffraction approximation
c
  t1=c2
  t3=c3*kave
  f=2*kave*(kave-wk)+c3/2*(kbar(2,j)-kbar(1,j))
c
  aa(j-1)=t1
  bb(j-1)=t3-2.*t1+f/2.
  cc(j-1)=t1
  dd(j-1)=-t1*alast(j+1)+(t3+2*t1-f/2)*alast(j)-t1*alast(j-1)
c
  endif
c
  if(idf.eq.1) then
c large angle diffraction approximation
c
  t1=c2/2.*(3.-wk/kave)
  t2=c2*c3/4./kave
  t3=c3*kave
  f=2*kave*(kave-wk)+c3/2*(kbar(2,j)-kbar(1,j))
c
  aa(j-1)=t1+t2
  bb(j-1)=t3-2.*(t1+t2)+f/2.
  cc(j-1)=t1+t2
  dd(j-1)=(t2-t1)*(alast(j+1)+alast(j-1))+(t3-2*(t2-t1)-f/2)
  & *alast(j)
  endif
c
  if(j.eq.2) then
c  if(IBC.eq.1) cc(1)=aa(1)+cc(1)
c reflective b.c. : a1=a3
  if(IBC.eq.1) bb(1)=aa(1)+bb(1)
c reflective b.c. : a1=a2
  if(IBC.eq.0) then
c transmitting b.c.

```

```
c
  if(isn.eq.0) then
c straight snell
  mip= (0.,1.)*wk*sin(theta)/2.
  mip=(1./dely-mip)/(1./dely+mip)
  else
c kirby's improved
  mip=(alast(2)-alast(1))/(alast(2)+alast(1))
  mip=(1.-mip)/(1.+mip)
  endif
c
  bb(1)=bb(1)+mip*aa(1)
  endif
  aa(j-1)=(0.,0.)
c
  endif
c
  if(j.eq.ndely) then
c   if(IBC.eq.1) aa(j-1)=aa(j-1)+cc(j-1)
c reflective b.c. : an=an-2
  if(IBC.eq.1) bb(j-1)=bb(j-1)+cc(j-1)
c reflective b.c. : an=an-1
  if(IBC.eq.0) then
c transmitting b.c.
c
  if(isn.eq.0) then
c straight snell
  mim= (0.,1.)*wk*sin(theta)/2.
  mim=(1./dely+mim)/(1./dely-mim)
  else
c kirby's improved
  mim=(alast(j+1)-alast(j))/(alast(j+1)+alast(j))
  mim=(1.+mim)/(1.-mim)
  endif
c
  bb(j-1)=bb(j-1)+mim*cc(j-1)
  endif
  cc(j-1)=(0.,0.)
  endif
c
200 continue
c-----
c
```

```

c          ***** compute the solution *****
c
c          neqs=ndely-1
c
c          call tridag(aa,bb,cc,dd,uu,neqs)
c
c          do 143 j=2,ndely
143      alast(j)=uu(j-1)
c load alast(j)
c
c          if(IBC.EQ.1) then
c      alast(1)=alast(3)
c reflective b.c.: a1=a3
c      alast(ndely+1)=alast(ndely-1)
c          : an=an-2
c      alast(1)=alast(2)
c reflective b.c.: a1=a2
c      alast(ndely+1)=alast(ndely)
c          : an=an-1
c      endif
c
c          if(IBC.EQ.0) then
c transmitting b.c.
c
c      alast(1)= mip*alast(2)
c      alast(ndely+1)= mim*alast(ndely)
c
c      endif
c
c transform back into phys. height
c      do 37 j=1,ndely+1
37      aphys(j)=2.*alast(j)/ccg(j)
c
c          ***** check for breaking *****
c
c      if(IBREAK.EQ.1) then
c      do 54 j=1,ndely+1
c      hb=bc*di(j)
c      rat=hb/cabs(aphys(j))
c      if(di(j).lt.0) rat=0.
c      if(rat.lt.1) then
c save point just before wave first breaks
c      if(ih(j).EQ.0) then

```

```

      hab(j)=cabs(aprev(j))
      rlb(j)=(lm-1)/real(ifx)
c calculate direction before breaking
      if(j.eq.ndely+1.or.ih(j+1).eq.1) then
xx=aimag((aprev(j)-aprev(j-1))/(dely*kbar(1,j)*aprev(j)))
      if(xx.gt.1) xx=1.
      if(xx.lt.-1.) xx=-1.
      dib(j)=asin(xx)
      else
xx=aimag((aprev(j+1)-aprev(j))/(dely*kbar(1,j)*aprev(j)))
      if(xx.gt.1) xx=1.
      if(xx.lt.-1.) xx=-1.
      dib(j)=asin(xx)
      endif
      dib(j)=270.-dib(j)*57.296-rot
      if(dib(j).lt.0) dib(j)=360+dib(j)
      ih(j)=1
      endif
      aphys(j)=rat*aphys(j)
      alast(j)=rat*alast(j)
      endif
54  continue
      endif
c
c *****
c
c... writing wave field
      if(nmx*(lm/nmx).eq.lm.or.lm.eq.1) then
      call wwave(aphys,ndely,nmy,dely,kbar)
      endif
c
      do 55 nn=1,ndely+1
      aprev(nn)=aphys(nn)
55  continue
c
100  continue
c
c... output prebreak heights and directions
      open(24,file='break.dat')
      write(24,'(/,18x,a)') '      REFRACTION - DIFFRACTION      '
      write(24,'(/,18x,a)') ' WAVE HEIGHT AND DIRECTION BEFORE BREAKING'
      write(24,'(/,15x,a,a,a,f5.1,a,f4.1)')
& ' site: ',name,' direction: ',dir,' period: ',per

```

```

        write(24,'(/,20x,a,6x,a,6x,a,9x,a,/)')
&'row',' H (m) ','col','dir'
        m=1
        write(24,'(18x,i4,f12.2,f12.1,f12.1)') m,hab(m),rlb(m),dib(m)
        alphas=dib(m)-shor
        irlb=NINT(rlb(m))+1
        breakd=(5.0/4.0)*hab(m)
***rasterize break point file m....ixbra
        ixbra=2405-m
        write(39,'(18x,i4,i4,f12.3,f12.1,f12.3)') ixbra,irlb,hab(m),
&alphas,breakd
        if(nmy.eq.1) then
            is=2
        else
            is=nmy
        endif
        mm=1
        do 888 m=is,ndely,nmy
            mm=mm+1
            write(24,'(18x,i4,f12.2,f12.1,f12.1)') mm,hab(m),rlb(m),dib(m)
            alphas=dib(m)-shor
            irlb=NINT(rlb(m))+1
            breakd=(5.0/4.0)*hab(m)
            ixbra=2405-mm
            write(39,'(18x,i4,i4,f12.3,f12.1,f12.3)')ixbra,irlb,hab(m),
&alphas,breakd
888    continue
c
c
        rewind (9)
        rewind (11)
c
c.....create wave height and wave angle arrays
        do 114 i=1,nx
            read(9) (wht(i,j),j=1,ny)
            read(11) (ang(i,j),j=1,ny)
114    continue
c
c.... write array values to:
c.... ascii depth, wave number, wave angle, wave height grid files
c
c
c2002    format(4644f12.2)

```

```

c
cccc Comment out old way of writing arrays
cccccccc do 134 i=1,nx
cccccccc write(33,2002) (wht(i,j),j=1,ny)
cccccccc write(34,2002) (ang(i,j),j=1,ny)
cccccccc134 continue
c
CCCCCC Raster way of writing arrays!!!!!!!!!!!!!!
  DO 176 j=ny,1,-1
    write(33,6666) (wht(i,j),i=1,nx)
    write(34,6666) (ang(i,j),i=1,nx)
  176 CONTINUE
6666 format(236f12.2)
6667 format(236f12.6)
c
c
  go to 901
900 write(*,'(20x,a,a,a)') '**** error **** ',ifile,' missing'
    write(*,'(20x,a)') ' press any key to continue '
    read(*,'(a)') idum
901 continue
    stop
    end
c
c-----
c
  subroutine tridag(a,b,c,r,u,n)
c
  parameter (nmax=250002)
  complex gam(nmax),a(n),b(n),c(n),r(n),u(n),bet
c
  bet=b(1)
  u(1)=r(1)/bet
  do 11 j=2,n
    gam(j)=c(j-1)/bet
    bet=b(j)-a(j)*gam(j)
    if(bet.eq.0)pause
    u(j)=(r(j)-a(j)*u(j-1))/bet
11 continue
  do 12 j=n-1,1,-1
    u(j)=u(j)-gam(j+1)*u(j+1)
12 continue
  return

```



```

    else
      aka=sqrt(a)*(1+a/6.*(1+a/5.))
    endif
    k=aka/d
    x=2*k*d
    cg=tpi*(f/k)*.5*(1+x/sinh(x))
    return
  end

c
c*****
c
c      subroutine intkcg(lm,kbar,ccg,di,ikount)
c
c          parameter(max=45000002)
c          real kbar(2,max)
c          dimension ccg(max),d(2,max),di(max)
c
c          save d
c          common /cut/ dc
c          common /grid/ ny,sy,sx,dely,delx,ndely,f,dcon,ify,ifx,tide
c          data  istart,ncol,eps/1,0,.0000001/
c
c... if this is the first call, load first two columns
c
c      go to (1,3) istart
1      istart=2
c... read in first 2 columns
      do 777 i=1,2
777      read(31,*) (d(i,j),j=1,ny)
      ncol=1
c... interpolate grid points for first row
      do 2 i=1,ndely
          y=1+real(i-1)/real(ify)+eps
          ym=amod(y,1.)
          iy=int(y)
          di(i)=d(1,iy)+ym*(d(1,iy+1)-d(1,iy))+tide
          call getkcg(di(i)*dcon,rk,cg)
          ccg(i)=cg
2      kbar(2,i)=rk
c
c... figure out which bathymetry grid columns should be used
c
3      icol=1+real(lm)/real(ifx)+eps

```

```
        if(icol.ne.ncol) then
            do 5 i=1,ny
5           d(1,i)=d(2,i)
            read(31,*,end=999) (d(2,j),j=1,ny)
999        ncol=icol
            endif
            dd1=d(1,100)
c
c... bilinear interpolate depths for new column of k and cg
c
15       x=1+real(lm)/real(ifx)+eps
           xm=amod(x,1.)
           do 20 i=1,ndely
               y=1+real(i-1)/real(ify)+eps
               ym=amod(y,1.)
               iy=int(y)
               di(i)=d(1,iy)+xm*(d(2,iy)-d(1,iy))+ym*(d(1,iy+1)-d(1,iy))+
& xm*ym*(d(2,iy+1)-d(1,iy+1)-d(2,iy)+d(1,iy))+tide
               if(di(i).le.01) then
                   di(i)=.01
               endif
c
c... shift k and ccg col 2 to 1 and calculate new 2's
c
           if(di(i).lt.dc) di(i)=dc
           kbar(1,i)=kbar(2,i)
           call getkcg(di(i)*dcon,rk,cg)
           kbar(2,i)=rk
20       ccg(i)=cg
           kbar(1,ndely+1)=kbar(1,ndely)
           kbar(2,ndely+1)=kbar(2,ndely)
           ccg(ndely+1)=ccg(ndely)
           di(ndely+1)=di(ndely)
c
           return
           end
```

AMEC, Environment & Infrastructure, Inc.
Hydrodynamic Modeling of Storm Drain Discharges in
the Neighborhood of ASBS 29 in La Jolla, California
Revised: 13 March 2013

APPENDIX D

CODE FOR THE OCEANBAT BATHYMETRY RETRIEVAL MODULE

Appendix D: Code for the OCEANBAT Bathymetry Retrieval Module

```
c*****
c
c       Bathymetry data base retrieval module oceanbat.f
c       Scott A. Jenkins & Joseph Wasyl Jan 10, 2001
c
c*****
c
c  THE LATTITUDE AND LONGITUDE OF THE UPPER LEFT CORNER OF A
c  BATHYMETRY GRID REQUIRED.
c  (The dimensions are specified in number of 3 second lat/lon points)
c  (we have been using a default value of 200 x 200)
c
c  reads packed grid files for the Southern California Bight
c  and writes the data to an 200x200 formatted data file, 'site'.grd.
c
c*****
c       integer*2 gdata(1201,801),dlist(12,10)
c       character name*8,ofile*20,ifile*60,lfile*13,cfile*13
c       character name2*60
c       dimension ilat(3),ilon(3)
c               real*4 latmin,latmax,lonmin,lonmax
c       common /param/ ixo,iyo,ix,iy,ixmin
c       common /int/ dx,dy,dgx,dgy,ang,ngx,ngy
c
c... initialize the disk list
c
c       call list(dlist)
c
c... get name of the active study area
c       open(11,file='oceanbat.inp',status='old')
c
c       read(11,'(a)') name
c
c
c       read(11,'(a)') name2
c       write(namesub,'(a)') name2
c
c       nn=8
c       do 2 m=8,1,-1
c         if(name(m:m).eq.' ') nn=m-1
2       continue
c
c       write(lfile,'(a,a)') name(:nn),'.log'
c
```

```
        open(8,file=lfile)
4      continue
c
        write(*,'(//,a)')
        &' OCEAN BATHYMETRY MODULE FOR THE CALIFORNIA COASTLINE
DATABASE'
c
c
c
        read(11,*) ilat(1)
        read(11,*) z
        ilat(2)=int(z)
        ilat(3)=nint(60.*(z-int(z)))
        read(11,*) ilon(1)
        read(11,*) z2
        ilon(2)=int(z2)
        ilon(3)=nint(60.*(z2-int(z2)))
c
        read(11,*) nx
        ngx=nx
c
        read(11,*) ny
        ngy=ny
c
c.....read in upper left corner as origin lat lon
c.....write files across from left to right starting at origin
        nrot=3
c
c... figure out dimension of 3 sec by 3 sec grid
c
        dy=92.6
        rlat=real(ilat(1))+real(ilat(2))/60+real(ilat(3))/3600
        dx=dy*cos(rlat*.017453)
c
        if(nrot.eq.1.or.nrot.eq.3) then
            dsave=dx
            dx=dy
            dy=dsave
        endif
c
c
c
        imx=0
        imy=0
c
c...output information to log file
c
        write(8,'(6i4,a)') ilat,ilon
```

```
    write(8,'(2f5.1,a)') dx,dy
    write(8,'(2i5,a)') ngx,ngy
    write(8,'(a)') ' 0 0 0 0'
c
    ang=0
    ang=pi*ang/180
    if(ang.lt.0) ang=2*pi+ang
c
c... truncate origin to a grid point
c
    ilat(3)=3*(nint(real(ilat(3))/3.))
    ilon(3)=3*(nint(real(ilon(3))/3.))
c
    iyo=ilat(1)*1200+ilat(2)*20+ilat(3)/3-imy
    ixo=150000-(ilon(1)*1200+ilon(2)*20+ilon(3)/3)-imx
c
c... adjust origin based on rotation
c
    if(nrot.eq.1) then
        ixo=ixo-ngy+1
        nsave=ngy
        ngy=ngx
        ngx=nsave
    elseif(nrot.eq.2) then
        ixo=ixo-ngx+1
        iyo=iyo-ngy+1
    elseif(nrot.eq.3) then
        iyo=iyo-ngx+1
        nsave=ngx
        ngx=ngy
        ngy=nsave
    endif
c
c... find range of necessary input data in both lat/lon and
c database units.
c
c
c
    ixmin=ixo
    ixmax=ixo+ngx-1
    iymn=iyo
    iymax=iyo+ngy-1
c
c
c... convert back to lat/lon coordinates
c
    latmin=real(iymn-1)/1200.
    latmax=real(iymax)/1200.
```

```
lonmax=(150000.-(ixmin+1))/1200.  
lonmin=(150000.-ixmax)/1200.  
c  
print *, ' lat/lon range ',latmin,latmax,lonmin,lonmax  
c  
do 60 i=latmin,latmax  
nggx=1  
nggy=1  
    iy=i*1200  
    nys=iymin-iy  
    nye=iymax-iy  
    if(nys.lt.1) then  
        nggy=abs(nys)+2  
        nys=1  
    endif  
    if(nye.gt.1200) then  
    if(nye.gt.2400) then  
        nye=1200  
    else  
        nye=1200  
        nggy=1  
    endif  
    endif  
do 60 j=lonmax,lonmin,-1  
    ix=150000-(j+1)*1200-1  
    nxs=ixmin-ix  
    nxe=ixmax-ix  
    if(nxs.lt.1) then  
        nggx=abs(nxs)+2  
        nxs=1  
    endif  
    if(nxe.gt.1200) then  
c        if(nxe.gt.2400) then  
c            nxe=1200  
c            nggx=1201  
c            else  
c                nggx=1  
c                nxe=1200  
            endif  
c        endif  
c  
c... figure out which bathymetry file to read  
c  
    il=i-31  
    jl=j-116  
    ndisk=dlist(il,jl)  
c
```

```
45  continue
c
c
    write(ifile,1000)name2(1:LSTGDCHR(name2)), i,j
c
1000  format(a,',',i2,i3,'pg.dta')
c
    close(20)
    print *, ' searching: ',ifile
    open(20,file=ifile,status='old',form='unformatted',err=50)
    go to 51
50  write(*,'(a,a,a)')
+ ' ?????? unable to find  ',ifile,' on the disk ?????? '
    write(*,'(a,\)') ' abort loading ? (y/n) : '
    read(*,*) ans
    if(ans.eq.'y'.or.ans.eq.'Y') then
        stop
    else
        go to 45
    endif
c
51  continue
c
    call unpack(gdata,nxs,nxe,nys,nye,nggx,nggy)
c
60  continue
c
c... output the grid array, one s to n column at a time from w to e
c
    write(ofile,2000) name(:nn)
2000  format(a,',grd')
c
    open(12,file=ofile)
c
c... output depends on rotation
c
2009  format(200f8.3)
    if(nrot.eq.1) then
        do 70 j=1,ngy
            write(12,2009) (real(gdata(i,j))* .1+.853,i=ngx,1,-1)
70  continue
        elseif(nrot.eq.2) then
            do 71 i=ngx,1,-1
                write(12,2009) (real(gdata(i,j))* .1+.853,j=ngy,1,-1)
71  continue
            elseif(nrot.eq.3) then
                do 72 j=ngy,1,-1
```

```

        write(12,2009) (real(gdata(i,j))* .1+.853,i=1,ngx)
72    continue
        else
        do 73 i=1,ngx
        write(12,2009) (real(gdata(i,j))* .1+.853,j=1,ngy)
73    continue
        endif
c
c... make the default contour commmand file for the base map
c
c... maximum length is 5.5 inches
c
        rlmax=max(real(ngx)*dx,real(ngy)*dy)
        h=6.5*real(ngy)*dy/rlmax
        w=6.5*real(ngx)*dx/rlmax
        write(cfile,'(a,a)' name(:nn),'.cnt')
        open(7,file=cfile)
        write(7,'(a,a)' 'file ',ofile)
        write(7,'(a,a)' 'format  binary')
        write(7,*) 'axes ',lonmax,lonmin,latmin,latmax
        write(7,'(a)') 'xlabel Latitude'
        write(7,'(a)') 'ylabel Longitude'
        write(7,'(a)') 'caption'
        write(7,'(a)') 'title  Depth Contours (meters from MSL)'
        write(7,'(a)') 'letter  .1 .1 .1 .1 .1'
        write(7,'(a,f5.2)') 'width  ',w
        write(7,'(a,f5.2)') 'height ',h
        write(7,'(a,i4,i4)') 'read  ',ngx,ngy
        write(7,*) 'plot ',.5*(8.5-w),.5*(11.-h)
        write(7,'(a)') 'stop'
c
c.....
c.....write ascii bathymetry
c    rewind(12)
c
c
c... open ascii bathymetry file
c    write(ofile1,'(a,a)' name(:nn),'.dep')
c    open(17,file=ofile1)
c
c
c    end
c
c
c*****
c
        subroutine unpack(gdata,nxs,nxe,ns,ne,ngx,ngy)

```

```
c
c... longitudes are reversed as read in to array since opposite of xy coor.
c
  integer*2 gdata(1201,801),dum
  integer*2 rec(1200),pdata(1200),idata(1200),dmin,dmax
  common /param/ ixo,iyo,ix,iy,ixmin
  data dmin,dmax/5001,-999/
c
c
c... loop through the files with desired data
c
  read(20) rec
c
c... read records
c
  ny=ngy
  do 100 i=1,ne
c   print *, ' reading rec ',i
c... unpacking data
c
c... check if record only contains deep water or land
c
  if(rec(i).lt.0) then
  if(i.lt.ns) go to 100
  if(rec(i).eq.-1) then
    depth=3050
  else
    depth=-20
  endif
  do 33 m=1,1200
33   idata(m)=depth
    go to 91
  endif
c
c... unpack the row
c
  icnt=1201
c
  if(i.lt.ns) then
  read(20) dum
  go to 100
  endif
c
  read(20) (pdata(m),m=1,rec(i))
c
  do 90 j=1,rec(i)
```

```
c
  if(pdata(j).lt.-10000) then
    if(pdata(j).lt.-20000) then
      ncnt=abs(pdata(j)+20000)
      depth=-20
    else
      ncnt=abs(pdata(j)+10000)
      depth=3050
    endif
    do 85 m=1,ncnt
      icnt=icnt-1
85    idata(icnt)=depth
      go to 90
    endif
  c
  icnt=icnt-1
  idata(icnt)=pdata(j)
  c
90  continue
  c
c... place desired data from record into grid array
  c
91  continue
  nx=ngx
  c
  do 92 jj=nxs,nxe
  c
  gdata(nx,ny)=idata(jj)
  c  dmax=max0(gdata(kx,ky),dmax)
  c  dmin=min0(gdata(kx,ky),dmin)
92  nx=nx+1
  c
98  ny=ny+1
  c
c.... save rec
  c
100 continue
  c  print *,dmin,dmax
  c
  c  ngx=nx
  c  ngy=ny
  return
  end
  c
  c
c*****
c
```

```

      subroutine list(dlist)
c
c... contains the floppy disk no. for grid files i=lat-31; j=lon-116
      integer*2 dlist(12,10)
c
      do 10 i=1,12
      do 10 j=1,10
      dlist(i,j)=-1
10    continue
c
      dlist(1,1)=1
      dlist(1,2)=1
      dlist(1,3)=1
      dlist(2,2)=1
      dlist(2,1)=2
      dlist(2,3)=2
      dlist(3,2)=2
      dlist(4,4)=2
      dlist(2,4)=3
      dlist(5,5)=3
      dlist(3,3)=3
      dlist(3,4)=4
      dlist(4,5)=4
      dlist(5,6)=5
c
      return
      end
c*****
      INTEGER FUNCTION LSTGDCHR(NAMESUB)

      CHARACTER*(*)  NAMESUB
      INTEGER  II,CLEN,INDEX

      CLEN = LEN(NAMESUB)
      DO 100 II = CLEN,1,-1
100  IF( ICHAR(NAMESUB(II:II)) .GT. 60 .AND.
      1   ICHAR(NAMESUB(II:II)) .LT. 127 )GOTO 101
101  INDEX=II

      LSTGDCHR = INDEX
      RETURN

      END

```

AMEC, Environment & Infrastructure, Inc.
Hydrodynamic Modeling of Storm Drain Discharges in
the Neighborhood of ASBS 29 in La Jolla, California
Revised: 13 March 2013

APPENDIX E

CODE FOR THE SEDXPORT TRANSPORT MODEL

Appendix E: Code for the SEDXPORT Transport Model

```
c*****
c
c sedxport3.for Transport Model - (bottom, surfzone, outfall sources)
c   with NULL POINT January. 24, 2005 & selected grid point - 10:00
c   TIME STEP MODE beach outfall source and canyon sink modules
c   Littoral Advection/Diffusion
c   Fine Sediment Dispersion MODEL
c   written by Scott A.Jenkins & Joseph Wasyl
c
c
c*****
c
c*****
c
c   parameter (ni=200, nj=200)
c
c   real*4 n0,n0_1
c
c   character name*8,infil1*12,infil2*12
c   character infile3*12,infile2*12
c   Dimension wnum(ni,nj),wht(ni,nj),depth(ni,nj)
c   dimension iyb(nj),ixb(nj),bh(nj),ba(nj),bd(nj)
c   dimension ubr(nj),dxbr(nj),dxbave(nj),ubave(nj)
c   dimension zw(5)
c   dimension r7(10,5),revr7(10,5)
c   dimension d(10),rcp(10),rc(10),rcsp(10),rszcp(10)
c   dimension rrs(10),rrsp(10)
c
c*****null point arrays*****
c   dimension type(ni,nj)
c*****
c ... second outfall arrays
c   dimension rrs2(10),rrsp2(10)
c   dimension rrivr2(10,5),pnrr2(10,5)
c*****
c
c
c   dimension rsurf(10,5),rriv(10,5),rbot(10,5)
c   dimension pns(10,5),pnr(10,5),pnb(10,5),pnt(10,5)
c   dimension sp(10),sp2(10),spp(10)
```

```

c
  dimension suml1(ni,nj),suml2(ni,nj)
  dimension suml3(ni,nj),suml4(ni,nj),b(ni,nj),b2(ni,nj)
  dimension ux(ni,nj),uy(ni,nj)
c
c
c.....arrays unique to selected grid point loop
  dimension sum2(101),zw3(101),dep2(101),slope(101),a4402(101)
  dimension r72(10,101),revr72(10,101),dep(100)
  dimension rsurf2(10,101),rriv2(10,101),rbot2(10,101)
  dimension pns2(10,101),pnr2(10,101),pnb2(10,101),pnt2(10,101)
c
c*****
c ... second outfall arrays unique to selected grid point
  dimension rriv2r2(10,101),pnr2r2(10,101)
c*****
c*****
c..Salinity module arrays
  dimension salmean(5),sal2mean(101)
  dimension sriv1(5),sriv2(5),salr7(5)
  dimension s2riv1(101),s2riv2(101),sal2r7(101)
  dimension sall1(ni,nj),sall2(ni,nj),sall3(ni,nj)
  dimension sall4(ni,nj)
  dimension acdom1(ni,nj),acdom2(ni,nj),acdom3(ni,nj)
  dimension acdom4(ni,nj),a440(101)
c*****
c
C
c
c
c
  open(18,file='CEM_sedxport3.inp',status='old')
c
  read(18,'(a)') name
  read(18,*) nx
  read(18,*) ny
  read(18,*) igrdx
  read(18,*) igrdy
  read(18,*) sx
  read(18,*) sy
  read(18,*) persw
  read(18,*) perwin
  read(18,*) hsw

```

```
read(18,*) hwin
read(18,*) tanbeta
read(18,*) aks
read(18,*) akb
read(18,*) ak2
  read(18,*) rci
  read(18,*) rszi
read(18,*) ak
read(18,*) q
read(18,*) irx
read(18,*) iry
read(18,*) dr
read(18,*) rwidth
read(18,*) rrsi
read(18,*) q2
read(18,*) irx2
read(18,*) iry2
read(18,*) dr2
read(18,*) rwidth2
read(18,*) rrsi2
read(18,*) ak3
read(18,*) ak4
read(18,*) ak5
read(18,*) ibins
read(18,*) verdat
read(18,*) numlay
read(18,*) alay1
read(18,*) alay2
read(18,*) alay3
read(18,*) alay4
read(18,*) surf
read(18,*) river
read(18,*) river2
read(18,*) bottom
read(18,*) rhos
read(18,*) rhosr
read(18,*) rhosr2
read(18,*) tcon
read(18,*) tconriv
read(18,*) deltat
read(18,*) timestep
read(18,*) n0
read(18,*) gamma
```

```
read(18,*) salo
read(18,*) w0sal
read(18,*) ak3s
read(18,*) ak5s
read(18,*) aksal
read(18,*) domslope
read(18,*) dominter
read(18,*) domback
read(18,*) tconsal
read(18,*) ak7
read(18,*) ilat1
read(18,*) z
read(18,*) two_layer
read(18,*) v
read(18,*) ak8
read(18,*) p_mbar
read(18,*) dmix_for
read(18,*) dmix
read(18,*) ak2_1
read(18,*) ak_1
read(18,*) ak3_1
read(18,*) ak5_1
read(18,*) tcon_1
read(18,*) tconriv_1
read(18,*) n0_1
read(18,*) gamma_1
read(18,*) delsal_1
read(18,*) w0sal_1
read(18,*) ak3s_1
read(18,*) ak5s_1
read(18,*) aksal_1
read(18,*) tconsal_1
```

c

c...convert time to seconds

```
time=deltat*60*60
```

c.....convert tcon by multiplying by 10 E-6

```
tcon=tcon*0.001
```

c

```
if(timestep.NE.0.0)then
open(27,file='dmix_wind.dat',status='old')
read(27,*) dmix_old
read(27,*) epsilonw_old
dmix_old=dmix_old
```

```

    close(27)
    else
c.....when no forecast available dmix_old is set to nowcast n0_1 at t=0
    dmix_old=n0_1
    endif
c
c.....convert background in mg/l to number of grains
    n0=n0*100
c
c
    ilat2=int(z)
    ilat3=nint(60.*(z-int(z)))
    theta=real(ilat1)+real(ilat2)/60+real(ilat3)/3600
    v=v*0.5148*100.0
    ak8=0.00009/((v**0.5)+1.1103)
    ustar=(ak8*(v**2))**0.5
    rot_e=0.000072685
    rho_a=0.001293*(p_mbar/760)**0.714285714
    f=2.0*rot_e*SIND(theta)
c
c
c.....calculate for residual from previous time step
c.....epsilonw is in cgs units
    epsilonw=0.0000043*(v**2)
    if(v.LE.600)epsilonw=0.0000000102*(v**3)
    if(timestep.EQ.0.0)epsilonw_old=epsilonw
c
c..calculate sediment layer depth in meters when dmix_for=0 (no forecast)
    if(dmix_for.EQ.0.0)then
        dmix=0.4*ustar/(f*100)
    endif
c
c...if a forecast dmix is used do not modify from previous timestep
    if(dmix_for.NE.0)go to 1867
    dmix=dmix+((dmix_old-dmix)*
    &EXP(-1.0*epsilonw_old*time/(dmix_old*100.0)**2))
1867  continue
c
c.....in a single layer system dmix is set to 500 meters!!
    if(two_layer.EQ.0.0)dmix=500.0
c
c
c.....dmix still in meters prior to writing

```

```
    open(27,file='dmix_wind.dat',status='unknown')
    write(27,8030)dmix
    write(27,8030)epsilonw
8030  format(f20.10)
c
c.....convert dmix back to centimeters for subsequent calculations
    dmix=dmix*100.0
c
    alay3=(dmix-100)
    alay4=(dmix+100)
c
c
    open(19,file='bulk_density.dat',status='old')
    read(19,*) rci1
    read(19,*) rci2
    read(19,*) rci3
    read(19,*) rci4
    read(19,*) rci5
    read(19,*) rci6
    read(19,*) rci7
    read(19,*) rci8
    read(19,*) rci9
    read(19,*) rci10
    read(19,*) rci11
    read(19,*) rci12
    read(19,*) rci13
    read(19,*) rci14
c
    ires=101
    riv2=river2
    riv=river
    bot=bottom
c
c
    salmax=(domback-dominter)/domslope*(-1.0)
c
c....divide n0 grains among the first 5 grain size bins
    an0b1=n0*.767
    an0b2=n0*.179
    an0b3=n0*.0376
    an0b4=n0*.00886
    an0b5=n0*.00609
    an0b6=n0*.00142
```

```
an0b7=n0*.000248
an0b8=n0*.000121
an0b9=n0*.0000484
if(an0b1.LE.2.0)an0b1=2.0
if(an0b2.LE.2.0)an0b2=2.0
if(an0b3.LE.2.0)an0b3=2.0
if(an0b4.LE.2.0)an0b4=2.0
if(an0b5.LE.2.0)an0b5=2.0
if(an0b6.LE.2.0)an0b6=2.0
if(an0b7.LE.2.0)an0b7=2.0
if(an0b8.LE.2.0)an0b8=2.0
if(an0b9.LE.2.0)an0b9=2.0
c
c
  per=persw
c
  numlay=4
  if(numlay.GE.4)numlay=4
c

c.....open array of bulk density values from previous time step
c
c
  OPEN(2, FILE='timestep.sed', ACCESS='DIRECT', RECL=24,
  & FORM='UNFORMATTED')
c
c.....open planview of grain number output files
c
c
c... open ascii file layer 1 grain number / cc
  open(41,file='layer1.sed')
  open(81,file='layer1.sal')
  open(85,file='layer1.dom')
  open(91,file='layer1.slp')
c
c
c... open ascii file layer 1 grain number / cc
  open(42,file='layer2.sed')
  open(82,file='layer2.sal')
  open(86,file='layer2.dom')
  open(92,file='layer2.slp')
c
  if(two_layer.NE.0)then
```

```
c... open ascii file layer 1 grain number / cc
    open(43,file='layer3.sed')
    open(83,file='layer3.sal')
    open(87,file='layer3.dom')
c
c... open ascii file layer 1 grain number / cc
    open(44,file='layer4.sed')
    open(84,file='layer4.sal')
    open(88,file='layer4.dom')
c
    endif
c
c
c
    freq=1/per
    pi=acos(-1.)
    g=980.0
    ro=1.03
    omega=2*pi/per
c
c
    nn=8
    do 3 m=8,1,-1
3    if(name(m:m).eq.' ') nn=m-1
c
c
c... open grain size and mass percent file 'masstotal.dat'
c
    open(26,file='masstotal.dat',status='old')
c
c... read data from file
c
    nfact=1
    do 44 i=1,ibins
    read(26,*)d(i),rcp(i),rcsp(i),rrsp(i),rrsp2(i)
c ..... convert microns to centimeters
    d(i)=d(i)*.0001
    rc(i)=rcp(i)*rci
    rszcp(i)=rcsp(i)*rszi
    rrs(i)=rrsp(i)*rrsi
    rrs2(i)=rrsp2(i)*rrsi2
    nfact=nfact*i
44  continue
```

```
c
c...open selected point file at selected grid point(igrdx,igrdy)
      open(99,file='profile.sed',status='unknown')
c
c
c*****NULL POINT*****
c... open bottom type classification file (from grass)
      open(29,file='bottom_type.dat',status='old')
c
c
c
c...open bottom distribution file at selected crossection(igrdy)
c.....this part of program commented out for integrated cwc model
c....  open(50,file='nullpt.dat',status='unknown')
c

c.....open bottom distribution file at selected point(igrdx,igrdy)
c.....this part commented out for integrated model
c.    open(88,file='nullpt.igrdx')
c
c*****
c
c... open ascii wave number file from swell component
      write(ifile2,'(a,a)') name(:nn),'.wvn'
      open(32,file=ifile2,status='old')
c
c... open ascii depth file corrected to tide
      write(infil1,'(a,a)') name(:nn),'.dep'
      open(20,file=infil1,status='old')
c
c.....open total wave height file
      write(infil2,'(a,a)') name(:nn),'.wht'
      open(9,file=infil2,status='old')
c
c... open ascii file x-component of current
      open(45,file='xcur.xpt')
c
c... open ascii file y-component of current
      open(46,file='ycur.xpt')
c
c
c... read bathymetry, wave height, swell wave number x1, y=1,200
c....read x-component of current, y-component of current
```

```
c.....x1, y1 is bottom left corner looking at page by convention
c
c.....read into arrays depth, wave height, wave number
      do 111 i=1,nx
        read(20,*) (depth(i,j),j=1,ny)
        read(9,*)(wht(i,j),j=1,ny)
        read(32,*)(wnum(i,j),j=1,ny)
111  continue
c
c.....read in xcur, ycur, bot type verticle system reversed (raster)
      do 168 j=ny,1,-1
        read(45,*)(ux(i,j),i=1,nx)
        read(46,*)(uy(i,j),i=1,nx)
        read(29,*) (type(i,j),i=1,nx)
c
168  continue
c
c
c..... open breaker input file
      write(infile3,'(a,a)') name(:nn),'.bra'
      open(38,file=infile3)
c
c.... read x,y, breaker height, breaker angle, breaker depth
      do 150 n=1,ny
        read(38,*) iyb(n),ixb(n),bh(n),ba(n),bd(n)
c
c.....determine wave height, wnum at the break point
      ibpx=ixb(n)-1
      whtbc=wht(ibpx,n)*100
      wnumbc=wnum(ibpx,n)/100
      depthbc=depth(ibpx,n)*100
      wndepb=wnumbc*depthbc
c
c...create ix by 200 arrays of dxbr's and ubr's at the break point
      dxbr(n)=whtbc/SINH(wndepb)
      ubr(n)=dxbr(n)*omega
c
150  continue
c
c.....calculate average values dxbave and ubave
      do 151 i=1,200
c
      im1=i-1
```

```

    im2=i-2
    ip1=i+1
    ip2=i+2
    if(im1.LT.1)im1=1
    if(im2.LT.1)im2=1
    if(ip1.GT.200)ip1=200
    if(ip2.GT.200)ip2=200
    dxbave(i)=(dxbr(i)+dxbr(im1)+dxbr(im2)+dxbr(ip1)+dxbr(ip2))/5
    ubave(i)=(ubr(i)+ubr(im1)+ubr(im2)+ubr(ip1)+ubr(ip2))/5
c
151  continue
c
c.....initalize icount to 0 outside of iy,ix, and ipart loops
c.....and rtold,rsold,qsold,qs2old,salold,salold2 for timestep=0
    icount=0
    rtold=0.0
    rsold=0.0
    qsold=0.0
    qs2old=0.0
    salold=0.0
    salold2=0.0
c
c.....determine wave height, wnum at the outfall
c    whtrm=wht(irx,iry)*100
c    wnumrm=wnum(irx,iry)/100
c    depthrm=depth(irx,iry)*100
c    wndeprm=wnumrm*depthrm
c
c
c..... at the outfall
c    drm=whtrm/SINH(wndeprm)
c    urm=drm*omega
c
    do 1800 iy=1,ny
    allxbrk=0
c
    bd1=bd(iy)*100
    if(bd1.LT.10.0)bd1=10.0
    ba1=ba(iy)
    bh1=bh(iy)*100
c
c.....determine wave height, wnum at the break point
    ibpx=ixb(iy)-1

```

```
      whtbc=wht(ibpx,iy)*100
      wnumbc=wnum(ibpx,iy)/100
      depthbc=depth(ibpx,iy)*100
      wndepb=wnumbc*depthbc
c
c..... at the break point
      dxb=whtbc/SINH(wndepb)
      ub=dxb*omega
c
c
c
      stopdep=bd(iy)
c
      do 1801 ix=1,nx
c
c*****null point - bottom type*****
      if(type(ix,iy).LE.100)go to 7006
c
      if(type(ix,iy).LE.200)then
      rci=(rci2-rci1)*(type(ix,iy)-100)/100+rci1
      go to 7007
      endif
c
      if(type(ix,iy).LE.300)then
      rci=(rci3-rci2)*(type(ix,iy)-200)/100+rci2
      go to 7007
      endif
c
      if(type(ix,iy).LE.400)then
      rci=(rci4-rci3)*(type(ix,iy)-300)/100+rci3
      go to 7007
      endif
c
      if(type(ix,iy).LE.500)then
      rci=(rci5-rci4)*(type(ix,iy)-400)/100+rci4
      go to 7007
      endif
c
      if(type(ix,iy).LE.200)then
      rci=(rci2-rci1)*(type(ix,iy)-100)/100+rci1
      go to 7007
      endif
c
```

```
    if(type(ix,iy).LE.300)then
      rci=(rci3-rci2)*(type(ix,iy)-200)/100+rci2
      go to 7007
    endif
c
    if(type(ix,iy).LE.400)then
      rci=(rci4-rci3)*(type(ix,iy)-300)/100+rci3
      go to 7007
    endif
c
    if(type(ix,iy).LE.500)then
      rci=(rci5-rci4)*(type(ix,iy)-400)/100+rci4
      go to 7007
    endif
c
    if(type(ix,iy).LE.600)then
      rci=(rci6-rci5)*(type(ix,iy)-500)/100+rci5
      go to 7007
    endif
c
    if(type(ix,iy).LE.700)then
      rci=(rci7-rci6)*(type(ix,iy)-600)/100+rci6
      go to 7007
    endif
c
    if(type(ix,iy).LE.800)then
      rci=(rci8-rci7)*(type(ix,iy)-700)/100+rci7
      go to 7007
    endif
c
    if(type(ix,iy).LE.900)then
      rci=(rci9-rci8)*(type(ix,iy)-800)/100+rci8
      go to 7007
    endif
c
    if(type(ix,iy).LE.1000)then
      rci=(rci10-rci9)*(type(ix,iy)-900)/100+rci9
      go to 7007
    endif
c
    if(type(ix,iy).LE.1100)then
      rci=(rci11-rci10)*(type(ix,iy)-1000)/100+rci10
      go to 7007
```

```

    endif
c
    if(type(ix,iy).LE.1200)then
    rci=(rci12-rci11)*(type(ix,iy)-1100)/100+rci11
    go to 7007
    endif
c
    if(type(ix,iy).LE.1300)then
    rci=(rci13-rci12)*(type(ix,iy)-1200)/100+rci12
    go to 7007
    endif
c
    if(type(ix,iy).LE.1400)then
    rci=(rci14-rci13)*(type(ix,iy)-1300)/100+rci13
    go to 7007
    endif
c
    if(type(ix,iy).GT.1400)then
    rci=rci14
    go to 7007
    endif
c
7006   rci=rci1
7007   continue
c
    distbp=((201-ix)-ixb(iy))*sx*100
c*****
c
    uy1=uy(ix,iy)+0.000001
    ux1=ux(ix,iy)+0.000001
c
c
c
c.....ADD resident sediment volume
c..... initialize total grain variable at each x,y location
    suml1(ix,iy)=n0
    suml2(ix,iy)=n0
    suml3(ix,iy)=n0
    suml4(ix,iy)=n0
c
    sall1(ix,iy)=salo
    sall2(ix,iy)=salo
    sall3(ix,iy)=salo

```

```
sall4(ix,iy)=salo
c
b(ix,iy)=gamma
b2(ix,iy)=gamma
c
c
if(depth(ix,iy).LE.stopdep)then
allxbrk=1.0
do 478 irt=ix,nx
suml1(irt,iy)=-1.0
suml2(irt,iy)=-1.0
suml3(irt,iy)=-1.0
suml4(irt,iy)=-1.0
c
sall1(irt,iy)=-1.0
sall2(irt,iy)=-1.0
sall3(irt,iy)=-1.0
sall4(irt,iy)=-1.0
c
acdom1(irt,iy)=-1.0
acdom2(irt,iy)=-1.0
acdom3(irt,iy)=-1.0
acdom4(irt,iy)=-1.0
c
c
b(irt,iy)=-1.0
b2(irt,iy)=-1.0

478 continue
go to 479
endif
c
c
c
c ..... convert wave hieght, water depth, and wave number into cgs
whtc=wht(ix,iy)*100
wnumc=wnum(ix,iy)/100
depthc=depth(ix,iy)*100
wndep=wnumc*depthc
c
d0=whtc/SINH(wndep)
u=omega*d0
c
```

```

c
c
c
  do 1776 ipart=1,ibins
c
  dip=d(ipart)
  rrsfix2=rrs2(ipart)
  rrsfix=rrs(ipart)
  respfix=rszcp(ipart)
c
c*****null point begin*****
c
  d0np=d0
  dm=ak7*d0np
  unp=rszi/(rhos*pi*dm)
  unpd1=unp*d(1)
  if(unpd1.GT.ibins)unp=ibins/d(1)
  if(unp.LT.ibins/(100*d(1)))unp=ibins/(100*d(1))
  unpdip=unp*dip
  rc(ipart)=rci*6.092*(((unp*dip)**ibins)/nfact)*EXP(-1*unp*dip)
  if(rc(ipart).LT.0.0000000000000001)rc(ipart)=0.0000000000000001
c
c.....nullpt selected grid write commented out
c  if(iy.NE.igrdy)go to 8001
c  if(ix.NE.igrdx)go to 8002
c  write(88,8003)dip,rc(ipart),depth(ix,iy),unpdip
c8003  format(4e10.3)
c8002  continue
c8001  continue
c*****null point end*****
  rcfix=rc(ipart)
c
c
  icount=icount+1
c
  if(timestep.EQ.0.0)go to 81
  read(2, REC=icount)rtold,rsold,qsold,qs2old,salold,salold2
81  continue
c
  if(ipart.EQ.1)w0=.00011
  if(ipart.EQ.2)w0=.00043
  if(ipart.EQ.3)w0=.0017
  if(ipart.EQ.4)w0=.0050

```

```

    if(ipart.EQ.5)w0=.0108
    if(ipart.EQ.6)w0=.044
    if(ipart.EQ.7)w0=.17
    if(ipart.EQ.8)w0=.38
    if(ipart.EQ.9)w0=.98
  c
  c*****
    if(iy.NE.igrdy)go to 4000
    if(ix.NE.igrdx)go to 4001
  c
    ipart2=ipart
  c
  c
    fw=EXP(5.2*((2.5*dip/d0)**0.2)-6.0)
  c
    delta=0.72*d0*(2.5*dip/d0)**0.25
    deltab=0.72*dxb*(2.5*dip/dxb)**0.25
    deltar=0.72*dxbave(iy)*(2.5*dip/dxbave(iy))**0.25
    deltas=0.72*dxbave(iy)*(0.000006625/dxbave(iy))**0.25
  c
  c
  c.....for the outfall sediment flux use running mean values of ub *dxb
    shieldr=ubave(iy)**2/((rhos/ro-1.0)*g*dip)
    epsilon_r_1=0.00035*ak3_1*((ubave(iy)/w0)**0.68)*
    &(shieldr**0.4)*deltar*g*per
    if(epsilon_r_1.LT.0.0000000001)epsilon_r_1 = 0.0000000001
    epsilon_r=epsilon_r_1+epsilon_w
  c**
  c.....for the outfall plume salinity use running mean values of ub *dxb
    shieldrs=ubave(iy)**2/(.03*g*dr)
    epsilon_rs_1=0.00035*ak3s*((ubave(iy)/w0sal)**0.68)*
    &(shieldrs**0.4)*deltas*g*per
    if(epsilon_rs_1.LT.0.0000000001)epsilon_rs_1 = 0.0000000001
    epsilon_rs=epsilon_rs_1+epsilon_w
  c
  c.....at the local break point
    shieldb=ub**2/((rhos/ro-1.0)*g*dip)
    epsilon_b_1=0.00035*ak3*((ub/w0)**0.68)*(shieldb**0.4)
    &*deltab*g*per
    if(epsilon_b_1.EQ.0)epsilon_b_1=0.0000000001
    epsilon_b=epsilon_b_1+epsilon_w
  c
  c.....at the local break point for disequilibrium profile

```

```

        epsilonbs_1=0.00035*ak3s*((ub/w0sal)**0.68)*(shieldrs**0.4)
        &*deltas*g*per
        if(epsilonbs_1.EQ.0.0000000001)epsilonbs_1 = 0.0000000001
        epsilonbs=epsilonbs_1+epsilonw
c
c.....offshore
        shield=u**2/((rhos/ro-1.0)*g*dip)
        epsilon_1=0.00035*ak2*((u/w0)**0.68)*(shield**0.4)*delta*g*per
        if(epsilon_1.EQ.0.0000000001)epsilon_1 = 0.0000000001
        epsilon=epsilon_1+epsilonw
c
c.....outfall shields and epsilon calculated in RIVERM subroutine
c**
c**
        rrsfix2=rrs2(ipart2)
        rrsfix=rrs(ipart2)
        respfix=rszcp(ipart2)
        rcfix=rc(ipart2)
c
        if(riv.EQ.1)then
            CALL RIVERM(epsilonnr,dr,rwidth,q,ux1,uy1,ix,iy,irx,iry,sx,
&sy,rrsfix,ak5,w0,deltab,rhosr,ro,dip,g,per,ak3,time,qsold,
&depthc,tconriv,qs)
            CALL SALM1(epsilonnr,dr,rwidth,q,ux1,uy1,ix,iy,irx,iry,sx,
&sy,salo,ak5s,w0sal,deltas,rhosr,ro,dip,g,per,ak3,time,salold,
&depthc,tconsal,sal)
c
            else
                continue
            endif
c
        if(riv2.EQ.1)then
            CALL RIVER2M(epsilonnr,dr2,rwidth2,q2,ux1,uy1,ix,iy,irx2,iry2,sx,
&sy,rrsfix2,ak5,w0,deltab,rhosr2,ro,dip,g,per,ak3,time,qs2old,
&depthc,tconriv,qs2)
c**
c**
            CALL SALM2(epsilonnr,dr2,rwidth2,q2,ux1,uy1,ix,iy,irx2,iry2,sx,
&sy,salo,ak5s,w0sal,deltas,rhosr2,ro,dip,g,per,ak3,time,salold2,
&depthc,tconsal,sal2)
c
            else
                continue
        
```

```

endif
c
if(surf.EQ.1)then
CALL SURFLM(epsilon,bd1,ba1,bh1,ibpx,ix,iy,
&ak4,aks,akb,dip,w0,pi,g,rhos,ro,tanbeta,rcspfix,time,rsold,
&depthc,tcon,rs)
else
continue
endif
c
c
if(bot.EQ.1)then
c**
c**
CALL BOTTOMM(ix,iy,u,shield,fw,ak,pi,wndep,rcfix,time,rtold,
&depthc,tcon,rt,w0,epsilon)
else
continue
endif
c
do 2002 k2=1,ires
zw3(k2)=depthc/100*(k2-1)
dep2(k2)=depthc/100*(ires-k2)
if(k2.EQ.1)zw3(k2)=delta
if(k2.EQ.1)dep2(k2)=depthc-delta
c
c ....sediment transport calculations
c.....initialize sal2mean(k2)
sal2mean(k2)=salo
a4402(k2)=dominter-domslope*sal2mean(k2)
if(sal2mean(k2).GE.salmax)a4402(k2)=domback
if(dmix.GE.dep2(k2))then
sal2r7(k2)=(-1.0)*dep2(k2)*aksal*w0sal/epsilonbs
else
sal2r7(k2)=(-1.0)*dep2(k2)*aksal*((dimx/4.21)**2.4)
&*w0sal/epsilonbs_1
endif
c
if((depthc-dmix).GE.zw3(k2))then
r72(ipart2,k2)=(-1.0)*zw3(k2)*w0/epsilon_1
else
r72(ipart2,k2)=(-1.0)*zw3(k2)*w0*(dmix/dip)**2.4/epsilon
endif

```

```

    if((depthc-dmix).LT.0.0)r72(ipart2,k2)=(-1.0)
    &*zw3(k2)*w0/epsilon
c
    if(dmix.GE.dep2(k2))then
    revr72(ipart2,k2)=(-1.0)*dep2(k2)*w0/epsilonb
    else
    revr72(ipart2,k2)=(-1.0)*dep2(k2)*w0*
    &(dmix/dip)**2.4/epsilonb_1
    endif
c**
c**
    if(surf.EQ.1)then
    rsurf2(ipart2,k2)=rs*EXP(r72(ipart2,k2))
    pns2(ipart2,k2)=(6.0/(pi*dip**3))*rsurf2(ipart2,k2)/rhos
    else
    pns2(ipart2,k2)=0
    endif
C
    if(riv.EQ.1)then
    s2riv1(k2)=sal*EXP(sal2r7(k2))
    rivsum=s2riv1(k2)
    sal2mean(k2)=salo-s2riv1(k2)
    a4402(k2)=dominter-domslope*sal2mean(k2)
    if(sal2mean(k2).GE.salmax)a4402(k2)=domback
    rrv2(ipart2,k2)=qs*EXP(revr72(ipart2,k2))
    pnr2(ipart2,k2)=(6.0/(pi*dip**3))*rrv2(ipart2,k2)/rhosr
    else
    pnr2(ipart2,k2)=0
    endif
C**
C**
    if(riv2.EQ.1)then
    s2riv2(k2)=sal2*EXP(sal2r7(k2))
    rivsum=s2riv1(k2)+s2riv2(k2)
    if(rivsum.GT.salo)then
    rivsum=salo
    endif
    sal2mean(k2)=salo-rivsum
    a4402(k2)=dominter-domslope*sal2mean(k2)
    if(sal2mean(k2).GE.salmax)a4402(k2)=domback
    rrv2r2(ipart2,k2)=qs2*EXP(revr72(ipart2,k2))
    pnr2r2(ipart2,k2)=(6.0/(pi*dip**3))*rrv2r2(ipart2,k2)/rhosr2
    else

```

```

    pnr2r2(ipart2,k2)=0
  endif
c
  if(bot.EQ.1)then
    rbot2(ipart2,k2)=rt*EXP(r72(ipart2,k2))
    pnb2(ipart2,k2)=(6.0/(pi*dip**3))*rbot2(ipart2,k2)/rhos
  else
    pnb2(ipart2,k2)=0
  endif
C**
C**
  pnt2(ipart2,k2)=pns2(ipart2,k2)+pnr2(ipart2,k2)+pnb2(ipart2,k2)
  &+pnr2r2(ipart2,k2)
  if(pnt2(ipart2,k2).GT.9999999)pnt2(ipart2,k2)=9999999
  if(pnt2(ipart2,k2).LT.-1000)pnt2(ipart2,k2)=-55555
c
2002  continue
c
2005  continue
c
c
4001  continue
4000  continue
c
c
c*****
c
  fw=EXP(5.2*((2.5*dip/d0)**0.2)-6.0)
c
  delta=0.72*d0*(2.5*dip/d0)**0.25
  deltab=0.72*dxb*(2.5*dip/dxb)**0.25
  deltar=0.72*dxbave(iy)*(2.5*dip/dxbave(iy))**0.25
  deltas=0.72*dxbave(iy)*(0.000006625/dxbave(iy))**0.25
c
c
c.....for the outfall sediment flux use running mean values of ub *dxb
  shieldr=ubave(iy)**2/((rhos/ro-1.0)*g*dip)
  epsilon_r_1=0.00035*ak3_1*((ubave(iy)/w0)**0.68)*
  &(shieldr**0.4)*deltar*g*per
  if(epsilon_r_1.LT.0.0000000001)epsilon_r_1 = 0.0000000001
  epsilon_r=epsilon_r_1+epsilon_w
c
c.....for the accretion wave use running mean values of ub *dxb

```

```

    shieldrs=ubave(iy)**2/(.03*g*dr)
    epsilonrs_1=0.00035*ak3s*((ubave(iy)/w0sal)**0.68)*
    &(shieldrs**0.4)*deltas*g*per
    if(epsilonrs_1.LT.0.0000000001)epsilonrs_1 = 0.0000000001
    epsilonrs=epsilonrs_1+epsilonw
c
c
    shieldb=ub**2/((rhos/ro-1.0)*g*dip)
    epsilonb_1=0.00035*ak3*((ub/w0)**0.68)*
    &(shieldb**0.4)*deltab*g*per
    if(epsilonb_1.EQ.0)epsilonb_1=0.0000000001
    epsilonb=epsilonb_1+epsilonw
c
c.....offshore
    shield=u**2/((rhos/ro-1.0)*g*dip)
    epsilon_1=0.00035*ak2*((u/w0)**0.68)*
    &(shield**0.4)*delta*g*per
    if(epsilon_1.LT.0.0000000001)epsilon_1 = 0.0000000001
    epsilon=epsilon_1+epsilonw
c
c
c.....at the local break point for salinity
    epsilonbs_1=0.00035*ak3s*((ub/w0sal)**0.68)
    &*(shieldrs**0.4)*deltas*g*per
    if(epsilonbs_1.LT.0.0000000001)epsilonbs_1 = 0.0000000001
    epsilonbs=epsilonbs_1+epsilonw
c
c.....outfall shields and epsilon calculated in RIVERM subroutine
c
c
c
c
    if(riv.EQ.1)then
      CALL RIVERM(epsilonnr,dr,rwidth,q,ux1,uy1,ix,iy,irx,iry,sx,
    &sy,rrsfix,ak5,w0,delta,rhosr,ro,dip,g,per,ak3,time,qsold,
    &depthc,tconriv,qs)
c
    CALL SALM1(epsilonnr,dr,rwidth,q,ux1,uy1,ix,iy,irx,iry,sx,
    &sy,salo,ak5s,w0sal,deltas,rhosr,ro,dip,g,per,ak3,time,salold,
    &depthc,tconsal,sal)
c
    else
      continue
  
```

```
endif
c
C
  if(riv2.EQ.1)then
    CALL RIVER2M(epsilon_r,dr2,rwidth2,q2,ux1,uy1,ix,iy,irx2,iry2,sx,
    &sy,rrsfix2,ak5,w0,deltab,rhosr2,ro,dip,g,per,ak3,time,qs2old,
    &depthc,tconriv,qs2)
c
    CALL SALM2(epsilon_rs,dr2,rwidth2,q2,ux1,uy1,ix,iy,irx2,iry2,sx,
    &sy,salo,ak5s,w0sal,deltas,rhosr2,ro,dip,g,per,ak3,time,salold2,
    &depthc,tconsal,sal2)
c
    else
      continue
    endif
c
c
  if(surf.EQ.1)then
    CALL SURFLM(epsilon_b,bd1,ba1,bh1,ibpx,ix,iy,
    &ak4,aks,akb,dip,w0,pi,g,rhos,ro,tanbeta,rcspfix,time,rsold,
    &depthc,tcon,rs)
    else
      continue
    endif
c
c
  if(bot.EQ.1)then
    CALL BOTTOMM(ix,iy,u,shield,fw,ak,pi,wndep,rcfix,time,rtold,
    &depthc,tcon,rt,w0,epsilon)
    else
      continue
    endif
c
c
c
  if(verdat.EQ.1)datum=depthc
  if(verdat.NE.1)datum=delta
c
  if(verdat.EQ.1)datmod=-1.0
  if(verdat.NE.1)datmod=1.0
c
  do 200 k=1,4
    if(k.EQ.1)zw(k)=depthc-100.0
```

```

    if(k.EQ.2)zw(k)=delta+100.0
    if(k.EQ.3)zw(k)=depthc-alay3
    if(k.EQ.4)zw(k)=depthc-alay4
  c
    if(zw(k).GT.depthc)zw(k)=depthc
    if(zw(k).LT.delta)zw(k)=delta
    dep(k)=depthc-zw(k)
  c
  c ...erosion calculations
    salmean(k)=salo
    a440(k)=dominter-domslope*salmean(k)
    if(salmean(k).GE.salmax)a440(k)=domback
    if(dmix.GE.dep(k))then
      salr7(k)=(-1.0)*dep(k)*aksal*w0sal/epsilonbs
    else
      salr7(k)=(-1.0)*dep(k)*aksal*((dimx/4.21)**2.4)
      &*w0sal/epsilonbs_1
    endif
  c
    if((depthc-dmix).GE.zw(k))then
      r7(ipart,k)=(-1.0)*zw(k)*w0/epsilon_1
    else
      r7(ipart,k)=(-1.0)*zw(k)*w0*(dmix/dip)**2.4/epsilon
  c*****my fix 10-21-94*****
    if(k.EQ.2)r7(ipart,k)=(-1.0)*zw(k)*w0/epsilon_1
  c*****
    endif
    if((depthc-dmix).LT.0.0)r7(ipart,k)=(-1.0)
    &*zw(k)*w0/epsilon
  c
    if(dmix.GE.dep(k))then
      revr7(ipart,k)=(-1.0)*dep(k)*w0/epsilonb
    else
      revr7(ipart,k)=(-1.0)*dep(k)*w0*
      &(dmix/dip)**2.4/epsilonb_1
    endif
  c**
  c
    if(surf.EQ.1)then
      rsurf(ipart,k)=rs*EXP(r7(ipart,k))
      pns(ipart,k)=(6.0/(pi*dip**3))*rsurf(ipart,k)/rhos
    else
      pns(ipart,k)=0
  
```

```
endif
C
if(riv.EQ.1)then
sriv1(k)=sal*EXP(salr7(k))
rivsum=sriv1(k)
salmean(k)=salo-sriv1(k)
a440(k)=dominter-domslope*salmean(k)
if(salmean(k).GE.salmax)a440(k)=domback
rriv(ipart,k)=qs*EXP(revr7(ipart,k))
pnr(ipart,k)=(6.0/(pi*dip**3))*rriv(ipart,k)/rhosr
else
pnr(ipart,k)=0
endif
C
C
if(riv2.EQ.1)then
sriv2(k)=sal2*EXP(salr7(k))
rivsum=sriv1(k)+sriv2(k)
if(rivsum.GT.salo)then
rivsum=salo
endif
salmean(k)=salo-rivsum
a440(k)=dominter-domslope*salmean(k)
if(salmean(k).GE.salmax)a440(k)=domback
rrivr2(ipart,k)=qs2*EXP(revr7(ipart,k))
pnrr2(ipart,k)=(6.0/(pi*dip**3))*rrivr2(ipart,k)/rhosr2
else
pnrr2(ipart,k)=0
endif
c
C
if(bot.EQ.1)then
rbot(ipart,k)=rt*EXP(r7(ipart,k))
pnb(ipart,k)=(6.0/(pi*dip**3))*rbot(ipart,k)/rhos
else
pnb(ipart,k)=0
endif
C
pnt(ipart,k)=pns(ipart,k)+pnr(ipart,k)+pnb(ipart,k)
&+pnrr2(ipart,k)
c
200 CONTINUE
c
```

```

1095  FORMAT(F8.5,3x,F8.3,3x,F17.4,3x,F12.8,f12.8)
c
499  continue
c
c.....sum numbers from each size bin together
      suml1(ix,iy)=pnt(ipart,1)+suml1(ix,iy)
      suml2(ix,iy)=pnt(ipart,2)+suml2(ix,iy)
      suml3(ix,iy)=pnt(ipart,3)+suml3(ix,iy)
      suml4(ix,iy)=pnt(ipart,4)+suml4(ix,iy)
c
c
      write(2, REC=icount)rt,rs,qs,qs2,sal,sal2
1776  continue
c
c
c*****null point write*****
c.....null point write commented out
c.....  if(iy.NE.igrdy)go to 6005
c..  write(50,3000)rc(1),rc(2),rc(3),rc(4),rc(5),rc(6),rc(7),
c..  &rc(8),rc(9),unp
c..3000  format(10e10.3)
c..6005  continue
c*****
c
c
c.....put salinity values int x-y array
      sall1(ix,iy)=salmean(1)
      sall2(ix,iy)=salmean(2)
      sall3(ix,iy)=salmean(3)
      sall4(ix,iy)=salmean(4)
      acdom1(ix,iy)=a440(1)
      acdom2(ix,iy)=a440(2)
      acdom3(ix,iy)=a440(3)
      acdom4(ix,iy)=a440(4)
c
c
      if(suml1(ix,iy).GT.9999999)suml1(ix,iy)=9999999
      if(suml2(ix,iy).GT.9999999)suml2(ix,iy)=9999999
      if(suml3(ix,iy).GT.9999999)suml3(ix,iy)=9999999
      if(suml4(ix,iy).GT.9999999)suml4(ix,iy)=9999999
c
c
      if(suml1(ix,iy).LT.-1000)suml1(ix,iy)=-1000

```

```
if(suml2(ix,iy).LT.-1000)suml2(ix,iy)=-1000
if(suml3(ix,iy).LT.-1000)suml3(ix,iy)=-1000
if(suml4(ix,iy).LT.-1000)suml4(ix,iy)=-1000
```

c

c

c...add fractional grains to the first 5 bins at surface & bottom

```
pnt(1,1)=pnt(1,1)+an0b1
pnt(2,1)=pnt(2,1)+an0b2
pnt(3,1)=pnt(3,1)+an0b3
pnt(4,1)=pnt(4,1)+an0b4
pnt(5,1)=pnt(5,1)+an0b5
pnt(6,1)=pnt(6,1)+an0b6
pnt(7,1)=pnt(7,1)+an0b7
pnt(8,1)=pnt(8,1)+an0b8
pnt(9,1)=pnt(9,1)+an0b9
```

c

c

```
pnt(1,2)=pnt(1,2)+an0b1
pnt(2,2)=pnt(2,2)+an0b2
pnt(3,2)=pnt(3,2)+an0b3
pnt(4,2)=pnt(4,2)+an0b4
pnt(5,2)=pnt(5,2)+an0b5
pnt(6,2)=pnt(6,2)+an0b6
pnt(7,2)=pnt(7,2)+an0b7
pnt(8,2)=pnt(8,2)+an0b8
pnt(9,2)=pnt(9,2)+an0b9
```

c

c

c

```
kounts=0
sumsp=0
do 1790 is=1,3
isp1=is+1
sp(is)=ABS((LOG(pnt(isp1,1)/pnt(is,1)))/(LOG(d(isp1)/d(is))))
sumsp=sumsp+sp(is)
if(sp(is).LT.0.1)go to 1789
kounts=kounts+1
```

1789 continue

1790 continue

c

```
kountb=0
sumsp2=0
do 1788 is=1,3
```

```

    isp1=isp+1
    sp2(is)=ABS((LOG(pnt(isp1,2)/pnt(is,2)))/(LOG(d(isp1)/d(is))))
    sumsp2=sumsp2+sp2(is)
    if(sp2(is).LT.0.1)go to 1787
    kountb=kountb+1
1787 continue
1788 continue
c
    b(ix,iy)=sumsp/(kounts+1)
    b2(ix,iy)=sumsp2/(kountb+1)
    if(b(ix,iy).GT.gamma)b(ix,iy)=gamma
    if(b(ix,iy).LT.1.0)b(ix,iy)=1.0
    if(b2(ix,iy).GT.gamma)b2(ix,iy)=gamma
    if(b2(ix,iy).LT.1.0)b2(ix,iy)=1.0
c
1791 continue
c
c
c*****selected grid loop start with ix,iy EQ igrdx igrdy***
    if(iy.NE.igrdy)go to 4002
    if(ix.NE.igrdx)go to 4003
    do 2006 k3=1,ires

c.....initialize sum2(k3) to background level n0
    sum2(k3)=n0
    do 2007 ipart3=1,ibins
c
c-----Slope Calculation for selected grid point-----
c...add fractional grains to the first 5 bins at each point in water
    pnt2(1,k3)=pnt2(1,k3)+an0b1
    pnt2(2,k3)=pnt2(2,k3)+an0b2
    pnt2(3,k3)=pnt2(3,k3)+an0b3
    pnt2(4,k3)=pnt2(4,k3)+an0b4
    pnt2(5,k3)=pnt2(5,k3)+an0b5
    pnt2(6,k3)=pnt2(6,k3)+an0b6
    pnt2(7,k3)=pnt2(7,k3)+an0b7
    pnt2(8,k3)=pnt2(8,k3)+an0b8
    pnt2(9,k3)=pnt2(9,k3)+an0b9
c
c
c.....sum numbers from each size bin together for selected location
    sum2(k3)=pnt2(ipart3,k3)+sum2(k3)
    if(sum2(k3).GT.9999999)sum2(k3)=9999999

```

```

2007  continue
c
c
2006  continue
c
c
      do 1462 k4=ires,1,-1
c.....calculate slope of profile.....
      sumspp=0
      kountp=0
c
      do 1795 is=1,3
      isp1=is+1
      spp(is)=ABS((LOG(pnt2(isp1,k4)/
&pnt2(is,k4)))/(LOG(d(isp1)/d(is))))
      sumspp=sumspp+spp(is)
      if(spp(is).LT.0.1)go to 1794
      kountp=kountp+1
1794  continue
1795  continue
c
      slope(k4)=sumspp/(kountp+1)
      if(slope(k4).GT.gamma)slope(k4)=gamma
      if(slope(k4).LT.1.0)slope(k4)=1.0
      write(99,3001)dep2(k4),char(9),sum2(k4),char(9),
&slope(k4),char(9),sal2mean(k4),char(9),a4402(k4)
1462  continue
4003  continue
4002  continue
c*****end write selected grid pt file*****
c
1801  continue
479   continue
c
      ixdum=100
      write(*,*)ixdum,iy,suml1(100,iy)
      write(*,*)epsilonb
c
1800  continue
c
1096  format(200f8.4)
1097  format(200f10.0)
1098  format(200f8.3)

```

3001 format(f9.3,1a,f10.0,1a,f8.3,1a,f8.3,1a,f8.4)

c

```
do 1935 iy=ny,1,-1
  write(81,1098) (sall1(ix,iy),ix=1,nx)
  write(85,1096) (acdom1(ix,iy),ix=1,nx)
  write(82,1098) (sall2(ix,iy),ix=1,nx)
  write(86,1096) (acdom2(ix,iy),ix=1,nx)
```

```
if(two_layer.NE.0)then
  write(83,1098) (sall3(ix,iy),ix=1,nx)
  write(87,1096) (acdom3(ix,iy),ix=1,nx)
  write(84,1098) (sall4(ix,iy),ix=1,nx)
  write(88,1096) (acdom4(ix,iy),ix=1,nx)
endif
```

1935 continue

c

```
do 1802 ix=1,nx
  write(41,1097) (suml1(ix,iy),iy=1,ny)
  write(91,1098) (b(ix,iy),iy=1,ny)
  write(42,1097) (suml2(ix,iy),iy=1,ny)
  write(92,1098) (b2(ix,iy),iy=1,ny)
```

c

```
if(two_layer.NE.0)then
  write(43,1097) (suml3(ix,iy),iy=1,ny)
  write(44,1097) (suml4(ix,iy),iy=1,ny)
endif
```

c

1802 continue

c

c

```
stop
END
```

c

c*****Outfall Subroutine*****

```
SUBROUTINE RIVERM(epsilon,dr,rwidth,q,ux1,uy1,ix,iy,irx,iry,sx,
&sy,rrsfix,ak5,w0,deltab,rhosr,ro,dip,g,per,ak3,time,qsold,
&depthc,tconriv,qs)
```

c

c

```
drc=dr*100.0
rwidthc=rwidth*100.0
qc=q*1000000.0
```

c

c...modification to produce sediment plots using variable current

c..... (RADIANS).....

c

```

  uvdir=ATAN2(uy1,ux1)
  rxyr=((iry-iy+.000001)*sy)/(ABS(irx-ix+.000001)*sx)
  thta=uvdir+ATAN(rxyr)
  ut=qc/(rwidthc*drc)
  ur=ut*COS(thta)-((ux1**2+uy1**2)**0.5)*SIN(thta)

```

c.....

c

c

```

  e2r=ak5*(ur-(ur**2+4*w0*epsilon)**0.5)/(2*epsilon)

```

c

```

  rsr1=(ABS(ut*rrsfix))/(ut**2+4*w0*epsilon)**0.5
  rsr3=e2r*(((irx-ix)*sx)**2)+(((iry-iy)*sy)**2)**0.5
  rsr2=EXP(rsr3)
  timedec=(time*tconriv*w0/depthc)
  if(timedec.GT.1.0)timedec=1.0
  timedec2=0.03116*(ux1**2+uy1**2)**0.5
  qsnew=rsr1*rsr2
  qfosl=qsold*(1-timedec)
  if(qsnew.GT.qfosl)then
    qs=qsnew+qfosl
  else
    qs=qsnew+qfosl*EXP(-1.0*timedec2)
  endif
  return
end

```

c

c

c*****End Outfall Subroutine*****

c

c

```

  SUBROUTINE SURFLM(epsilonb,bd1,ba1,bh1,ibpx,ix,iy,
    &ak4,aks,akb,dip,w0,pi,g,rhos,ro,tanbeta,rcspfix,time,
    &rsold,depthc,tcon,rs)

```

c

c*****Begin Surf1 Subroutine*****

c

```

  us=ABS((g*bd1)**0.5*COS(ba1)**2)
  e2=(us-(us**2+4*ak4*w0*epsilonb)**0.5)/(2*epsilonb)
  denom=pi*dip**3*(rhos-ro)*akb*bd1**2*9240.0/tanbeta
  rn=(24*aks*ro*bh1**2*(g*bd1)**0.5)/denom

```

```

rr=pi*dip**3*rn*rhos/6
rs1=(rr/(us**2+4*w0*epsilonb)**0.5)
rs3=(e2*ABS(ibpx-ix)*77.5)
rs2=EXP(rs3)
rs=rs1*rs2*rcspx+rsold*(1-(EXP(-1.0*depthc*tcon/(2*time*w0))))
c
return
end
c
c*****End Surf1 Subroutine*****
c
c
SUBROUTINE BOTTOMM(ix,iy,u,shield,fw,ak,pi,wndep,rcfix,time,
&rtold,depthc,tcon,rt,w0,epsilon)
c
***** Begin Bottom Subroutine*****
c
if (u.LT..000001) then
  nomo=1
  rt1=0.0
  go to 399
endif
c
rt5=shield*fw
if(rt5.le..05)then
  nomo=1
  rt1=0.0
  go to 399
endif
c
c
rt2=(0.05/(rt5))**.5
rt4=ACOS(rt2)
rt1=ak*(fw*shield-0.05)*(2/pi)*rt4
399 continue
rt=rt1+(rtold*(1-(EXP(-1.0*depthc*tcon/(2*time*w0))))))
c
c*****rcfix section was commented out Sept 12, 1994 10:00
if(rt.GT.rcfix)then
  rt1=rcfix
  rt=rt1+(rtold*(1-(EXP(-1.0*depthc*tcon/(2*time*w0))))))
endif
c

```

```

c
  return
end
c
c*****End Bottom Subroutine*****
c
c*****Outfall2 Subroutine*****
  SUBROUTINE RIVER2M(epsilon,dr2,rwidth2,q2,ux1,uy1,ix,iy,irx2,iry2
    &,sx,sy,rrsfix2,ak5,w0,deltab,rhosr2,ro,dip,g,per,ak3,time,
    &qs2old,depthc,tconriv,qs2)
c
c
  drc=dr2*100.0
  rwidthc=rwidth2*100.0
  qc=q2*1000000.0
c
c...modification to produce sediment plots using variable current
c..... (RADIANS).....
c
  uvdir=ATAN2(uy1,ux1)
  rxyr=((iry2-iy+.000001)*sy)/(ABS(irx2-ix+.000001)*sx)
  thta=uvdir+ATAN(rxyr)
  ut=qc/(rwidthc*drc)
  ur=ut*COS(thta)-((ux1**2+uy1**2)**0.5)*SIN(thta)
c.....
c
  e2r=ak5*(ur-(ur**2+4*w0*epsilon)**0.5)/(2*epsilon)
c
  rsr1=(ABS(ut*rrsfix2))/(ut**2+4*w0*epsilon)**0.5
  rsr3=e2r*(((irx2-ix)*sx)**2)+(((iry2-iy)*sy)**2)**0.5
  rsr2=EXP(rsr3)
  timedec=(time*tconriv*w0/depthc)
  if(timedec.GT.1.0)timedec=1.0
  timedec2=0.03116*(ux1**2+uy1**2)**0.5
  qsnew=rsr1*rsr2
  qfosl=qs2old*(1-timedec)
  if(qsnew.GT.qfosl)then
    qs2=qsnew+qfosl
  else
    qs2=qsnew+qfosl*EXP(-1.0*timedec2)
  endif
c
  return

```

```

end
c
c
c*****End Outfall2 Subroutine*****
c
c*****Accretion Outfall 1 Subroutine*****
SUBROUTINE SALM1(epsilon,dr,rwidth,q,ux1,uy1,ix,iy,irx,iry,sx,
&sy,salo,ak5s,w0sal,deltas,rhosr,ro,dip,g,per,ak3,time,salold,
&depthc,tconsal,sal)
c
c
drc=dr*100.0
rwidthc=rwidth*100.0
qc=q*1000000.0
c
c...modification to produce sediment plots using variable current
c..... (RADIANS).....
c
uvdir=ATAN2(uy1,ux1)
rxyr=((iry-iy+.000001)*sy)/(ABS(irx-ix+.000001)*sx)
thta=uvdir+ATAN(rxyr)
ut=qc/(rwidthc*drc)
ur=ut*COS(thta)-((ux1**2+uy1**2)**0.5)*SIN(thta)
c.....
c
c
e2r=ak5s*(ur-(ur**2+4*w0sal*epsilon)**0.5)/(2*epsilon)
c
rsr1=(ABS(ut*salo))/(ut**2+4*w0sal*epsilon)**0.5
rsr3=e2r*(((irx-ix)*sx)**2)+(((iry-iy)*sy)**2)**0.5
rsr2=EXP(rsr3)
timedec=(time*tconsal*w0sal/depthc)
if(timedec.GT.1.0)timedec=1.0
timedec2=0.03116*(ux1**2+uy1**2)**0.5
snew=rsr1*rsr2
sfosl=salold*(1-timedec)
if(snew.GT.sfosl)then
sal=snew+sfosl
else
sal=snew+sfosl*EXP(-1.0*timedec2)
endif
return
end

```

```

c
c
c*****End Accretion Outfall 1 Subroutine*****
c
c
c*****Salinity Outfall2 Subroutine*****
  SUBROUTINE SALM2(epsilon,dr2,rwidth2,q2,ux1,uy1,ix,iy,irx2,iry2
    &,sx,sy,salo,ak5s,w0sal,delta,rsr2,ro,dip,g,per,ak3,time,
    &salold2,depthc,tconsal,sal2)
c
c
  drc=dr2*100.0
  rwidthc=rwidth2*100.0
  qc=q2*1000000.0
c
c...modification to produce sediment plots using variable current
c..... (RADIANS).....
c
  uvdir=ATAN2(uy1,ux1)
  rxyr=((iry2-iy+.000001)*sy)/(ABS(irx2-ix+.000001)*sx)
  thta=uvdir+ATAN(rxyr)
  ut=qc/(rwidthc*drc)
  ur=ut*COS(thta)-((ux1**2+uy1**2)**0.5)*SIN(thta)
c.....
c
c
  e2r=ak5s*(ur-(ur**2+4*w0sal*epsilon)**0.5)/(2*epsilon)
c
  rsr1=(ABS(ut*salo))/(ut**2+4*w0sal*epsilon)**0.5
  rsr3=e2r*(((irx2-ix)*sx)**2)+(((iry2-iy)*sy)**2)**0.5
  rsr2=EXP(rsr3)
  timedec=(time*tconsal*w0sal/depthc)
  if(timedec.GT.1.0)timedec=1.0
  timedec2=0.03116*(ux1**2+uy1**2)**0.5
  snw=rsr1*rsr2
  sfosl=salold2*(1-timedec)
  if(snw.GT.sfosl)then
    sal2=snw+sfosl
  else
    sal2=snw+sfosl*EXP(-1.0*timedec2)
  endif
c
  return

```

AMEC, Environment & Infrastructure, Inc.
Hydrodynamic Modeling of Storm Drain Discharges in
the Neighborhood of ASBS 29 in La Jolla, California
Revised: 13 March 2013

end

c

c

c*****End Accretion Outfall2 Subroutine*****

AMEC, Environment & Infrastructure, Inc.
Hydrodynamic Modeling of Storm Drain Discharges in
the Neighborhood of ASBS 29 in La Jolla, California
Revised: 13 March 2013

APPENDIX F

CODE FOR THE MULTINODE DILUTION MODEL

Appendix F: Code for the Multinode Dilution Model

```
c*****
c
c   multinode.for - 18 June 2004
c**with verticle loop
c reads in raster 200 row 200 column arrays of:
c depths, wave heights, wave numbers, x- and y-directed current components
c Surface and Bottom Salinity & calculates Dilution from these
c   written by Scott A. Jenkins & Joseph Wasyl
c
c   character*26 infile1,infile2,infile4,infile5
c
c   DIMENSION depth(200,200),wht(200,200),wvn(200,200)
c   DIMENSION xcur(200,200),ycur(200,200),col(200,200)
c
c   dimension z(5),s(5),ps1(5),ps1b(5),ps1bav(5)
c   integer ipt(5),ix(5),iy(5)
c   dimension pnx(200,200),pny(200,200),pn(200,200),pn_l(200,200)
c   dimension brx(200,200),bry(200,200),brn(200,200),dmix(200,200)
c   dimension salsur(200,200),salbrn(200,200),saldep(200,200)
c   dimension dilriv(200,200),dildep(200,200),colriv(200,200)
c   dimension dilbrn(200,200),dbrnav(200,200),sbrnav(200,200)
c   dimension brxav(200,200),bryav(200,200),brnav(200,200)
c   character*12 ifile,ofile1,ofile2,ofile3,ofile4,ofile5,ofile6
c   character*12 ofile7,ofile8,ofile9,ofil10,ofil11,ofil12,ofil13
c
c
c   open(42,file='multinode_agua_3.inp',status='old')
c   read(42,3000)ifile
c   read(42,3000)infile1
c   read(42,3111)infile2
c   read(42,3200)infile4
c   read(42,3200)infile5
c   read(42,3000)ofile1
c   read(42,3000)ofile2
c   read(42,3000)ofile3
c   read(42,3000)ofile4
c   read(42,3000)ofile5
c   read(42,3000)ofile6
c   read(42,3000)ofile7
c   read(42,3000)ofile8
```

```
read(42,3000)ofile9
read(42,3000)ofil10
read(42,3000)ofil11
read(42,3000)ofil12
read(42,3000)ofil13
read(42,*)num
read(42,*)imax
read(42,*)jmax
read(42,*)srivx1
read(42,*)srivx2
read(42,*)srivx3
read(42,*)srivx4
read(42,*)srivx5
read(42,*)srivy1
read(42,*)srivy2
read(42,*)srivy3
read(42,*)srivy4
read(42,*)srivy5
read(42,*)ub
read(42,*)vb
read(42,*)u2
read(42,*)v2
read(42,*)sx
read(42,*)sy
read(42,*)akx1_1
read(42,*)aky1_1
read(42,*)akx1_2
read(42,*)aky1_2
read(42,*)akx1_3
read(42,*)aky1_3
read(42,*)akx1_4
read(42,*)aky1_4
read(42,*)akx1_5
read(42,*)aky1_5
read(42,*)ak2_1
read(42,*)ak2_2
read(42,*)ak2_3
read(42,*)ak2_4
read(42,*)ak2_5
read(42,*)akz_1
read(42,*)akz_2
read(42,*)akz_3
read(42,*)akz_4
```

read(42,*)akz_5
read(42,*)thresh
read(42,*)back
read(42,*)salo
read(42,*)cline
read(42,*)isal
read(42,*)pnman
read(42,*)upper
read(42,*)brine
read(42,*)upperb
read(42,*)ibrn
read(42,*)brnman
read(42,*)per
read(42,*)ruf
read(42,*)rhos
read(42,*)wind
read(42,*)deglat
read(42,*)ibadx
read(42,*)ibady
read(42,*)qsa
read(42,*)qtc
read(42,*)widsa
read(42,*)widtc
read(42,*)akr_3
read(42,*)akr_4
read(42,*)u_blend
read(42,*)aksal
read(42,*)surdz
read(42,*)botdz
read(42,*)shrdec
read(42,*)swrdec
read(42,*)surmix
read(42,*)aksur
read(42,*)surhb
read(42,*)thermo
read(42,*)xmag
read(42,*)ymag
read(42,*)akocs
read(42,*)depo
read(42,*)thrm dz
read(42,*)coli
read(42,*)deep
read(42,*)akzav

c

rawbrn=2.0*salo

C**read in oceanbat .grd, oceanrds_200x200_raster and tidecur_agua arrays

c

OPEN(UNIT=51,FILE=infile1,STATUS='OLD')

OPEN(UNIT=52,FILE=infile2,STATUS='OLD')

OPEN(UNIT=54,FILE=infile4,STATUS='OLD')

OPEN(UNIT=55,FILE=infile5,STATUS='OLD')

C

DO 8001 J=1,200

READ(51,*)(depth(I,J),I=1,200)

READ(52,*)(wht(I,J),I=1,200)

READ(54,*)(xcur(I,J),I=1,200)

READ(55,*)(ycur(I,J),I=1,200)

8001 CONTINUE

c

3000 format(a12)

3111 format(a26)

3200 format(a22)

c

surhb=surhb*100.0

surdz=surdz*100.0

botdz=botdz*100.0

cline=cline*100.0

depo=depo*100.0

thrm dz=thrm dz*100.0

freq=1.0/per

pi=ACOS(-1.0)

g=980.0

rho=1.03

sigma=2.0*pi*freq

deepl=2.0*pi*g/(sigma**2.0)

wind=wind*0.5148*100.0

ak8=0.00009/((wind**0.5)+1.1103)

ustar=(ak8*(wind**2))**0.5

rot_e=0.000072685

f=2.0*rot_e*SIND(deglat)

dmix_test=4.0*ustar/(f*100.0)

c.....epsilonw is in cgs units

epsilonw=0.0000043*(wind**2.0)

if(wind.LE.600)epsilonw=0.0000000102*(wind**3.0)

c

c

```
open(20,file=ifile,status='old')
open(21,file=ofile1,status='unknown')
open(22,file=ofile2,status='unknown')
open(23,file=ofile3,status='unknown')
open(24,file=ofile4,status='unknown')
open(25,file=ofile5,status='unknown')
open(26,file=ofile6,status='unknown')
open(27,file=ofile7,status='unknown')
open(28,file=ofile8,status='unknown')
open(29,file=ofile9,status='unknown')
open(30,file=ofil10,status='unknown')
open(31,file=ofil11,status='unknown')
open(32,file=ofil12,status='unknown')
open(33,file=ofil13,status='unknown')
c
c
c... open node file
do 100 i=1,num
read(20,1000) ipt(i),ix(i),iy(i),z(i)
100 continue
1000 format(i2,2i4,f7.2)
c
c..covert x and y coordinates to nearest integer
c..calculate or assign strength to each source
c
c**initialize particle output array
do 870 iay=1,jmax
do 860 iax=1,imax
pn(iax,iay)=0.0
pnx(iax,iay)=0.0
pny(iax,iay)=0.0
brn(iax,iay)=0.0
brx(iax,iay)=0.0
bry(iax,iay)=0.0
brnav(iax,iay)=0.0
brxav(iax,iay)=0.0
bryav(iax,iay)=0.0
xcur(iax,iay)=xmag*xcur(iax,iay)
ycur(iax,iay)=ymag*ycur(iax,iay)
c
depth(iax,iay)=depth(iax,iay)*100.0
c**make land in bays negative in increasing iax direction
if(iland.EQ.1)depth(iax,iay)=-200.0
```


cPick each x location of grid(iax) solve dx relative to x location of source ix(i)

```

do 800 iax=1,imax
dx=(iax-ix(i))*sx
do 850 iay=1,jmax
dmix(iax,iay)=4.0*ustar/(f*100.0)
if(dmix(iax,iay).LE.cline)dmix(iax,iay)=cline
if(depth(iax,iay).GT.0.0.AND.xcur(iax,iay).EQ.0.0)
&xcur(iax,iay)=0.00001
if(depth(iax,iay).GT.0.0.AND.ycur(iax,iay).EQ.0.0)
&ycur(iax,iay)=0.00001
dy=(iay-iy(i))*sy
dr=((dx**2.0)+(dy**2.0))**0.5
drxy=((sx**2.0)+(sy**2.0))**0.5
if(dr.LT.drxy)dr=drxy
theta=ABS(dx/dr)
d0=wht(iax,iay)/SINH(wvn(iax,iay)*depth(iax,iay))+0.001
uwav=sigma*d0
ucur=(xcur(iax,iay)**2.0+ycur(iax,iay)**2.0)**0.5
u=ucur+uwav
C-----
fw=EXP(5.2*((2.5*ruf/d0)**0.2)-6.0)
delta=0.72*d0*(2.5*ruf/d0)**0.25
shield=(u**2/((rhos/rho-1.0)*g*ruf))*fw
C-----
C*****SIO_1 UTFALL X-LOOP (ipt=1) lat=33 39' 19"N, lon=117 58' 57"W*****
if(ipt(i).EQ.1)then
if(depth(iax,iay).LT.10.0)then
ps1(i)=0.0
ps1b(i)=0.0
ps1bav(i)=0.0
etr=0.0
etrb=0.0
go to 4521
endif
s(i)=srivx1
ak1=akx1_1
ak2=ak2_1
surdec=-1.0*((depth(iax,iay)/surhb)**aksur)
epsur=surmix*(EXP(surdec))
c
c*U_BLEND logic
uave=(u_blend*ucur+u)/(u_blend+1)
dxb=uave*per

```

```

deltar=0.72*dxb*(2.5*ruf/dxb)**0.25
fw=EXP(5.2*((2.5*ruf/dxb)**0.2)-6.0)
shield=(uave**2/((rhos/rho-1.0)*g*ruf))*fw
epsilon_1=0.00035*ak2*(uave**0.68)*(shield**0.4)*deltar*g*per
if(xcur(iax,iay).LT.0.0)then
uwav=-1.0*uave
else
uwav=uave
endif
u0=xcur(iax,iay)+uwav+ub
u0abs=ABS(u0)
c
if(epsilon_1.EQ.0.0)epsilon_1=0.0000000001
eps=epsilon_1+epsilon_w
depmdz=depth(iax,iay)-botdz
botx=-1.0*akz_1*(botdz**1.0)/eps
botav=-1.0*akzav*(depth(iax,iay)**1.0)/eps
decbot=EXP(botx)
decav=EXP(botav)
if(dmix(iax,iay).GE.depth(iax,iay).AND.depth(iax,iay).GT.0.0)
&dmix(iax,iay)=depth(iax,iay)
if(dmix(iax,iay).GT.depmdz)decbot=decbot**shrdec
ps1b(i)=s(i)*decbot/((uave**2+4.0*ruf*(eps+epsur))**0.5)
ps1bav(i)=ps1b(i)*decav/decbot
c SIO_1 Inshore
if(iax.EQ.237.AND.iay.EQ.133)write(*,*)iax,iay,epsilon_1,epsur,
&ps1b(i),etrb
c SIO_1 Inshore
if(iax.EQ.173.AND.iay.EQ.96)write(*,*)iax,iay,epsilon_1,epsur,
&ps1b(i),etrb
c SIO_1 Inshore
if(iax.EQ.179.AND.iay.EQ.94)write(*,*)iax,iay,epsilon_1,epsur,
&ps1b(i),etrb
c SIO_1 Inshore
if(iax.EQ.163.AND.iay.EQ.97)write(*,*)iax,iay,epsilon_1,epsur,
&ps1b(i),etrb
if(u0.GE.0.0.AND.dx.GT.0.0)then
etr=-1.0*ak1*((u0-theta*u0)+((4.0*ruf*eps)**0.5))/(2.0*eps)
endif
if(u0.GE.0.0.AND.dx.LT.0.0)then
etr=-1.0*ak1*((u0+theta*u0)+((4.0*ruf*eps)**0.5))/(2.0*eps)
endif
if(u0.LT.0.0.AND.dx.LT.0.0)then

```

```

    etr=-1.0*ak1*(-1.0*(u0-theta*u0)+((4.0*ruf*eps)**0.5))/
&(2.0*eps)
  endif
  if(u0.LT.0.0.AND.dx.GT.0.0)then
    etr=-1.0*ak1*(-1.0*(u0+theta*u0)+((4.0*ruf*eps)**0.5))/
&(2.0*eps)
  endif
  au0=ABS(u0)
  if(dx.EQ.0.0)then
    etr=-1.0*ak1*(au0+((4.0*ruf*eps)**0.5))/
&(2.0*eps)
  endif
c
  if(u0.GE.0.0.AND.dx.GT.0.0)then
    etrb=-1.0*ak1*((u0-theta*u0)+((4.0*ruf*eps)**0.5))/
&(2.0*eps)
  endif
  if(u0.GE.0.0.AND.dx.LT.0.0)then
    etrb=-1.0*ak1*((u0+theta*u0)+((4.0*ruf*eps)**0.5))/
&(2.0*eps)
  endif
  if(u0.LT.0.0.AND.dx.LT.0.0)then
    etrb=-1.0*ak1*(-1.0*(u0-theta*u0)+(4.0*ruf*eps)**0.5)/
&(2.0*eps)
  endif
  if(u0.LT.0.0.AND.dx.GT.0.0)then
    etrb=-1.0*ak1*(-1.0*(u0+theta*u0)+((4.0*ruf*eps)**0.5))/
&(2.0*eps)
  endif
  au0=ABS(u0)
  if(dx.EQ.0.0)then
    etrb=-1.0*ak1*(au0+((4.0*ruf*eps)**0.5))/
&(2.0*eps)
  endif
  endif
4521 continue
c*****END                SIO_1                OUTFALL                X-
LOOP*****
c
C*****SIO_3 OUTFALL X-LOOP (ipt=2) *****
  if(ipt(i).EQ.2)then
    if(depth(iax,iay).LT.10.0)then
      ps1(i)=0.0

```

```

ps1b(i)=0.0
etr=0.0
etrb=0.0
go to 4522
endif
if(xcur(iax,iay).LT.0.0)uwav=-1.0*uwav
u0=xcur(iax,iay)+uwav+u2
s(i)=srivx2
ak1=akx1_2
ak2=ak2_2
epsilon_1=0.00035*ak2*(u**0.68)*(shield**0.4)*delta*g*per
if(epsilon_1.EQ.0.0)epsilon_1=0.0000000001
eps=epsilon_1+epsilonw
dmxmdz=dmix(iax,iay)-thrmz
if(thrmz.NE.0)then
if(dmxmdz.GT.depth(iax,iay).AND.depth(iax,iay).GT.0.0)
&thrmz=dmxmdz-depth(iax,iay)+thrmz
endif
thrmx=-1.0*akz_2*(thrmz**1.0)
dcthrm=EXP(thrmx)
if(depth(iax,iay).LE.depo)then
ps1(i)=(s(i)*dcthrm/((u**2+4.0*ruf*eps)**0.5))*
&((depth(iax,iay)/depo)**akocs)
else
ps1(i)=(s(i)*dcthrm/((u**2+4.0*ruf*eps)**0.5))*
&((depth(iax,iay)/depo)**(akocs/deep))
endif
if(u0.GE.0.0.AND.dx.GT.0.0)then
etr=-1.0*ak1*((u0-theta*u0)+((4.0*ruf*eps)**0.5))/(2.0*eps)
endif
if(u0.GE.0.0.AND.dx.LT.0.0)then
etr=-1.0*ak1*((u0+theta*u0)+((4.0*ruf*eps)**0.5))/(2.0*eps)
endif
if(u0.LT.0.0.AND.dx.LT.0.0)then
etr=-1.0*ak1*(-1.0*(u0-theta*u0)+((4.0*ruf*eps)**0.5))/
&(2.0*eps)
endif
if(u0.LT.0.0.AND.dx.GT.0.0)then
etr=-1.0*ak1*(-1.0*(u0+theta*u0)+((4.0*ruf*eps)**0.5))/
&(2.0*eps)
endif
au0=ABS(u0)
if(dx.EQ.0.0)then

```

```

    etr=-1.0*ak1*(au0+((4.0*ruf*eps)**0.5)/
    &(2.0*eps)
    endif
  endif
4522 continue
c*****END                SIO_3                OUTFALL                X-
LOOP*****
c
C*****SIO_2 Outfall X-LOOP (ipt=3) *****
  if(ipt(i).EQ.3)then
    if(depth(iax,iay).LT.10.0)then
      ps1(i)=0.0
      ps1b(i)=0.0
      etr=0.0
      etrb=0.0
      go to 4523
    endif
    drc=z(i)*100.0
    wid=widsa*100.0
    qc=qsa*92903.0
    uvdir=ATAN2(ycur(iax,iay),xcur(iax,iay))
    ut0=qc/(drc*wid)
    ut=ut0/((((dx+0.00001)**2+(dy+0.00001)**2)**0.5)**akr_3)
    u0=xcur(iax,iay)-ut*COS(uvdir)
    uave=(u_blend*ucur+u)/(u_blend+1)
    dxb=uave*per
    deltar=0.72*dxb*(2.5*ruf/dxb)**0.25
    fw=EXP(5.2*((2.5*ruf/dxb)**0.2)-6.0)
    shield=(uave**2/((rhos/rho-1.0)*g*ruf))*fw
    s(i)=srivx3
    ak1=akx1_3
    ak2=ak2_3
    epsilon_l=0.00035*ak2*(uave**0.68)*(shield**0.4)*deltar*g*per
    if(epsilon_l.EQ.0.0)epsilon_l=0.0000000001
    eps=epsilon_l+epsilonw
c***diagnostic
CCCCCCC   if(iay.EQ.118)write(*,*)iax,iay,ur,shield,deltar,eps
c***diagnostic
    surx=-1.0*akz_3*(surdz**1.0)
    decsur=EXP(surx)
    if(dmix(iax,iay).GE.depth(iax,iay).AND.depth(iax,iay).GT.0.0)
    &dmix(iax,iay)=depth(iax,iay)
    if(dmix(iax,iay).LT.surdz)decsur=decsur**thermo

```

```

ps1(i)=s(i)*decsur/((u0**2+4.0*ruf*eps)**0.5)
if(u0.GE.0.0.AND.dx.GT.0.0)then
etr=-1.0*ak1*((u0-theta*u0)+((4.0*ruf*eps)**0.5))/(2.0*eps)
endif
if(u0.GE.0.0.AND.dx.LT.0.0)then
etr=-1.0*ak1*((u0+theta*u0)+((4.0*ruf*eps)**0.5))/(2.0*eps)
endif
if(u0.LT.0.0.AND.dx.LT.0.0)then
etr=-1.0*ak1*(-1.0*(u0-theta*u0)+((4.0*ruf*eps)**0.5))/
&(2.0*eps)
endif
if(u0.LT.0.0.AND.dx.GT.0.0)then
etr=-1.0*ak1*(-1.0*(u0+theta*u0)+((4.0*ruf*eps)**0.5))/
&(2.0*eps)
endif
au0=ABS(u0)
if(dx.EQ.0.0)then
etr=-1.0*ak1*(au0+((4.0*ruf*eps)**0.5))/
&(2.0*eps)
endif
endif
4523 continue
c*****END SIO_2 Outfall X-LOOP*****
c
C*****SIO_4 OUTFALL X-LOOP (ipt=4) *****
if(ipt(i).EQ.4)then
if(depth(iax,iay).LT.10.0)then
ps1(i)=0.0
ps1b(i)=0.0
etr=0.0
etrb=0.0
go to 4524
endif
drc=z(i)*100.0
wid=widtc*100.0
qc=qtc*92903.0
uvdir=ATAN2(ycur(iax,iay),xcur(iax,iay))
ut0=qc/(drc*wid)
ut=ut0/((((dx+0.00001)**2+(dy+0.00001)**2)**0.5)**akr_4)
u0=xcur(iax,iay)-ut*COS(uvdir)
uave=(u_blend*ucur+u)/(u_blend+1)
dxb=uave*per
deltar=0.72*dxb*(2.5*ruf/dxb)**0.25

```

```

fw=EXP(5.2*((2.5*ruf/dxb)**0.2)-6.0)
shield=(uave**2/((rhos/rho-1.0)*g*ruf))*fw
s(i)=srivx4
ak1=akx1_4
ak2=ak2_4
epsilon_1=0.00035*ak2*(uave**0.68)*(shield**0.4)*deltar*g*per
if(epsilon_1.EQ.0.0000000001)epsilon_1=0.0000000001
eps=epsilon_1+epsilon_w
c***diagnostic
CCCCCCC if(iay.EQ.118)write(*,*)iax,iay,ur,shield,deltar,eps
c***diagnostic
surx=-1.0*akz_4*(surdz**2.0)/eps
decsur=EXP(surx)
if(dmix(iax,iay).GE.depth(iax,iay).AND.depth(iax,iay).GT.0.0)
&dmix(iax,iay)=depth(iax,iay)
if(dmix(iax,iay).LT.surdz)decsur=decsur**thermo
ps1(i)=s(i)*decsur/((u0**2+4.0*ruf*eps)**0.5)
if(u0.GE.0.0.AND.dx.GT.0.0)then
etr=-1.0*ak1*((u0-theta*u0)+((4.0*ruf*eps)**0.5))/(2.0*eps)
endif
if(u0.GE.0.0.AND.dx.LT.0.0)then
etr=-1.0*ak1*((u0+theta*u0)+((4.0*ruf*eps)**0.5))/(2.0*eps)
endif
if(u0.LT.0.0.AND.dx.LT.0.0)then
etr=-1.0*ak1*(-1.0*(u0-theta*u0)+((4.0*ruf*eps)**0.5))/
&(2.0*eps)
endif
if(u0.LT.0.0.AND.dx.GT.0.0)then
etr=-1.0*ak1*(-1.0*(u0+theta*u0)+((4.0*ruf*eps)**0.5))/
&(2.0*eps)
endif
au0=ABS(u0)
if(dx.EQ.0.0)then
etr=-1.0*ak1*(au0+((4.0*ruf*eps)**0.5))/
&(2.0*eps)
endif
endif
4524 continue
c*****END SIO_4 X-LOOP*****
c
C*****SIO_ Offshore OUTFALL X-LOOP (ipt=5) *****
if(ipt(i).EQ.5)then
if(depth(iax,iay).LT.10.0)then

```

```

    ps1(i)=0.0
    ps1b(i)=0.0
    etr=0.0
    etrb=0.0
    go to 4525
  endif
  if(xcur(iax,iay).LT.0.0)uwav=-1.0*uwav
  u0=xcur(iax,iay)+uwav
  s(i)=srivx5
  ak1=akx1_5
  ak2=ak2_5
  epsilon_l=0.00035*ak2*(u**0.68)*(shield**0.4)*delta*g*per
  if(epsilon_l.EQ.0.0000000001)epsilon_l=0.0000000001
  eps=epsilon_l+epsilonw
  ps1(i)=s(i)/((u**2+4.0*ruf*eps)**0.5)
  if(u0.GE.0.0.AND.dx.GT.0.0)then
    etr=-1.0*ak1*((u0-theta*u0)+((4.0*ruf*eps)**0.5))/(2.0*eps)
  endif
  if(u0.GE.0.0.AND.dx.LT.0.0)then
    etr=-1.0*ak1*((u0+theta*u0)+((4.0*ruf*eps)**0.5))/(2.0*eps)
  endif
  if(u0.LT.0.0.AND.dx.LT.0.0)then
    etr=-1.0*ak1*(-1.0*(u0-theta*u0)+((4.0*ruf*eps)**0.5))/
&(2.0*eps)
  endif
  if(u0.LT.0.0.AND.dx.GT.0.0)then
    etr=-1.0*ak1*(-1.0*(u0+theta*u0)+((4.0*ruf*eps)**0.5))/
&(2.0*eps)
  endif
  au0=ABS(u0)
  if(dx.EQ.0.0)then
    etr=-1.0*ak1*(au0+((4.0*ruf*eps)**0.5))/
&(2.0*eps)
  endif
  endif
4525 continue
c*****END          SIO          Offshore          OUTFALL          X-
LOOP*****
c
  ps3=etr*((dx**2)+(dy**2))**0.5
  ps3b=etrb*((dx**2)+(dy**2))**0.5
c***
  ps2=EXP(ps3)

```

```

    ps2b=EXP(ps3b)
    pnx(iax,iay)=pnx(iax,iay)+(ps1(i)*ps2)
    brx(iax,iay)=brx(iax,iay)+(ps1b(i)*ps2b)
    brxav(iax,iay)=brxav(iax,iay)+(ps1bav(i)*ps2b)
  c
  c
  850  continue
  800  continue
  799  continue
  c
  C*****V LOOPS *****
  c
  cPick each Source, use x and y location arrays ix(i), iy(i) of source
    do 1799 i=1,num
  cPick each x location of grid(iax) solve dx relative to x location of source ix(i)
    do 1800 iay=1,jmax
      dy=(iay-iy(i))*sy
  c
    do 1850 iax=1,imax
      dmix(iax,iay)=4.0*ustar/(f*100.0)
      if(dmix(iax,iay).LE.cline)dmix(iax,iay)=cline
      if(iax.EQ.ibadx.AND.iay.EQ.ibady)then
        ps1(i)=0.0
        ps1b(i)=0.0
        ps1bav(i)=0.0
        etr=0.0
        etrb=0.0
        go to 1777
      endif
      if(depth(iax,iay).GT.0.0.AND.xcur(iax,iay).EQ.0.0)
&xcur(iax,iay)=0.00001
        if(depth(iax,iay).GT.0.0.AND.ycur(iax,iay).EQ.0.0)
&ycur(iax,iay)=0.00001
          dx=(iax-ix(i))*sx
          dr=((dx**2.0)+(dy**2.0))**0.5
          drxy=((sx**2.0)+(sy**2.0))**0.5
          if(dr.LT.drxy)dr=drxy
          beta=ABS(dy/dr)
  c
    d0=wht(iax,iay)/SINH(wvn(iax,iay)*depth(iax,iay))+0.001
    uwav=sigma*d0
    ucur=(xcur(iax,iay)**2.0+ycur(iax,iay)**2.0)**0.5
    u=ucur+uwav

```

C-----

```
fw=EXP(5.2*((2.5*ruf/d0)**0.2)-6.0)
delta=0.72*d0*(2.5*ruf/d0)**0.25
shield=(u**2/((rhos/rho-1.0)*g*ruf))*fw
```

C-----

c*****SIO_1 OUTFALL Y-LOOP*****

```
if(ipt(i).EQ.1)then
if(depth(iax,iay).LT.10.0)then
ps1(i)=0.0
ps1b(i)=0.0
ps1bav(i)=0.0
etr=0.0
etrb=0.0
go to 4530
endif
s(i)=srivy1
ak1=aky1_1
ak2=ak2_1
surdec=-1.0*((depth(iax,iay)/surhb)**aksur)
epsur=surmix*(EXP(surdec))
```

c

c* U_BLEND logic

```
uave=(u_blend*ucur+u)/(u_blend+1)
dxb=uave*per
deltar=0.72*dxb*(2.5*ruf/dxb)**0.25
fw=EXP(5.2*((2.5*ruf/dxb)**0.2)-6.0)
shield=(uave**2/((rhos/rho-1.0)*g*ruf))*fw
epsilon_1=0.00035*ak2*(uave**0.68)*(shield**0.4)*deltar*g*per
if(ycur(iax,iay).LT.0.0)then
uwav=-1.0*uave
else
uwav=uave
endif
v0=ycur(iax,iay)+uwav+vb
v0abs=ABS(v0)
```

c

```
if(epsilon_1.EQ.0.0)epsilon_1=0.0000000001
eps=epsilon_1+epsilonw
depmdz=depth(iax,iay)-botdz
botx=-1.0*akz_1*(botdz**1.0)/eps
botav=-1.0*akzav*(depth(iax,iay)**1.0)/eps
decbot=EXP(botx)
decav=EXP(botav)
```

```

    if(dmix(iax,iay).GE.depth(iax,iay).AND.depth(iax,iay).GT.0.0)
&dmix(iax,iay)=depth(iax,iay)
    if(dmix(iax,iay).GT.depmdz)decbot=decbot**shrdec
    ps1b(i)=s(i)*decbot/((uave**2+4.0*ruf*(eps+epsur))**0.5)
    ps1bav(i)=ps1b(i)*decav/decbot
    if(v0.GE.0.0.AND.dy.GT.0.0)then
    etr=-1.0*ak1*((v0-beta*v0)+((4.0*ruf*eps)**0.5))/(2.0*eps)
    endif
    if(v0.GE.0.0.AND.dy.LT.0.0)then
    etr=-1.0*ak1*((v0+beta*v0)+((4.0*ruf*eps)**0.5))/(2.0*eps)
    endif
    if(v0.LT.0.0.AND.dy.LT.0.0)then
    etr=-1.0*ak1*(-1.0*(v0-beta*v0)+((4.0*ruf*eps)**0.5))/
&(2.0*eps)
    endif
    if(v0.LT.0.0.AND.dy.GT.0.0)then
    etr=-1.0*ak1*(-1.0*(v0+beta*v0)+((4.0*ruf*eps)**0.5))/
&(2.0*eps)
    endif
    av0=ABS(v0)
    if(dy.EQ.0.0)then
    etr=-1.0*ak1*(av0+((4.0*ruf*eps)**0.5))/
&(2.0*eps)
    endif
c
    if(v0.GE.0.0.AND.dy.GT.0.0)then
    etrb=-1.0*ak1*((v0-beta*v0)+((4.0*ruf*eps)**0.5))/(2.0*eps)
    endif
    if(v0.GE.0.0.AND.dy.LT.0.0)then
    etrb=-1.0*ak1*((v0+beta*v0)+((4.0*ruf*eps)**0.5))/(2.0*eps)
    endif
    if(v0.LT.0.0.AND.dy.LT.0.0)then
    etrb=-1.0*ak1*(-1.0*(v0-beta*v0)+((4.0*ruf*eps)**0.5))/
&(2.0*eps)
    endif
    if(v0.LT.0.0.AND.dy.GT.0.0)then
    etrb=-1.0*ak1*(-1.0*(v0+beta*v0)+(4.0*ruf*eps)**0.5)/
&(2.0*eps)
    endif
    av0=ABS(v0)
    if(dy.EQ.0.0)then
    etrb=-1.0*ak1*(av0+(4.0*ruf*eps)**0.5)/
&(2.0*eps)

```

```

    endif
  endif
4530 continue
C*****END SIO_1 Y-LOOP*****
c
c*****SIO_3 OUTFALL Y-LOOP*****
  if(ipt(i).EQ.2)then
    if(depth(iax,iay).LT.10.0)then
      ps1(i)=0.0
      ps1b(i)=0.0
      etr=0.0
      etrb=0.0
      go to 4531
    endif
    if(ycur(iax,iay).LT.0.0)uwav=-1.0*uwav
    v0=ycur(iax,iay)+uwav+v2
    s(i)=srivy2
    ak1=aky1_2
    ak2=ak2_2
    epsilon_1=0.00035*ak2*(u**0.68)*(shield**0.4)*delta*g*per
    if(epsilon_1.EQ.0.000000001)epsilon_1=0.000000001
    eps=epsilon_1+epsilonw
    dmixmapz=dmix(iax,iay)-thrmxz
    if(thrmxz.NE.0)then
      if(dmixmapz.GT.depth(iax,iay).AND.depth(iax,iay).GT.0.0)
&thrmxz=dmixmapz-depth(iax,iay)+thrmxz
    endif
    thrmx=-1.0*akz_2*(thrmxz**1.0)
    dcthmx=EXP(thrmx)
    if(depth(iax,iay).LE.depo)then
      ps1(i)=(s(i)/((u**2+4.0*ruf*eps)**0.5))*
&((depth(iax,iay)/depo)**akocs)
    else
      ps1(i)=(s(i)/((u**2+4.0*ruf*eps)**0.5))*
&((depth(iax,iay)/depo)**(akocs/deep))
    endif
    if(v0.GE.0.0.AND.dy.GT.0.0)then
      etr=-1.0*ak1*((v0-beta*v0)+((4.0*ruf*eps)**0.5))/(2.0*eps)
    endif
    if(v0.GE.0.0.AND.dy.LT.0.0)then
      etr=-1.0*ak1*((v0+beta*v0)+((4.0*ruf*eps)**0.5))/(2.0*eps)
    endif
    if(v0.LT.0.0.AND.dy.LT.0.0)then

```

```

    etr=-1.0*ak1*(-1.0*(v0-beta*v0)+((4.0*ruf*eps)**0.5))/
&(2.0*eps)
    endif
    if(v0.LT.0.0.AND.dy.GT.0.0)then
    etr=-1.0*ak1*(-1.0*(v0+beta*v0)+((4.0*ruf*eps)**0.5))/
&(2.0*eps)
    endif
    av0=ABS(v0)
    if(dy.EQ.0.0)then
    etr=-1.0*ak1*(av0+((4.0*ruf*eps)**0.5))/
&(2.0*eps)
    endif
    endif
4531 continue
c
C*****END SIO_3 OUTFALL Y-LOOP*****
c
C*****SIO_2 Outfall Y-LOOP*****
    if(ipt(i).EQ.3)then
    if(depth(iax,iay).LT.10.0)then
    ps1(i)=0.0
    ps1b(i)=0.0
    etr=0.0
    etrb=0.0
    go to 4532
    endif
    drc=z(i)*100.0
    wid=widsa*100.0
    qc=qsa*92903.0
    uvdir=ATAN2(ycur(iax,iay),xcur(iax,iay))
    ut0=qc/(drc*wid)
    ut=ut0/((((dx+0.00001)**2+(dy+0.00001)**2)**0.5)**akr_3)
    v0=ycur(iax,iay)+ut*SIN(uvdir)
    uave=(u_blend*ucur+u)/(u_blend+1)
    dxb=uave*per
    deltar=0.72*dxb*(2.5*ruf/dxb)**0.25
    fw=EXP(5.2*((2.5*ruf/dxb)**0.2)-6.0)
    shield=(uave**2/((rhos/rho-1.0)*g*ruf))*fw
    s(i)=srivy3
    ak1=aky1_3
    ak2=ak2_3
    epsilon_1=0.00035*ak2*(uave**0.68)*(shield**0.4)*deltar*g*per
    if(epsilon_1.EQ.0.0)epsilon_1=0.0000000001

```

```

    eps=epsilon_1+epsilonw
    surx=-1.0*akz_3*(surdz**1.0)
    decsur=EXP(surx)
    if(dmix(iax,iay).GE.depth(iax,iay).AND.depth(iax,iay).GT.0.0)
&dmix(iax,iay)=depth(iax,iay)
    if(dmix(iax,iay).LT.surdz)decsur=decsur**thermo
    ps1(i)=s(i)*decsur/((v0**2+4.0*ruf*eps)**0.5)
    if(v0.GE.0.0.AND.dy.GT.0.0)then
    etr=-1.0*ak1*((v0-beta*v0)+((4.0*ruf*eps)**0.5))/(2.0*eps)
    endif
    if(v0.GE.0.0.AND.dy.LT.0.0)then
    etr=-1.0*ak1*((v0+beta*v0)+((4.0*ruf*eps)**0.5))/(2.0*eps)
    endif
    if(v0.LT.0.0.AND.dy.LT.0.0)then
    etr=-1.0*ak1*(-1.0*(v0-beta*v0)+((4.0*ruf*eps)**0.5))/
&(2.0*eps)
    endif
    if(v0.LT.0.0.AND.dy.GT.0.0)then
    etr=-1.0*ak1*(-1.0*(v0+beta*v0)+((4.0*ruf*eps)**0.5))/
&(2.0*eps)
    endif
    av0=ABS(v0)
    if(dy.EQ.0.0)then
    etr=-1.0*ak1*(av0+((4.0*ruf*eps)**0.5))/
&(2.0*eps)
    endif
    endif
4532 continue
c
C*****END SIO_2 Y-LOOP*****
c
c*****SIO_4 Y-LOOP*****
    if(ipt(i).EQ.4)then
    if(depth(iax,iay).LT.10.0)then
    ps1(i)=0.0
    ps1b(i)=0.0
    etr=0.0
    etrb=0.0
    go to 4533
    endif
    drc=z(i)*100.0
    wid=widtc*100.0
    qc=qtc*92903.0

```

```

uvdir=ATAN2(ycur(iax,iay),xcur(iax,iay))
ut0=qc/(drc*wid)
ut=ut0/((((dx+0.00001)**2+(dy+0.00001)**2)**0.5)**akr_4)
v0=ycur(iax,iay)+ut*SIN(uvdir)
uave=(u_blend*ucur+u)/(u_blend+1)
dxb=uave*per
deltar=0.72*dxb*(2.5*ruf/dxb)**0.25
fw=EXP(5.2*((2.5*ruf/dxb)**0.2)-6.0)
shield=(uave**2/((rhos/rho-1.0)*g*ruf))*fw
s(i)=srivy4
ak1=aky1_4
ak2=ak2_4
epsilon_l=0.00035*ak2*(uave**0.68)*(shield**0.4)*deltar*g*per
if(epsilon_l.EQ.0.0000000001)epsilon_l=0.0000000001
eps=epsilon_l+epsilon_w
surx=-1.0*akz_4*(surdz**2.0)/eps
decsur=EXP(surx)
if(dmix(iax,iay).GE.depth(iax,iay).AND.depth(iax,iay).GT.0.0)
&dmix(iax,iay)=depth(iax,iay)
if(dmix(iax,iay).LT.surdz)decsur=decsur**thermo
ps1(i)=s(i)*decsur/((v0**2+4.0*ruf*eps)**0.5)
if(v0.GE.0.0.AND.dy.GT.0.0)then
etr=-1.0*ak1*((v0-beta*v0)+((4.0*ruf*eps)**0.5))/(2.0*eps)
endif
if(v0.GE.0.0.AND.dy.LT.0.0)then
etr=-1.0*ak1*((v0+beta*v0)+((4.0*ruf*eps)**0.5))/(2.0*eps)
endif
if(v0.LT.0.0.AND.dy.LT.0.0)then
etr=-1.0*ak1*(-1.0*(v0-beta*v0)+((4.0*ruf*eps)**0.5))/
&(2.0*eps)
endif
if(v0.LT.0.0.AND.dy.GT.0.0)then
etr=-1.0*ak1*(-1.0*(v0+beta*v0)+((4.0*ruf*eps)**0.5))/
&(2.0*eps)
endif
av0=ABS(v0)
if(dy.EQ.0.0)then
etr=-1.0*ak1*(av0+((4.0*ruf*eps)**0.5))/
&(2.0*eps)
endif
endif

```

4533 continue

c

```

C*****END SIO_4 Y-LOOP*****
c
c*****SIO Offshore OUTFALL Y-LOOP*****
  if(ipt(i).EQ.5)then
    if(depth(iax,iay).LT.10.0)then
      ps1(i)=0.0
      ps1b(i)=0.0
      etr=0.0
      etrb=0.0
      go to 4534
    endif
    if(ycur(iax,iay).LT.0.0)uwav=-1.0*uwav
    v0=ycur(iax,iay)+uwav
    s(i)=srivy5
    ak1=aky1_5
    ak2=ak2_5
    epsilon_1=0.00035*ak2*(u**0.68)*(shield**0.4)*delta*g*per
    if(epsilon_1.EQ.0.0000000001)epsilon_1=0.0000000001
    eps=epsilon_1+epsilon_w
    ps1(i)=s(i)/((u**2+4.0*d1*eps)**0.5)
    if(v0.GE.0.0.AND.dy.GT.0.0)then
      etr=-1.0*ak1*((v0-beta*v0)+((4.0*ruf*eps)**0.5))/(2.0*eps)
    endif
    if(v0.GE.0.0.AND.dy.LT.0.0)then
      etr=-1.0*ak1*((v0+beta*v0)+((4.0*ruf*eps)**0.5))/(2.0*eps)
    endif
    if(v0.LT.0.0.AND.dy.LT.0.0)then
      etr=-1.0*ak1*(-1.0*(v0-beta*v0)+((4.0*ruf*eps)**0.5))/
&(2.0*eps)
    endif
    if(v0.LT.0.0.AND.dy.GT.0.0)then
      etr=-1.0*ak1*(-1.0*(v0+beta*v0)+((4.0*ruf*eps)**0.5))/
&(2.0*eps)
    endif
    av0=ABS(v0)
    if(dy.EQ.0.0)then
      etr=-1.0*ak1*(av0+((4.0*ruf*eps)**0.5))/
&(2.0*eps)
    endif
  endif
4534 continue
c
C*****END SIO Offshore OUTFALL Y-LOOP*****

```

```

c
1777  continue
      ps3=etr*((dx**2)+(dy**2))**0.5
      ps3b=etrb*((dx**2)+(dy**2))**0.5
c***
      ps2=EXP(ps3)
      ps2b=EXP(ps3b)
      pny(iax,iay)=pny(iax,iay)+(ps1(i)*ps2)
      bry(iax,iay)=bry(iax,iay)+(ps1b(i)*ps2b)
      bryav(iax,iay)=bryav(iax,iay)+(ps1bav(i)*ps2b)
c
1850  continue
1800  continue
1799  continue
c*****END V LOOPS*****
c
c sum pnx and pny together
      do 2800 iax=1,imax
      do 2850 iay=1,jmax
c      if(pnx(iax,iay).LE.0.00000001)pnx(iax,iay)=0.00000001
c      if(pny(iax,iay).LE.0.00000001)pny(iax,iay)=0.00000001
c      if(pnx(iax,iay).GE.1000000000.0)pnx(iax,iay)=1000000000.0
c      if(pny(iax,iay).GE.1000000000.0)pny(iax,iay)=1000000000.0
      pn(iax,iay)=(pnx(iax,iay)+pny(iax,iay))/2.0
c      pn_l(iax,iay)=LOG(pn(iax,iay))
      brn(iax,iay)=(brx(iax,iay)+bry(iax,iay))/2.0
      brnav(iax,iay)=(brxav(iax,iay)+bryav(iax,iay))/2.0
c
c
2850  continue
2800  continue
c
      if(isal.EQ.1)then
c find maximum pnmax
      pnmax=0.0
      brnmax=0.0
      do 2900 iax=1,imax
      do 2950 iay=1,jmax
      if(pn(iax,iay).GT.pnmax)pnmax=pn(iax,iay)
      if(brn(iax,iay).GT.brnmax)brnmax=brn(iax,iay)
2950  continue
2900  continue
      else

```

```

    brnmax=0.0
    do 2902 iax=1,imax
    do 2953 iay=1,jmax
    if(brn(iax,iay).GT.brnmax)brnmax=brn(iax,iay)
2953  continue
2902  continue
    pnmax=pnman
    endif
c
    if(ibrn.EQ.0)brnmax=brnman
    pnmx_1=LOG(pnmax)
    write(*,*)pnmax,brnmax
c
c*****SALINITY LOOP
    do 3100 iax=1,imax
    do 3150 iay=1,jmax
c**salinity at depth increment surdz below surface
    salsur(iax,iay)=salo*(1.0-((pn(iax,iay)/pnmax)**aksal))
    if(salsur(iax,iay).LT.0.0)salsur(iax,iay)=0.0
    if(depth(iax,iay).LE.0.0)salsur(iax,iay)=0.0
c**salinity at elevation botdz above the bottom
    salbrn(iax,iay)=salo*(1-(brn(iax,iay)/brnmax))+brine*
    &(brn(iax,iay)/brnmax)
c**depth averaged brine salinity
    sbrnav(iax,iay)=salo*(1-(brnav(iax,iay)/brnmax))+brine*
    &(brnav(iax,iay)/brnmax)
    if(iax.EQ.150.AND.iay.EQ.92)write(*,*)salbrn(iax,iay)
    if(iax.EQ.150.AND.iay.EQ.92)write(*,*)sbrnav(iax,iay)
c**salinity of sewage at depth increment thrmdz above thermocline
    saldep(iax,iay)=salo*(1.0-((pn(iax,iay)/pnmax)**aksal))
    if(saldep(iax,iay).LT.0.0)saldep(iax,iay)=0.0
    if(depth(iax,iay).LE.0.0)saldep(iax,iay)=0.0
c
c SIO_1 Inshore
    if(iax.EQ.174.AND.iay.EQ.94)write(*,*)iax,iay,pn(iax,iay),
    &salsur(iax,iay),salbrn(iax,iay),dmix(iax,iay)
c upper left (NW) corner of grid
    if(iax.EQ.1.AND.iay.EQ.1)write(*,*)iax,iay,pn(iax,iay),
    &salsur(iax,iay),salbrn(iax,iay),dmix(iax,iay)
c SIO_3 Inshore
    if(iax.EQ.173.AND.iay.EQ.96)write(*,*)iax,iay,pn(iax,iay),
    &salsur(iax,iay),salbrn(iax,iay),dmix(iax,iay)
c SIO_2

```

```

      if(iax.EQ.193.AND.iay.EQ.100)write(*,*)iax,iay,pn(iax,iay),
      &salsur(iax,iay),salbrn(iax,iay),dmix(iax,iay)
c SIO_4 Outfall
      if(iax.EQ.204.AND.iay.EQ.109)write(*,*)iax,iay,pn(iax,iay),
      &salsur(iax,iay),salbrn(iax,iay),dmix(iax,iay)
3150  continue
3100  continue
c
C****SALINITY MAXIMUM AND MINIMUM LOOP
      salsmx=0.0
      saldmx=0.0
      salbmn=33.52
      do 3160 iax=1,imax
      do 3170 iay=1,jmax
      if(salsur(iax,iay).GT.salsmx)salsmx=salsur(iax,iay)
      if(saldep(iax,iay).GT.saldmx)saldmx=saldep(iax,iay)
      if(salbrn(iax,iay).LT.salbmn)salbmn=salbrn(iax,iay)
3170  continue
3160  continue
      write(*,*)salsmx,saldmx,salbmn
c
c****DILUTION LOOP
      do 3180 iax=1,imax
      do 3190 iay=1,jmax
c dilution of storm water sources at depth increment surdz below surface
      dilriv(iax,iay)=LOG10(salsmx/(salsmx-salsur(iax,iay)+back))
c**storm waterdilution at elevation botdz above the bottom
      dilbrn(iax,iay)=LOG10((rawbrn-salbmn)/
      &(salbrn(iax,iay)-salbmn+back))
c**depth averaged brine dilution
      dbrnav(iax,iay)=LOG10((rawbrn-salbmn)/
      &(sbrnav(iax,iay)-salbmn+back))
      if(iax.EQ.150.AND.iay.EQ.92)write(*,*)dilbrn(iax,iay)
      if(iax.EQ.150.AND.iay.EQ.92)write(*,*)dbrnav(iax,iay)
c dilution of storm water at depth increment thrmdz above thermocline
      dildep(iax,iay)=LOG10(saldmx/(saldmx-saldep(iax,iay)+back))
c TSS counts of storm water at depth thrmdz above thermocline
      col(iax,iay)=LOG10(coli)-dildep(iax,iay)
      if(col(iax,iay).LT.0.0)col(iax,iay)=0.0
c
c TSS counts of outfall source at depth surdz below surface
      colriv(iax,iay)=LOG10(coli)-dilriv(iax,iay)
      if(colriv(iax,iay).LT.0.0)colriv(iax,iay)=0.0

```

```
c
3190  continue
3180  continue
c
c
  do 901 iay=1,jmax
  write(21,999)(pn(iax,iay),iax=1,imax)
901  continue
c
  close(21)
c
  do 902 iay=1,jmax
  write(22,999)(pn_1(iax,iay),iax=1,imax)
902  continue
c
  close(22)
c
c
  do 888 iax=1,imax
  do 887 iay=1,jmax
  if(depth(iax,iay).LT.surdz)salsur(iax,iay)=-2.0
  if(depth(iax,iay).LE.0.0)salsur(iax,iay)=-2.0
  if(depth(iax,iay).LT.botdz)salbrn(iax,iay)=-2.0
  if(depth(iax,iay).LE.0.0)salbrn(iax,iay)=-2.0
  if(depth(iax,iay).LE.0.0)dilbrn(iax,iay)=-2.0
  if(depth(iax,iay).LE.0.0)dildep(iax,iay)=-2.0
  if(depth(iax,iay).LE.0.0)saldep(iax,iay)=-2.0
  if(depth(iax,iay).LE.0.0)col(iax,iay)=-2.0
  if(depth(iax,iay).LE.0.0)colriv(iax,iay)=-2.0
  if(depth(iax,iay).LE.0.0)sbrnav(iax,iay)=-2.0
  if(depth(iax,iay).LE.0.0)dbnav(iax,iay)=-2.0
887  continue
888  continue
c
  do 903 iay=1,jmax
  write(23,995)(salsur(iax,iay),iax=1,imax)
903  continue
c
  close(23)
c
c
  do 905 iay=1,jmax
  write(25,995)(salbrn(iax,iay),iax=1,imax)
```

```
905  continue
c
    close(25)
c
c
    do 906 iay=1,jmax
        write(26,995)(dilbrn(iax,iay),iax=1,imax)
906  continue
c
    close(26)
c
    do 904 iay=1,jmax
        write(24,999)(dilriv(iax,iay),iax=1,imax)
904  continue
c
    close(24)
cc
    do 907 iay=1,jmax
        write(27,995)(saldep(iax,iay),iax=1,imax)
907  continue
c
    close(27)
c
c
    do 908 iay=1,jmax
        write(28,995)(dildep(iax,iay),iax=1,imax)
908  continue
c
    close(28)
c
c
    do 909 iay=1,jmax
        write(29,995)(col(iax,iay),iax=1,imax)
909  continue
c
    close(29)
c
    do 910 iay=1,jmax
        write(30,995)(dmix(iax,iay),iax=1,imax)
910  continue
c
    close(30)
c
```

```
      do 911 iay=1,jmax
        write(31,995)(colriv(iax,iay),iax=1,imax)
911    continue
      c
        close(31)
      c
      c
        do 912 iay=1,jmax
          write(32,995)(sbrnav(iax,iay),iax=1,imax)
912    continue
      c
        close(32)
      c
      c
        do 913 iay=1,jmax
          write(33,995)(dbrnav(iax,iay),iax=1,imax)
913    continue
      c
        close(33)
      c
999    format(200e12.3)
995    format(200e15.6)
      c
        stop
      end
```

AMEC, Environment & Infrastructure, Inc.
Hydrodynamic Modeling of Storm Drain Discharges in
the Neighborhood of ASBS 29 in La Jolla, California
Revised: 13 March 2013

APPENDIX G

AMEC MONITORING DATA

Appendix G: AMEC Monitoring Data

Station Code	Sample Date	Time	Units	Result	Collection Device Name	Agency
906SDL062OD	03/Nov/11	8:45 PST	inches	0	Hach tipping bucket rain gauge	AMEC
906SDL062OD	03/Nov/11	9:00 PST	inches	0	Hach tipping bucket rain gauge	AMEC
906SDL062OD	03/Nov/11	9:15 PST	inches	0	Hach tipping bucket rain gauge	AMEC
906SDL062OD	03/Nov/11	9:30 PST	inches	0	Hach tipping bucket rain gauge	AMEC
906SDL062OD	03/Nov/11	9:45 PST	inches	0	Hach tipping bucket rain gauge	AMEC
906SDL062OD	03/Nov/11	10:00 PST	inches	0	Hach tipping bucket rain gauge	AMEC
906SDL062OD	03/Nov/11	10:15 PST	inches	0	Hach tipping bucket rain gauge	AMEC
906SDL062OD	03/Nov/11	10:30 PST	inches	0	Hach tipping bucket rain gauge	AMEC
906SDL062OD	03/Nov/11	10:45 PST	inches	0	Hach tipping bucket rain gauge	AMEC
906SDL062OD	03/Nov/11	11:00 PST	inches	0	Hach tipping bucket rain gauge	AMEC
906SDL062OD	03/Nov/11	11:15 PST	inches	0	Hach tipping bucket rain gauge	AMEC
906SDL062OD	03/Nov/11	11:30 PST	inches	0	Hach tipping bucket rain gauge	AMEC
906SDL062OD	03/Nov/11	11:45 PST	inches	0	Hach tipping bucket rain gauge	AMEC
906SDL062OD	03/Nov/11	12:00 PST	inches	0	Hach tipping bucket rain gauge	AMEC
906SDL062OD	03/Nov/11	12:15 PST	inches	0	Hach tipping bucket rain gauge	AMEC
906SDL062OD	03/Nov/11	12:30 PST	inches	0	Hach tipping bucket rain gauge	AMEC
906SDL062OD	03/Nov/11	12:45 PST	inches	0	Hach tipping bucket rain gauge	AMEC
906SDL062OD	03/Nov/11	13:00 PST	inches	0	Hach tipping bucket rain gauge	AMEC
906SDL062OD	03/Nov/11	13:15 PST	inches	0	Hach tipping bucket rain gauge	AMEC
906SDL062OD	03/Nov/11	13:30 PST	inches	0	Hach tipping bucket rain gauge	AMEC
906SDL062OD	03/Nov/11	13:45 PST	inches	0	Hach tipping bucket rain gauge	AMEC
906SDL062OD	03/Nov/11	14:00 PST	inches	0	Hach tipping bucket rain gauge	AMEC
906SDL062OD	03/Nov/11	14:15 PST	inches	0	Hach tipping bucket rain gauge	AMEC
906SDL062OD	03/Nov/11	14:30 PST	inches	0	Hach tipping bucket rain gauge	AMEC
906SDL062OD	03/Nov/11	14:45 PST	inches	0	Hach tipping bucket rain gauge	AMEC
906SDL062OD	03/Nov/11	15:00 PST	inches	0	Hach tipping bucket rain gauge	AMEC
906SDL062OD	03/Nov/11	15:15 PST	inches	0	Hach tipping bucket rain gauge	AMEC
906SDL062OD	03/Nov/11	15:30 PST	inches	0	Hach tipping bucket rain gauge	AMEC
906SDL062OD	03/Nov/11	15:45 PST	inches	0	Hach tipping bucket rain gauge	AMEC
906SDL062OD	03/Nov/11	16:00 PST	inches	0	Hach tipping bucket rain gauge	AMEC
906SDL062OD	03/Nov/11	16:15 PST	inches	0	Hach tipping bucket rain gauge	AMEC
906SDL062OD	03/Nov/11	16:30 PST	inches	0	Hach tipping bucket rain gauge	AMEC
906SDL062OD	03/Nov/11	16:45 PST	inches	0	Hach tipping bucket rain gauge	AMEC
906SDL062OD	03/Nov/11	17:00 PST	inches	0	Hach tipping bucket rain gauge	AMEC
906SDL062OD	03/Nov/11	17:15 PST	inches	0	Hach tipping bucket rain gauge	AMEC
906SDL062OD	03/Nov/11	17:30 PST	inches	0	Hach tipping bucket rain gauge	AMEC
906SDL062OD	03/Nov/11	17:45 PST	inches	0	Hach tipping bucket rain gauge	AMEC
906SDL062OD	03/Nov/11	18:00 PST	inches	0	Hach tipping bucket rain gauge	AMEC
906SDL062OD	03/Nov/11	18:15 PST	inches	0	Hach tipping bucket rain gauge	AMEC
906SDL062OD	03/Nov/11	18:30 PST	inches	0	Hach tipping bucket rain gauge	AMEC
906SDL062OD	03/Nov/11	18:45 PST	inches	0	Hach tipping bucket rain gauge	AMEC
906SDL062OD	03/Nov/11	19:00 PST	inches	0	Hach tipping bucket rain gauge	AMEC
906SDL062OD	03/Nov/11	19:15 PST	inches	0	Hach tipping bucket rain gauge	AMEC
906SDL062OD	03/Nov/11	19:30 PST	inches	0	Hach tipping bucket rain gauge	AMEC
906SDL062OD	03/Nov/11	19:45 PST	inches	0	Hach tipping bucket rain gauge	AMEC
906SDL062OD	03/Nov/11	20:00 PST	inches	0	Hach tipping bucket rain gauge	AMEC
906SDL062OD	03/Nov/11	20:15 PST	inches	0	Hach tipping bucket rain gauge	AMEC
906SDL062OD	03/Nov/11	20:30 PST	inches	0	Hach tipping bucket rain gauge	AMEC
906SDL062OD	03/Nov/11	20:45 PST	inches	0	Hach tipping bucket rain gauge	AMEC
906SDL062OD	03/Nov/11	21:00 PST	inches	0	Hach tipping bucket rain gauge	AMEC
906SDL062OD	03/Nov/11	21:15 PST	inches	0	Hach tipping bucket rain gauge	AMEC
906SDL062OD	03/Nov/11	21:30 PST	inches	0	Hach tipping bucket rain gauge	AMEC
906SDL062OD	03/Nov/11	21:45 PST	inches	0	Hach tipping bucket rain gauge	AMEC
906SDL062OD	03/Nov/11	22:00 PST	inches	0	Hach tipping bucket rain gauge	AMEC

Station Code	Sample Date	Time	Agency	Location	Result	Collection Device Name
906SDL062OD	20/Nov/11	14:00	AMEC	Pipe	0 cfs	Hach 950 Flow Meter
906SDL062OD	20/Nov/11	14:15	AMEC	Pipe	0 cfs	Hach 950 Flow Meter
906SDL062OD	20/Nov/11	14:30	AMEC	Pipe	0 cfs	Hach 950 Flow Meter
906SDL062OD	20/Nov/11	14:45	AMEC	Pipe	0 cfs	Hach 950 Flow Meter
906SDL062OD	20/Nov/11	15:00	AMEC	Pipe	0 cfs	Hach 950 Flow Meter
906SDL062OD	20/Nov/11	15:15	AMEC	Pipe	0 cfs	Hach 950 Flow Meter
906SDL062OD	20/Nov/11	15:30	AMEC	Pipe	0 cfs	Hach 950 Flow Meter
906SDL062OD	20/Nov/11	15:45	AMEC	Pipe	0 cfs	Hach 950 Flow Meter
906SDL062OD	20/Nov/11	16:00	AMEC	Pipe	0 cfs	Hach 950 Flow Meter
906SDL062OD	20/Nov/11	16:15	AMEC	Pipe	0 cfs	Hach 950 Flow Meter
906SDL062OD	20/Nov/11	16:30	AMEC	Pipe	0 cfs	Hach 950 Flow Meter
906SDL062OD	20/Nov/11	16:45	AMEC	Pipe	0 cfs	Hach 950 Flow Meter
906SDL062OD	20/Nov/11	17:00	AMEC	Pipe	0 cfs	Hach 950 Flow Meter
906SDL062OD	20/Nov/11	17:15	AMEC	Pipe	0 cfs	Hach 950 Flow Meter
906SDL062OD	20/Nov/11	17:30	AMEC	Pipe	0 cfs	Hach 950 Flow Meter
906SDL062OD	20/Nov/11	17:45	AMEC	Pipe	1.29 cfs	Hach 950 Flow Meter
906SDL062OD	20/Nov/11	18:00	AMEC	Pipe	1.76 cfs	Hach 950 Flow Meter
906SDL062OD	20/Nov/11	18:15	AMEC	Pipe	5.48 cfs	Hach 950 Flow Meter
906SDL062OD	20/Nov/11	18:30	AMEC	Pipe	8.77 cfs	Hach 950 Flow Meter
906SDL062OD	20/Nov/11	18:45	AMEC	Pipe	9.44 cfs	Hach 950 Flow Meter
906SDL062OD	20/Nov/11	19:00	AMEC	Pipe	10.44 cfs	Hach 950 Flow Meter
906SDL062OD	20/Nov/11	19:15	AMEC	Pipe	9.33 cfs	Hach 950 Flow Meter
906SDL062OD	20/Nov/11	19:30	AMEC	Pipe	6.54 cfs	Hach 950 Flow Meter
906SDL062OD	20/Nov/11	19:45	AMEC	Pipe	4.83 cfs	Hach 950 Flow Meter
906SDL062OD	20/Nov/11	20:00	AMEC	Pipe	4.45 cfs	Hach 950 Flow Meter
906SDL062OD	20/Nov/11	20:15	AMEC	Pipe	4.05 cfs	Hach 950 Flow Meter
906SDL062OD	20/Nov/11	20:30	AMEC	Pipe	3.62 cfs	Hach 950 Flow Meter
906SDL062OD	20/Nov/11	20:45	AMEC	Pipe	3.7 cfs	Hach 950 Flow Meter
906SDL062OD	20/Nov/11	21:00	AMEC	Pipe	4.5 cfs	Hach 950 Flow Meter
906SDL062OD	20/Nov/11	21:15	AMEC	Pipe	3.67 cfs	Hach 950 Flow Meter
906SDL062OD	20/Nov/11	21:30	AMEC	Pipe	3.52 cfs	Hach 950 Flow Meter
906SDL062OD	20/Nov/11	21:45	AMEC	Pipe	3.39 cfs	Hach 950 Flow Meter
906SDL062OD	20/Nov/11	22:00	AMEC	Pipe	3.14 cfs	Hach 950 Flow Meter
906SDL062OD	20/Nov/11	22:15	AMEC	Pipe	2.63 cfs	Hach 950 Flow Meter
906SDL062OD	20/Nov/11	22:30	AMEC	Pipe	2.09 cfs	Hach 950 Flow Meter
906SDL062OD	20/Nov/11	22:45	AMEC	Pipe	1.66 cfs	Hach 950 Flow Meter
906SDL062OD	20/Nov/11	23:00	AMEC	Pipe	1.39 cfs	Hach 950 Flow Meter
906SDL062OD	20/Nov/11	23:15	AMEC	Pipe	1.32 cfs	Hach 950 Flow Meter
906SDL062OD	20/Nov/11	23:30	AMEC	Pipe	1.62 cfs	Hach 950 Flow Meter
906SDL062OD	20/Nov/11	23:45	AMEC	Pipe	4.59 cfs	Hach 950 Flow Meter
906SDL062OD	21/Nov/11	0:00	AMEC	Pipe	6.12 cfs	Hach 950 Flow Meter
906SDL062OD	21/Nov/11	0:15	AMEC	Pipe	3.99 cfs	Hach 950 Flow Meter
906SDL062OD	21/Nov/11	0:30	AMEC	Pipe	3.16 cfs	Hach 950 Flow Meter
906SDL062OD	21/Nov/11	0:45	AMEC	Pipe	3.12 cfs	Hach 950 Flow Meter
906SDL062OD	21/Nov/11	1:00	AMEC	Pipe	2.75 cfs	Hach 950 Flow Meter
906SDL062OD	21/Nov/11	1:15	AMEC	Pipe	2.15 cfs	Hach 950 Flow Meter
906SDL062OD	21/Nov/11	1:30	AMEC	Pipe	1.59 cfs	Hach 950 Flow Meter
906SDL062OD	21/Nov/11	1:45	AMEC	Pipe	1.11 cfs	Hach 950 Flow Meter
906SDL062OD	21/Nov/11	2:00	AMEC	Pipe	0.761 cfs	Hach 950 Flow Meter
906SDL062OD	21/Nov/11	2:15	AMEC	Pipe	0.53 cfs	Hach 950 Flow Meter
906SDL062OD	21/Nov/11	2:30	AMEC	Pipe	0.339 cfs	Hach 950 Flow Meter
906SDL062OD	21/Nov/11	2:45	AMEC	Pipe	0.249 cfs	Hach 950 Flow Meter
906SDL062OD	21/Nov/11	3:00	AMEC	Pipe	0.204 cfs	Hach 950 Flow Meter
906SDL062OD	21/Nov/11	3:15	AMEC	Pipe	0.146 cfs	Hach 950 Flow Meter

Station Code	Sample Date	Time	Agency	Location	Result	Units	Collection Device Name
906SDL062OD	07/Feb/12	14:00	AMEC	Pipe	0	cfs	Hach 950 Flow Meter
906SDL062OD	07/Feb/12	14:15	AMEC	Pipe	0	cfs	Hach 950 Flow Meter
906SDL062OD	07/Feb/12	14:30	AMEC	Pipe	0	cfs	Hach 950 Flow Meter
906SDL062OD	07/Feb/12	14:45	AMEC	Pipe	0	cfs	Hach 950 Flow Meter
906SDL062OD	07/Feb/12	15:00	AMEC	Pipe	0	cfs	Hach 950 Flow Meter
906SDL062OD	07/Feb/12	15:15	AMEC	Pipe	0.01	cfs	Hach 950 Flow Meter
906SDL062OD	07/Feb/12	15:30	AMEC	Pipe	0.095	cfs	Hach 950 Flow Meter
906SDL062OD	07/Feb/12	15:45	AMEC	Pipe	0.28	cfs	Hach 950 Flow Meter
906SDL062OD	07/Feb/12	16:00	AMEC	Pipe	1.9	cfs	Hach 950 Flow Meter
906SDL062OD	07/Feb/12	16:15	AMEC	Pipe	2.2	cfs	Hach 950 Flow Meter
906SDL062OD	07/Feb/12	16:30	AMEC	Pipe	1.33	cfs	Hach 950 Flow Meter
906SDL062OD	07/Feb/12	16:45	AMEC	Pipe	2.23	cfs	Hach 950 Flow Meter
906SDL062OD	07/Feb/12	17:00	AMEC	Pipe	4.44	cfs	Hach 950 Flow Meter
906SDL062OD	07/Feb/12	17:15	AMEC	Pipe	6.56	cfs	Hach 950 Flow Meter
906SDL062OD	07/Feb/12	17:30	AMEC	Pipe	5.14	cfs	Hach 950 Flow Meter
906SDL062OD	07/Feb/12	17:45	AMEC	Pipe	2.47	cfs	Hach 950 Flow Meter
906SDL062OD	07/Feb/12	18:00	AMEC	Pipe	2.04	cfs	Hach 950 Flow Meter
906SDL062OD	07/Feb/12	18:15	AMEC	Pipe	1.02	cfs	Hach 950 Flow Meter
906SDL062OD	07/Feb/12	18:30	AMEC	Pipe	0.293	cfs	Hach 950 Flow Meter
906SDL062OD	07/Feb/12	18:45	AMEC	Pipe	0.047	cfs	Hach 950 Flow Meter
906SDL062OD	07/Feb/12	19:00	AMEC	Pipe	0	cfs	Hach 950 Flow Meter
906SDL062OD	07/Feb/12	19:15	AMEC	Pipe	0	cfs	Hach 950 Flow Meter
906SDL062OD	07/Feb/12	19:30	AMEC	Pipe	0	cfs	Hach 950 Flow Meter
906SDL062OD	07/Feb/12	19:45	AMEC	Pipe	0	cfs	Hach 950 Flow Meter
906SDL062OD	07/Feb/12	20:00	AMEC	Pipe	0	cfs	Hach 950 Flow Meter
906SDL062OD	07/Feb/12	20:15	AMEC	Pipe	0	cfs	Hach 950 Flow Meter
906SDL062OD	07/Feb/12	20:30	AMEC	Pipe	0	cfs	Hach 950 Flow Meter
906SDL062OD	07/Feb/12	20:45	AMEC	Pipe	0	cfs	Hach 950 Flow Meter
906SDL062OD	07/Feb/12	21:00	AMEC	Pipe	0	cfs	Hach 950 Flow Meter

AMEC, Environment & Infrastructure, Inc.
Hydrodynamic Modeling of Storm Drain Discharges in
the Neighborhood of ASBS 29 in La Jolla, California
Revised: 13 March 2013

Station Code	Sample Date	Time	Agency	Location	Result	Units	Collection Device Name
906SDL062OD	16/Mar/12	17:45	AMEC	Pipe	0	cfs	Hach 950 Flow Meter
906SDL062OD	16/Mar/12	18:00	AMEC	Pipe	0	cfs	Hach 950 Flow Meter
906SDL062OD	16/Mar/12	18:15	AMEC	Pipe	0	cfs	Hach 950 Flow Meter
906SDL062OD	16/Mar/12	18:30	AMEC	Pipe	0	cfs	Hach 950 Flow Meter
906SDL062OD	16/Mar/12	18:45	AMEC	Pipe	0	cfs	Hach 950 Flow Meter
906SDL062OD	16/Mar/12	19:00	AMEC	Pipe	0	cfs	Hach 950 Flow Meter
906SDL062OD	16/Mar/12	19:15	AMEC	Pipe	0	cfs	Hach 950 Flow Meter
906SDL062OD	16/Mar/12	19:30	AMEC	Pipe	0	cfs	Hach 950 Flow Meter
906SDL062OD	16/Mar/12	19:45	AMEC	Pipe	0	cfs	Hach 950 Flow Meter
906SDL062OD	16/Mar/12	20:00	AMEC	Pipe	0	cfs	Hach 950 Flow Meter
906SDL062OD	16/Mar/12	20:15	AMEC	Pipe	0	cfs	Hach 950 Flow Meter
906SDL062OD	16/Mar/12	20:30	AMEC	Pipe	0	cfs	Hach 950 Flow Meter
906SDL062OD	16/Mar/12	20:45	AMEC	Pipe	0	cfs	Hach 950 Flow Meter
906SDL062OD	16/Mar/12	21:00	AMEC	Pipe	0	cfs	Hach 950 Flow Meter
906SDL062OD	16/Mar/12	21:15	AMEC	Pipe	0	cfs	Hach 950 Flow Meter
906SDL062OD	16/Mar/12	21:30	AMEC	Pipe	0	cfs	Hach 950 Flow Meter
906SDL062OD	16/Mar/12	21:45	AMEC	Pipe	0	cfs	Hach 950 Flow Meter
906SDL062OD	16/Mar/12	22:00	AMEC	Pipe	0	cfs	Hach 950 Flow Meter
906SDL062OD	16/Mar/12	22:15	AMEC	Pipe	0	cfs	Hach 950 Flow Meter
906SDL062OD	16/Mar/12	22:30	AMEC	Pipe	0	cfs	Hach 950 Flow Meter
906SDL062OD	16/Mar/12	22:45	AMEC	Pipe	0	cfs	Hach 950 Flow Meter
906SDL062OD	16/Mar/12	23:00	AMEC	Pipe	0	cfs	Hach 950 Flow Meter
906SDL062OD	16/Mar/12	23:15	AMEC	Pipe	0	cfs	Hach 950 Flow Meter
906SDL062OD	16/Mar/12	23:30	AMEC	Pipe	0	cfs	Hach 950 Flow Meter
906SDL062OD	16/Mar/12	23:45	AMEC	Pipe	0	cfs	Hach 950 Flow Meter
906SDL062OD	17/Mar/12	0:00	AMEC	Pipe	0	cfs	Hach 950 Flow Meter
906SDL062OD	17/Mar/12	0:15	AMEC	Pipe	0	cfs	Hach 950 Flow Meter
906SDL062OD	17/Mar/12	0:30	AMEC	Pipe	0	cfs	Hach 950 Flow Meter
906SDL062OD	17/Mar/12	0:45	AMEC	Pipe	0	cfs	Hach 950 Flow Meter
906SDL062OD	17/Mar/12	1:00	AMEC	Pipe	0	cfs	Hach 950 Flow Meter
906SDL062OD	17/Mar/12	1:15	AMEC	Pipe	0.053	cfs	Hach 950 Flow Meter
906SDL062OD	17/Mar/12	1:30	AMEC	Pipe	0.428	cfs	Hach 950 Flow Meter
906SDL062OD	17/Mar/12	1:45	AMEC	Pipe	0.252	cfs	Hach 950 Flow Meter
906SDL062OD	17/Mar/12	2:00	AMEC	Pipe	0.065	cfs	Hach 950 Flow Meter
906SDL062OD	17/Mar/12	2:15	AMEC	Pipe	0.011	cfs	Hach 950 Flow Meter
906SDL062OD	17/Mar/12	2:30	AMEC	Pipe	0.031	cfs	Hach 950 Flow Meter
906SDL062OD	17/Mar/12	2:45	AMEC	Pipe	0.031	cfs	Hach 950 Flow Meter
906SDL062OD	17/Mar/12	3:00	AMEC	Pipe	0.017	cfs	Hach 950 Flow Meter
906SDL062OD	17/Mar/12	3:15	AMEC	Pipe	0.017	cfs	Hach 950 Flow Meter
906SDL062OD	17/Mar/12	3:30	AMEC	Pipe	0.014	cfs	Hach 950 Flow Meter
906SDL062OD	17/Mar/12	3:45	AMEC	Pipe	0.01	cfs	Hach 950 Flow Meter
906SDL062OD	17/Mar/12	4:00	AMEC	Pipe	0.01	cfs	Hach 950 Flow Meter
906SDL062OD	17/Mar/12	4:15	AMEC	Pipe	0.225	cfs	Hach 950 Flow Meter
906SDL062OD	17/Mar/12	4:30	AMEC	Pipe	0.44	cfs	Hach 950 Flow Meter
906SDL062OD	17/Mar/12	4:45	AMEC	Pipe	0.361	cfs	Hach 950 Flow Meter
906SDL062OD	17/Mar/12	5:00	AMEC	Pipe	0.493	cfs	Hach 950 Flow Meter
906SDL062OD	17/Mar/12	5:15	AMEC	Pipe	1.74	cfs	Hach 950 Flow Meter
906SDL062OD	17/Mar/12	5:30	AMEC	Pipe	1.68	cfs	Hach 950 Flow Meter
906SDL062OD	17/Mar/12	5:45	AMEC	Pipe	2.23	cfs	Hach 950 Flow Meter
906SDL062OD	17/Mar/12	6:00	AMEC	Pipe	2.18	cfs	Hach 950 Flow Meter
906SDL062OD	17/Mar/12	6:15	AMEC	Pipe	4.25	cfs	Hach 950 Flow Meter
906SDL062OD	17/Mar/12	6:30	AMEC	Pipe	1.62	cfs	Hach 950 Flow Meter
906SDL062OD	17/Mar/12	6:45	AMEC	Pipe	1.78	cfs	Hach 950 Flow Meter
906SDL062OD	17/Mar/12	7:00	AMEC	Pipe	2.13	cfs	Hach 950 Flow Meter

Station Code	Sample Date	Time	Agency	Location	Result	Units	Collection Device Name
906SDL157OD	20/Nov/11	9:15	AMEC	Pipe	0	cfs	Hach 950 Flow Meter
906SDL157OD	20/Nov/11	9:30	AMEC	Pipe	0	cfs	Hach 950 Flow Meter
906SDL157OD	20/Nov/11	9:45	AMEC	Pipe	0	cfs	Hach 950 Flow Meter
906SDL157OD	20/Nov/11	10:00	AMEC	Pipe	0	cfs	Hach 950 Flow Meter
906SDL157OD	20/Nov/11	10:15	AMEC	Pipe	0	cfs	Hach 950 Flow Meter
906SDL157OD	20/Nov/11	10:30	AMEC	Pipe	0	cfs	Hach 950 Flow Meter
906SDL157OD	20/Nov/11	10:45	AMEC	Pipe	0	cfs	Hach 950 Flow Meter
906SDL157OD	20/Nov/11	11:00	AMEC	Pipe	0	cfs	Hach 950 Flow Meter
906SDL157OD	20/Nov/11	11:15	AMEC	Pipe	0	cfs	Hach 950 Flow Meter
906SDL157OD	20/Nov/11	11:30	AMEC	Pipe	0	cfs	Hach 950 Flow Meter
906SDL157OD	20/Nov/11	11:45	AMEC	Pipe	0	cfs	Hach 950 Flow Meter
906SDL157OD	20/Nov/11	12:00	AMEC	Pipe	0	cfs	Hach 950 Flow Meter
906SDL157OD	20/Nov/11	12:15	AMEC	Pipe	0	cfs	Hach 950 Flow Meter
906SDL157OD	20/Nov/11	12:30	AMEC	Pipe	0	cfs	Hach 950 Flow Meter
906SDL157OD	20/Nov/11	12:45	AMEC	Pipe	0	cfs	Hach 950 Flow Meter
906SDL157OD	20/Nov/11	13:00	AMEC	Pipe	0	cfs	Hach 950 Flow Meter
906SDL157OD	20/Nov/11	13:15	AMEC	Pipe	0	cfs	Hach 950 Flow Meter
906SDL157OD	20/Nov/11	13:30	AMEC	Pipe	0	cfs	Hach 950 Flow Meter
906SDL157OD	20/Nov/11	13:45	AMEC	Pipe	0	cfs	Hach 950 Flow Meter
906SDL157OD	20/Nov/11	14:00	AMEC	Pipe	0	cfs	Hach 950 Flow Meter
906SDL157OD	20/Nov/11	14:15	AMEC	Pipe	0	cfs	Hach 950 Flow Meter
906SDL157OD	20/Nov/11	14:30	AMEC	Pipe	0	cfs	Hach 950 Flow Meter
906SDL157OD	20/Nov/11	14:45	AMEC	Pipe	0	cfs	Hach 950 Flow Meter
906SDL157OD	20/Nov/11	15:00	AMEC	Pipe	0	cfs	Hach 950 Flow Meter
906SDL157OD	20/Nov/11	15:15	AMEC	Pipe	0	cfs	Hach 950 Flow Meter
906SDL157OD	20/Nov/11	15:30	AMEC	Pipe	0	cfs	Hach 950 Flow Meter
906SDL157OD	20/Nov/11	15:45	AMEC	Pipe	0	cfs	Hach 950 Flow Meter
906SDL157OD	20/Nov/11	16:00	AMEC	Pipe	0	cfs	Hach 950 Flow Meter
906SDL157OD	20/Nov/11	16:15	AMEC	Pipe	0	cfs	Hach 950 Flow Meter
906SDL157OD	20/Nov/11	16:30	AMEC	Pipe	0	cfs	Hach 950 Flow Meter
906SDL157OD	20/Nov/11	16:45	AMEC	Pipe	0	cfs	Hach 950 Flow Meter
906SDL157OD	20/Nov/11	17:00	AMEC	Pipe	0	cfs	Hach 950 Flow Meter
906SDL157OD	20/Nov/11	17:15	AMEC	Pipe	0	cfs	Hach 950 Flow Meter
906SDL157OD	20/Nov/11	17:30	AMEC	Pipe	0.003	cfs	Hach 950 Flow Meter
906SDL157OD	20/Nov/11	17:45	AMEC	Pipe	0.56	cfs	Hach 950 Flow Meter
906SDL157OD	20/Nov/11	18:00	AMEC	Pipe	1.26	cfs	Hach 950 Flow Meter
906SDL157OD	20/Nov/11	18:15	AMEC	Pipe	1.25	cfs	Hach 950 Flow Meter
906SDL157OD	20/Nov/11	18:30	AMEC	Pipe	2.73	cfs	Hach 950 Flow Meter
906SDL157OD	20/Nov/11	18:45	AMEC	Pipe	2.96	cfs	Hach 950 Flow Meter
906SDL157OD	20/Nov/11	19:00	AMEC	Pipe	3.22	cfs	Hach 950 Flow Meter
906SDL157OD	20/Nov/11	19:15	AMEC	Pipe	2.26	cfs	Hach 950 Flow Meter
906SDL157OD	20/Nov/11	19:30	AMEC	Pipe	1.76	cfs	Hach 950 Flow Meter
906SDL157OD	20/Nov/11	19:45	AMEC	Pipe	1.49	cfs	Hach 950 Flow Meter
906SDL157OD	20/Nov/11	20:00	AMEC	Pipe	0.96	cfs	Hach 950 Flow Meter
906SDL157OD	20/Nov/11	20:15	AMEC	Pipe	0.94	cfs	Hach 950 Flow Meter
906SDL157OD	20/Nov/11	20:30	AMEC	Pipe	0.92	cfs	Hach 950 Flow Meter
906SDL157OD	20/Nov/11	20:45	AMEC	Pipe	1.72	cfs	Hach 950 Flow Meter
906SDL157OD	20/Nov/11	21:00	AMEC	Pipe	1.68	cfs	Hach 950 Flow Meter
906SDL157OD	20/Nov/11	21:15	AMEC	Pipe	1.08	cfs	Hach 950 Flow Meter
906SDL157OD	20/Nov/11	21:30	AMEC	Pipe	0.93	cfs	Hach 950 Flow Meter
906SDL157OD	20/Nov/11	21:45	AMEC	Pipe	0.97	cfs	Hach 950 Flow Meter
906SDL157OD	20/Nov/11	22:00	AMEC	Pipe	0.95	cfs	Hach 950 Flow Meter
906SDL157OD	20/Nov/11	22:15	AMEC	Pipe	0.84	cfs	Hach 950 Flow Meter
906SDL157OD	20/Nov/11	22:30	AMEC	Pipe	0.75	cfs	Hach 950 Flow Meter

Station Code	Sample Date	Time	Agency	Location	Result	Units	Collection Device Name
906SDL157OD	07/Feb/12	14:00	AMEC	Pipe	0	cfs	Hach 950 Flow Meter
906SDL157OD	07/Feb/12	14:15	AMEC	Pipe	0	cfs	Hach 950 Flow Meter
906SDL157OD	07/Feb/12	14:30	AMEC	Pipe	0	cfs	Hach 950 Flow Meter
906SDL157OD	07/Feb/12	14:45	AMEC	Pipe	0	cfs	Hach 950 Flow Meter
906SDL157OD	07/Feb/12	15:00	AMEC	Pipe	0.001	cfs	Hach 950 Flow Meter
906SDL157OD	07/Feb/12	15:15	AMEC	Pipe	0.11	cfs	Hach 950 Flow Meter
906SDL157OD	07/Feb/12	15:30	AMEC	Pipe	0.13	cfs	Hach 950 Flow Meter
906SDL157OD	07/Feb/12	15:45	AMEC	Pipe	0.16	cfs	Hach 950 Flow Meter
906SDL157OD	07/Feb/12	16:00	AMEC	Pipe	0.45	cfs	Hach 950 Flow Meter
906SDL157OD	07/Feb/12	16:15	AMEC	Pipe	1.31	cfs	Hach 950 Flow Meter
906SDL157OD	07/Feb/12	16:30	AMEC	Pipe	1.34	cfs	Hach 950 Flow Meter
906SDL157OD	07/Feb/12	16:45	AMEC	Pipe	2.52	cfs	Hach 950 Flow Meter
906SDL157OD	07/Feb/12	17:00	AMEC	Pipe	2.88	cfs	Hach 950 Flow Meter
906SDL157OD	07/Feb/12	17:15	AMEC	Pipe	3.48	cfs	Hach 950 Flow Meter
906SDL157OD	07/Feb/12	17:30	AMEC	Pipe	3.15	cfs	Hach 950 Flow Meter
906SDL157OD	07/Feb/12	17:45	AMEC	Pipe	3.17	cfs	Hach 950 Flow Meter
906SDL157OD	07/Feb/12	18:00	AMEC	Pipe	2.73	cfs	Hach 950 Flow Meter
906SDL157OD	07/Feb/12	18:15	AMEC	Pipe	2.07	cfs	Hach 950 Flow Meter
906SDL157OD	07/Feb/12	18:30	AMEC	Pipe	1.64	cfs	Hach 950 Flow Meter
906SDL157OD	07/Feb/12	18:45	AMEC	Pipe	1.27	cfs	Hach 950 Flow Meter
906SDL157OD	07/Feb/12	19:00	AMEC	Pipe	0.77	cfs	Hach 950 Flow Meter
906SDL157OD	07/Feb/12	19:15	AMEC	Pipe	0.51	cfs	Hach 950 Flow Meter
906SDL157OD	07/Feb/12	19:30	AMEC	Pipe	0.24	cfs	Hach 950 Flow Meter
906SDL157OD	07/Feb/12	19:45	AMEC	Pipe	0.1	cfs	Hach 950 Flow Meter
906SDL157OD	07/Feb/12	20:00	AMEC	Pipe	0.022	cfs	Hach 950 Flow Meter
906SDL157OD	07/Feb/12	20:15	AMEC	Pipe	0.003	cfs	Hach 950 Flow Meter
906SDL157OD	07/Feb/12	20:30	AMEC	Pipe	0	cfs	Hach 950 Flow Meter
906SDL157OD	07/Feb/12	20:45	AMEC	Pipe	0	cfs	Hach 950 Flow Meter
906SDL157OD	07/Feb/12	21:00	AMEC	Pipe	0	cfs	Hach 950 Flow Meter

Station Code	Sample Date	Time	Agency	Location	Result	Units	Collection Device Name
906SDL157OD	16/Mar/12	17:45	AMEC	Pipe	0	cfs	Hach 950 Flow Meter
906SDL157OD	16/Mar/12	18:00	AMEC	Pipe	0	cfs	Hach 950 Flow Meter
906SDL157OD	16/Mar/12	18:15	AMEC	Pipe	0	cfs	Hach 950 Flow Meter
906SDL157OD	16/Mar/12	18:30	AMEC	Pipe	0	cfs	Hach 950 Flow Meter
906SDL157OD	16/Mar/12	18:45	AMEC	Pipe	0	cfs	Hach 950 Flow Meter
906SDL157OD	16/Mar/12	19:00	AMEC	Pipe	0	cfs	Hach 950 Flow Meter
906SDL157OD	16/Mar/12	19:15	AMEC	Pipe	0	cfs	Hach 950 Flow Meter
906SDL157OD	16/Mar/12	19:30	AMEC	Pipe	0	cfs	Hach 950 Flow Meter
906SDL157OD	16/Mar/12	19:45	AMEC	Pipe	0	cfs	Hach 950 Flow Meter
906SDL157OD	16/Mar/12	20:00	AMEC	Pipe	0	cfs	Hach 950 Flow Meter
906SDL157OD	16/Mar/12	20:15	AMEC	Pipe	0	cfs	Hach 950 Flow Meter
906SDL157OD	16/Mar/12	20:30	AMEC	Pipe	0	cfs	Hach 950 Flow Meter
906SDL157OD	16/Mar/12	20:45	AMEC	Pipe	0	cfs	Hach 950 Flow Meter
906SDL157OD	16/Mar/12	21:00	AMEC	Pipe	0	cfs	Hach 950 Flow Meter
906SDL157OD	16/Mar/12	21:15	AMEC	Pipe	0	cfs	Hach 950 Flow Meter
906SDL157OD	16/Mar/12	21:30	AMEC	Pipe	0	cfs	Hach 950 Flow Meter
906SDL157OD	16/Mar/12	21:45	AMEC	Pipe	0	cfs	Hach 950 Flow Meter
906SDL157OD	16/Mar/12	22:00	AMEC	Pipe	0	cfs	Hach 950 Flow Meter
906SDL157OD	16/Mar/12	22:15	AMEC	Pipe	0	cfs	Hach 950 Flow Meter
906SDL157OD	16/Mar/12	22:30	AMEC	Pipe	0	cfs	Hach 950 Flow Meter
906SDL157OD	16/Mar/12	22:45	AMEC	Pipe	0	cfs	Hach 950 Flow Meter
906SDL157OD	16/Mar/12	23:00	AMEC	Pipe	0	cfs	Hach 950 Flow Meter
906SDL157OD	16/Mar/12	23:15	AMEC	Pipe	0	cfs	Hach 950 Flow Meter
906SDL157OD	16/Mar/12	23:30	AMEC	Pipe	0	cfs	Hach 950 Flow Meter
906SDL157OD	16/Mar/12	23:45	AMEC	Pipe	0	cfs	Hach 950 Flow Meter
906SDL157OD	17/Mar/12	0:00	AMEC	Pipe	0	cfs	Hach 950 Flow Meter
906SDL157OD	17/Mar/12	0:15	AMEC	Pipe	0	cfs	Hach 950 Flow Meter
906SDL157OD	17/Mar/12	0:30	AMEC	Pipe	0	cfs	Hach 950 Flow Meter
906SDL157OD	17/Mar/12	0:45	AMEC	Pipe	0	cfs	Hach 950 Flow Meter
906SDL157OD	17/Mar/12	1:00	AMEC	Pipe	0	cfs	Hach 950 Flow Meter
906SDL157OD	17/Mar/12	1:15	AMEC	Pipe	0	cfs	Hach 950 Flow Meter
906SDL157OD	17/Mar/12	1:30	AMEC	Pipe	0	cfs	Hach 950 Flow Meter
906SDL157OD	17/Mar/12	1:45	AMEC	Pipe	0	cfs	Hach 950 Flow Meter
906SDL157OD	17/Mar/12	2:00	AMEC	Pipe	0	cfs	Hach 950 Flow Meter
906SDL157OD	17/Mar/12	2:15	AMEC	Pipe	0	cfs	Hach 950 Flow Meter
906SDL157OD	17/Mar/12	2:30	AMEC	Pipe	0	cfs	Hach 950 Flow Meter
906SDL157OD	17/Mar/12	2:45	AMEC	Pipe	0	cfs	Hach 950 Flow Meter
906SDL157OD	17/Mar/12	3:00	AMEC	Pipe	0	cfs	Hach 950 Flow Meter
906SDL157OD	17/Mar/12	3:15	AMEC	Pipe	0	cfs	Hach 950 Flow Meter
906SDL157OD	17/Mar/12	3:30	AMEC	Pipe	0	cfs	Hach 950 Flow Meter
906SDL157OD	17/Mar/12	3:45	AMEC	Pipe	0	cfs	Hach 950 Flow Meter
906SDL157OD	17/Mar/12	4:00	AMEC	Pipe	0	cfs	Hach 950 Flow Meter
906SDL157OD	17/Mar/12	4:15	AMEC	Pipe	0	cfs	Hach 950 Flow Meter
906SDL157OD	17/Mar/12	4:30	AMEC	Pipe	0	cfs	Hach 950 Flow Meter
906SDL157OD	17/Mar/12	4:45	AMEC	Pipe	0	cfs	Hach 950 Flow Meter
906SDL157OD	17/Mar/12	5:00	AMEC	Pipe	0	cfs	Hach 950 Flow Meter
906SDL157OD	17/Mar/12	5:15	AMEC	Pipe	0.001	cfs	Hach 950 Flow Meter
906SDL157OD	17/Mar/12	5:30	AMEC	Pipe	0.045	cfs	Hach 950 Flow Meter
906SDL157OD	17/Mar/12	5:45	AMEC	Pipe	0.19	cfs	Hach 950 Flow Meter
906SDL157OD	17/Mar/12	6:00	AMEC	Pipe	0.51	cfs	Hach 950 Flow Meter
906SDL157OD	17/Mar/12	6:15	AMEC	Pipe	0.9	cfs	Hach 950 Flow Meter
906SDL157OD	17/Mar/12	6:30	AMEC	Pipe	1.14	cfs	Hach 950 Flow Meter
906SDL157OD	17/Mar/12	6:45	AMEC	Pipe	0.78	cfs	Hach 950 Flow Meter
906SDL157OD	17/Mar/12	7:00	AMEC	Pipe	0.39	cfs	Hach 950 Flow Meter

Station Code	Date	Time	Result	Units	TSS (mg/L)	TSS Load (kg/min)
906SDL062OD	20/Nov/11	14:00		0 cfs	260	0.0000
906SDL062OD	20/Nov/11	14:15		0 cfs	260	0.0000
906SDL062OD	20/Nov/11	14:30		0 cfs	260	0.0000
906SDL062OD	20/Nov/11	14:45		0 cfs	260	0.0000
906SDL062OD	20/Nov/11	15:00		0 cfs	260	0.0000
906SDL062OD	20/Nov/11	15:15		0 cfs	260	0.0000
906SDL062OD	20/Nov/11	15:30		0 cfs	260	0.0000
906SDL062OD	20/Nov/11	15:45		0 cfs	260	0.0000
906SDL062OD	20/Nov/11	16:00		0 cfs	260	0.0000
906SDL062OD	20/Nov/11	16:15		0 cfs	260	0.0000
906SDL062OD	20/Nov/11	16:30		0 cfs	260	0.0000
906SDL062OD	20/Nov/11	16:45		0 cfs	260	0.0000
906SDL062OD	20/Nov/11	17:00		0 cfs	260	0.0000
906SDL062OD	20/Nov/11	17:15		0 cfs	260	0.0000
906SDL062OD	20/Nov/11	17:30		0 cfs	260	0.0000
906SDL062OD	20/Nov/11	17:45		1.29 cfs	260	0.5698
906SDL062OD	20/Nov/11	18:00		1.76 cfs	260	0.7775
906SDL062OD	20/Nov/11	18:15		5.48 cfs	260	2.4208
906SDL062OD	20/Nov/11	18:30		8.77 cfs	260	3.8741
906SDL062OD	20/Nov/11	18:45		9.44 cfs	260	4.1701
906SDL062OD	20/Nov/11	19:00		10.44 cfs	260	4.6118
906SDL062OD	20/Nov/11	19:15		9.33 cfs	260	4.1215
906SDL062OD	20/Nov/11	19:30		6.54 cfs	260	2.8890
906SDL062OD	20/Nov/11	19:45		4.83 cfs	260	2.1336
906SDL062OD	20/Nov/11	20:00		4.45 cfs	260	1.9658
906SDL062OD	20/Nov/11	20:15		4.05 cfs	260	1.7891
906SDL062OD	20/Nov/11	20:30		3.62 cfs	260	1.5991
906SDL062OD	20/Nov/11	20:45		3.7 cfs	260	1.6344
906SDL062OD	20/Nov/11	21:00		4.5 cfs	260	1.9878
906SDL062OD	20/Nov/11	21:15		3.67 cfs	260	1.6212
906SDL062OD	20/Nov/11	21:30		3.52 cfs	260	1.5549
906SDL062OD	20/Nov/11	21:45		3.39 cfs	260	1.4975
906SDL062OD	20/Nov/11	22:00		3.14 cfs	260	1.3871
906SDL062OD	20/Nov/11	22:15		2.63 cfs	260	1.1618
906SDL062OD	20/Nov/11	22:30		2.09 cfs	260	0.9232
906SDL062OD	20/Nov/11	22:45		1.66 cfs	260	0.7333
906SDL062OD	20/Nov/11	23:00		1.39 cfs	260	0.6140
906SDL062OD	20/Nov/11	23:15		1.32 cfs	260	0.5831
906SDL062OD	20/Nov/11	23:30		1.62 cfs	260	0.7156
906SDL062OD	20/Nov/11	23:45		4.59 cfs	260	2.0276
906SDL062OD	21/Nov/11	0:00		6.12 cfs	260	2.7035
906SDL062OD	21/Nov/11	0:15		3.99 cfs	260	1.7626
906SDL062OD	21/Nov/11	0:30		3.16 cfs	260	1.3959
906SDL062OD	21/Nov/11	0:45		3.12 cfs	260	1.3782
906SDL062OD	21/Nov/11	1:00		2.75 cfs	260	1.2148
906SDL062OD	21/Nov/11	1:15		2.15 cfs	260	0.9497
906SDL062OD	21/Nov/11	1:30		1.59 cfs	260	0.7024
906SDL062OD	21/Nov/11	1:45		1.11 cfs	260	0.4903
906SDL062OD	21/Nov/11	2:00		0.761 cfs	260	0.3362
906SDL062OD	21/Nov/11	2:15		0.53 cfs	260	0.2341
906SDL062OD	21/Nov/11	2:30		0.339 cfs	260	0.1498
906SDL062OD	21/Nov/11	2:45		0.249 cfs	260	0.1100
906SDL062OD	21/Nov/11	3:00		0.204 cfs	260	0.0901

Station Code	Date	Time	Result	Units	TSS (mg/L)	TSS Load (kg/min)
906SDL062OD	07/Feb/12	14:00	0	cfs	130	0.0000
906SDL062OD	07/Feb/12	14:15	0	cfs	130	0.0000
906SDL062OD	07/Feb/12	14:30	0	cfs	130	0.0000
906SDL062OD	07/Feb/12	14:45	0	cfs	130	0.0000
906SDL062OD	07/Feb/12	15:00	0	cfs	130	0.0000
906SDL062OD	07/Feb/12	15:15	0.01	cfs	130	0.0022
906SDL062OD	07/Feb/12	15:30	0.095	cfs	130	0.0210
906SDL062OD	07/Feb/12	15:45	0.28	cfs	130	0.0618
906SDL062OD	07/Feb/12	16:00	1.9	cfs	130	0.4197
906SDL062OD	07/Feb/12	16:15	2.2	cfs	130	0.4859
906SDL062OD	07/Feb/12	16:30	1.33	cfs	130	0.2938
906SDL062OD	07/Feb/12	16:45	2.23	cfs	130	0.4925
906SDL062OD	07/Feb/12	17:00	4.44	cfs	130	0.9807
906SDL062OD	07/Feb/12	17:15	6.56	cfs	130	1.4489
906SDL062OD	07/Feb/12	17:30	5.14	cfs	130	1.1353
906SDL062OD	07/Feb/12	17:45	2.47	cfs	130	0.5456
906SDL062OD	07/Feb/12	18:00	2.04	cfs	130	0.4506
906SDL062OD	07/Feb/12	18:15	1.02	cfs	130	0.2253
906SDL062OD	07/Feb/12	18:30	0.293	cfs	130	0.0647
906SDL062OD	07/Feb/12	18:45	0.047	cfs	130	0.0104
906SDL062OD	07/Feb/12	19:00	0	cfs	130	0.0000
906SDL062OD	07/Feb/12	19:15	0	cfs	130	0.0000
906SDL062OD	07/Feb/12	19:30	0	cfs	130	0.0000
906SDL062OD	07/Feb/12	19:45	0	cfs	130	0.0000
906SDL062OD	07/Feb/12	20:00	0	cfs	130	0.0000
906SDL062OD	07/Feb/12	20:15	0	cfs	130	0.0000
906SDL062OD	07/Feb/12	20:30	0	cfs	130	0.0000
906SDL062OD	07/Feb/12	20:45	0	cfs	130	0.0000
906SDL062OD	07/Feb/12	21:00	0	cfs	130	0.0000
						99.57
27,050					130	99.57
Total Flow (cf)						Total Load (kg/event)

Station Code	Date	Time	Result	Units	TSS (mg/L)	TSS Load (kg/min)
906SDL062OD	16/Mar/12	17:45	0	cfs	81	0.0000
906SDL062OD	16/Mar/12	18:00	0	cfs	81	0.0000
906SDL062OD	16/Mar/12	18:15	0	cfs	81	0.0000
906SDL062OD	16/Mar/12	18:30	0	cfs	81	0.0000
906SDL062OD	16/Mar/12	18:45	0	cfs	81	0.0000
906SDL062OD	16/Mar/12	19:00	0	cfs	81	0.0000
906SDL062OD	16/Mar/12	19:15	0	cfs	81	0.0000
906SDL062OD	16/Mar/12	19:30	0	cfs	81	0.0000
906SDL062OD	16/Mar/12	19:45	0	cfs	81	0.0000
906SDL062OD	16/Mar/12	20:00	0	cfs	81	0.0000
906SDL062OD	16/Mar/12	20:15	0	cfs	81	0.0000
906SDL062OD	16/Mar/12	20:30	0	cfs	81	0.0000
906SDL062OD	16/Mar/12	20:45	0	cfs	81	0.0000
906SDL062OD	16/Mar/12	21:00	0	cfs	81	0.0000
906SDL062OD	16/Mar/12	21:15	0	cfs	81	0.0000
906SDL062OD	16/Mar/12	21:30	0	cfs	81	0.0000
906SDL062OD	16/Mar/12	21:45	0	cfs	81	0.0000
906SDL062OD	16/Mar/12	22:00	0	cfs	81	0.0000
906SDL062OD	16/Mar/12	22:15	0	cfs	81	0.0000
906SDL062OD	16/Mar/12	22:30	0	cfs	81	0.0000
906SDL062OD	16/Mar/12	22:45	0	cfs	81	0.0000
906SDL062OD	16/Mar/12	23:00	0	cfs	81	0.0000
906SDL062OD	16/Mar/12	23:15	0	cfs	81	0.0000
906SDL062OD	16/Mar/12	23:30	0	cfs	81	0.0000
906SDL062OD	16/Mar/12	23:45	0	cfs	81	0.0000
906SDL062OD	17/Mar/12	0:00	0	cfs	81	0.0000
906SDL062OD	17/Mar/12	0:15	0	cfs	81	0.0000
906SDL062OD	17/Mar/12	0:30	0	cfs	81	0.0000
906SDL062OD	17/Mar/12	0:45	0	cfs	81	0.0000
906SDL062OD	17/Mar/12	1:00	0	cfs	81	0.0000
906SDL062OD	17/Mar/12	1:15	0.053	cfs	81	0.0073
906SDL062OD	17/Mar/12	1:30	0.428	cfs	81	0.0589
906SDL062OD	17/Mar/12	1:45	0.252	cfs	81	0.0347
906SDL062OD	17/Mar/12	2:00	0.065	cfs	81	0.0089
906SDL062OD	17/Mar/12	2:15	0.011	cfs	81	0.0015
906SDL062OD	17/Mar/12	2:30	0.031	cfs	81	0.0043
906SDL062OD	17/Mar/12	2:45	0.031	cfs	81	0.0043
906SDL062OD	17/Mar/12	3:00	0.017	cfs	81	0.0023
906SDL062OD	17/Mar/12	3:15	0.017	cfs	81	0.0023
906SDL062OD	17/Mar/12	3:30	0.014	cfs	81	0.0019
906SDL062OD	17/Mar/12	3:45	0.01	cfs	81	0.0014
906SDL062OD	17/Mar/12	4:00	0.01	cfs	81	0.0014
906SDL062OD	17/Mar/12	4:15	0.225	cfs	81	0.0310
906SDL062OD	17/Mar/12	4:30	0.44	cfs	81	0.0606
906SDL062OD	17/Mar/12	4:45	0.361	cfs	81	0.0497
906SDL062OD	17/Mar/12	5:00	0.493	cfs	81	0.0678
906SDL062OD	17/Mar/12	5:15	1.74	cfs	81	0.2395
906SDL062OD	17/Mar/12	5:30	1.68	cfs	81	0.2312
906SDL062OD	17/Mar/12	5:45	2.23	cfs	81	0.3069
906SDL062OD	17/Mar/12	6:00	2.18	cfs	81	0.3000
906SDL062OD	17/Mar/12	6:15	4.25	cfs	81	0.5849
906SDL062OD	17/Mar/12	6:30	1.62	cfs	81	0.2229
906SDL062OD	17/Mar/12	6:45	1.78	cfs	81	0.2450
906SDL062OD	17/Mar/12	7:00	2.13	cfs	81	0.2931

Station Code	Date	Time	Result	Units	TSS (mg/L)	TSS Load (kg/min)
906SDL157OD	20/Nov/11	9:15	0	cfs		340 0.0000
906SDL157OD	20/Nov/11	9:30	0	cfs		340 0.0000
906SDL157OD	20/Nov/11	9:45	0	cfs		340 0.0000
906SDL157OD	20/Nov/11	10:00	0	cfs		340 0.0000
906SDL157OD	20/Nov/11	10:15	0	cfs		340 0.0000
906SDL157OD	20/Nov/11	10:30	0	cfs		340 0.0000
906SDL157OD	20/Nov/11	10:45	0	cfs		340 0.0000
906SDL157OD	20/Nov/11	11:00	0	cfs		340 0.0000
906SDL157OD	20/Nov/11	11:15	0	cfs		340 0.0000
906SDL157OD	20/Nov/11	11:30	0	cfs		340 0.0000
906SDL157OD	20/Nov/11	11:45	0	cfs		340 0.0000
906SDL157OD	20/Nov/11	12:00	0	cfs		340 0.0000
906SDL157OD	20/Nov/11	12:15	0	cfs		340 0.0000
906SDL157OD	20/Nov/11	12:30	0	cfs		340 0.0000
906SDL157OD	20/Nov/11	12:45	0	cfs		340 0.0000
906SDL157OD	20/Nov/11	13:00	0	cfs		340 0.0000
906SDL157OD	20/Nov/11	13:15	0	cfs		340 0.0000
906SDL157OD	20/Nov/11	13:30	0	cfs		340 0.0000
906SDL157OD	20/Nov/11	13:45	0	cfs		340 0.0000
906SDL157OD	20/Nov/11	14:00	0	cfs		340 0.0000
906SDL157OD	20/Nov/11	14:15	0	cfs		340 0.0000
906SDL157OD	20/Nov/11	14:30	0	cfs		340 0.0000
906SDL157OD	20/Nov/11	14:45	0	cfs		340 0.0000
906SDL157OD	20/Nov/11	15:00	0	cfs		340 0.0000
906SDL157OD	20/Nov/11	15:15	0	cfs		340 0.0000
906SDL157OD	20/Nov/11	15:30	0	cfs		340 0.0000
906SDL157OD	20/Nov/11	15:45	0	cfs		340 0.0000
906SDL157OD	20/Nov/11	16:00	0	cfs		340 0.0000
906SDL157OD	20/Nov/11	16:15	0	cfs		340 0.0000
906SDL157OD	20/Nov/11	16:30	0	cfs		340 0.0000
906SDL157OD	20/Nov/11	16:45	0	cfs		340 0.0000
906SDL157OD	20/Nov/11	17:00	0	cfs		340 0.0000
906SDL157OD	20/Nov/11	17:15	0	cfs		340 0.0000
906SDL157OD	20/Nov/11	17:30	0.003	cfs		340 0.0017
906SDL157OD	20/Nov/11	17:45	0.56	cfs		340 0.3235
906SDL157OD	20/Nov/11	18:00	1.26	cfs		340 0.7279
906SDL157OD	20/Nov/11	18:15	1.25	cfs		340 0.7221
906SDL157OD	20/Nov/11	18:30	2.73	cfs		340 1.5770
906SDL157OD	20/Nov/11	18:45	2.96	cfs		340 1.7099
906SDL157OD	20/Nov/11	19:00	3.22	cfs		340 1.8601
906SDL157OD	20/Nov/11	19:15	2.26	cfs		340 1.3055
906SDL157OD	20/Nov/11	19:30	1.76	cfs		340 1.0167
906SDL157OD	20/Nov/11	19:45	1.49	cfs		340 0.8607
906SDL157OD	20/Nov/11	20:00	0.96	cfs		340 0.5546
906SDL157OD	20/Nov/11	20:15	0.94	cfs		340 0.5430
906SDL157OD	20/Nov/11	20:30	0.92	cfs		340 0.5315
906SDL157OD	20/Nov/11	20:45	1.72	cfs		340 0.9936
906SDL157OD	20/Nov/11	21:00	1.68	cfs		340 0.9705
906SDL157OD	20/Nov/11	21:15	1.08	cfs		340 0.6239
906SDL157OD	20/Nov/11	21:30	0.93	cfs		340 0.5372
906SDL157OD	20/Nov/11	21:45	0.97	cfs		340 0.5603
906SDL157OD	20/Nov/11	22:00	0.95	cfs		340 0.5488
906SDL157OD	20/Nov/11	22:15	0.84	cfs		340 0.4852

Station Code	Date	Time	Result	Units	TSS (mg/L)	TSS Load (kg/min)
906SDL157OD	07/Feb/12	14:00	0	cfs	230	0.0000
906SDL157OD	07/Feb/12	14:15	0	cfs	230	0.0000
906SDL157OD	07/Feb/12	14:30	0	cfs	230	0.0000
906SDL157OD	07/Feb/12	14:45	0	cfs	230	0.0000
906SDL157OD	07/Feb/12	15:00	0.001	cfs	230	0.0004
906SDL157OD	07/Feb/12	15:15	0.11	cfs	230	0.0430
906SDL157OD	07/Feb/12	15:30	0.13	cfs	230	0.0508
906SDL157OD	07/Feb/12	15:45	0.16	cfs	230	0.0625
906SDL157OD	07/Feb/12	16:00	0.45	cfs	230	0.1758
906SDL157OD	07/Feb/12	16:15	1.31	cfs	230	0.5119
906SDL157OD	07/Feb/12	16:30	1.34	cfs	230	0.5236
906SDL157OD	07/Feb/12	16:45	2.52	cfs	230	0.9847
906SDL157OD	07/Feb/12	17:00	2.88	cfs	230	1.1254
906SDL157OD	07/Feb/12	17:15	3.48	cfs	230	1.3599
906SDL157OD	07/Feb/12	17:30	3.15	cfs	230	1.2309
906SDL157OD	07/Feb/12	17:45	3.17	cfs	230	1.2387
906SDL157OD	07/Feb/12	18:00	2.73	cfs	230	1.0668
906SDL157OD	07/Feb/12	18:15	2.07	cfs	230	0.8089
906SDL157OD	07/Feb/12	18:30	1.64	cfs	230	0.6409
906SDL157OD	07/Feb/12	18:45	1.27	cfs	230	0.4963
906SDL157OD	07/Feb/12	19:00	0.77	cfs	230	0.3009
906SDL157OD	07/Feb/12	19:15	0.51	cfs	230	0.1993
906SDL157OD	07/Feb/12	19:30	0.24	cfs	230	0.0938
906SDL157OD	07/Feb/12	19:45	0.1	cfs	230	0.0391
906SDL157OD	07/Feb/12	20:00	0.022	cfs	230	0.0086
906SDL157OD	07/Feb/12	20:15	0.003	cfs	230	0.0012
906SDL157OD	07/Feb/12	20:30	0	cfs	230	0.0000
906SDL157OD	07/Feb/12	20:45	0	cfs	230	0.0000
906SDL157OD	07/Feb/12	21:00	0	cfs	230	0.0000
						164.45
25,250					230	164.45
Total Flow (cf)						Total Load (kg/event)

Station Code	Date	Time	Result	Units	TSS (mg/L)	TSS Load (kg/min)
906SDL157OD	16/Mar/12	17:45	0	cfs	170	0.0000
906SDL157OD	16/Mar/12	18:00	0	cfs	170	0.0000
906SDL157OD	16/Mar/12	18:15	0	cfs	170	0.0000
906SDL157OD	16/Mar/12	18:30	0	cfs	170	0.0000
906SDL157OD	16/Mar/12	18:45	0	cfs	170	0.0000
906SDL157OD	16/Mar/12	19:00	0	cfs	170	0.0000
906SDL157OD	16/Mar/12	19:15	0	cfs	170	0.0000
906SDL157OD	16/Mar/12	19:30	0	cfs	170	0.0000
906SDL157OD	16/Mar/12	19:45	0	cfs	170	0.0000
906SDL157OD	16/Mar/12	20:00	0	cfs	170	0.0000
906SDL157OD	16/Mar/12	20:15	0	cfs	170	0.0000
906SDL157OD	16/Mar/12	20:30	0	cfs	170	0.0000
906SDL157OD	16/Mar/12	20:45	0	cfs	170	0.0000
906SDL157OD	16/Mar/12	21:00	0	cfs	170	0.0000
906SDL157OD	16/Mar/12	21:15	0	cfs	170	0.0000
906SDL157OD	16/Mar/12	21:30	0	cfs	170	0.0000
906SDL157OD	16/Mar/12	21:45	0	cfs	170	0.0000
906SDL157OD	16/Mar/12	22:00	0	cfs	170	0.0000
906SDL157OD	16/Mar/12	22:15	0	cfs	170	0.0000
906SDL157OD	16/Mar/12	22:30	0	cfs	170	0.0000
906SDL157OD	16/Mar/12	22:45	0	cfs	170	0.0000
906SDL157OD	16/Mar/12	23:00	0	cfs	170	0.0000
906SDL157OD	16/Mar/12	23:15	0	cfs	170	0.0000
906SDL157OD	16/Mar/12	23:30	0	cfs	170	0.0000
906SDL157OD	16/Mar/12	23:45	0	cfs	170	0.0000
906SDL157OD	17/Mar/12	0:00	0	cfs	170	0.0000
906SDL157OD	17/Mar/12	0:15	0	cfs	170	0.0000
906SDL157OD	17/Mar/12	0:30	0	cfs	170	0.0000
906SDL157OD	17/Mar/12	0:45	0	cfs	170	0.0000
906SDL157OD	17/Mar/12	1:00	0	cfs	170	0.0000
906SDL157OD	17/Mar/12	1:15	0	cfs	170	0.0000
906SDL157OD	17/Mar/12	1:30	0	cfs	170	0.0000
906SDL157OD	17/Mar/12	1:45	0	cfs	170	0.0000
906SDL157OD	17/Mar/12	2:00	0	cfs	170	0.0000
906SDL157OD	17/Mar/12	2:15	0	cfs	170	0.0000
906SDL157OD	17/Mar/12	2:30	0	cfs	170	0.0000
906SDL157OD	17/Mar/12	2:45	0	cfs	170	0.0000
906SDL157OD	17/Mar/12	3:00	0	cfs	170	0.0000
906SDL157OD	17/Mar/12	3:15	0	cfs	170	0.0000
906SDL157OD	17/Mar/12	3:30	0	cfs	170	0.0000
906SDL157OD	17/Mar/12	3:45	0	cfs	170	0.0000
906SDL157OD	17/Mar/12	4:00	0	cfs	170	0.0000
906SDL157OD	17/Mar/12	4:15	0	cfs	170	0.0000
906SDL157OD	17/Mar/12	4:30	0	cfs	170	0.0000
906SDL157OD	17/Mar/12	4:45	0	cfs	170	0.0000
906SDL157OD	17/Mar/12	5:00	0	cfs	170	0.0000
906SDL157OD	17/Mar/12	5:15	0.001	cfs	170	0.0003
906SDL157OD	17/Mar/12	5:30	0.045	cfs	170	0.0130
906SDL157OD	17/Mar/12	5:45	0.19	cfs	170	0.0549
906SDL157OD	17/Mar/12	6:00	0.51	cfs	170	0.1473
906SDL157OD	17/Mar/12	6:15	0.9	cfs	170	0.2599
906SDL157OD	17/Mar/12	6:30	1.14	cfs	170	0.3293
906SDL157OD	17/Mar/12	6:45	0.78	cfs	170	0.2253
906SDL157OD	17/Mar/12	7:00	0.39	cfs	170	0.1126